Pediatric Wheelchair Transportation Safety: Transit Manual Wheelchair Design Guidelines and Injury Risk of 6-year-old Children in a Frontal Motor Vehicle Impact

by

DongRan Ha

BS, Carnegie Mellon University, 1998

MS, University of Pittsburgh, 2000

Submitted to the Graduate Faculty of

the School of Health and Rehabilitation Science in partial fulfillment

of the requirements for the degree of

Ph.D. of Rehabilitation Science and Technology

University of Pittsburgh

2004

UNIVERSITY OF PITTSBURGH

School of Health and Rehabilitation Science

This dissertation was presented

by

DongRan Ha

It was defended on

October 28, 2004

and approved by

Rory A. Cooper, PhD, Rehabilitation Science and Technology, University of Pittsburgh

Douglas A. Hobson, PhD, Rehabilitation Science and Technology, University of Pittsburgh

C. Gregory Shaw, PhD, Mechanical and Aerospace Engineering, University of Virginia

Dissertation Director: Gina E. Bertocci, PhD, Mechanical Engineering, University of Louisville

Pediatric Wheelchair Transportation Safety:
Transit Manual Wheelchair Design Guidelines and
Injury Risk of 6-year-old Children in a Frontal Motor Vehicle Impact

DongRan Ha, PhD

University of Pittsburgh, 2004

Children with disabilities often cannot be seated in standard child seats or automobile seats because of physical deformities or poor trunk and head control. Therefore, when children with disabilities are transported to schools and developmental facilities, they often remain seated in their wheelchairs in vehicles such as school buses and family vans. Children who must travel seated in their wheelchairs are excluded from the protections dictated by the federal and state laws related to child protection in motor vehicle crashes. This dissertation investigated the safety of children in wheelchairs in transit, mainly using computer simulation software. Three pediatric manual wheelchairs were tested with a Hybrid III 6-year-old ATD in accordance with the ANSI/RESNA WC-19 standard. Using sled test data, a computer model representing a Zippie wheelchair seated with a Hybrid III 6-year-old ATD subjected to a 20g/48kph frontal crash was developed and validated in MADYMO. The injury risks of 6-year-old wheelchair occupants in a frontal impact motor vehicle crash was investigated by analyzing sled test data and by using the pediatric wheelchair computer model. The loads imposed on the wheelchair and occupant restraint system under 20g/48kph frontal impact conditions with varying wheelchair setup conditions was also investigated using the computer model. The study results showed that a 6-year-old wheelchair seated occupant may be subjected to a risk of neck and chest injuries in a frontal impact motor vehicle crash. Results also showed that altering wheelchair settings does have impact on kinematics and injury risk of a 6-year-old wheelchair occupant in a frontal motor vehicle crash. Changing wheelchair settings also had impact on wheelchair kinematics and loads imposed on the wheelchair and occupant restraint system. The study results presented in this dissertation will provide guidelines for manufacturers designing pediatric transit wheelchairs, seating, and occupant restraint system. The pediatric wheelchair model developed in this study will provide a foundation for studying the response of a manual pediatric wheelchair and a child occupant in crashes. Moreover, the model will promote the study of associated injury risks for pediatric wheelchair users in motor vehicle crashes.

PREFACE

I would like thank my committee members, Dr. Gina Bertocci, Dr. Rory Cooper, Dr. Douglas Hobson and Dr. Gregory Shaw, for their guidance and insightful comments throughout my dissertation study. Especially, I'm very grateful to Dr. Bertocci, who has helped me in so many ways in past six years. She has been a permanent source of advice and support.

Very special thanks go to my parents and husband:

My parents, Il-boo Ha and Hwa-ja Park, nicknamed me 'Curie' (Marie Curie, a great woman scientist who won two Nobel Prizes) and often told me that I would be a great scientist like Marie Curie. I dedicate this dissertation to my parents who always believed in me, love me and support me.

My dear husband, Hosik Nam, has always been extremely patient and supportive. Without him, my dissertation study could not have been completed. Hosik, thank you for loving me and being always there for me!

I would deeply thank my mother-in-law, Mi-young Nam, for her prayers, understanding, and unconditional support.

I wish to give many thanks to my three older sisters, Young-ran Ha, Hye-ran Ha, and Ju-ran Ha, and in-laws, Ki-young Kim, Jung-min Lee, Moon-jung Ooi and David Ooi, for their loving encouragement and for being there.

I would also like to thank my friends and colleagues, especially Linda van Roosmalen and Sue Furman, for their encouragement and support. And, special thanks also go to the staff of the department of Rehabilitation Science and Technology, especially Joe Ruffing, for assistant with many aspects associated with my study.

I wish to express great appreciation to Rohit Jategaonkar for his expertise in developing a computer model and to Miriam Manary and Lawrence Schneider for their expertise in conducting sled tests.

Lastly, but not least, I would like to thank God for leading me to all these great people and giving me knowledge and strength to achieve this goal.

This research was funded by the National Institute of Disability and Rehabilitation Research (NIDRR), Rehabilitation Engineering Research Center (RERC) on Wheelchair Transportation Safety, grant # H133E010302.

TABLE OF CONTENTS

LIST OF FIGURES

LIST OF TABLES

DEFINITIONS AND ABBREVIATIONS

ADA: Americans with Disabilities Act

ANSI: American National Standards Institute

ATD: anthropomorphic test device

CG: the center of gravity

CG_{WC} : the center of gravity of the wheelchair

FMVSS: Federal Motor Vehicle Safety Standards

Four-point Tiedown: A wheelchair securement system that attaches to the wheelchair at four separate securement points and that also anchors to the vehicle at four separate anchor points.

g: Abbreviation for acceleration due to gravity measured at seat level; one g is equal to 9.8 m/s/s

HIC: head injury criterion

H-pt: a point located on the buttock/pelvis region of an ATD that represents the approximate human hip joint location

IDEA: Individuals with Disabilities Education Act

ISO: International Standards Organization

MADYMO: MAthmatical DYnamic Model is a name of crash simulation software package

MVC: motor vehicle crash

NHTSA: National Highway Traffic Safety Administration

N_{ij}; neck injury criteria

OIAM: occupant injury assessment measurement values such as HIC_{15}, N_{ij}, and chest acceleration

ORS: occupant restraint system

RESNA: Rehabilitation Engineering and Assistive Technology Society of North America

SAE: Society of Automotive Engineers

SBA: seat back angle

SOWHAT: Subcommittee on Wheelchairs and Transportation

SP: securement point

STBI: seat-to-back intersection

SWCB: surrogate wheelchair base is a repeatable and reusable wheelchair frame to which wheelchair seating systems can be attached

$VAR_{time\_history}$: variables used in the comparison of time histories between sled test and computer simulation model

$VAR_{hor\_excursion}$: variables used in the comparison of peak horizontal excursions between sled test and computer simulation model

WCSS: wheelchair seating system consists of wheelchair seat pan and wheelchair seat back

WTORS: wheelchair tiedown and occupant restraint systems

1 INTRODUCTION

In this dissertation, the safety of children in wheelchairs in transit was investigated using computer simulation software, MADYMO. This dissertation consists of seven chapters as follow: Chapter 1 presents background literature and comparison of computer simulation software packages. Specific aims of the dissertation are stated at the end of Chapter 1. Chapter 2 describes the development and validation of a computer simulation model representing a 6-year-old occupant seated in a manual pediatric wheelchair. Chapter 3 assesses the injury risks for a 6-year-old occupant using a wheelchair as a vehicle seat during a frontal impact. Chapter 3 is based on the sled test results, and computer simulation is not involved in the chapter. Chapter 4 investigates the effect of different manual wheelchair settings on injury risks of a 6-year-old wheelchair occupant in transit during a frontal motor vehicle crash. The results of the parametric sensitivity analysis study conducted in the chapter are related to the injury risk measures specified in the current transit wheelchair standards and federal motor vehicle safety standards (FMVSS). Chapter 5 investigates the effect of different manual wheelchair settings on pediatric manual wheelchair and WTORS loading during a frontal crash. In Chapter 6, injury risks associated with children seated in wheelchairs riding school buses are compared to those associated with children in bus seats during a frontal crash. Finally, Chapter 7 states conclusions and limitations of this study.

1.1 BACKGROUND

In the United States, injuries related to motor vehicle crashes (MVCs) are the leading cause of death for children over the age of one [1]. To protect children from injuries and death in MVCs, extensive research has been conducted in the automotive industries, and federal and state laws related to child protection in MVCs have been established. Federal Motor Vehicle Safety

Standard (FMVSS) 213 regulates the child restraint systems designed for children weighing 50 lbs (22.7 kg) or less [2]. A child weighing less than 40 lbs (18.1 kg) is required to be seated in a convertible car seat; a child who has outgrown a car seat is required to be seated in a belt-positioning booster seat until he/she reaches 50 lbs (22.7 kg). Recently, there has been an increase in concerns related to children who have outgrown booster seats but who have not yet reached adult stature. The result has been a proposal to extend the FMVSS 213 regulation to children weighing more than 50 lbs (22.7 kg) [3].

Children with disabilities often cannot be seated in standard booster seats or automobile seats because of physical deformities or poor trunk and head control; they may differ anatomically from children who do not have disabilities or may not have sufficient balance while sitting due to lack of trunk or head stability. The results of the survey study on transportation of children with disabilities conducted by Everly et al. show that a large percentage of children (44%) transported daily have poor head and trunk control and are therefore unable to sit upright without support (see Figure 1) [4]. Therefore, children with disabilities who must travel seated in their wheelchairs are often excluded from the protections dictated by the FMVSS 213, as well as by other laws relating to child protection in MVCs.

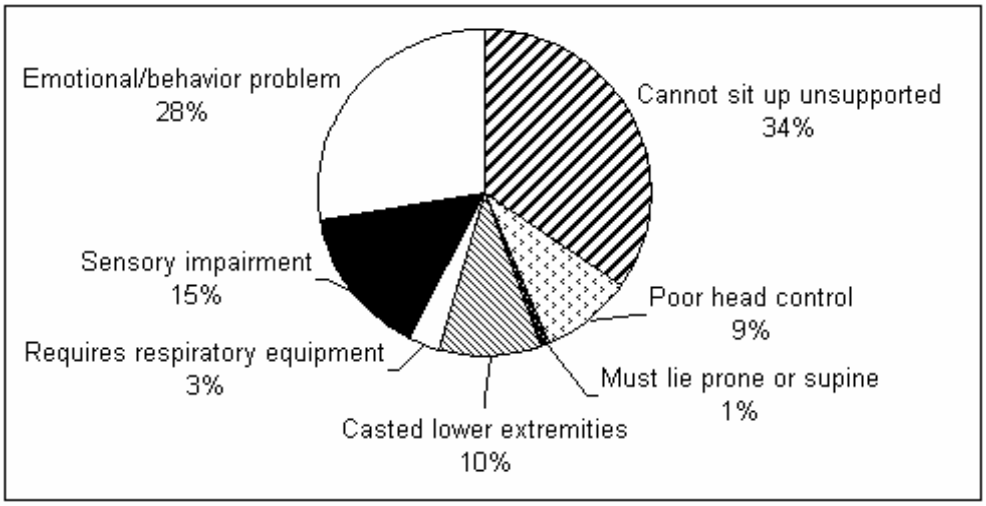

Figure 1 Conditions of children with disabilities transported [4]

Federal laws, such as the Americans with Disabilities Act (ADA) and the Individuals with Disabilities Education Act (IDEA), prohibit discrimination against children with disabilities. IDEA (formerly called Education for all Handicapped Children Act of 1975) requires "public schools to make available to all eligible children with disabilities a free appropriate public education in the least restrictive environment appropriate to their individual needs" [5]. Therefore, many children with disabilities receive their education along with non-disabled children in the same mainstreamed schools, and these disabled children are transported on a daily basis to schools and developmental facilities. The Everly et al. survey study shows that a majority of children using transportation services are school aged children, six to 17 years old (see Figure 2) [4]. This study also showed that a majority of children with disabilities were transported to and from schools, community agencies, and rehabilitation facilities by 66 passenger school buses (see Figure 3) [4]. Because of the US Department of Transportation's requirements for compartmentalization on large school buses and the inherent safety associated with larger vehicles, children seated in OEM vehicle seats are approximately eight times safer in

school buses than in their parents' cars [6]. "School bus transportation is one of the safest forms of transportation in the United States" [6]. However, children with disabilities who are seated in their wheelchairs while riding school buses do not benefit from compartmentalization and are not as protected as non-disabled children.

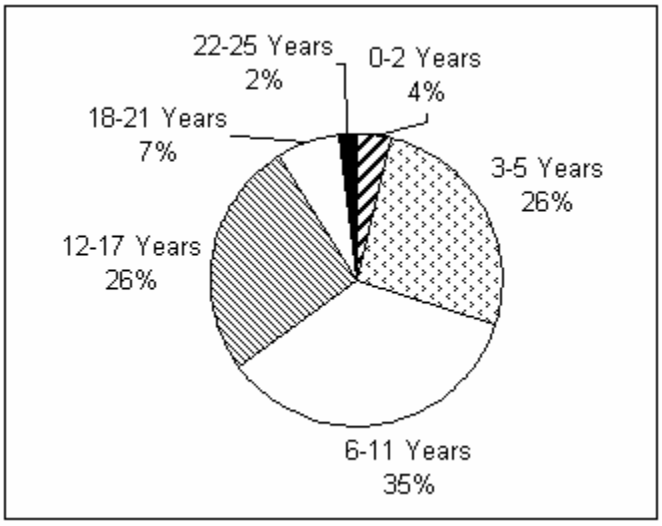

Figure 2 Age categories of children transported [4]

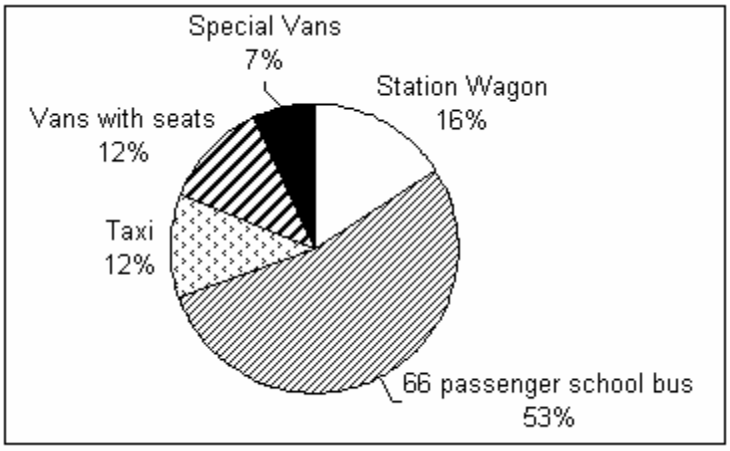

Figure 3 Vehicle types used by respondents to transport children [4]

The number of travelers with disabilities who sit in their wheelchairs in public or private transportation has increased since the passage of the ADA. Children often remain seated in their wheelchairs in vehicles such as school buses and family vans when they are transported. Because wheelchairs are not typically designed to serve as vehicle seats, concerns about the safety of both the wheelchair user and the other occupants in the vehicles have been raised. In order to improve the safety of wheelchair-seated travelers and other vehicle occupants, voluntary standards, which have not been mandated by state or federal laws, have been established by national and international organizations. These organizations include the Society of Automotive Engineers (SAE) Adaptive Devices Subcommittee, American National Standards Institute (ANSI)/Rehabilitation Engineering and Assistive Technology Society of North America (RESNA) Subcommittee on Wheelchairs and Transportation (SOWHAT), and International Standards Organization (ISO) Working Group 6 [7] [8] [9] [10]. However, except for the ANSI/RESNA WC-19 standard, test setup and performance requirements stated in the standards address only adult anthropomorphic test devices (ATDs) and adult wheelchairs. Moreover, studies and research conducted to-date on wheelchair transportation safety, such as wheelchair tiedown and occupant restraint systems (WTORS), wheelchair and seating system crashworthiness, transit wheelchair design criteria, wheelchair occupant injuries in a crash, etc, have focused on adult wheelchair users. There have been no studies published on pediatric transit wheelchairs and the injury risks for pediatric wheelchair users in crashes.

1.2 WHEELCHAIR TRANSPORTATION STANDARDS

1.2.1 Wheelchair Securement and Occupant Restraint Standards

In order to provide effective protection to wheelchair occupants and other passengers in vehicles, the three systems of wheelchair safety should all function together. Those include a

wheelchair tiedown system which secures a wheelchair to the vehicle floor, a wheelchair frame and seating system which supports an occupant, and a wheelchair occupant restraint system. Voluntary wheelchair standards contain design and performance requirements for those systems and provide guidance for the manufacture of transport-safe products.

1.2.1.1 SAE RP J2249: Wheelchair Tiedowns and Occupant Restraint Systems

The Society of Automotive Engineers (SAE) developed the recommended practice (RP) for aftermarket products of wheelchair tiedowns and occupant restraint systems (WTORS) [7]. This standard specifies design requirements, test methods, and performance requirements of a device or system that secures a wheelchair and that restrains a wheelchair-seated occupant, WTORS. It applies to all type of WTORS used for forward-facing wheelchair-seated children and adults.

The standard provides the recommended angles and locations of front and rear tiedown straps from wheelchair securement points to vehicle anchor points (see Figure 4). Specified angles can be applied to both adult and pediatric wheelchairs. The standard also provides the range of angles and locations for pelvic restraints and their anchor points (Figure 5). For shoulder restraints, the preferred zones for location of the belt on the occupant's torso and on the shoulder restraint upper vehicle anchor point are provided for different occupant sizes (Table 1 and Figure 6).

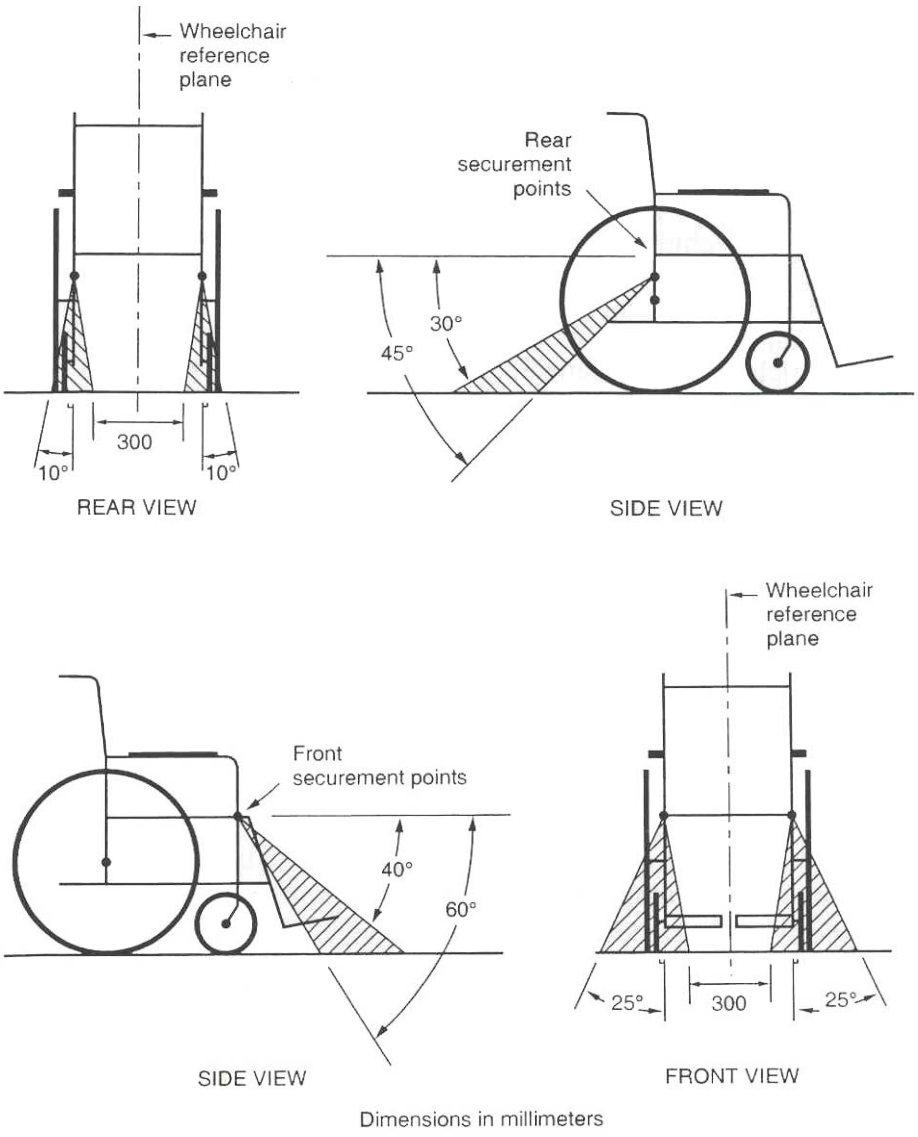

Figure 4 Preferred angles and locations of rear tie-down (top) and front tie-down (bottom) [7]

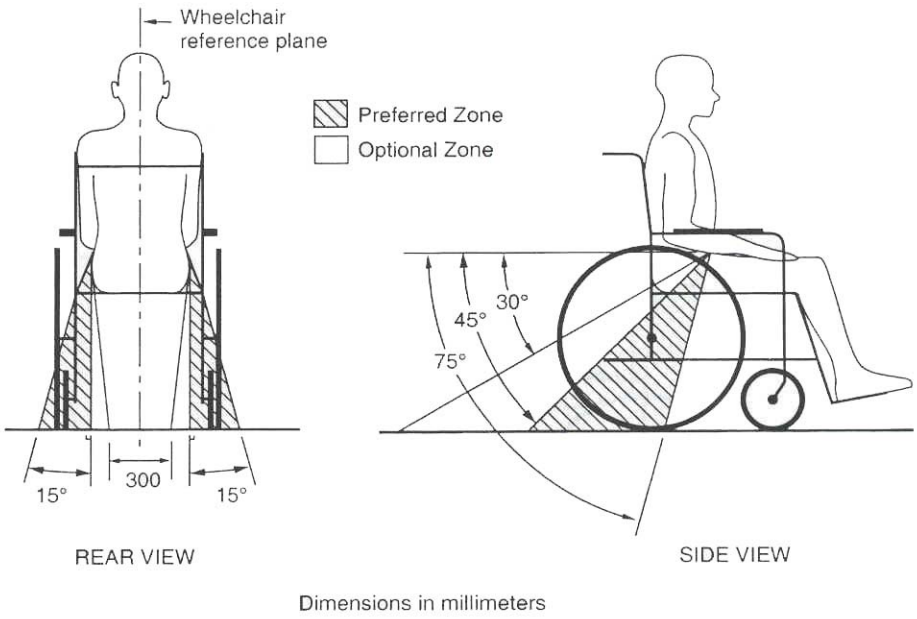

Figure 5 Range of required angles and locations for pelvic restraints and pelvic-restraint anchor points [7]

Table 1 Recommended belt-fit values for Figure 6 (mm) [7]

Occupant Size	**N1**	**N2**	**SR**
6-year-old	52	91	273
mall female	66	109	353
midsize male	76	127	406
large male	81	135	432

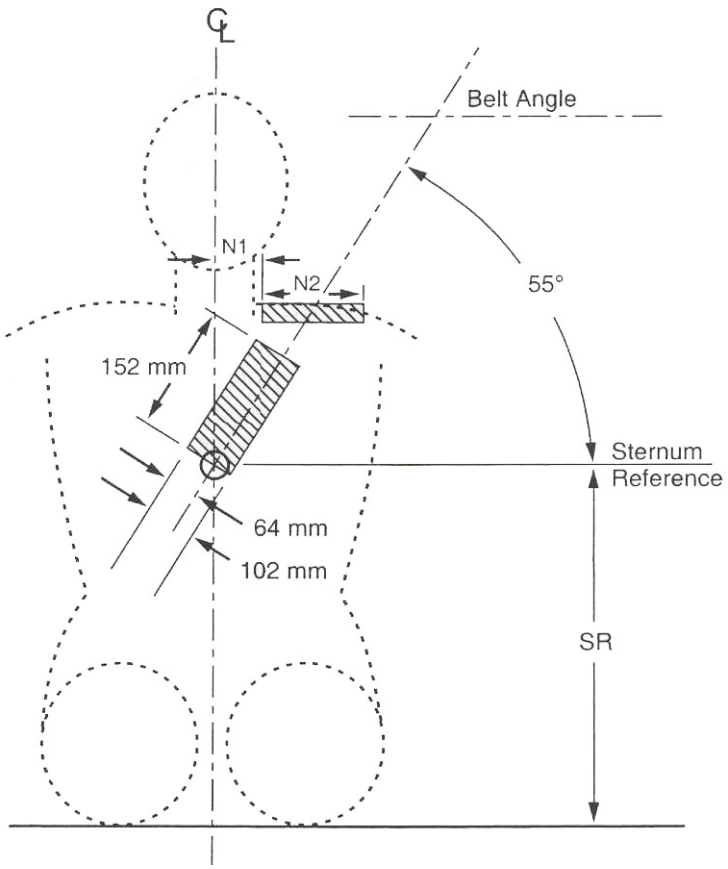

Figure 6 Preferred zones for location of shoulder belt on occupant's torso [7]

SAE J2249 requires WTORS to perform successfully in a 20g/48kph (30mph) sled-generated frontal crash pulse. A surrogate wheelchair representing an adult-sized electrically-powered wheelchair and 76.3 kg anthropomorphic test dummy (ATD) representing a midsize male are used for the frontal impact test in the standard. Although it was noted that a 6-year-old ATD or a small female ATD could be used to test the product intended for use by children, the horizontal excursion limits of the test dummy and the test wheelchair, as shown in Table 2, are provided for the midsize male ATD and not for the smaller ATDs.

Table 2 SAE J2249 - Wheelchair and dummy horizontal excursion limits (mm) [7]

Measurement Point	Excursion Variable	Pelvic & Shoulder Restraint
Test Wheelchair	X_{wc}	200
ATD Knee	X_{knee}	375
ATD Head	X_{head}	650

where

X_{wc} = the horizontal distance relative to the sled platform between the contrast target placed at or near point P on the test wheelchair at time t_0, to the point P target at the time of peak wheelchair excursion;

X_{knee} = the horizontal distance relative to the sled platform between the dummy knee-joint target at time t_0, to the knee joint target at the time of peak knee excursion; and

X_{head} = the horizontal distance relative to the sled platform between the most forward point on the dummy's head above the nose at time t_0, to the most forward point on the dummy's head at the time of peak head excursion.

1.2.1.2 ISO 10542: Wheelchair Tiedown and Occupant Restraint Systems

The *ISO 10542 Part 1: Requirements and Test Methods for all Systems* has in large part been harmonized with SAE RP J2249. The ISO 10542 Part 1 also specifies design requirements, test methods, and performance requirements of WTORS in a frontal impact [8]. However, design and testing of the products intended for use by children and for pediatric wheelchairs are not included in the standard. It requires the same range of angles and locations for pelvic restraints and their anchor points as SAE J2249, but it designates the preferred location of the shoulder restraint only for adult occupants, not for children. In Part 2 of ISO 10542, *Four-Point, Strap-Type Tiedown Systems,* the recommended angles and locations of front and rear tiedown straps are included and are the same specifications as those indicated in SAE J2249. ISO 10542 Part 2 applies to WTORS that use belt-type occupant restrains and four-point strap-type wheelchair tiedowns. For a docking system, ISO 10542 Part 3, which is under development, applies. ISO 10542 also requires WTORS to be dynamically tested with a 20g/48kph (30mph)

frontal crash pulse. The horizontal excursion limits of the test dummy and the test wheelchair specified in the standard are for the 50th percentile male ATD only.

1.2.2 Transit Wheelchair Standards

Even though a wheelchair may be properly secured to a vehicle floor and a wheelchair occupant may be well restrained, if the wheelchair fails to support an occupant, there is a greater likelihood that the occupant will be injured. Design and performance requirements of wheelchairs used as seats in motor vehicles are addressed in the following standards.

1.2.2.1 ANSI/RESNA WC-19: Wheelchairs for Use in Motor Vehicles

SOWHAT (Subcommittee on Wheelchairs and Transportation), a subcommittee of the Rehabilitation Engineering and Assistive Technology Society of North America (RESNA) Technical Guidelines Committee, developed a transit wheelchair standard in order to enhance the safety performance of production wheelchairs. This standard, *ANSI/RESNA WC-19: Wheelchairs for Use in Motor Vehicles*, was approved by the American National Standards Institute (ANSI) in April 2000 [9].

The WC-19 standard contains design and performance requirements, as well as test procedures for wheelchairs used as forward-facing seats in motor vehicles. This standard applies to manual wheelchairs, powerbase wheelchairs, and scooters designed for adults and children with a body mass of 22 kg (48 lbs). It requires a wheelchair to be provided with two front and two rear securement points for attachment to a four-point, strap-type tiedown system. The standard also requires that the wheelchair, including wheelchair frame and seating systems, be sled-impact tested using a 20g/48kph (30mph) frontal crash pulse. The performance requirements of the frontal impact sled test are as follows:

a) The wheelchair securement points shall not show signs of material failure, other than deformation or yielding.

b) The wheelchair securement points shall not show deformation or distortion that prevents manual disengagement and removal of the hook end fittings of the surrogate tiedown system.

c) At the end of the test, the wheelchair shall be in an upright position on the test platform.

d) At the end of the test, the ATD shall be retained in the wheelchair seat in a seated posture, as determined by the ATD torso being oriented at not more than 45 degrees to the vertical when viewed from any direction.

Note: The angle of the ATD torso can be estimated by aligning the edge of an inclinometer with an imaginary line connecting the center of the ATD's head and the ATD's H-point.

e) Rigid components, parts, equipment, or accessories in excess of 100 grams shall not become detached from the wheelchair during the test.

f) Wheelchair components that may contact the occupant shall not fragment or separate in a manner that produces sharp edges with a radius of less than 2 mm.

g) Primary occupant load-carrying parts and components, including but not limited to the seat, backrest, wheels, casters, axles, frame members, occupant restraint belts and occupant restraint anchorages, shall not show visible signs of structural failure, other than deformation or yielding, unless:

i) the component is designed to fail in a controlled manner and this is indicated by the wheelchair manufacturer, or

ii) there is a backup mechanism or component specified by the manufacturer that does not show signs of failure.

h) Detachable seating inserts shall not break free from the wheelchair frame at any attachment point.

i) The peak horizontal excursions of the ATD and wheelchair shall not exceed the values in Table 3.

j) The wheelchair shall not impose forward loads on the ATD, which is considered to be achieved if the peak ATD knee excursion exceeds the peak wheelchair Point-P excursion by 10%:

$X_{knee}/X_{wc} > 1.1$

k) The posttest height of the average of left and right ATD H-points relative to the wheelchair ground plane shall not decrease by more than 20% from the pretest height.

l) Batteries of powered wheelchairs, or their surrogate replacement parts, shall

i) not move completely outside the wheelchair footprint,

ii) remain attached or tethered to the battery compartment, and

iii) not move into the wheelchair user's space (e.g., shall not contact the back of the ATD's legs) [9].

In the WC-19 standard, the horizontal excursion limits of the test dummy and the test wheelchair for the midsized male, small female and 6-year-old ATDs are specified as shown in Table 3. Moreover, the ATD's head excursion is limited in two directions, forward and rearward.

Table 3 ANSI/RESNA WC-19 Wheelchair and dummy horizontal excursion limits (mm) [9]

		ATD		
Measurement Point	Excursion Variable	6-Year-old	Small Female	Midsize and Large Male
Wheelchair Point P	X_{wc}	150	200	200
ATD Knee Center	X_{knee}	300	375	375
ATD Front of Head	X_{headF}	450	550	650
ATD Back of Head	X_{headR}	-300	-350	-400

Note: negative signs in last row indicate rearward excursion limits

where,

X_{headF} = the horizontal distance relative to the sled platform between the most forward point on the dummy's head above the nose at time t_0, to the most forward point on the dummy's head at the time of peak forward head excursion, and

X_{headR} = the horizontal distance relative to the sled platform between the most rearward point on the dummy's head at time t_0, to the most rearward point on the dummy's head at the time of peak rearward head excursion.

1.2.2.2 ISO 7176-Part 19: Wheeled Mobility Devices for Use in Motor Vehicles

The ISO 7176-Part 19 standard has in large part been harmonized with the ANSI/RESNA WC-19 standard, and also contains design and performance requirements, and test procedures for wheelchairs used as forward facing seats in motor vehicles [10]. The standard applies to all manual and powered wheelchairs, including scooters, designed for an adult occupant with a mass greater than 36 kg (79.4 lb). Children are not currently addressed in this standard. The ISO 7176-19 standard also requires that the wheelchairs be sled-impact tested using a 20g/48kph (30mph) frontal crash pulse. Because the standard applies to adult wheelchairs only, the horizontal excursion limits of the test dummy and the test wheelchair are specified only for the midsize male ATD.

The wheelchair securement and occupant restraint standards (1.2.1) and transit wheelchair standards (1.2.2) described above require a product, including a wheelchair and WTORS, to be sled tested using a 20g/48kph (30 mph) frontal impact crash pulse. This requirement is based on existing federal motor vehicle safety standards for private passenger vehicles (1.3.1 and 1.3.2) [2] [11]. In the automotive industry, the frontal crash test has been the primary priority in occupant protection in motor vehicle crashes because more than half of crashes resulting in serious injury or fatalities occurred in frontal crashes [12]. 48kph refers to velocity change, ΔV, of an impact vehicle during a crash and represents approximately "the 95th-percentile crash severity in terms of real-world frontal crashes for passenger cars" [13]. That means approximately "95% of real-world frontal crashes of passenger cars, minivans, and sport utility vehicles are less than [48kph] in severity" [13]. The 20g deceleration corridor specified in the wheelchair transportation standards is based on FMVSS 213 (1.3.1) [2] and was developed through an interlaboratory study involving various sled test facilities [14].

1.3 AUTOMOTIVE INDUSTRY STANDARDS

In order to study the level of protection of pediatric wheelchair users in vehicles, the Federal Motor Vehicle Safety Standards (FMVSS) that cover the safety of the pediatric population and wheelchair occupants were reviewed.

1.3.1 FMVSS 571.213: Child Restraint Systems

FMVSS 213 specifies requirements for child restraint systems, including devices designed for use in motor vehicles used to restrain or position children weighing 50 lbs (22.7 kg) or less [2]. The approximate weight of an average 6-year-old child is 50 lbs, therefore, the standard can be thought of as addressing restraint systems designed for use by children 6 years old or younger. This standard requires the restraint system to be frontal-impact tested at a velocity change of 48 kph (30 mph) with the acceleration pulse to fall within the curve shown in Figure 7. Depending upon the mass and height for which the restraint system is designed, a different sized dummy (including a new-born dummy, a 9-month-old dummy, a 3-year-old dummy, and a 6-year-old dummy (49 CFR Part 572 Subpart I)) could be used in the frontal impact barrier test. The dynamic performance requirements of restraint systems are specified in the standard as follows:

> Each child restraint system,
>
> (a) Exhibit no complete separation of any load bearing structural element and no partial separation exposing either surfaces with a radius of less than 1⁄4 inch or surfaces with protrusions greater than 3.8 inch above the immediate adjacent surrounding contactable surface of any structural element of the system.
>
> (b) If adjustable to different positions, remain in the same adjustment position during the testing that it was in immediately before the testing.

(c) If a front facing child restraint system, not allow the angle between the system's back support surfaces for the child and the system's seating surface to be less than 45 degrees at the completion of the test. [2]

Injury criteria, also specified under dynamic performance requirements, include a head injury criterion (HIC) of 1000 and a maximum resultant acceleration of the upper thorax sustained for three consecutive milliseconds < 60 g. The test dummy's head and knee excursion limits are specified relative to a reference point, 'Point Z', which is located at the seatback pivot point of the standard bench seat; these values are either 720mm or 813 mm for the head (depending on the restraint types) and 915 mm for the knee (see Figure 8). For built-in child restraint systems, the knee excursion limit is specified as 305 mm forward of the pre-test position of the knee pivot point.

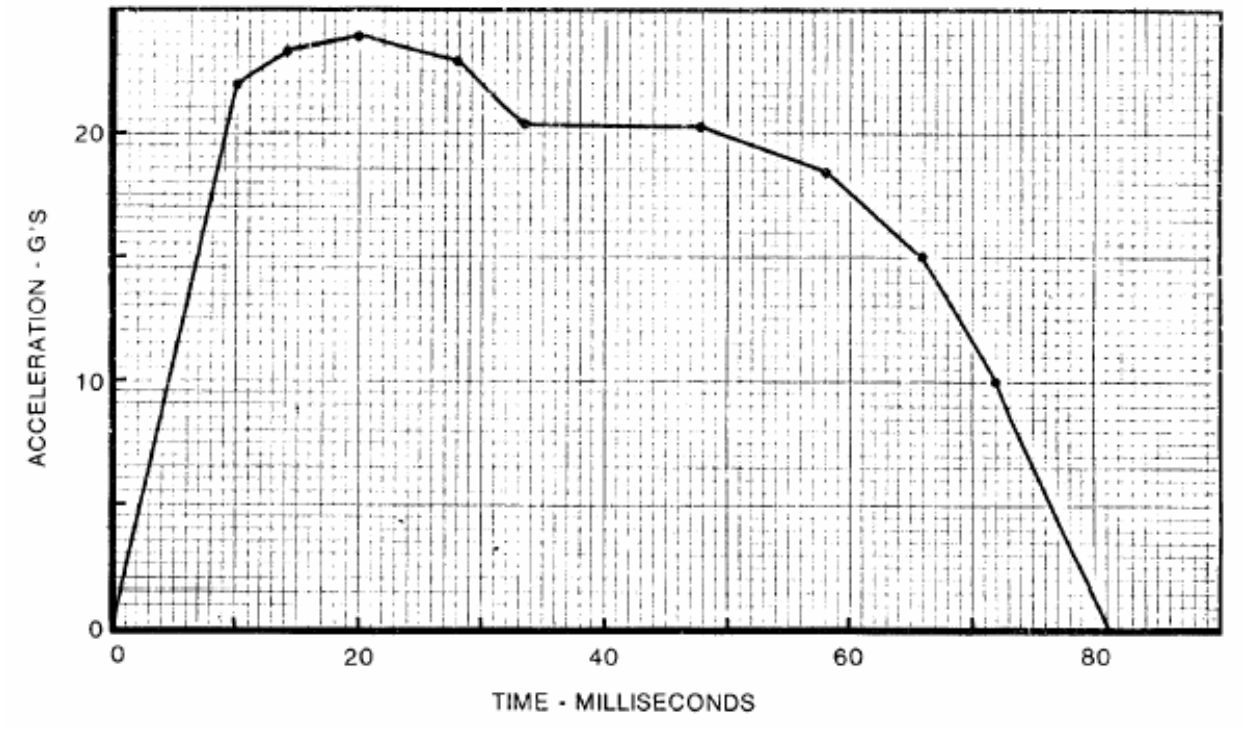

Figure 7 Acceleration function for ΔV = 30mph [2]

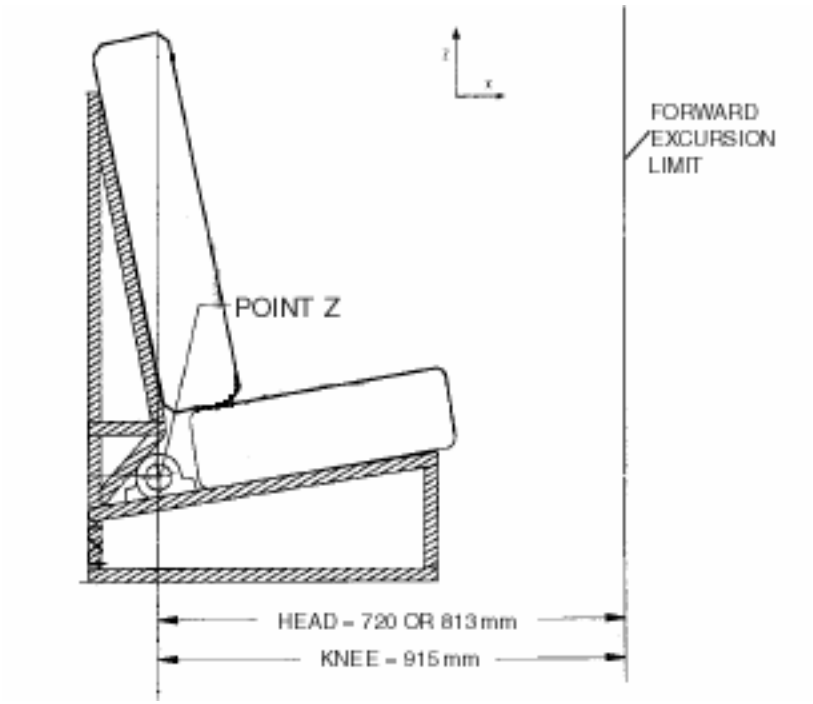

Figure 8 Location of Point Z and forward excursion limits (modified figure) [2]

1.3.2 FMVSS 571.208: Occupant Crash Protection

FMVSS 208 specifies vehicle performance requirements in terms of the acceleration and forces measured on anthropomorphic dummies in crash tests [11]. The purpose of the standard is to protect the vehicle occupants in crashes, so that the number of vehicle occupants who are injured or killed in crashes can be reduced. This standard, which applies to passenger cars, multipurpose passenger vehicles, trucks, and buses, requires a vehicle to meet frontal crash protection requirements. The standard specifies 48 kph (30 mph) frontal barrier crash test requirements and injury criteria for the 50th percentile Hybrid III male dummy.

FMVSS 208 also specifies requirements for air bag deployment. The rigid barrier test requirements, test procedures, and injury criteria for different sized dummies, including the 50th percentile adult male dummy, the 5th percentile adult female dummy, the 12-month-old CRABI dummy, the 3-year-old child dummy, and the 6-year-old child dummy, are specified in the

standard in order to minimize the risk of injury resulting from deployment of an air bag. Injury criteria for the Hybrid III 6-year-old child dummy (49 CFR Part 572 Subpart N) are as follows:

1. Head injury criteria.

(a) For any two points in time, t_1 and t_2, during the event which are separated by not more than a 15 millisecond time interval and where t_1 is less than t_2, the head injury criterion (HIC_{15}) shall be determined using the resultant head acceleration at the center of gravity of the dummy head, a_r, expressed as a multiple of g (the acceleration of gravity) and shall be calculated using the expression:

$$HIC_{15} = \left[\frac{1}{(t_2 - t_1)} \int_{t_1}^{t_2} a_r dt \right]^{2.5} (t_2 - t_1)$$

(b) The maximum calculated HIC_{15} value shall not exceed 700.

2. The resultant acceleration calculated from the output of the thoracic instrumentation shall not exceed 60 g's, except for intervals whose cumulative duration is not more than 3 milliseconds.

3. Compression deflection of the sternum relative to the spine, as determined by instrumentation, shall not exceed 40 mm (1.6 in).

4. Neck injury.

When measuring neck injury, each of the following injury criteria shall be met.

(a) Nij.

(1) The shear force (Fx), axial force (Fz), and bending moment (My) shall be measured by the dummy upper neck load cell for the duration of the crash event.

(2) During the event, the axial force (Fz) can be either in tension or compression while the occipital condyle bending moment (Mocy) can be in either flexion or extension. This results in four possible loading conditions for Nij: tension-extension (Nte), tension-flexion (Ntf), compression-extension (Nce), or compression-flexion (Ncf).

(3) When calculating Nij using equation 4.(a).(4), the critical values, Fzc and Myc, are:

(i) Fzc = 2800 N (629 lbf) when Fz is in tension

(ii) Fzc = 2800 N (629 lbf) when Fz is in compression

(iii) Myc = 93 Nm (69 lbf-ft) when a flexion moment exists at the occipital condyle

(iv) Myc = 37 Nm (27 lbf-ft) when an extension moment exists at the occipital condyle.

(4) At each point in time, only one of the four loading conditions occurs and the Nij value corresponding to that loading condition is computed and the three remaining loading modes shall be considered a value of zero. The expression for calculating each Nij loading condition is given by:

Nij = (Fz / Fzc) + (Mocy / Myc)

(5) None of the four Nij values shall exceed 1.0 at any time during the event.

(b) Peak tension.

Tension force (Fz), measured at the upper neck load cell, shall not exceed 1490 N (335 lbf) at any time.

(c) Peak compression.

Compression force (Fz), measured at the upper neck load cell, shall not exceed 1820 N (409 lbf) at any time. [11]

1.3.3 FMVSS 571.222: School bus passenger seating and crash protection

The purpose of FMVSS 222, which applies to school buses, is to reduce the number of deaths and the severity of injuries to school bus occupants in crashes and maneuvers [15]. The standard specifies design and performance requirements of seating (eg. seat height and seat back force/deflection), restraining barriers, and occupant impact zones in school buses. FMVSS 222 includes the requirements for wheelchair users in school buses, including both wheelchair securement devices and their anchorages and wheelchair occupant restraints and their anchorages. A school bus should be equipped so that a wheelchair can be secured in a forward-facing position with at least two front and two rear securement devices. Moreover, a wheelchair occupant restraint system, including both pelvic and upper torso restraints, should be provided at each wheelchair location. This standard also specifies the force that each anchorage system should withstand upon impact: 13344 N at wheelchair securement anchorage, 13344 N at wheelchair occupant restraint floor anchorage, and 6672 N at wheelchair occupant restraint

upper torso anchorage. FMVSS 222 requires that wheelchair securement device and wheelchair occupant restraint systems meet the requirements of FMVSS 209, *Seat Belt Assemblies*: the Type 1 belt system applies to wheelchair securement devices and the Type 2 belt system applies to wheelchair occupant restraints. Although FMVSS 222 states that the movement of the wheelchair should be limited, the excursion limits of the occupant and the wheelchair are not specified.

It should be noted that injury criteria for a 6-year-old ATD specified in FMVSS (1.3.1 and 1.3.2) and used in this dissertation are based on an average 6-year-old child without disabilities who has normal muscle tone and balance. Currently, injury criteria for people with disabilities are not available in any of the FMVSS standards, transit wheelchair standards, or the injury literature. Because children with disabilities often have less trunk or head stability than that of an average 6-year-old child without disabilities, children with disabilities seated in wheelchairs may be more susceptible to severe and fatal injuries in circumstances that would not be injurious to children without disabilities. Therefore, even if the study results presented in this dissertation meet the injury criteria limits for a 6-year-old ATD specified in FMVSS, children with disabilities may still be at increased risk of injuries as compared to children without disabilities.

1.4 ANTHROPOMORPHIC TEST DUMMY

The 6-year-old test dummy required to be used in FMVSS 213 *Child Restraint Systems* is Hybrid II ATD (49 CFR Part 572 Subpart I). Segmented weights and dimensions of the Hybrid II 6-year-old child dummy (Hybrid II 6) are listed in Appendix A. The Hybrid II 6 can be equipped to measure head acceleration, chest acceleration, pelvis acceleration, and femur forces. FMVSS 208 requires to use Hybrid III 6-year-old child dummy (Hybrid III 6) (49 CFR Part 572

Subpart N) in air bag deployment tests. Segmented weights and dimensions of the Hybrid III 6 are also listed in Appendix A. Hybrid III 6 has more advanced instrumentation capabilities than Hybrid II. In addition to the instrumentation available with Hybrid II 6, the Hybrid III 6 is also capable of measuring chest deflection and neck forces and moments. Replacement of Hybrid II 6 with Hybrid III 6 in FMVSS 213 has been proposed [3] in order to improve the evaluation of child restraint system performance by adopting injury criteria that the Hybrid II 6 cannot measure, such as chest deflection and neck injury.

The 6-year-old test dummies available for compliance testing in FMVSS represent an average 6-year-old child who does not have disabilities. Children with disabilities often have physical deformities and differ anatomically from children who do not have disabilities. Moreover, a child with a disability often has less trunk or head stability than that of an average 6-year-old child without disabilities. Therefore, a Hybrid II 6 or Hybrid III 6 does not adequately represent the population being studied in this dissertation, 6-year-old children with disabilities. Currently available test dummies represent the non-disabled population, and there are no test dummies available that represent people with disabilities. Because a dummy representing a child with a disability was not available at the time of this study, a Hybrid III 6, which provides improved biofidelity and instrumentation capability over Hybrid II 6, was used in this dissertation study.

1.5 COMPUTER SIMULATION STUDIES ON WHEELCHAIRS AND WHEELCHAIR OCCUPANTS

Computer simulation has been implemented by researchers in the automotive industry since the 1960's and has aided in the development of crashworthy automobiles and occupant protection systems [16] [17] [18]. Computer simulation models have been also developed for

use in crash behavior studies involving wheelchairs and wheelchair occupants, and the risk of injury in wheelchair occupants in crashes.

1.5.1 Power Wheelchair Computer Models

A commercial powerbase wheelchair seated with a 50th percentile male ATD subjected to a 20g/48kph (30mph) were developed and validated using two sets of sled test data in a study done by Bertocci et al. [19]. The wheelchair was secured using a four-point strap tiedown system, and the ATD was restrained using a three-point belt system consisting of a lap and shoulder restraint. In the study, gross motions of the occupant and wheelchair were captured during the computer simulation and compared to sled impact testing. Moreover, time histories profiles of simulation-generated occupant restraint and tiedown loads, and accelerations of wheelchair, ATD head and chest along with wheel and ATD head excursions were compared to sled impact testing results for model validation. The comparisons of sled test and computer simulation-generated variables showed reasonable correlation between the two methods [19]. Based on the results of the study, the authors concluded that "the model provides an adequate representation of the subject powerbase and occupant exposed to a 20g/30 mph frontal motor vehicle crash" [19].

Computer simulations were also used to aid in the development of crashworthy wheelchair and seating design criteria. In the study done by Bertocci et al., the effects of a 20g, 48 kph frontal crash on the wheelchair were evaluated using the ISO/SAE surrogate wheelchair model [20]. The computer model consists of a SAE/ISO surrogate wheelchair, which represents an 85 kg typical power wheelchair, 50th percentile male ATD, four-point strap tiedown system, and three-point occupant restraint system. Wheelchair acceleration, vertical excursion of the front wheels, and loads on wheelchair securement point, seat, lap belt anchor, and wheels were evaluated under three different securement configurations: the rear securement points 19 cm

above the wheelchair's vertical CG, the rear securement level with the CG, and the rear securement 19 cm below the CG. Figure 9 shows the crash response of a wheelchair and occupant at 90 ms into the crash event at three different securement configurations. The results of the study showed that "positioning of rear securement points near the wheelchair center of gravity can serve as an effective strategy for managing crash response and loadings on the wheelchair" [20].

In the study, *Development of frontal impact crashworthy wheelchair seating design criteria using computer simulation*, seat and seat-back loading in a frontal crash were explored using a previously validated computer simulation model [21]. The model consisted of a powerbase wheelchair and a seated 50th percentile male ATD exposed to a 20g/30mph frontal impact. To evaluate the influence of seat and seat-back surface stiffness and seat-back angle on wheelchair seat and seat back loading, parametric analyses were conducted. Seat and seat back surface stiffness were varied from 25% to 200% of the baseline, which were 500 lb/in for the seat and 1650 lb/in for the seat-back. Seat-back angle was varied from 0° to 30°. The results of the study showed that seating surface stiffness and seat-back angle were found to influence seating loads under frontal crash conditions. Seat loading varied with stiffness, ranging from 819 lb to 3273 lb, while seat-back loading was found to be between 1427 lb to 2691 lb, depending upon seat-back stiffness and recline angle.

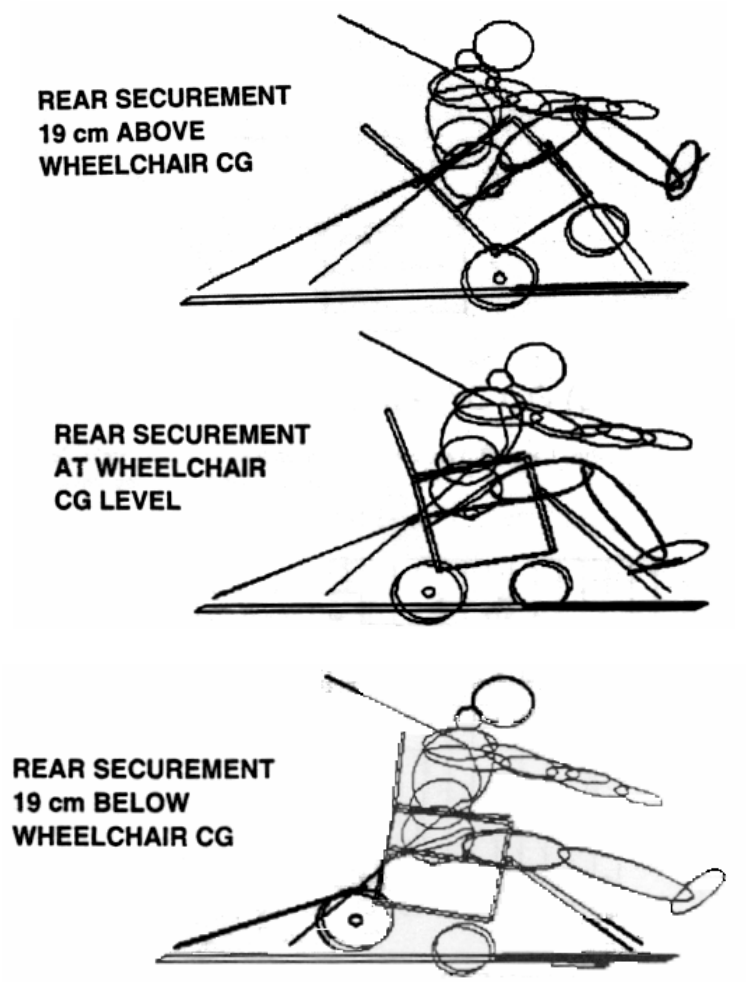

Figure 9 Wheelchair-occupant crash response at time = 90ms for varying securement point configurations [20]

1.5.2 Manual Wheelchair Computer Models

A 21 kg (46 lb) manual wheelchair seated with a 50th percentile male ATD subjected to a 20g/48kph (30mph) were developed and validated in a study done by Leary and Bertocci [22]. The manual wheelchair was also secured using a four-point strap tiedown system, and the ATD was restrained using a three-point belt system. Gross occupant and wheelchair kinematics of the sled test and computer simulation at different time frames were compared. Moreover, occupant restraint and tiedown loads and accelerations of wheelchair, ATD chest and pelvis were compared between sled test data and computer generated data. The results of the study showed

that the peaks and profiles of two data (sled test and computer simulation) matched quite well. The authors stated, “overall ATD and wheelchair kinematics, belt tensions, and accelerations confirm that the computer model is a reasonably valid representation of the sled test” [22].

In the same study, the authors investigated the loads imposed upon manual wheelchairs during frontal impact using the validated model. The influences of seat stiffness and rear securement point location on wheel loads, rear securement point loads, and seat loads were assessed. The rear securement point positions varied from 2.5” (6.4 cm) below the rear hub to 5.5” (14 cm) above the rear hub. The results showed that vertical rear securement point position had relatively little effect on tiedown force but greatly influenced wheel loading and wheelchair stability. Seat stiffness also had great influence on seat loading: ones with lower stiffness led to the lower seat loads [22].

Computer simulations have been used to aid in the development of transit wheelchair, wheelchair seating system, and WTORS standards [23] [14] [24]. The Standards Committee on Wheelchairs and Transportation (SOWHAT) of ANSI/RESNA is currently developing a standard which will evaluate the design and performance of wheelchair seating systems (WCSSs) independent of a specific wheelchair frame. The standard requires frontal impact sled testing of a WCSS using a surrogate wheelchair base (SWCB). The SWCB is a repeatable and reusable wheelchair frame to which WCSSs can be attached. WCSSs are used with both a manual and a power wheelchair bases, and therefore, a SWCB should represent characteristics of both type of wheelchair bases. While developing a SWCB for the WCSS standard, issues related to the characteristics of manual wheelchairs and their impact on failure mechanisms of WCSSs during crashes should be considered in addition to the characteristics of powered wheelchairs. A

SWCB should produce worst-case seating system loading conditions and failure modes for a range of commercial manual wheelchair bases and securement point locations.

In order to assist development of SWCB that can be a good representation of commercial manual wheelchair bases, influence of various wheelchair design parameters (seat back angle, rear securement point vertical location with respect to wheelchair CG, and seat-to-back intersection location with respect to rear hub) on wheelchair seat and seat back loading in a manual wheelchair was investigated using computer simulation [24]. A parametric sensitivity analysis was conducted using a previously validated computer model representing an adult manual wheelchair seated with a 50th percentile male Hybrid III ATD [22]. The results of the study showed that seat back loading was influenced by all three parameters: the seat back load increased as the seat back angle was decreased, the height of the rear securement point location was increased, and the seat-to-back intersection location was moved horizontally toward the back of the wheelchair. The effect of these three design parameters on seat pan loading was not substantial, except for the seat-to-back intersection location, which had a slight influence on the seat pan load.

1.5.3 WC User Injury Risk Studies

Computer simulations have also been used in the studies on injury risk assessment of wheelchair users in motor vehicle crashes. Paskoff assessed neck injury risk of wheelchair users in rear collisions using Dynaman computer simulation [25]. The model consisted of a 25 kg (55 lb) powered wheelchair and a seated 50th percentile male ATD modeled with Rear Impact Dummy (RID) neck, which was designed to simulate the head-neck response of a human exposed to a low speed collision [25]. The wheelchair was secured using a four-point strap

tiedown system, and the ATD was restrained using a lap and a shoulder belts. The model was not validated with actual rear impact sled test data.

The study examined the effects of seat back height, seat back stiffness, and the effectiveness of a head restraint at two different speeds, 8 kph (5 mph) and 16.1 kph (10 mph), on head/chest angle, head torque, and neck axial loads. The results of the study showed that "a head restraint of any kind is extremely beneficial in reducing the moment experienced by the head about the occipital condyles" [25]. The maximum moments resulted in all simulations without a headrest were above the ligamentous damage threshold, 57 N-m. The effect of back height on the occupant kinematics was not substantial at low speeds. However, back stiffness showed a large effect on the neck forces and moments. In the low speed simulations (8 kph), head/chest angle and head torque were reduced as back stiffness was increased. But, in the high speed simulations (16.1 kph), "the soft back had the greatest effect in reducing maximum moment about the occipital condyles" [25].

Injury risk of a manual wheelchair user in a frontal impact motor vehicle crash was analyzed using data collected from six frontal impact sled tests [26]. In the study, two types of seating systems, 'sling-type' and 'rigid-type', were tested on a 20 kg manual wheelchair frame. An instrumented 50^{th} percentile male Hybrid III ATD was seated in the wheelchair and restrained using a tree-point belt system. The wheelchair was secured to the sled platform using a four strap-type tiedowns. The wheelchair and occupant were subjected to 48 kph (30mph) velocity change and average 20 g sled deceleration.

Collected sled test data was compared to ANSI/RESNA WC-19 wheelchair and dummy horizontal excursion limits (see Table 3) and various injury criteria [11] [27]. The results showed that the excursions of all tests were within the allowable limits. But "the neck forces

occurring in frontal impact may pose the greatest risk of injury": four of the six tests exceed the neck injury criteria [26]. Based on the results of the study, the wheelchairs users using rigid seats may be in higher risk of neck injury than the ones using sling seats.

As described in the above studies, computer models of a powerbase wheelchair and a manual wheelchair seated with a 50th percentile male ATD subjected to a 20g/48kph (30mph) were developed, validated, and used in transit wheelchair and occupant studies. Those models represent an adult wheelchair seated with an adult occupant (50th percentile male). Pediatric wheelchair occupants respond differently in crashes, and the 50th percentile male ATD is not appropriate for representing younger populations. In addition, pediatric transit wheelchairs are subjected to different loading conditions in a crash than are adult transit wheelchairs. Therefore, existing computer models are not suitable for studying pediatric wheelchairs in transit or associated occupant injury risks.

1.6 COMPUTER SIMULATION SOFTWARE

1.6.1 Dynaman

Dynaman (GESAC, Inc., MD) is a commercial version of the Articulated Total Body/Crash Victim Simulator (ATB/CVS), which was originally developed by the Department of Defense and the Department of Transportation in the United States to study motor vehicle occupants in a crash and aircrew members during aircraft ejection [28]. A body in ATB is represented by a lumped mass element and is visually represented by an ellipsoid. An ellipsoid is assigned a mass and moment of inertia and may be connected using different types of joints. A crash dummy and various wheelchair components can be created using ellipsoids. This program uses planes to create the surrounding environment, such as the vehicle floor or wall, which can be defined as contact surfaces. The program is also capable of representing air bags

and safety belts. The dummy data set used in the program is based on the 50th percentile male Hybrid III dummy. Mass, inertia, and joint properties of the 50th percentile male Hybrid III dummy were measured by Armstrong Aerospace Medical Research Laboratory, and the data set for the program was developed based on those measurements [29] [28]. The 50th percentile male ATB Hybrid III dummy contains 18 ellipsoid segments and 17 joints. The data set for smaller and larger dummies, such as a 6-year-old dummy, can be generated using the *Generator of Body Data* (GEBOD) program provided with Dynaman. GEBOD generates a scaled dummy data set based on input specifications such as height, weight, or population percentile [28].

The Dynaman software program includes a preprocessor, a simulation module, and a post processor. The preprocessor enables the user to build and view the input file, which includes properties of the occupant, the environment around the occupant, and the motion assigned to the environment. The simulation module reads the input file and generates pictures and plot files with kinematic variables. From the post processor, the user can view time-incremented images of the simulation, and tables and plots of kinetic and kinematic data. Dynaman has a DOS-based interface, therefore, selections can be made only through a keyboard, and all input values need to be typed in. In the program, created segments and planes are drawn with lines, therefore, representations of segments surfaces and planes are limited (see Figure 10-a). In the postprocessor, individual images at each time step can be captured and saved in files.

1.6.2 ATB3^{I}

ATB3^{I} (Veridian Co., VA) is a commercial version of the Articulated Total Body (ATB) simulation program. ATB3^{I} is basically identical to Dynaman, with the exception of ATB3^{I}'s improved user interface and graphics. ATB3^{I} has a Windows-based interface, so that both the keyboard and the mouse are used to make selections. In the preprocessor, data can either be typed or copied and pasted into spreadsheet-like tables. This program has 3-D solid object

graphics (see Figure 10-b). In the postprocessor, both an individual image and an animation of a crash simulation can be captured and saved in files. ATB3^{I} does not have plotting capability, therefore, time-history kinetic and kinematic data generated as tabular output files need to be exported to a plotting program, such as Excel (Microsoft), in order to generate plots. An input file created in Dynaman can be converted to an ATB3^{I} format input file in several steps. These conversion steps are listed in Appendix B.

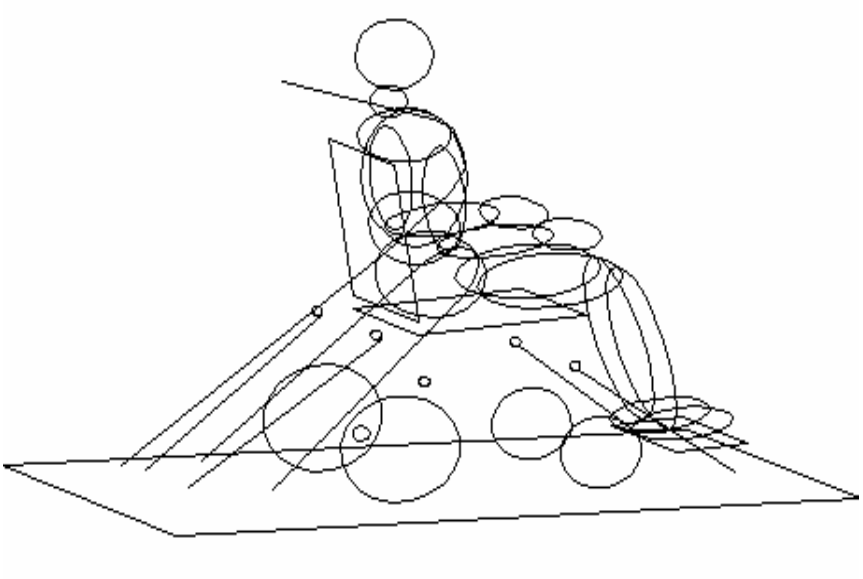

(a)

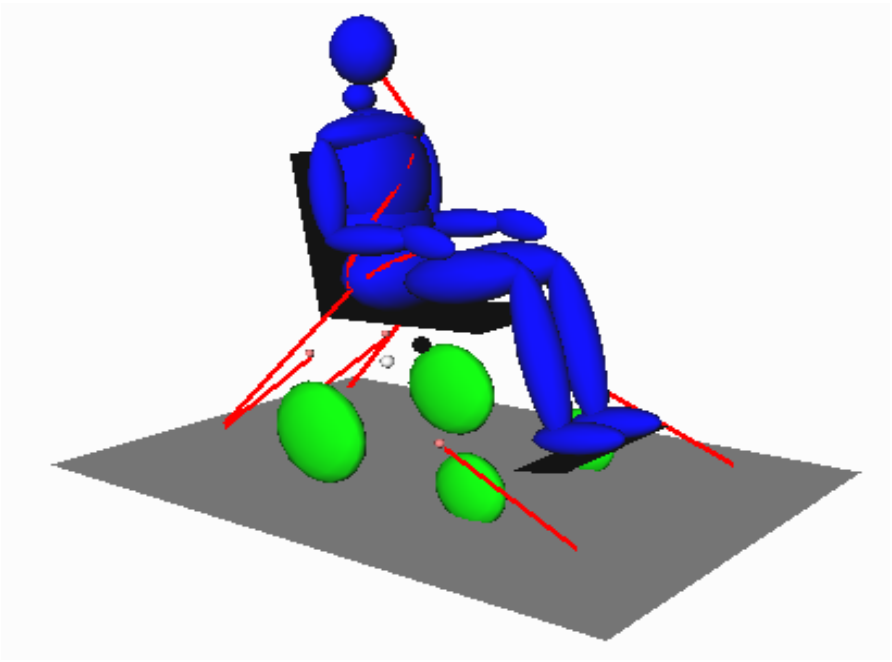

(b)

Figure 10 Graphics of computer crash simulation - (a) Dynaman and (b) ATB3[I]

1.6.3 MADYMO

MADYMO (MAthmatical DYnamic MOdel) (TNO Automotive, Netherlands) is a crash simulation software package originally designed for studying motor vehicle occupants in crashes [30]. MADYMO has the capability of analyzing both multi-body systems (similar to ATB) and finite element models in one program. For example, a model can consist of multi-body systems of a dummy and a vehicle seat with finite element structures of an airbag, a seat belt, and a dashboard. Similar to the ATB simulation program, a body in MADYMO is represented by a lumped mass element, which has a mass, moment of inertia, and center of gravity (CG), and can be connected to other bodies using different types of joints. Different from the ATB program, a body in MADYMO can be visually represented by three different types of surfaces, including ellipsoids, planes, and cylinders. Contacts can be defined between surfaces or surfaces and finite element structures.

MADYMO has a variety of dummy models representing crash dummies available in the industry. MADYMO dummy models are divided into four modules, frontal impact dummies, side impact dummies, child dummies, and pedestrian subsystems. Frontal impact adult dummies include the Hybrid III 5^{th} percentile female, 50^{th} percentile male, 95^{th} percentile male, 50^{th} percentile male standing, and a 50^{th} percentile male with a TNO Rear Impact Dummy (TRID) neck. Child dummies include the Hybrid III 3-year-old and 6-year-old, CRABI 12-month-old, and six other child dummies used in Europe. MADYMO dummy models are calibrated and validated through component tests such as neck extension and flexion, and complete dummy sled tests [31]. Details on dummy model descriptions and validation tests are available in the Database Manual [31]. MADYMO has three types of dummy models – the ellipsoid, the facet, and the finite element dummies. The ellipsoid model is similar to the ATB dummy model, which is created with lumped mass ellipsoid segments connected by joints. The Hybrid III 6-

year-old ellipsoid model available in MADYMO contains 28 bodies with 51 ellipsoid surfaces and 28 joints. The facet model is a more advanced ellipsoid model in which a structural deformation of dummy components, such as ribs and skins, are represented by deformable bodies [31]. In the FE model, several deformable parts of the dummy are modeled with finite elements. The facet models and the FE models are available only in a few dummy sizes which do not include the Hybrid III 6-year-old dummy.

An input file for MADYMO is created using Extensible Markup Language (XML) codes. Although any computer text editors can be used to create an XML file, a user can more easily create an input file using an advanced XML editor, such as Epic (Arbortext, Inc., MI) , Morphon (Morphon Technologies, Netherlands), and XML Spy (Altova, Austria). The XML editor has a Windows-based interface which allows a user to either type in or copy and paste data into spreadsheet-like tables. MADYMO reads in an XML input file, solves the simulation, and generates output files that have been specified in the input file. The program has the capability to calculate standard injury parameters such as Head Injury Criteria (HIC), neck injury criteria (N_{ij}), thoracic acceleration and deflection, femur loading, and tibia loading, and generate an associated file with time-history data. To view the animation outputs and plots of kinetic and kinematic data, a separate graphical post processor such as the CEM (EASi Co., MI) or the Hyperview (Altair, MI) should be used. These post processor programs have the capability of reading the output files generated by different simulation software, including MADYMO, and have advanced features that help the user to view, manipulate, and save the simulation animation and result plots. By using these post processors, animation and plots can be synchronized and displayed simultaneously (see Figure 11).

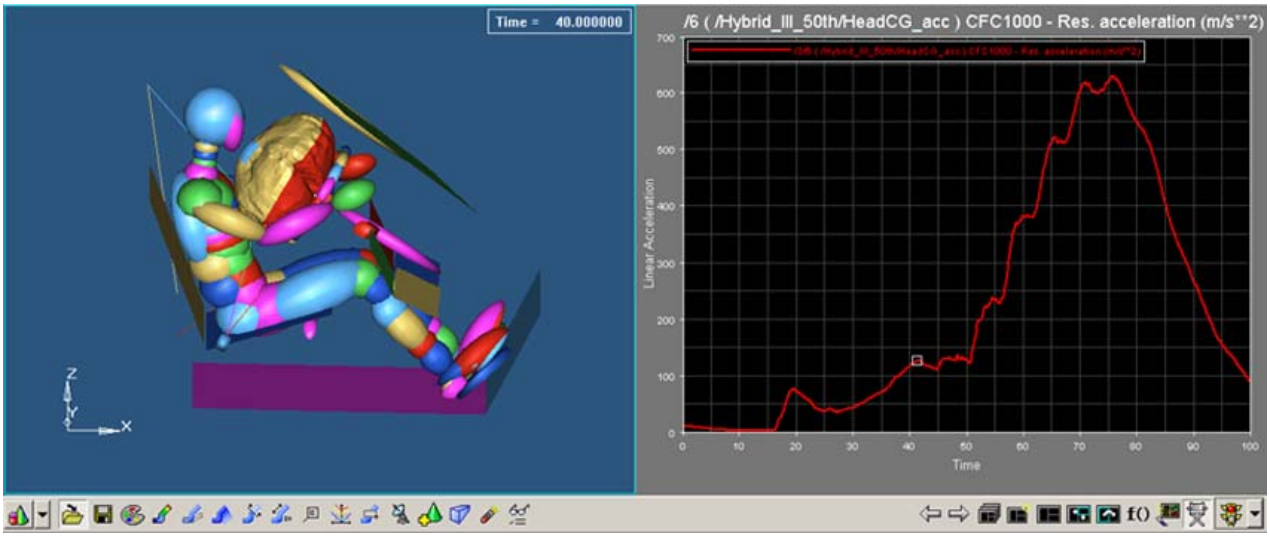

Figure 11 MADYMO output displayed in Hyperview - animation and plot

1.7 SPECIFIC AIMS

Children with disabilities who are seated in their wheelchairs while traveling in vehicles should be able to expect the same levels of safety and protection as those children who are not disabled. The following specific aims have been defined for the study:

1. Develop a pediatric manual wheelchair and a 6-year-old occupant computer crash simulation model, and validate the model using sled test data.
2. Assess injury risks for manual pediatric wheelchair occupants in a frontal impact motor vehicle crash.
3. Evaluate the effect of different wheelchair design parameters on dynamic response of a wheelchair occupant and occupant injury risk during a frontal motor vehicle crash.
4. Define pediatric transit manual wheelchair design criteria.
5. Assess frontal crash injury risks associated with children in wheelchairs riding in school buses

1.8 REFERENCES

1. Centers for Disease Control and Prevention. Leading causes of death reports. *Available at: http://webapp.cdc.gov/sasweb/ncipc/leadcaus.html*, February 2003
2. National Highway Traffic Safety Administration (NHTSA). (1979). *FMVSS 213 Child Restraint Systems* (October, 2000 ed. Vol. 49 CFR 571.213).
3. National Highway Traffic Safety Administration (NHTSA). (2002). *Notice of proposed rulemaking (NPRM) on Federal Motor Vehicle Safety Standards; Child Restraint Systems* (Docket No. NHTSA-02-11707): NHTSA.
4. Everly, J. S., Bull, M. J., Stroup, K. B., Goldsmith, J. J., Doll, J. P., & Russell, R. (1993). A Survey of Transportation Services for Children with Disabilities. *The American Journal of Occupational Therapy, 47*(9), 804-810.
5. U.S. Department of Justice Civil-Rights Division. (May 2000). *A Guide to Disability Rights Laws*. Washington, DC.
6. Hinch, J., McCray, L., Prasad, A., Sullivan, L., Willke, D., Hott, C., et al. (2002). *School Bus Safety: Crashworthiness Research*: National Highway Traffic Safety Administration.
7. Society of Automotive Engineers (SAE). (1997). *SAE J2249: Wheelchair Tiedowns and Occupant Restraint Systems for Use in Motor Vehicles* (No. SAE J2249): SAE.
8. International Standards Organization (ISO). (2001). *ISO 10542: Wheelchair Tiedown and Occupant Restraint Systems* (No. ISO 10542): ISO.
9. ANSI/RESNA Subcommittee on Wheelchairs and Transportation (SOWHAT). (2000). *ANSI/RESNA WC/Vol 1: Section 19 Wheelchairs - Wheelchairs Used as Seats in Motor Vehicles*: ANSI/RESNA.

10. International Standards Organization (ISO). (2000). *ISO 7176-19: Wheelchairs Used as Seats in Motor Vehicles* (No. ISO 7176-19): ISO.

11. National Highway Traffic Safety Administration (NHTSA). (1971). *FMVSS 208 Occupant Crash Protection* (October, 2000 ed. Vol. 49 CFR 571.208).

12. http://www-fars.nhtsa.dot.gov/.

13. http://www.rercwts.pitt.edu/RERC_WTS_FAQ/RERC_WTS_FAQ.html.

14. Shaw, G., Lapidot, A., & Scavnicky, M. (1994). Interlaboratory Study of Proposed Compliance Test Protocol for Wheelchair Tiedown and Occupant Restraint Systems. *SAE, SAE Paper No. 942229*, 355-370.

15. National Highway Traffic Safety Administration (NHTSA). (1976). *FMVSS 222 School Bus Passenger Seating and Crash Protection* (October, 2000 ed. Vol. 49 CFR 571.222).

16. McHenry, R. R., & Naab, K. N. (1966). Computer simulation of the crash victim - a validation study. *SAE, SAE Paper No. 660792*, 73-94.

17. Bartz, J. A. (1972). Development and validation of a computer simulation of a crash victim in three dimensions. *SAE, SAE Paper No. 720961*, 105-127.

18. Hou, J., Tomas, J., & Sparke, L. (1995). Optimization of driver-side airbag and restraint system by occupant dynamics simulation. *SAE, SAE Paper No. 952703*, 461-471.

19. Bertocci, G. E., Szobota, S., Hobson, D. A., & Digges, K. (1999). Computer Simulation and Sled Test Validation of a Powerbase Wheelchair and Occupant Subjected to Frontal Crash Conditions. *IEEE Transactions on Rehabilitation Engineering, 7*(2), 234-244.

20. Bertocci, G. E., Digges, K., & Hobson, D. (1996). Development of transportable wheelchair design criteria using computer crash simulation. *IEEE Transactions of Rehabilitation Engineering, 4*(3), 171-181.

21. Bertocci, G. E., Szobota, S., Ha, D., & vanRoosemalen, L. (2000). Development of Frontal Impact Crashworthy Wheelchair Seating Design Criteria Using Computer Simulation. *Journal of Rehab Research and Development, 37*(No. 5), 565-572.

22. Leary, A., & Bertocci, G. (2001). *Design Criteria for Manual Wheelchairs Used as Motor Vehicle Seats Using Computer Simulation.* Paper presented at the RESNA, Reno, Nevada.

23. Pilkey, W., Kang, W., & Shaw, G. (1994). *Crash Response of Wheelchair-occupant systems in transport.* Paper presented at the RESNA, Nashville, TN.

24. Ha, D., & Bertocci, G. E. (2003). *An Investigation of Manual Wheelchair Seat Pan and Seat Back Loading Associated with Various Wheelchair Design Parameters Using Computer Crash Simulation.* Paper presented at the RESNA, Atlanta, GA.

25. Paskoff, G. (1995). *Transportation of Wheelchair Users - An Assessment of Neck Injury Risk During Rear Collisions.* Unpublished Masters thesis, University of Virginia, Virginia.

26. Leary, A., & Bertocci, G. (2001). *Injury Risk Analysis of a Wheelchair User in a Frontal Impact Motor Vehicle Crash.* Paper presented at the RESNA, Reno, Nevada.

27. Nahlum, A., & Melvin, J. (1993). *Accidental injury-biomechanics and prevention*. NY: Springer-Verlag.

28. Digges, K. H. *Application of the ATB Model to Wheelchair Restraints*. Pittsburgh: University of Pittsburgh.

29. Kaleps, I., White, R., Beecher, R., & Obergafell, L. (1988). *Measurement of Hybrid III Dummy Properties and Analytical Simulation Database Development* (No. AAMRL-TR-88-005). Dayton, OH: Armstrong Aerospace Medical Research Laboratory.

30. TNO Automotive. (2001). *MADYMO V6.0 Theory Manual*. The Netherlands.

31. TNO Automotive. (2001). *MADYMO V6.0 Database Manual*. The Netherlands.

2 DEVELOPMENT AND VALIDATION OF A FRONTAL IMPACT 6 YEAR-OLD WHEELCHAIR-SEATED OCCUPANT COMPUTER MODEL

2.1 ABSTRACT

A computer model representing a Zippie pediatric wheelchair seated with a Hybrid III 6-year-old ATD subjected to a 20g/48kph frontal crash was developed in MADYMO. The wheelchair was secured using a four-point tiedown system, and the occupant was restrained using a three-point belt system. The occupant restraint system was developed through three steps: standard shoulder and lap belts in Step 1, standard shoulder belt with a FE belt segment and FE lap belt in Step 2, and FE shoulder and lap belts in Step 3. The time history profiles of the computer model were tuned to those of the sled test. Then, the peak value for each of the variables used in the time history comparison was compared between the sled test and the model. The peak horizontal excursions were also compared between the sled test and the model. To evaluate the shape (trend) of time histories of the model, Pearson's correlation coefficient (*r*) between the sled test and the model was computed for all variables used in time history comparison. The correlation coefficient ranged from 0.86 to 0.95 with an average *r* of 0.91. *r* above 0.8 indicates 'high' relationship between two compared groups. Therefore, r of 0.91 indicates that there are "high" correlations between the model and the sled test across all $VAR_{time\_history}$. The pediatric wheelchair model developed and validated in this study will provide a foundation for studying the response of a manual pediatric wheelchair in crashes and associated injury risks for pediatric wheelchair users.

Keywords: computer simulation, pediatric wheelchair, 6-year-old Hybrid III ATD, wheelchair testing

2.2 BACKGROUND

Federal laws, such as the Americans with Disabilities Act (ADA) and the Individuals with Disabilities Education Act (IDEA), prohibit discrimination against children with disabilities [1] [2]. IDEA requires education be provided to children with disabilities "in the least restrictive environment" [2], which means along with non-disabled children in the same main-stream schools. When children are transported to schools and developmental facilities, they often remain seated in their wheelchairs in vehicles, such as school buses and family vans. However, most wheelchairs are typically designed to provide mobility to individuals, and not necessarily to be used as vehicle seats. Therefore, in order to improve the safety of children seated in wheelchairs in vehicles, studies are needed to investigate the response of a pediatric wheelchair and occupant in crashes, and to investigate the associated injury risks.

Computer simulation has been implemented by researchers in the automotive industry since the 1960's and it has aided in the development of crashworthy automobiles and occupant protection systems [3] [4] [5]. Computer simulation models have also been developed and used in the field of wheelchair transportation safety to study crash behavior involving adult wheelchairs and wheelchair occupants, and their risk of injury in crashes [6] [7] [8] [9].

In a study done by Bertocci et al., a 116 kg commercial powerbase wheelchair seated with a 50th percentile male anthropomorphic test device (ATD) subjected to a 20g/48kph were developed and validated using two sets of sled test data [6]. The wheelchair was secured using a four-point strap tiedown system, and the ATD was restrained using a three-point belt system consisting of a lap and shoulder restraint. In the study, time history profiles of simulation-generated occupant restraint and tiedown loads and accelerations of wheelchair, ATD head and chest, along with wheel and ATD head excursions, were compared to sled impact testing results for model validation. Based on the results of the study, the authors concluded that "the model

provides an adequate representation of the powerbase and occupant exposed to a 20g/30 mph (48kph) frontal motor vehicle crash" [6]. This validated power wheelchair model has been used to aid in the development of frontal impact crashworthy wheelchair and seating design criteria [7] [8].

An adult manual wheelchair model was also developed and validated in a study done by Leary and Bertocci [9]. The model consisted of a 21 kg manual wheelchair with a seated 50th percentile male ATD, four-point strap tiedown system, and three-point occupant belt system. The occupant restraint and tiedown loads and accelerations of wheelchair, ATD chest and pelvis were compared between sled test data and computer simulation generated data. The results of the study showed that the peaks and profiles of the two data sets (sled test and computer simulation) matched quite well. Using the developed model, the authors investigated the loads imposed upon manual wheelchairs during frontal impact to provide design guidelines.

Computer simulation was also used in the study on injury risk assessment of a wheelchair user in a motor vehicle crash. Paskoff assessed neck injury risk of wheelchair users in rear collisions using computer simulation [10]. The model consisted of a 25 kg powered wheelchair (without the batteries) and a seated 50th percentile male ATD modeled with a Rear Impact Dummy (RID) neck, which was designed to simulate the head-neck response of a human exposed to a low speed collision [10]. The wheelchair was secured using a four-point strap tiedown system, and the ATD was restrained using lap and shoulder belts. The model was not validated with actual rear impact sled test data. The study examined the effects of seat back height, seat back stiffness, and the effectiveness of a head restraint on head/chest angle, head torque, and neck axial loads.

As described in the above studies, the computer models developed and used to date represent adult wheelchairs with a seated adult occupant (50^{th} percentile male). Pediatric wheelchair occupants likely respond differently in crashes, and the 50^{th} percentile male ATD is not appropriate for representing younger populations. In addition, pediatric transit wheelchairs are subjected to different loading conditions in a crash than are adult transit wheelchairs. Therefore, in order to study pediatric wheelchairs in transit or associated occupant injury risks, a computer model of a pediatric wheelchair, with a seated Hybrid III 6-year-old ATD (Hybrid III 6), was developed and validated in this study.

2.3 METHODS

2.3.1 Sled Testing

Three identical pediatric manual wheelchairs were sled tested in this study. For the purpose of computer simulation model development and validation, sled test data of successfully run wheelchair tests were needed. Therefore, among pediatric manual wheelchairs available on the market, one with the transit option was chosen for the study. A wheelchair with the transit option is defined as a wheelchair that has been tested in accordance with the ANSI/RESNA WC-19 standard, which requires a 20g/48kph (30 mph) frontal impact sled test. Sunrise Medical (Longmont, CO) Zippie is one of the most commonly used transit pediatric manual wheelchairs [11] [12]. The Zippie transit option includes four wheelchair securement points which interface with tiedown straps. The wheelchair seating system chosen for the study is the Sunrise Medical transit-tested standard conventional seating, which consists of a padded solid seat and solid back.

2.3.1.1 Instrumentation and Pretest Measurements

Frontal impact sled testing was conducted at the University of Michigan Transportation Research Institute (UMTRI). The sled at UMTRI operates on the rebound principle, which achieves a desired change in velocity by reversing its direction of motion during the impact

event. The Hybrid III 6-year-old ATD (Hybrid III 6) was used for the sled test. The Hybrid III 6 was equipped to measure head acceleration, chest (upper thorax) acceleration, chest compression (compression deflection of the thorax sternum relative to the spine), and forces and moments at the dummy's upper neck. Additionally, each wheelchair was equipped with an accelerometer (Endevco, Model 2264-2000, rated to 2000 g) located at its CG. Both the wheelchair tiedown and occupant restraint systems were equipped with webbing tension load cells: UMTRI Instrumented Rod End Load Cells (Model JP1, rated to 44480 N (10,000 lb)) on wheelchair tiedown belts and Denton Belt Load Cells (Model 3255, rated to 13344 N (3000 lb)) on occupant restraint belts.

Sled Test Setup (See Figure 12*)*

1. A ZIPPIE wheelchair with seating system was placed on the sled platform facing forward.

2. The instrumented Hybrid III 6-year-old ATD was place and positioned in the wheelchair.

3. The wheelchair was secured to the sled platform using a surrogate four-point, strap-type tiedown.

4. The ATD was restrained with a surrogate, vehicle-anchored, three-point belt which includes a lap and shoulder belt. The shoulder belt was taped to the dummy's shirt at the upper chest area to keep the shoulder belt positioned during the initial sled acceleration.*

5. Reflective markers were placed on the front hub, rear hub, wheelchair center of gravity (CG), point P, and knee joint.

Note: point P is a wheelchair seat reference point located approximately 50 mm above and 50 mm forward of the projected side-view intersection of the undepressed wheelchair seat back and undepressed wheelchair seat.

---

* Tape was used to temporarily attach the shoulder belt to the upper torso of the test dummy since WC-19 requires 75mm of shoulder belt slack simulating the belt pay out with a retractor [13]. Due to the slack, the shoulder belt was likely to slide off the ATD's shoulder. Therefore, tape was used to retain the shoulder belt in place during initial phase of the sled test.

6. Two cameras were placed on the side of the sled platform in order to capture both forward and rearward ATD head excursion.

Before conducting the sled test, the measurements described in Appendix C were taken from the test setup for use in the development of the computer model. Positions of accelerometers and load cells on the sled, wheelchair, ATD, and WTORS were also measured before testing. Table 4 shows the summary of the sled test setup conditions.

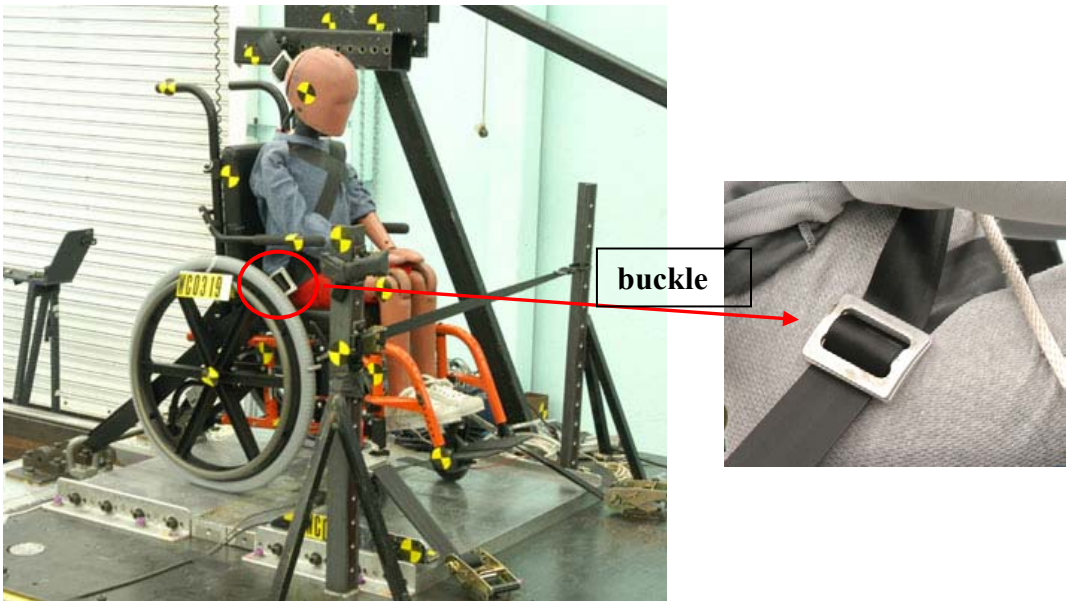

Figure 12 Sled test setup

Table 4 Sled test setup conditions

Wheelchair Type	Sunrise Medical Zippie
Wheelchair Securement	Surrogate 4-point strap-type tiedown
Occupant Restraint	Surrogate independent 3-point belt
Anthropomorphic Test Dummy	Hybrid III 6-year-old, 25kg
Target Impact Velocity (ΔV)	48 kph
Target Average Sled Deceleration	20g
Wheelchair	
Wheelchair Weight	18.6 kg
Wheelchair $CG_{vertical}$	359 mm above ground
Wheelchair $CG_{horizontal}$	188 mm front of rear hub
Wheelchair Rear Hub Height	280 mm above ground
Seating System	Sunrise Medical standard conventional seating (padded solid seat and solid back)
Seat depth	380 mm
Seat width	310 mm
Seat back height	380 mm
Seat back width	310 mm
Wheelchair Securement Points on Wheelchair	
Front Securement Point	419 mm front of rear hub
	191 mm above ground/ 89 mm below rear hub
Rear Securement Point to Rear Hub	105 mm behind rear hub
	315 mm above ground/ 35 mm above rear hub
Wheelchair Tiedown	
Front-Rear Floor Anchor Distance	1295 mm
Rear Tiedown Angle wrt Horizontal	38 º
Front Tiedown Angle wrt Horizontal	29 º
Lateral Dist Between Rear Floor Anchor Points	335 mm
Lateral Dist Between Front Floor Anchor Points	670 mm
Rear Tiedown Length	495 mm
Front Tiedown Length	419 mm
Rear Hub to Rear Tiedown Floor Anchor Dist	518 mm
Occupant Restraint	
Shoulder Belt Upper Anchor Point	305 mm behind ATD shoulder
	178 mm above ATD shoulder
	1045 mm above sled platform
	305 mm left of wheelchair centerline
Sagittal Plane Shoulder Belt Angle	30 º wrt Horizontal (behind shoulder)
Frontal Plane Shoulder Belt Angle	54 º wrt Horizontal Sternum Reference
Sagittal Plane Lap Belt Angle	42 º wrt Horizontal

2.3.1.2 Data collection

The 20g/48kph frontal impact pulse used for sled testing is shown in Figure 13 with the pulse requirements stated in ANSI/RESNA WC-19. Data collected during the sled test for use in the validation of the computer model were as follow: wheelchair acceleration, rear tiedown belt loads, shoulder belt load, lap belt load, ATD head acceleration, and ATD chest acceleration. Signals collected from the accelerometers and load cells were filtered following the requirements of SAE J211-2, instrumentation for impact testing.

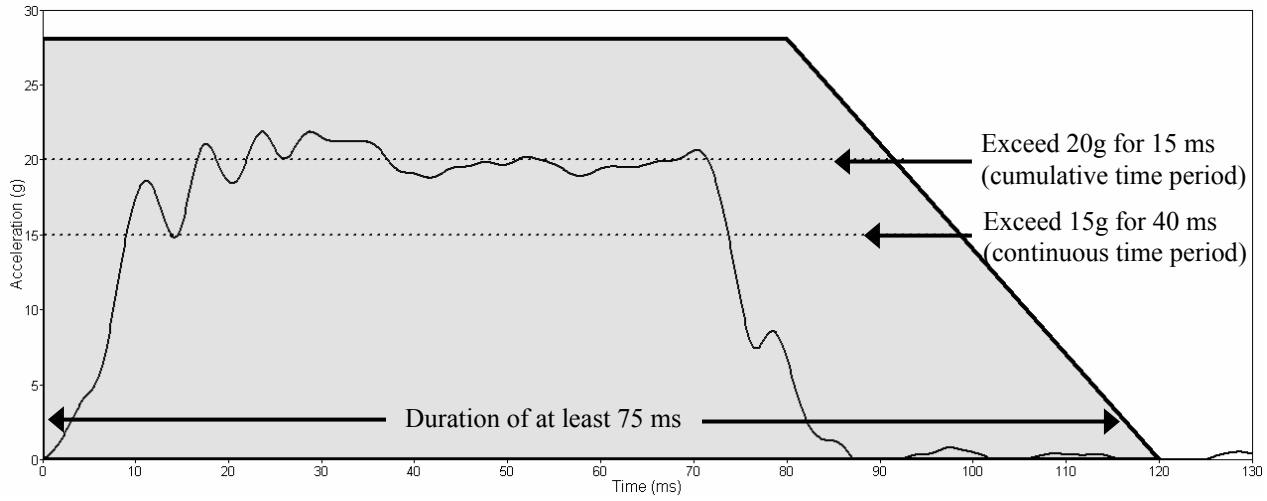

Figure 13 Sled deceleration pulse with ANSI/RESNA WC-19 corridor

During each sled test, the entire impact event was recorded using high-speed (1000 frames/sec) motion cameras (Kodak HG 2000 digital high speed video camera) positioned at the side of the sled track. Data collected and motion videos taken from the sled test were used in the validation of the computer model.

2.3.2 Selection of Computer Simulation Software

Prior to developing a computer simulation model of the pediatric manual wheelchair, three computer crash simulation software packages, Dynaman, ATB3I, and MADYMO, were

evaluated (see 1.6). After the evaluation, MADYMO V6.01 was chosen for the study for the following reasons:

- Availability of the validated Hybrid III 6-year-old child dummy model.
- Availability of features such as 16 joint types, three contact surface shapes, three hysteresis models, which support the user in developing a more sophisticated computer simulation model.
- Capability of analyzing both multi-body systems and finite element models.
- Capability of calculating standard injury parameters.
- Capability of generating output files which can be read from the post processors with advanced features that allow easy manipulation of data, animation, and plots.

2.3.3 MADYMO model development

Using the measurements taken from the sled test setup (sled_test_3), a computer model of the Zippie wheelchair with a seated Hybrid III 6 was developed (see Figure 14). The coordinate system used in the sled test and the computer model is shown in Figure 14.

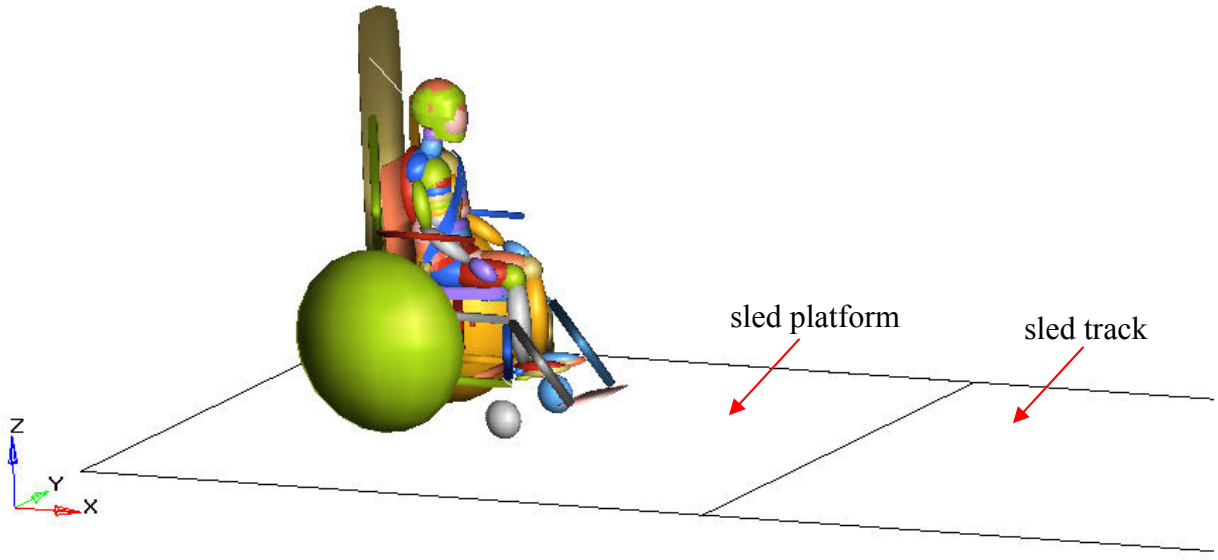

Figure 14 Pediatric manual wheelchair and Hybrid III 6-year-old ATD model in MADYMO

The Zippie wheelchair was modeled with seven bodies, representing two front casters, two rear wheels, wheelchair seat, wheelchair seat back, and wheelchair frame structure. Mass, moment of inertia, and CG of each wheelchair component were assigned to each body. The moment of inertia of four wheels, seat and seat back were estimated using the moment of inertia equations for *thin rectangular plate* and *thin disk*. The moment of inertia of wheelchair frame structure was estimated using the Parallel-Axis Theorem, $Ix = \bar{I}x' + m(\bar{y}^2 + \bar{z}^2)$, $Iy = \bar{I}y' + m(\bar{z}^2 + \bar{x}^2)$, $Iz = \bar{I}z' + m(\bar{x}^2 + \bar{y}^2)$, calculated at the CG of wheelchair frame (see Appendix D). To represent the complete wheelchair frame, including the armrests and the footrests, 20 ellipsoid surfaces were attached to the wheelchair frame body.

For a 6-year-old ATD, the MADYMO Hybrid III 6-year-old ATD model, which has been calibrated and validated through component tests and complete dummy sled tests, was used [14].

There are two types of belts available in MADYMO, the standard belt and the finite element (FE) belt. The standard belt is attached and fixed to a body surface, preventing belt slippage over the body surfaces. Conversely, the nodes of the FE belt are able to slide over the body surfaces. The four-point, strap-type tiedowns were modeled using standard belts which secured the wheelchair frame (two front securement points and two rear securement points) to the moving sled platform (two front anchor points and two rear anchor points).

The three-point occupant restraint system was developed through three steps as follow:

Step1. standard shoulder belt and standard lap belt **(Standard Belt model)**,

Step2. standard shoulder belt with FE segment and FE lap belt **(FE_Segment Belt model)**,

Step3. FE shoulder belt and FE lap belt **(Full_FE Belt model)**. (See Figure 15)

Belt slack was given to the shoulder belt in all models. Since the lap-to-shoulder belt buckle should move freely in space (see Figure 12), the buckle was modeled as a body with a free joint.

The acceleration pulse was applied to the moving sled platform, which was joined to the sled track using the translational joint.

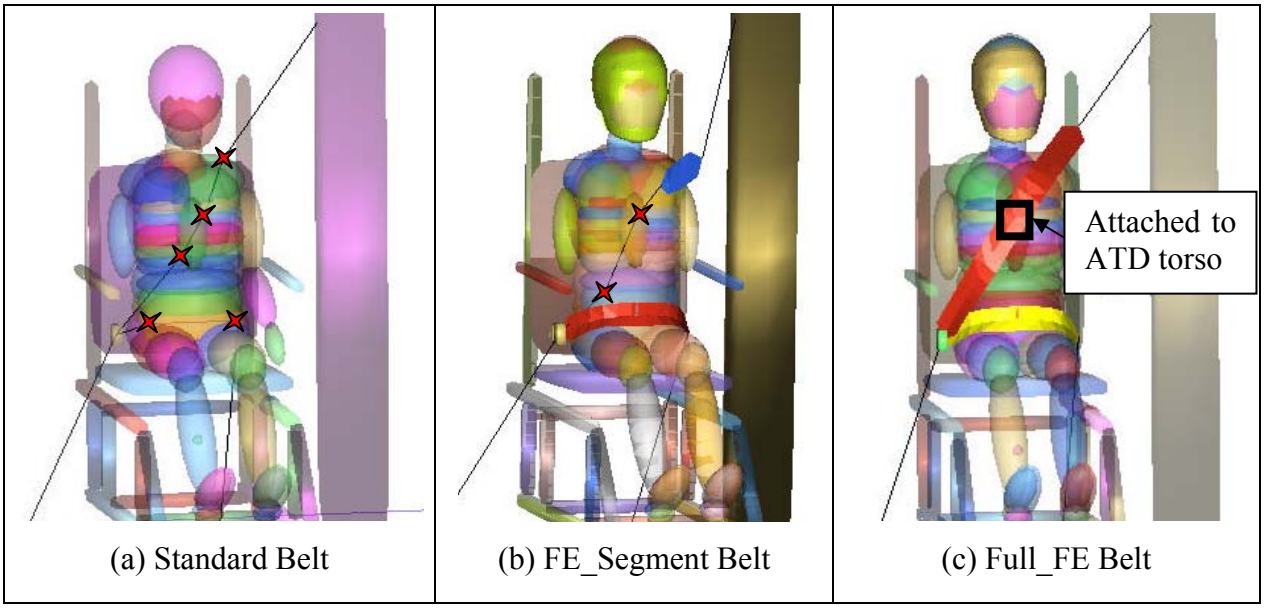

(a) Standard Belt (b) FE_Segment Belt (c) Full_FE Belt

Figure 15 Occupant belt models in MADYMO: (a) Standard Belt, (b) FE_Segment Belt, and (c) Full_FE Belt

2.3.4 MADYMO model validation

The model was tuned using the following sled test data: wheelchair acceleration measured at the wheelchair CG, wheelchair rear tiedown forces, occupant restraint shoulder and lap belt forces, and ATD head and chest accelerations. Trends and the peak of time history data from the computer simulation model were tuned to trends and the peak of time history data from the sled test. (Variables used in the comparison of time histories are termed, $\mathbf{VAR_{time\_history}}$.) For each $VAR_{time\_history}$, peak of time history resulted from the model was compared to the peak resulted from the sled test using % Peak difference (see Equation 1). The peak horizontal excursions of the wheelchair, ATD's head, and knee joint were obtained from sled test videos and compared to the model to evaluate the kinematics of a wheelchair and an ATD, and % Peak difference was also calculated. (Variables used in the comparison of peak horizontal excursions

are termed, $\mathbf{VAR_{hor\_excursion}}$) Visual comparison of the sled test video and the model animation output were also conducted.

Equation 1 % Peak difference

$$\% \text{ Peak difference} = \frac{\left| Peak_{sled\_test} - Peak_{simulation} \right|}{Peak_{sled\_test}} * 100$$

In the automotive crash research, comparison of the time history profiles is most typically used to validate computer simulation models [15] [16] [17] [18] [5] [19] [20]. In this study, after the comparison of the time history profiles was conducted, the model validation criteria stated below were applied to the final model (Full_FE Belt model). The model is defined to be a "validated model" only if it meets all of the following criteria:

Model Validation Criteria

(Note: the limit for each criterion was determined based on the previous crash simulation studies as well as accepted statistical assumptions [6] [21] [22] [23] [24] [25] – see 2.5 Discussion)

1. Average % Peak difference ($VAR_{time\_history}$) < 15 %
   - Evaluating the peaks in time history comparison
2. Average Pearson's correlation coefficient (r) > 0.8
   - Evaluating the shape of the time history profiles
3. Average % Peak difference ($VAR_{hor\_excursion}$) < 15 %
   - Evaluating kinematics of the wheelchair and the ATD

The Pearson's correlation coefficient (r) between the sled test and the Full_FE Belt model was computed for each of the $VAR_{time\_history}$. Data from the computer model was generated at the same rate as the data collected from the sled test. Therefore, each data point collected from the sled test was able to be paired with a data point generated from the computer

simulation. The time increment between data points was 0.1 ms. The Pearson's correlation coefficient was computed using values at individual data point of paired data.

2.3.5 Evaluation of the Full_FE Belt model

To further evaluate the validated model, 95% confidence interval (CI) of sled tests was constructed for each variable, $VAR_{time\_history}$, and time histories generated from the model were compared to the 95% CI of the sled tests. The model was also evaluated using the software package called *ADVISER* (TNO Automotive, Netherlands), which compared the computer simulation results to the sled test results and provided a quality rating for a computer model. Root-mean-square normalized error (RMSNE) and % Area difference were calculated and reported in this study, so those values can possibly be used as the comparison values in the future studies involving crash simulation model validation.

Linear regression analysis of the computer simulation versus the sled test was also conducted using SPSS 12.0.1 (SPSS Inc., Chicago, Illinois). To test whether a significant relationship exists between the peaks measured from the sled test and the peaks obtained from the model, the test statistic value of linear regression slope ('b' in $y = a + bx$) was used. The null hypothesis, H_0: b=0, was tested using the significance (alpha) level of 0.05.

2.4 RESULTS

2.4.1 Sled Testing

Time histories of data collected during three sled tests are shown in the Figure 16. Figure 17 shows the time-lapse images of the sled_test_3 at 20 ms intervals.

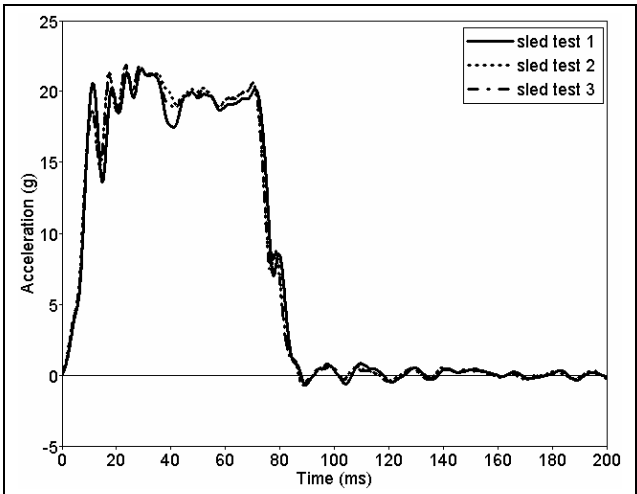

(a) sled acceleration

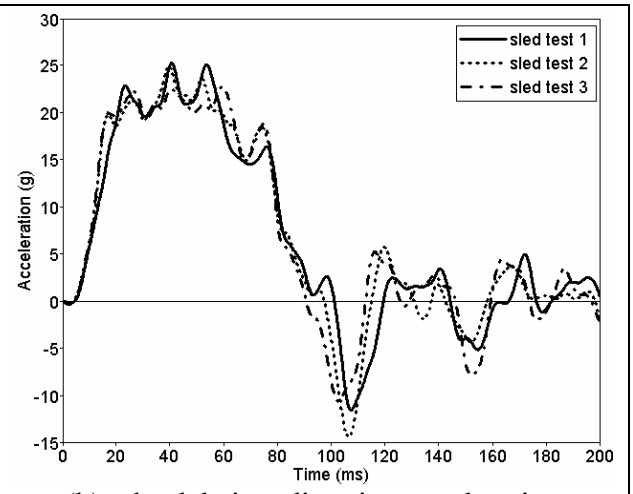

(b) wheelchair x-direction acceleration

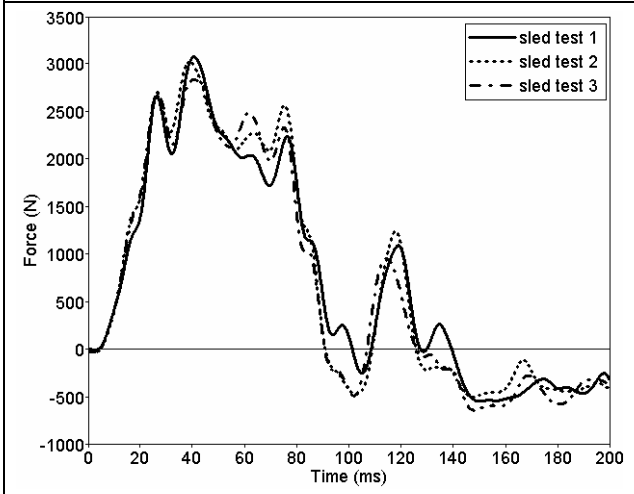

(c) rear right tiedown force

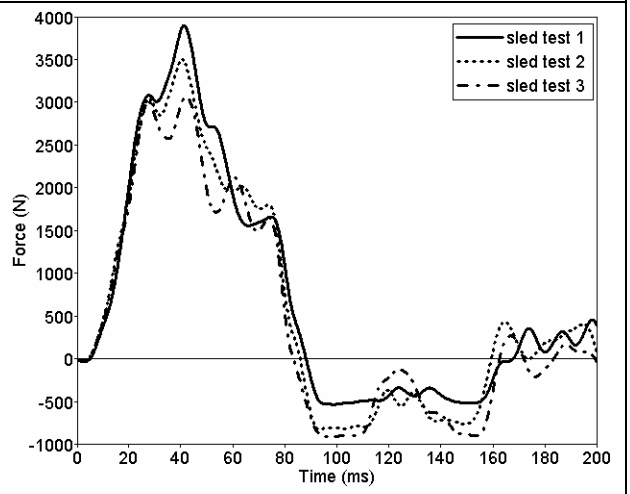

(d) rear left tiedown force

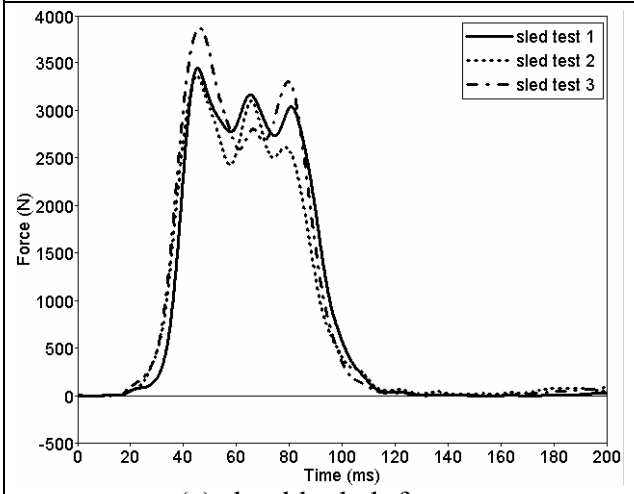

(e) shoulder belt force

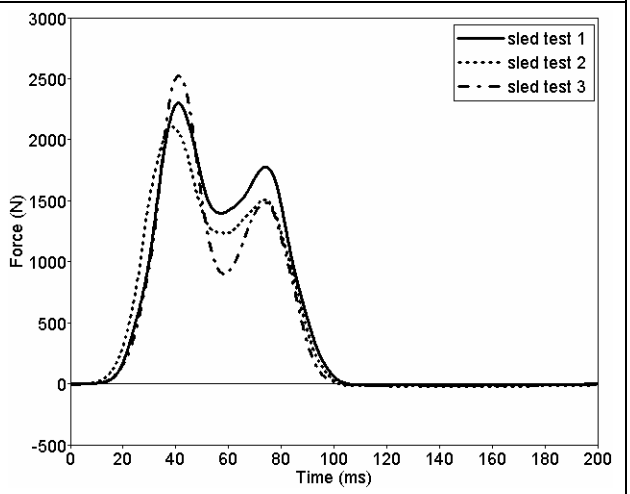

(f) lap belt force

(Continue)

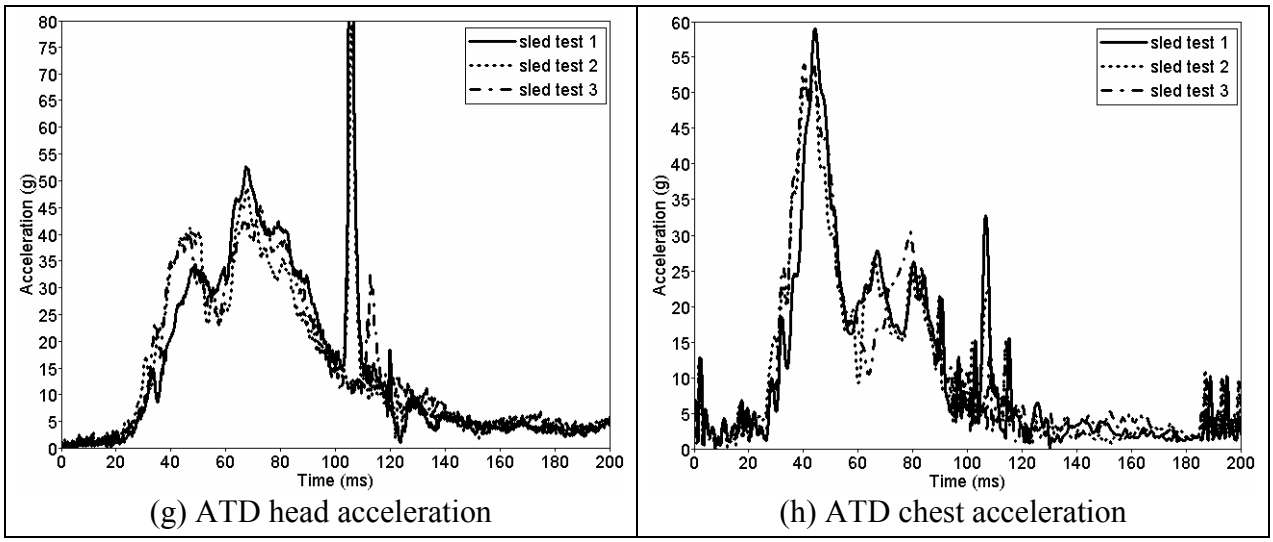

(g) ATD head acceleration (h) ATD chest acceleration

Figure 16 Time histories of (a) sled acceleration, (b) wheelchair x-direction acceleration, (c) rear right tiedown force, (d) rear left tiedown force, (e) shoulder belt force, (f) lap belt force, (g) ATD head acceleration, and (h) ATD chest acceleration – sled tests

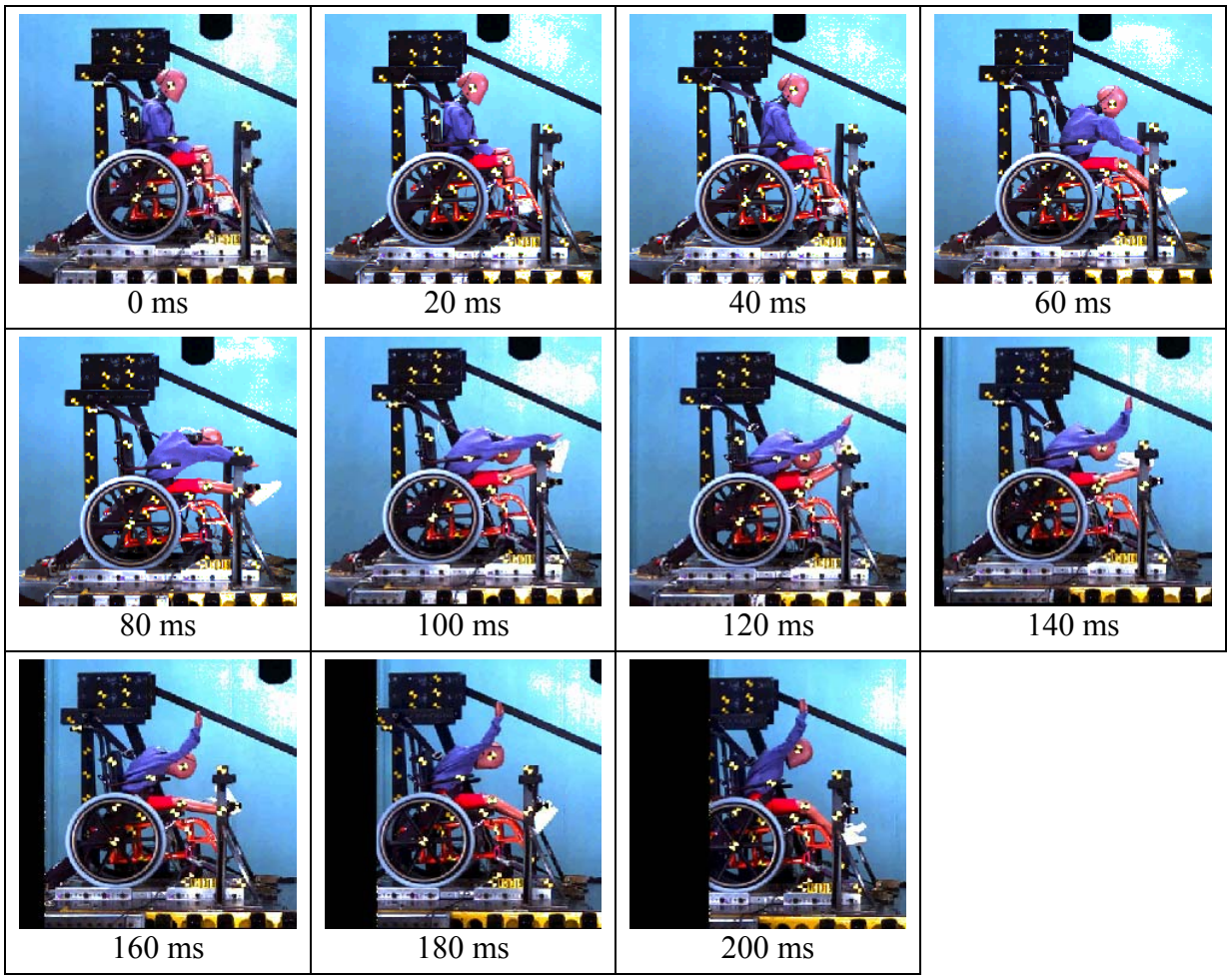

Figure 17 Images of the sled test 3 at 20 ms intervals

During each sled test, the ATD's head contacted its knee between 100 ms and 120 ms (see Figure 17). High peaks shown in the time histories of ATD head acceleration (see Figure 16-(g)) are the result of head contact. The shoulder belt slid off of the ATD's shoulder during all three sled tests (see Figure 18).

Figure 18 Post sled test – front view

2.4.2 MADYMO Model Development

2.4.2.1 Step 1: Standard Belt model

The three-point occupant restraint system was modeled first with the standard belt. As shown in Figure 15-(a), the belt is attached to the ATD's body surfaces at the left clavicle, upper left sternum, lower left sternum, right abdomen, and left abdomen (attachment points are marked with a "✗").

Comparison between sled test data and Standard Belt model data are shown in Figure 19. Time history profiles of the computer simulation were tuned with those of the sled tests for all variables, $VAR_{time\_history}$. Although the sled test results showed higher force on the rear left

tiedown than on the rear right tiedown (Figure 19 – (b) and (c)), the model had higher force on the right tiedown than on the left tiedown. As shown in Table 5, the peak value for each of the variables, $VAR_{time\_history}$, was compared between the sled test and the model using % Peak difference. The % peak difference across all $VAR_{time\_history}$ for the Standard Belt model ranged from 2.4 % to 11.0 % with the average % Peak difference of 5.1 %.

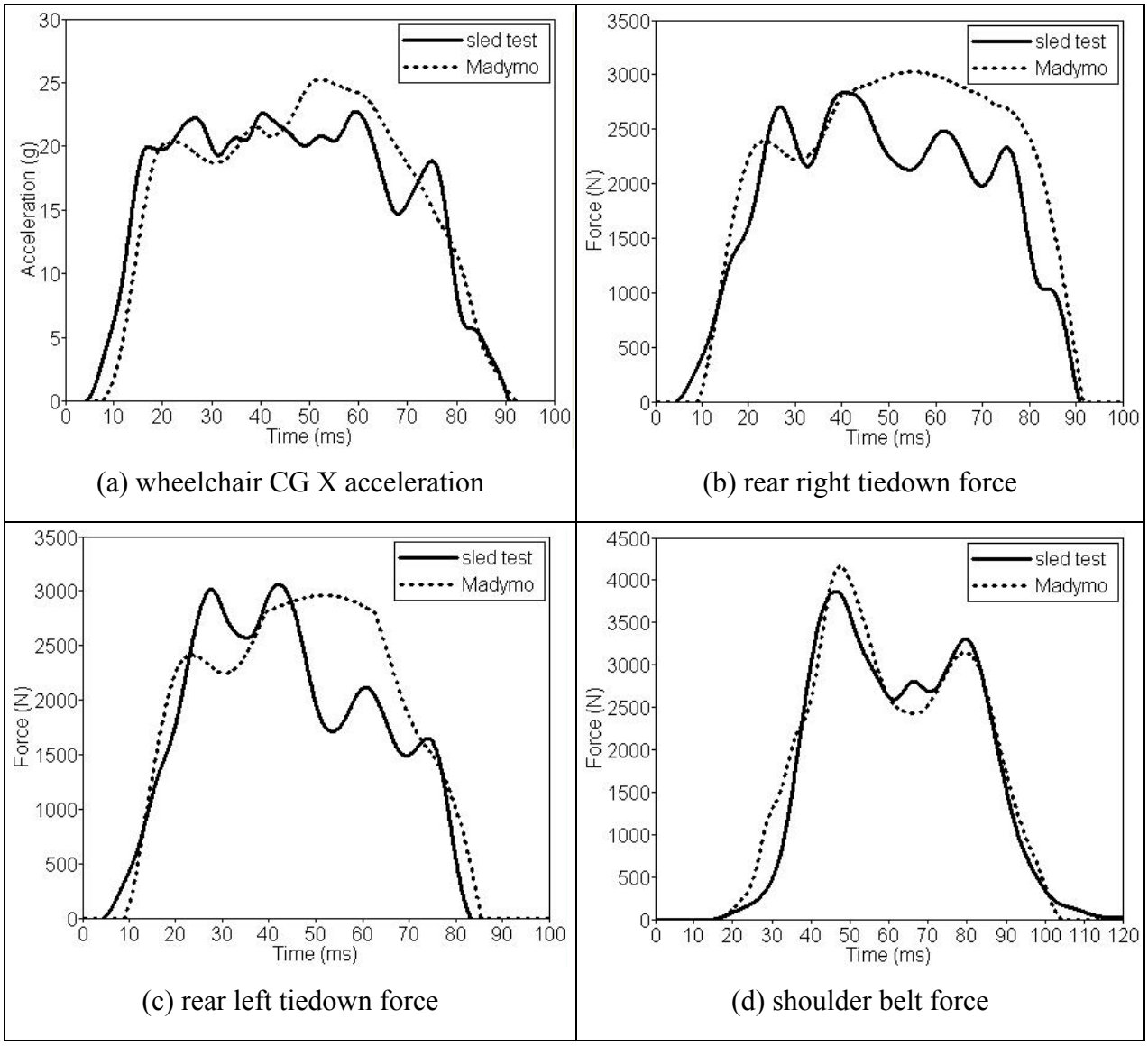

(a) wheelchair CG X acceleration

(b) rear right tiedown force

(c) rear left tiedown force

(d) shoulder belt force

(Continue)

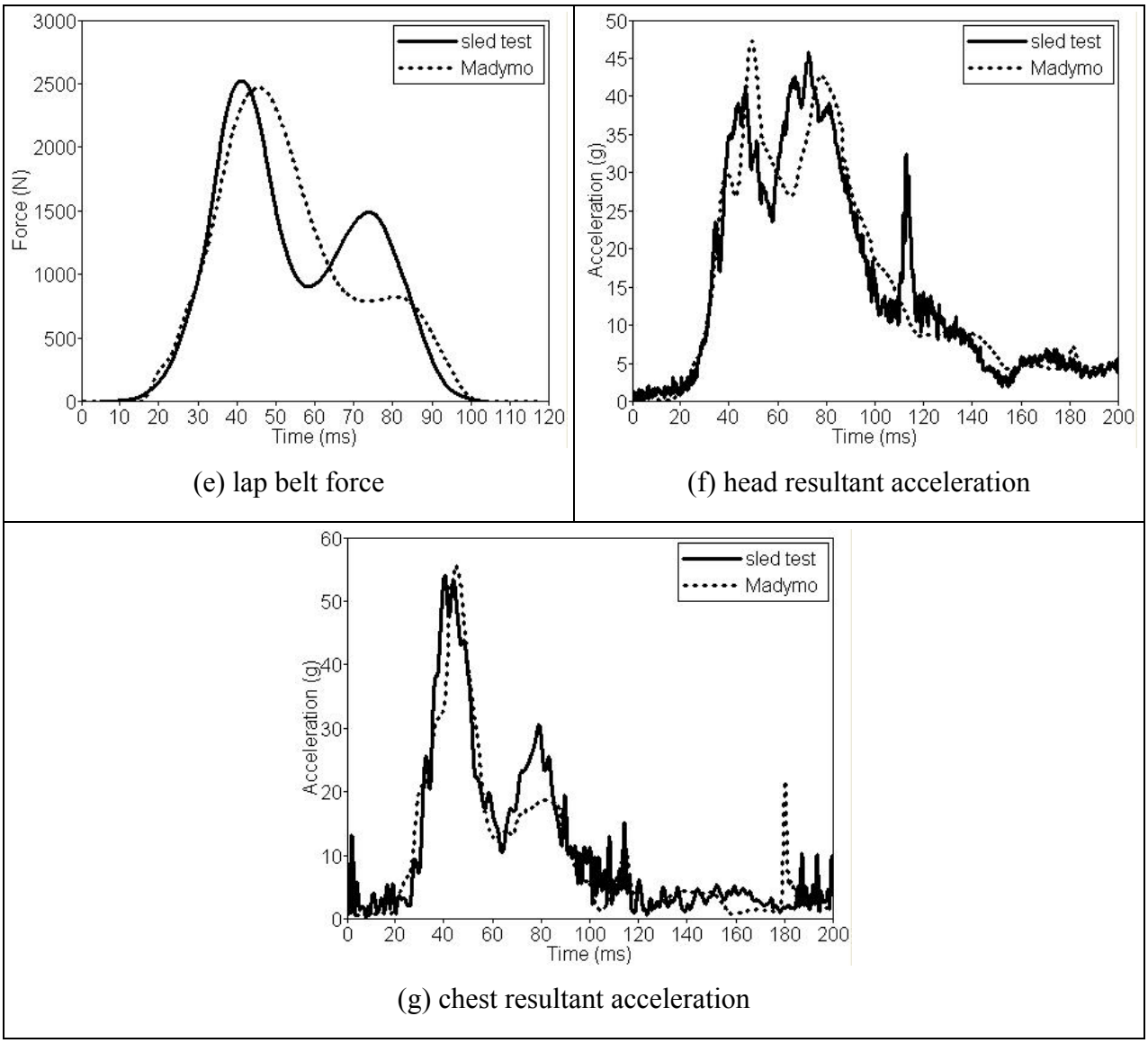

(e) lap belt force

(f) head resultant acceleration

(g) chest resultant acceleration

Figure 19 Comparison of sled test and simulation model – Standard Belt model

Table 5 Comparison of the peak values between sled test and Standard Belt model

$VAR_{time\ history}$	Sled test	Standard Belt model	% Peak difference
WC CG x-acceleration (g)	22.7	25.2	11.0
Rear right tiedown force (N)	2832	3020	6.6
Rear left tiedown force (N)	3055	2960	3.1
Shoulder belt force (N)	3862	4087	5.8
Lap belt force (N)	2519	2433	3.4
Head resultant acceleration (g)	45.7	47.2	3.3
Chest resultant acceleration (g)	54.0	55.3	2.4
Average % Peak difference (%)			**5.1**

A comparison of the wheelchair and occupant gross motions between the Standard Belt model and sled testing is shown in Figure 20. Wheelchair kinematics showed higher wheel deflection than the sled test results (see Figure 20-100 ms). During the rebound phase of the impact, the ATD was turning and shifting toward the upper shoulder belt anchor point side (see Figure 20 – 200 ms). As shown in Table 6, the peak horizontal excursion of a wheelchair, ATD head, and ATD knee joint ($VAR_{hor\_excursion}$) was also compared between the sled test and the model to evaluate kinematics of the wheelchair and the ATD. The % Peak difference across $VAR_{hor\_excursion}$ for the Standard Belt model ranged from 34.1 % to 376.9 % with the average % Peak difference of 150.9 %.

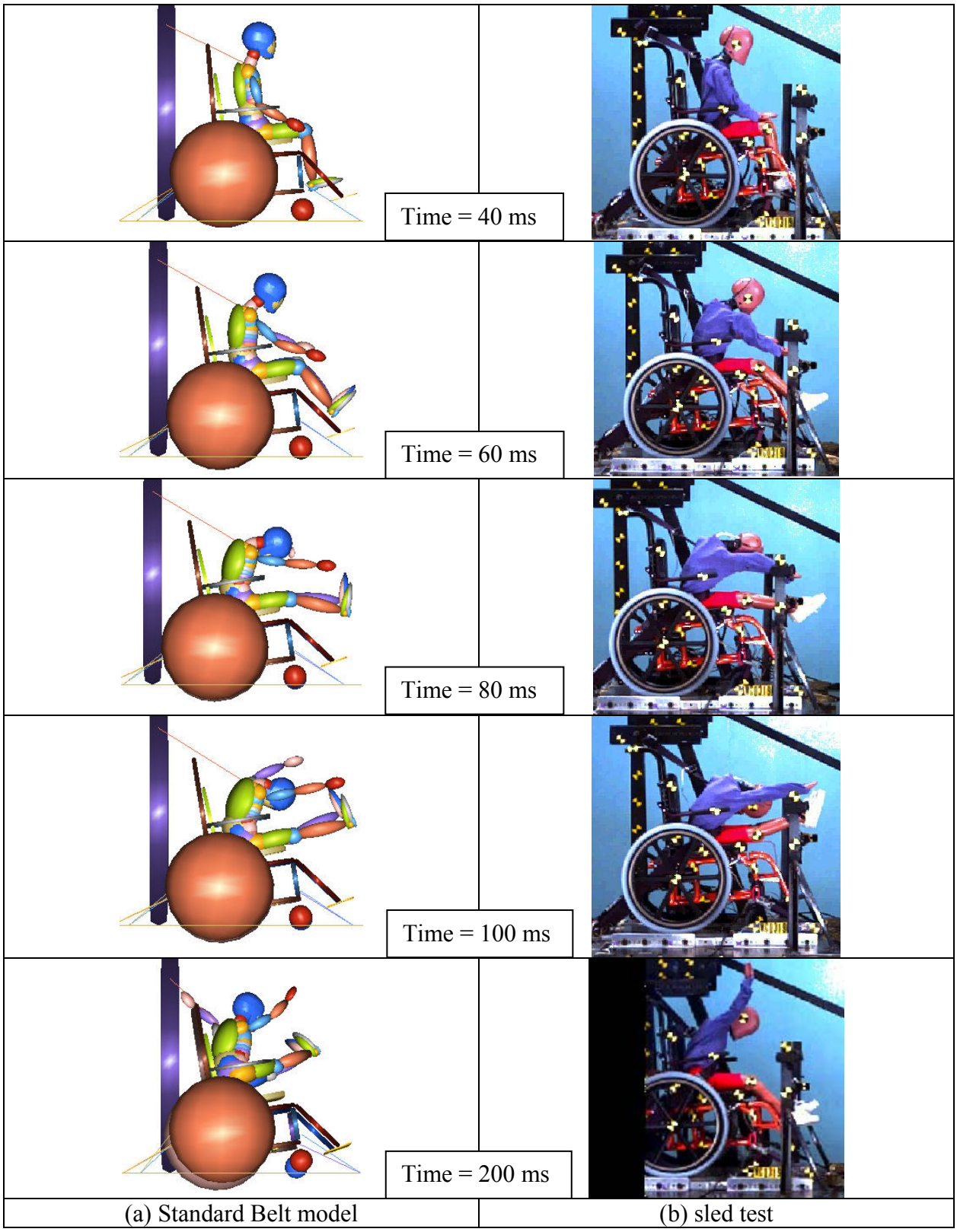

Figure 20 Wheelchair and occupant crash response – (a) Standard Belt model versus (b) sled test

Table 6 Peak horizontal excursions of sled test and Standard Belt model

$VAR_{hor\_excursion}$	Sled test (mm)	Standard Belt model (mm)	% Peak difference
Wheelchair excursion	13	62	376.9
Knee excursion	65	92	41.5
Head forward excursion	252	166	34.1
Average % Peak diff. (%)			**150.9**

2.4.2.2 Step 2: FE_Segment Belt model

The Standard Belt model showed high % Peak difference across all $VAR_{hor\_excursion}$ (especially wheelchair excursion). To improve the kinematics of a wheelchair and an ATD in the computer model, the Standard Belt model was modified and retuned using sled test data.

Although the upper section of the shoulder belt slid off of the ATD's shoulder during sled tests (see Figure 18), the occupant belt which was modeled using the standard belt did not slide over the dummy body surfaces in the Standard Belt model. To simulate the shoulder belt, which had a section taped to the dummy body and a section that slid off of the shoulder, a combination of standard belt and FE belt was used in the Step 2 model, FE_Segment Belt model. As shown in Figure 15-(b), the FE belt section of the shoulder belt allowed the belt to slide off of the shoulder, and the standard belt, which was attached to the dummy's upper chest (marked with a " ✕ "), simulated the taped section of the shoulder belt. The lap belt was modeled with an FE belt.

Comparison between sled test data and FE_Segment Belt model data are shown in Figure 21. Unlike the sled test results, which had higher force on the rear left tiedown than on the rear right tiedown (Figure 21 – (b) and (c)), the model had similar peak force on both sides of the rear tiedowns. The peak shoulder belt force of the model (3368 N) did not reach as high as did the sled test result (3862 N) (Figure 21 – (d)). The ATD head acceleration of the model reached higher than did the sled test result, while the chest acceleration of the model did not reach as high as did that of the sled test (Figure 21 – (f)). The peak value for each of the $VAR_{time\_history}$ was

compared between the sled test and the model as shown in Table 7. The % peak difference across all $VAR_{time\_history}$ for the FE_Segment Belt model ranged from 5.6 % to 22.2 % with the average % Peak difference of 11.8 %.

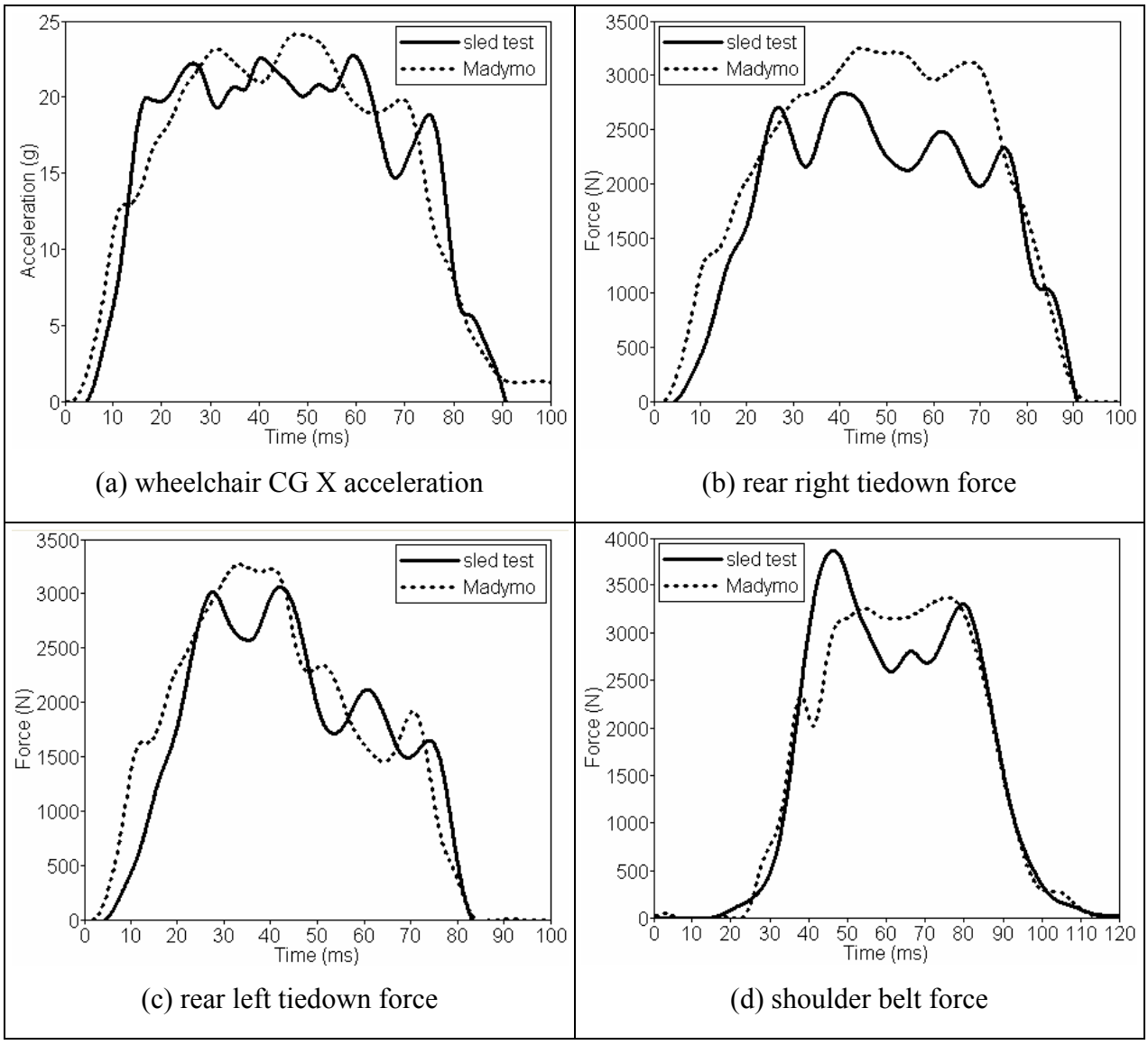

(a) wheelchair CG X acceleration

(b) rear right tiedown force

(c) rear left tiedown force

(d) shoulder belt force

(Continue)

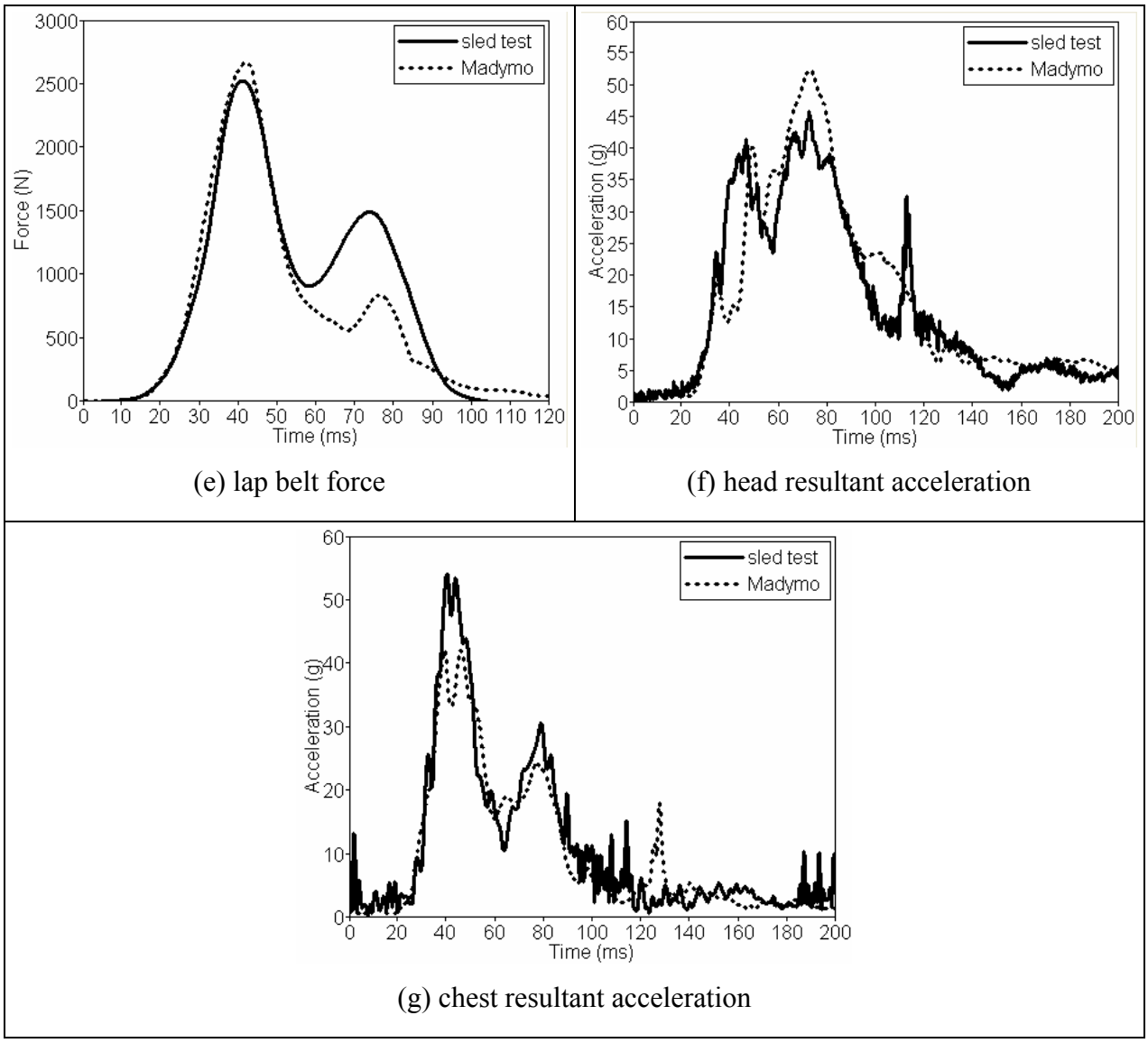

(e) lap belt force

(f) head resultant acceleration

(g) chest resultant acceleration

Figure 21 Comparison of sled test and simulation model – FE_Segment Belt model

Table 7 Comparison of the peak values between sled test and FE_Segment Belt model

$VAR_{time\ history}$	Sled test	FE_Segment Belt model	% Peak difference
WC CG x-acceleration (g)	22.7	24.1	6.2
Rear right tiedown force (N)	2832	3247	14.7
Rear left tiedown force (N)	3055	3263	6.8
Shoulder belt force (N)	3862	3368	12.8
Lap belt force (N)	2519	2661	5.6
Head resultant acceleration (g)	45.7	52.3	14.4
Chest resultant acceleration (g)	54.0	42.0	22.2
Average % Peak difference			**11.8**

A comparison of the wheelchair and occupant gross motions between the FE_Segment Belt model and sled testing is shown in Figure 22. Wheelchair kinematics are similar to those obtained through sled testing at each time interval. General motion of the ATD appears to be comparable between sled testing and the FE_Segment Belt model. The ATD kinematics in the rebound phase of the impact were similar between the two, except differences in leg extension. The peak horizontal excursions (wheelchair, ATD's head, and ATD knee joint) of the sled test and the FE_Segment Belt model are shown in Table 8. The % Peak difference across $VAR_{hor\_excursion}$ for the FE_Segment model ranged from 7.7 % to 17.8 % with the average % Peak difference of 11.4 %.

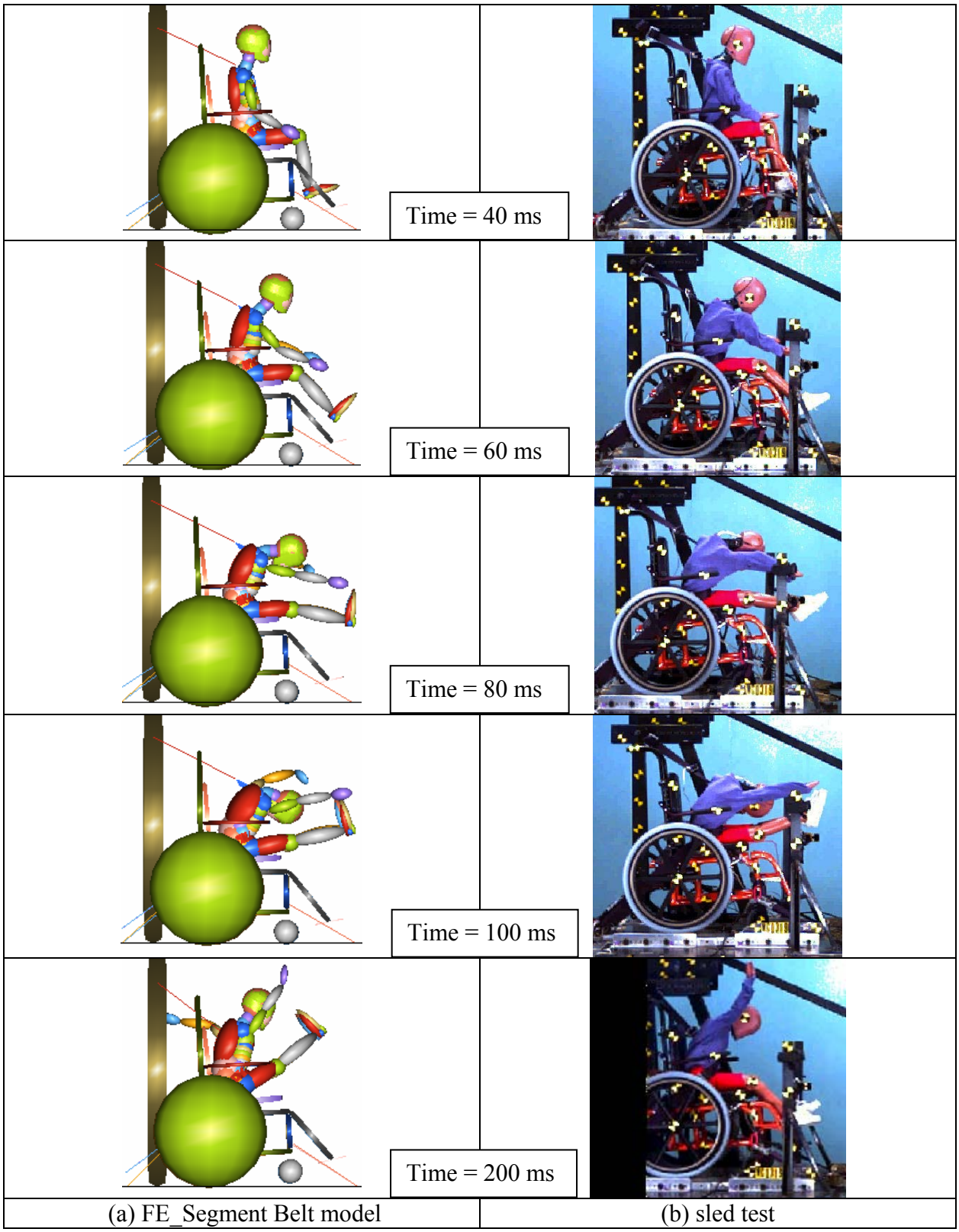

Figure 22 Wheelchair and occupant crash response – (a) FE_Segment Belt model versus (b) sled test

Table 8 Peak horizontal excursions of sled test and FE_Segment Belt model

$VAR_{hor\_excursion}$	Sled test (mm)	FE_Segment Belt model (mm)	% Peak difference
Wheelchair excursion	13	12	7.7
Knee excursion	65	76.6	17.8
Head forward excursion	252	230	8.7
Average % Peak diff. (%)			**11.4**

2.4.2.3 Step 3: Full_FE Belt model

Although using a small portion of an FE belt is not a standard way to model an occupant restraint belt, an FE belt segment was inserted into a standard shoulder belt in the FE_Segment Belt model. In the process of tuning the FE_Segment Belt model, the shoulder belt showed unstable behavior. For example, changing characteristic (force-deformation or force-elongation) of one of the input variables by a small fraction caused a large difference in the shoulder belt force time history. Moreover, in the FE_Segment Belt model, only the FE segment portion in the shoulder belt was able to slide over the ATD body while the standard belt portion was attached to the dummy's body. Therefore, in Step 3 of the model development, the shoulder belt was modeled with a full FE belt, Full_FE Belt model. In the Full_FE Belt model, both the shoulder and the lap belt were modeled with an FE belt. And, to simulate the taped portion of the shoulder belt, several nodes on the FE shoulder belt were attached to the ATD's upper chest (see Figure 15-(c)).

Comparison between sled test data and Full_FE Belt model data is shown in Figure 23. Visually the time histories compare well between the model and sled test, with a few exceptions. In the Full_FE Belt model, the maximum shoulder belt force occurred later in time than did the peak occurrence time observed during the sled test (Figure 23 – (d)). The spike in the head acceleration time history from the sled test (Figure 23 – (f)) indicates head-to-knee contact of the

ATD. The peak value for each of the $VAR_{time\_history}$ was compared between the sled test and the model in Table 9. The % peak difference across all $VAR_{time\_history}$ for the Full_FE Belt model ranged from 1.5 % to 15.8 % with the average % Peak difference of 8.1 %.

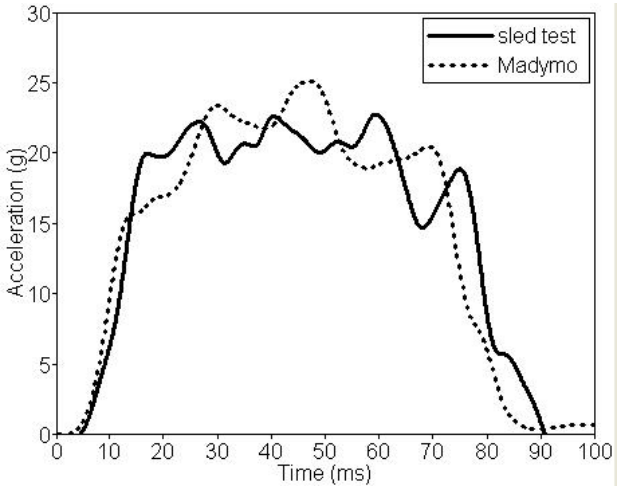

(a) Wheelchair CG X acceleration

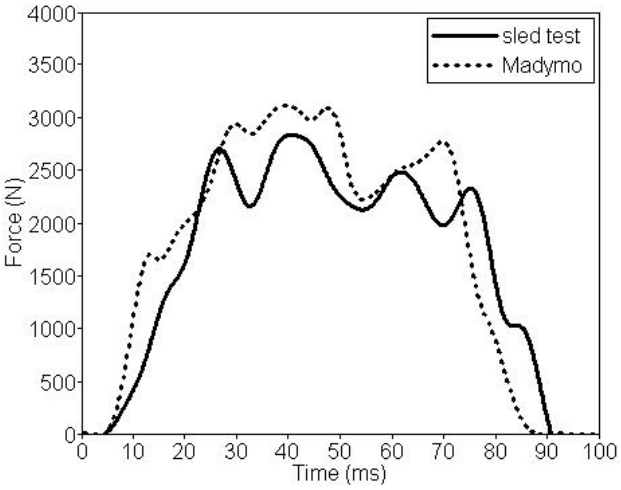

(b) Rear right tiedown force

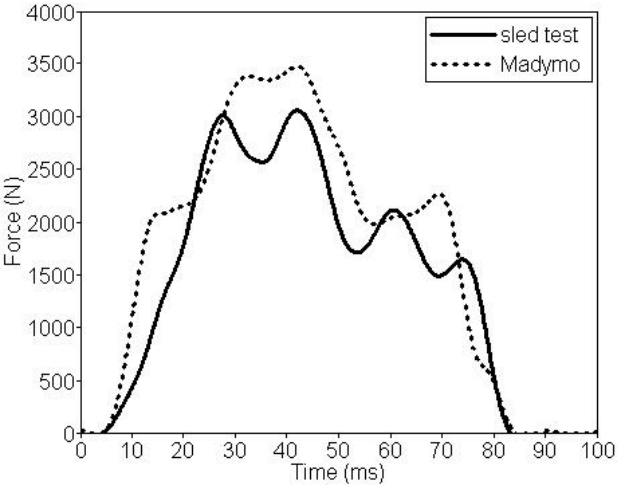

(c) Rear left tiedown force

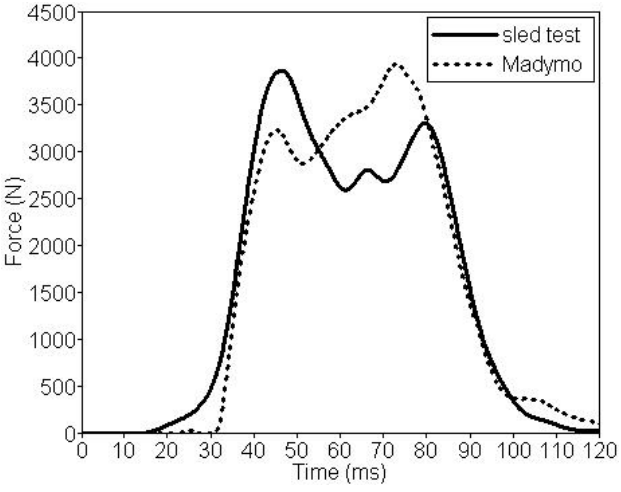

(d) Shoulder belt force

(Continue)

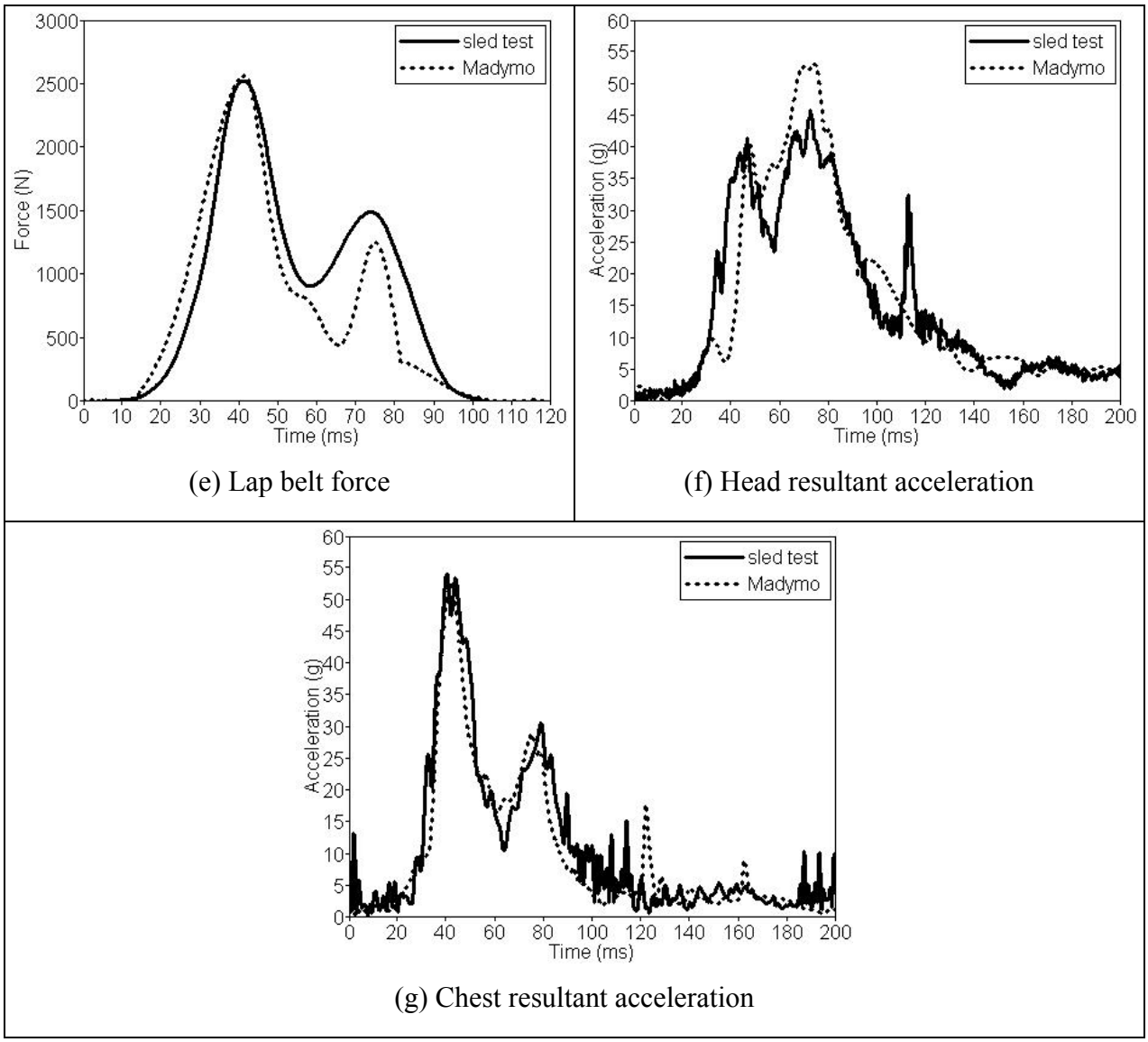

(e) Lap belt force

(f) Head resultant acceleration

(g) Chest resultant acceleration

Figure 23 Comparison of sled test and simulation model – Full_FE Belt model

Table 9 Comparison of the peak values between sled test and Full_FE Belt model

$VAR_{time\ history}$	Sled test	Full_FE Belt model	% Peak difference
WC CG x-acceleration (g)	22.7	25.1	10.6
Rear right tiedown force (N)	2832	3115	10.0
Rear left tiedown force (N)	3055	3471	13.6
Shoulder belt force (N)	3862	3931	1.8
Lap belt force (N)	2519	2558	1.5
Head resultant acceleration (g)	45.7	52.9	15.8
Chest resultant acceleration (g)	54.0	52.2	3.3
Average % Peak difference (%)			**8.1**

A comparison of the wheelchair and occupant gross motions between sled testing and the Full_FE Belt model is shown in Figure 24. Wheelchair kinematics are similar to those obtained through sled testing at each time interval. General motion of the ATD appears to be comparable between sled testing and the Full_FE Belt model. The ATD kinematics in the rebound phase of the impact were similar between the two, except differences were seen in extension of the legs. The peak horizontal excursions (wheelchair, ATD's head, and ATD knee joint) of the sled test and the Full_FE Belt model are shown in Table 10. The % Peak difference across $VAR_{hor\_excursion}$ for the Full_FE Belt model ranged from 7.7 % to 15.4 % with the average % Peak difference of 11.3 %.

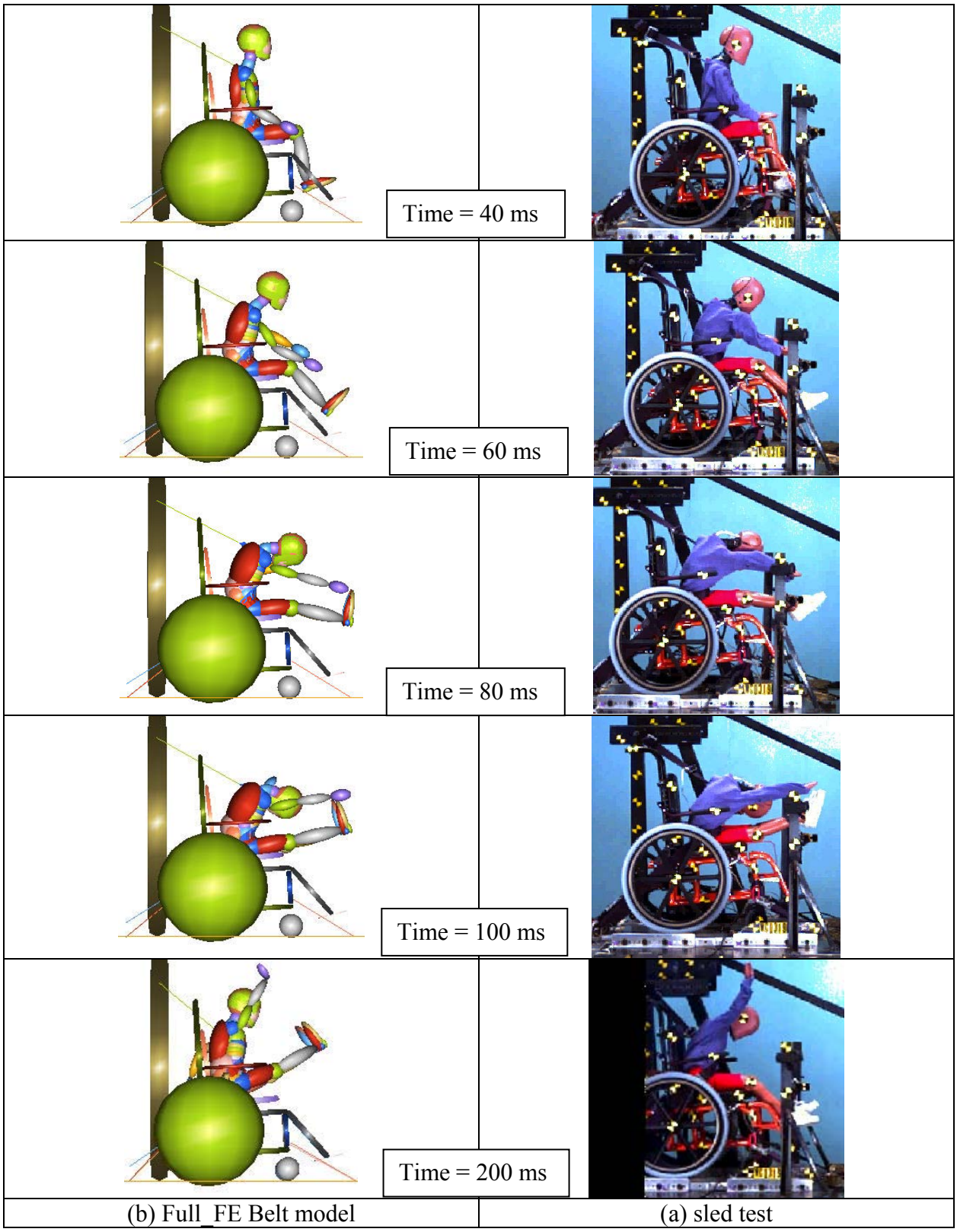

Figure 24 Wheelchair and occupant crash response – (a) Full_FE Belt model versus (b) sled test

Table 10 Peak horizontal excursions of sled test and Full_FE Belt model

$VAR_{hor\_excursion}$	Sled test (mm)	Full_FE Belt model (mm)	% Peak difference
Wheelchair excursion	13	15	15.4
Knee excursion	65	70	7.7
Head forward excursion	252	225	10.7
Average % Peak diff. (%)			**11.3**

2.4.3 Model Validation

Before applying the 'Model Validation Criteria' (stated in 2.3.4) to the final model, Full_FE Belt model, the Pearson's correlation coefficient (*r*) between the sled test and the model was computed for all $VAR_{time\_history}$ (see Table 11). Data between two time points where the sled test time history crossed the horizontal axis, 0 Y-value, were included in the calculation of *r* (see Figure 30). The time increment between data points was 0.1 ms. The correlation coefficients across all $VAR_{time\_history}$ for the Full_FE Belt model ranged from 0.86 to 0.95 with the average *r* of 0.91.

Table 11 Correlation coefficient (*r*) between the sled test and the Full_FE Belt model

$VAR_{time\_history}$	***r*** (sled test vs. Full_FE Belt model)
WC CG x-acceleration	0.90
Rear right tiedown force	0.88
Rear left tiedown force	0.91
Shoulder belt force	0.95
Lap belt force	0.91
Head resultant acceleration	0.86
Chest resultant acceleration	0.94
Average *r*	**0.91**

The Model Validation Criteria were applied to the results of the Full_FE belt model. As shown in Table 12, the model met all of the criteria. Therefore, the Full_FE Belt model is considered to be a validated model.

Table 12 Comparison between validation criteria and Full_FE Belt model

	Ave % Peak difference ($VAR_{time\_history}$)	Ave *r*	Ave % Peak difference ($VAR_{hor\_excursion}$)
Criterion	**< 15**	**> 0.8**	**< 15**
Full_FE Belt	8.1	0.91	11.3

2.4.4 Evaluation of Validated Full_FE Belt Model

2.4.4.1 95% Confidence Interval

95% confidence interval (CI) of sled tests was constructed for each variable used in time history comparison ($VAR_{time\_history}$) using Equation 2. *T-distribution*, "sampling distribution used to evaluate smaller samples" [26], was used in the calculation of CI due to small sample sizes (3 sled tests). Time histories generated from the model were compared to the 95% CI of sled tests as shown in Figure 25.

Equation 2 95% Confidence Interval

95% CI = $\overline{X} \pm (t) s_{\overline{X}}$

$\overline{X}$ = mean

t = critical value, **4.303** for 95% CI with 2 degrees of freedom

$s_{\overline{X}}$ = standard error of the mean

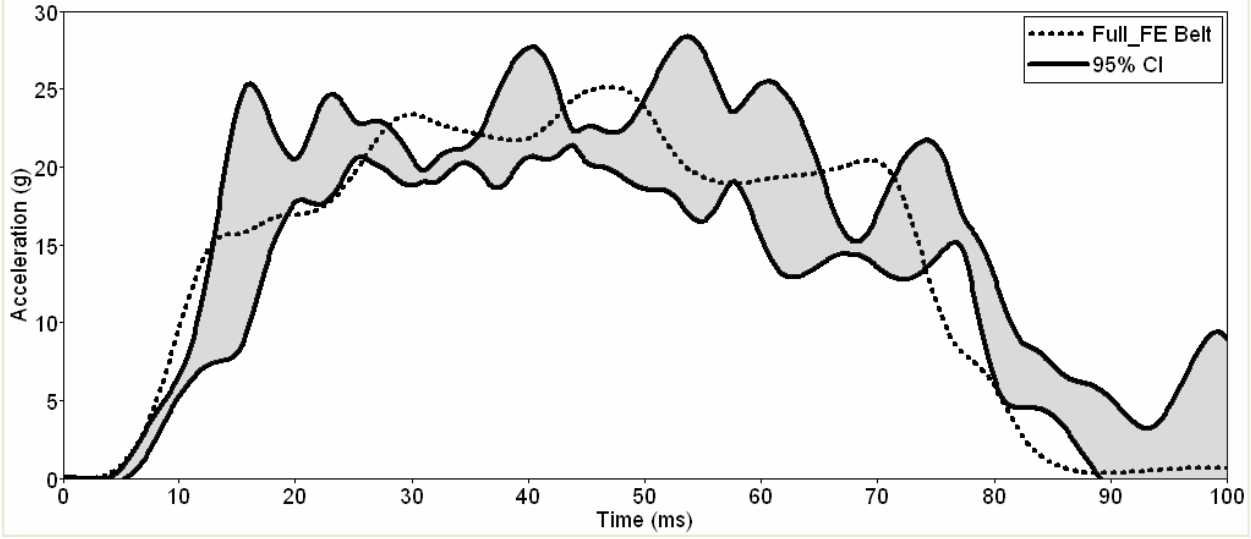

Wheelchair CG X acceleration

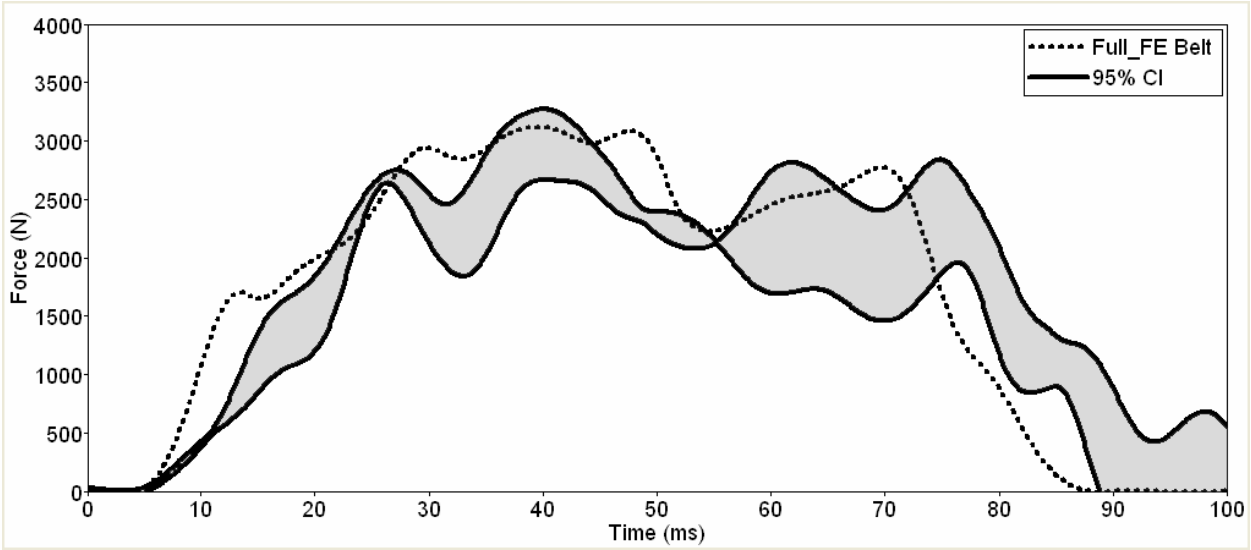

Rear right tiedown force

(Continue)

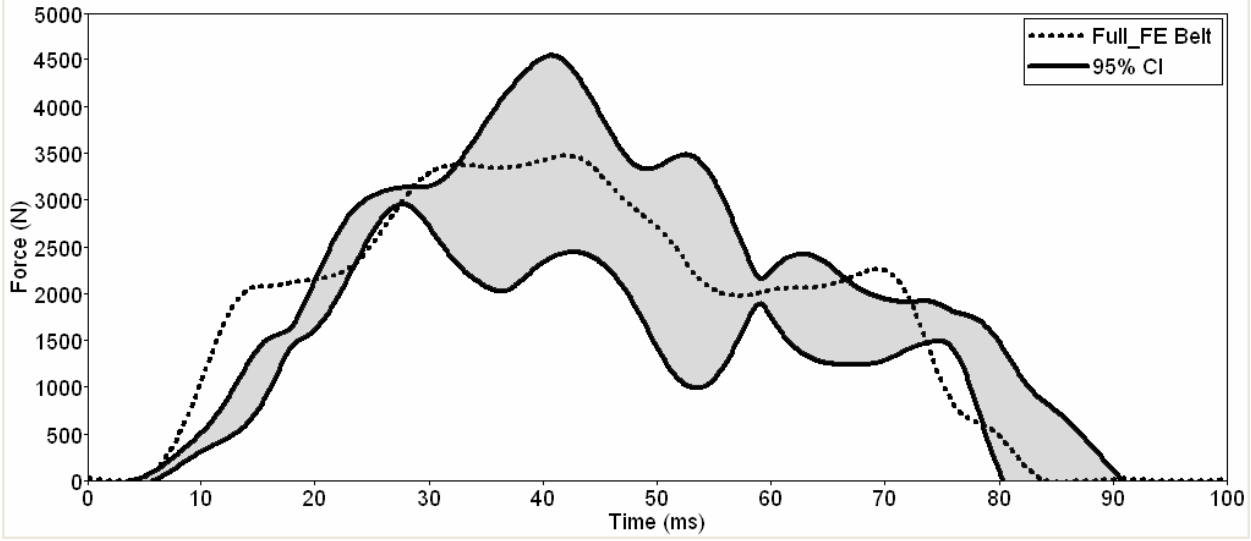

Rear left tiedown force

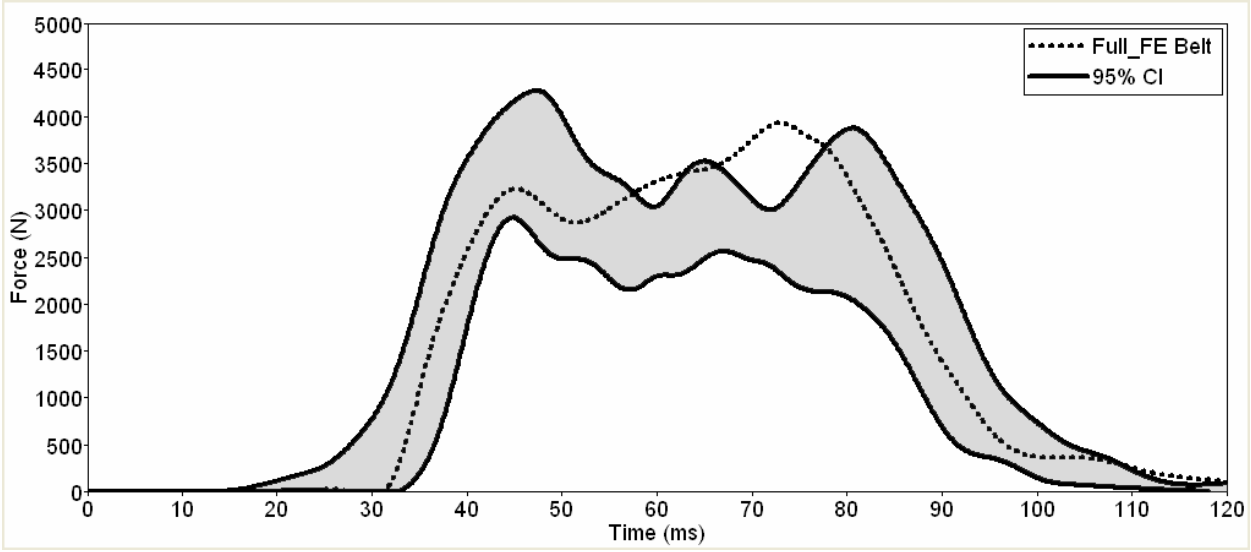

Shoulder belt force

(Continue)

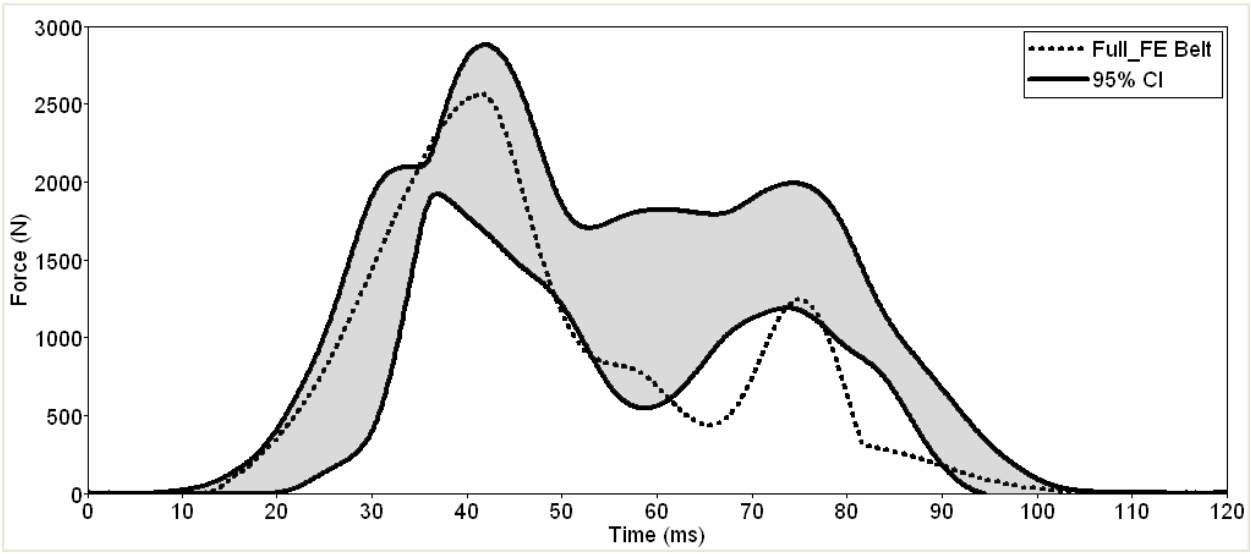

Lap belt force

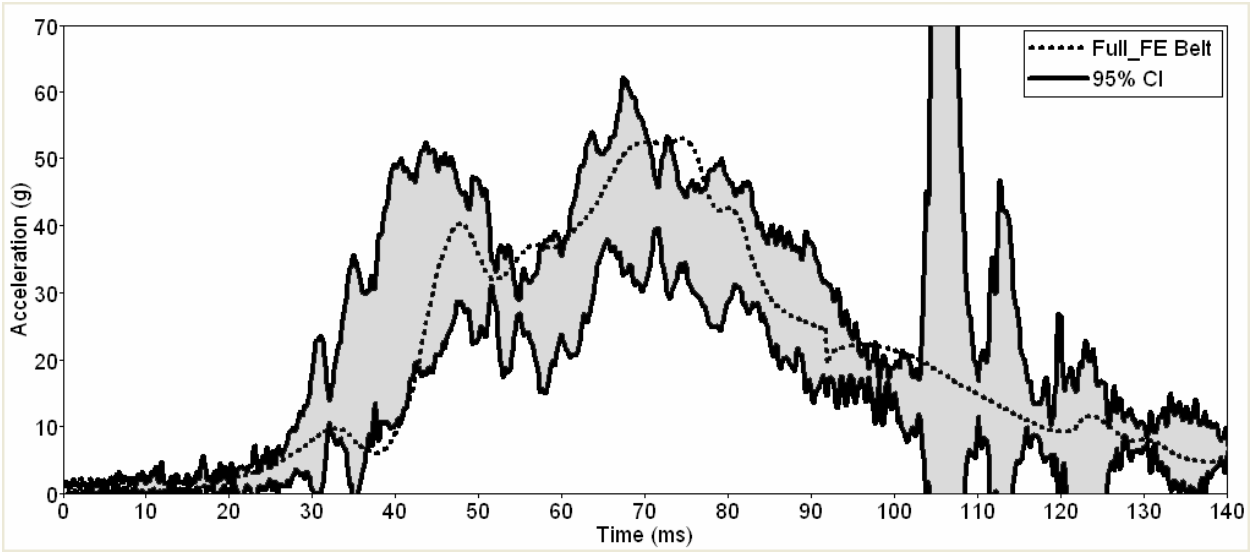

Head resultant acceleration

(Continue)

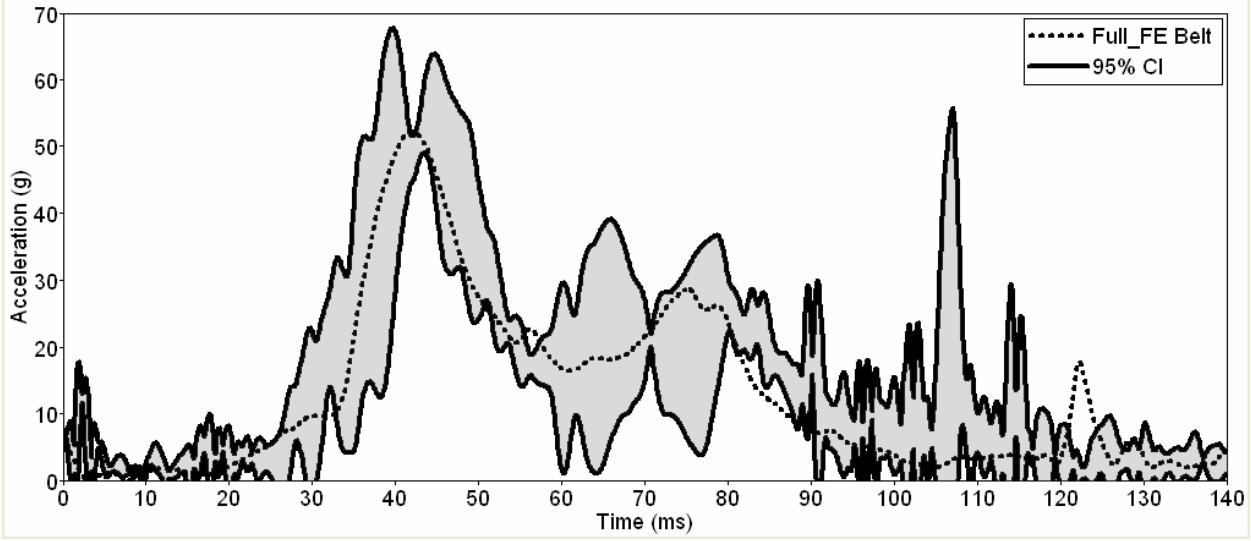

Chest resultant acceleration

Figure 25 Model output on 95% confidence interval of sled tests

2.4.4.2 Adviser

Adviser (TNO Automotive, Netherlands) is software which compares a numerical model to experimental results and provides a quality rating for a numerical model. The Full_FE Belt model was evaluated using the Beta version of Adviser.

As shown in the Figure 26, representing the 'input table', two categories (the peak and NISE, curve comparison command) were used in Adviser. Variables used in the comparison are:

- Peak: wheelchair acceleration, wheelchair rear left tiedown force, wheelchair rear right tiedown force, shoulder belt force, lap belt forces, ATD head acceleration, ATD chest acceleration, wheelchair excursion, ATD head excursion, and ATD knee excursion.
- NISE, curve comparison: wheelchair acceleration, wheelchair rear left tiedown force, wheelchair rear right tiedown force, shoulder belt force, lap belt forces, ATD head acceleration, ATD chest acceleration.

The sled test data were used as reference value ('Ref' in Figure 26) and compared to the data generated from the computer model ('Value' in Figure 26). 'Weight' in the input table reflects the importance of each category ('Peak' and 'NISE' in this study) and the importance of individual variable (WC acceleration, tiedown force, etc) in comparison. Range between 0 and 1 can be assigned to each category and variable. In this study, equal weight of "1" was assigned to both categories and all variables.

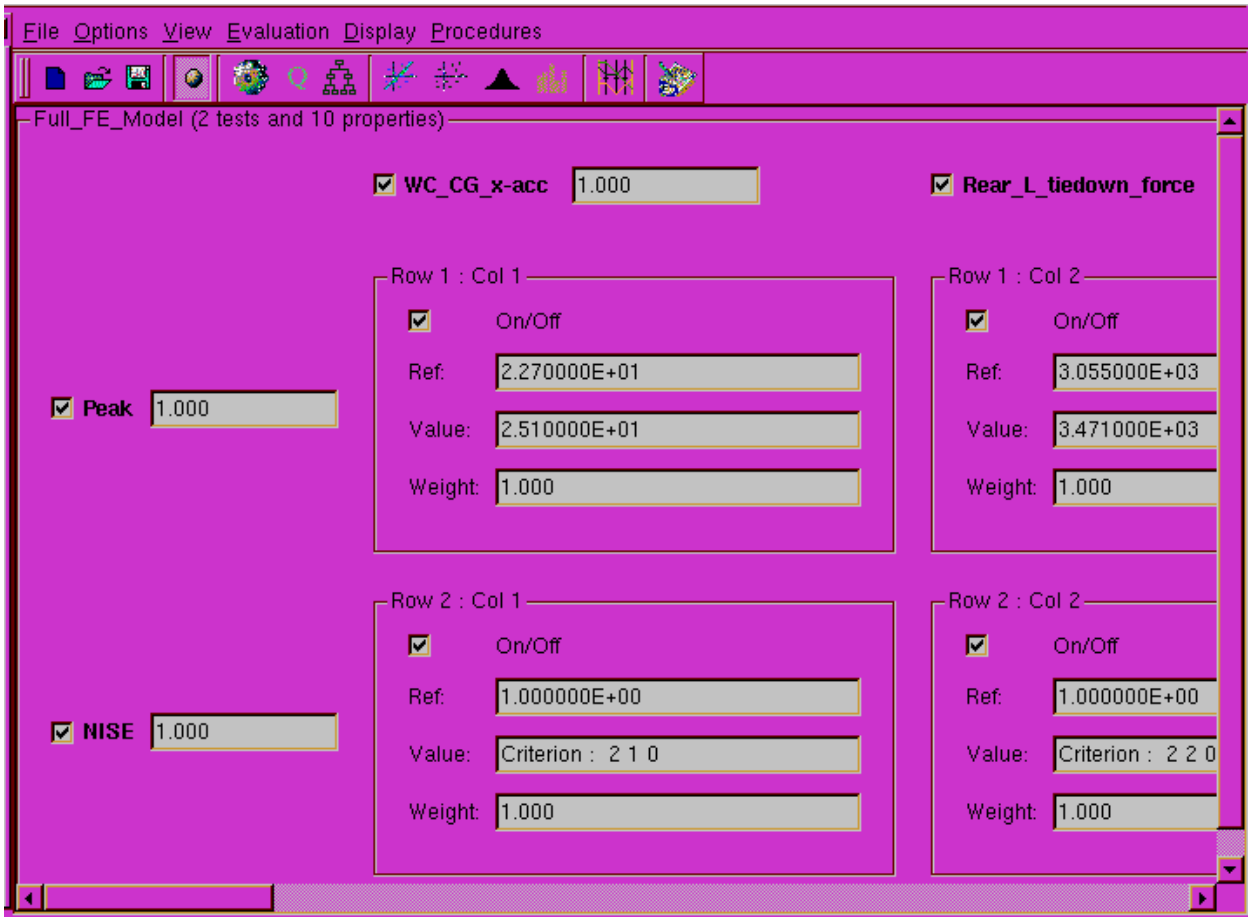

Figure 26 Adviser input table

In comparing of the computer model and sled test peaks, a rating ('Score') for individual variables was calculated in Adviser as follow [27]:

$$\text{Score}_{\text{Peak}} = 100 - [100 * \left| \frac{ref_{sled\_test} - value_{simulation}}{ref_{sled\_test}} \right|]$$

The Normalized Integral Square Error (NISE) was used in comparison of the time history curves between the pediatric wheelchair model and the sled test. NISE is "related in principle to the concept of Cumulative Variance" [27]. And, "the total NISE can be divided into phase shift, amplitude difference, and shape difference" [27]. The equation for NISE specified in *ADVISER Reference Guide* is as follow [27]:

$$NISE = 1 - \frac{2R_{xy}(0)}{R_{xx}(0) + R_{yy}(0)}$$

where

$$R_{xy}(0) = \frac{1}{N}\sum_{i=1}^{N} X_i Y_i$$

$$R_{xx}(0) = \frac{1}{N}\sum_{i=1}^{N} X_i X_i$$

$$R_{yy}(0) = \frac{1}{N}\sum_{i=1}^{N} Y_i Y_i$$

X_i = a digitised point of a data set
Y_i = a digitised point of another data set
N = number of digitised points in each data set

The result table generated from the Adviser includes a rating for individual variable and a rating for each category (see Figure 27). A 'Global Score' representing the quality rating for a model is also shown in the result table. The Adviser results are shown in Figure 28. The 'Global Score' is 92.96 % for the Full FE model. A model with the Global Score of 75 % or above is

considered to be a ‘good model’ which can be used in research studies and product development [28].

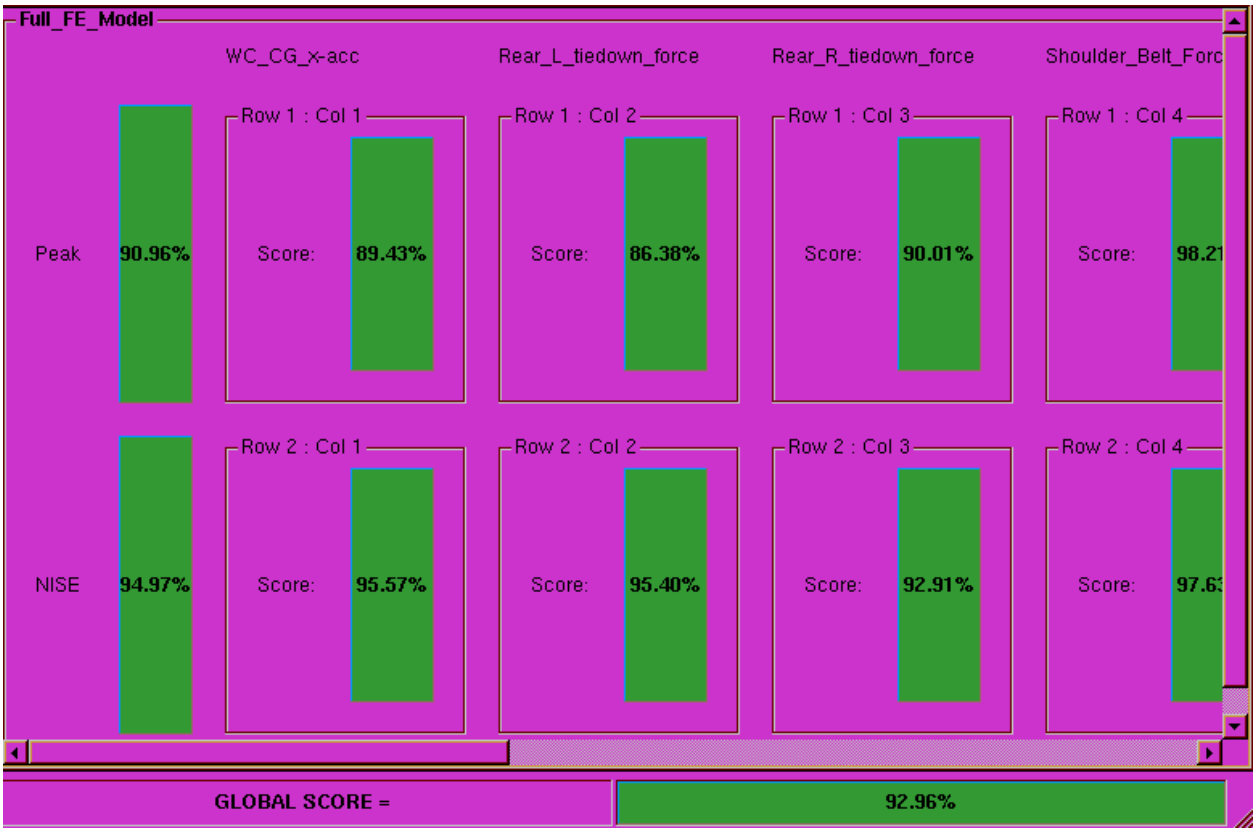

Figure 27 Adviser result table

Global score

Project name	Score
Full_FE_Model	92.96 %

Tests scores

Number	Name	Score
1	Peak	90.96 %
2	NISE	94.97 %

Elements scores

	WC_CG x-acc	Rear_L Tiedown F	Rear_R Tiedown F	Shoulder Belt Force	Lap Belt Force	Head Acc	Chest Acc	WC Excursion	Knee Excursion	Head Excursion
Peak	89.43 %	86.38 %	90.01 %	98.21 %	98.45 %	84.25 %	96.67 %	84.62 %	92.31 %	89.29 %
NISE	95.57 %	95.40 %	92.91 %	97.63 %	93.22 %	93.21 %	96.85 %	disabled	disabled	disabled

Figure 28 Full_FE Belt model Adviser results

2.4.4.3 Root-mean-square normalized error (RMSNE)

Peaks

The root-mean-square normalized error (RMSNE) was calculated to quantify an error between the peaks which resulted from a model and the peaks measured from a sled test (see Equation 3). m of 10 (7 $VAR_{time\_history}$ plus 3 $VAR_{hor\_excursion}$) was used in the calculation. The RMSNE for the Full_FE Belt model was 0.104.

Equation 3 RMSNE for peaks

$$\text{RMSNE} = \sqrt{\frac{\sum_{i=1}^{m} (Error_i)^2}{m}}$$

$$Error_i = \frac{(Peak_{sled\_test,i} - Peak_{simulation,i})}{Peak_{sled\_test,i}}$$

i = variable, m = number of variables

Trend

To quantitatively evaluate how well the trends of time histories between a model and a sled test were matched, the RMSNE was also calculated for $VAR_{time\_history}$ using Equation 4. As shown in Figure 29, the RMSNE for evaluating trends in time histories is "based on taking small 'slices' of time and measuring the deviation of [the simulation model's] line from the target (sled test) at each of these times." [29]

Equation 4 RMSNE for trends

$$\text{RMSNE} = \sqrt{\frac{\sum_{i=1}^{m} (Error_i)^2}{m}}$$

$$Error_i = \frac{(X_{sled\_test,i} - X_{simulation,i})}{X_{sled\_test,i}}$$

$X_{sled\_test,i}$ *and* $X_{simulation,i}$ = value at time point i

m = number of time points within the interval

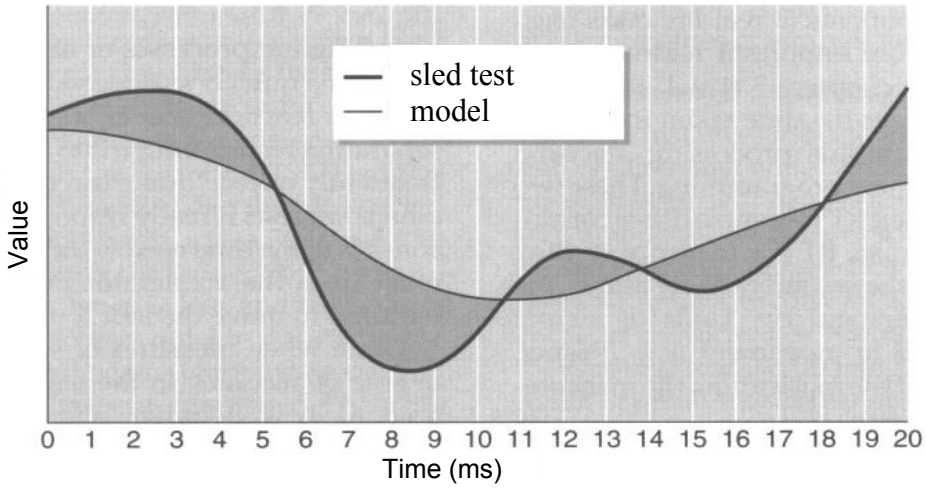

Figure 29 Representation of RMSNE [29]

The RMSNE was calculated using the time interval between two time points where the sled test time history crossed the horizontal axis, 0 Y-value (see Figure 30). The time increment used in the calculation was 0.1 ms. The first and the last sections of data, where data points were not stable, were excluded in calculation since it caused very high *Error* values and increased the RMSNE value substantially. The RMSNE value for each $VAR_{time\_history}$ of the Full_FE Belt model was calculated using the stabilized data points and presented in Table 13. The shoulder belt force showed the lowest RMSNE and lap belt force showed the highest RMSNE among all variables. The RMSNE values were very sensitive to a time interval, and depending on the time interval included, the RMSNE values varied.

Table 13 RMSNE for comparing trends of time histories

$VAR_{time\_history}$	Full_FE Belt
WC CG x-acc	0.323
Rear_R tiedown F	0.356
Rear_L tiedown F	0.290
Shoulder belt F	0.257
Lap belt F	0.425
Head acc	0.352
Chest acc	0.345
Average RMSNE	**0.34**

2.4.4.4 % Area difference

RMSNE "represents essentially (but not exactly) the area between [the model and the sled test], as shown by the shaded portions of Figure 29." [29] Therefore, to quantitatively evaluate how well the trends of time histories between a model and a sled test were matched, % Area difference was developed in this study (see Equation 5) and calculated for all $VAR_{time\_history}$ of the Full_FE Belt model. The % Area difference represents the area that is *not common* (A_{nc}) between two curves over the total area ($A_c + A_{nc}$) of two curves (see Figure 30). 0 % area

difference indicates complete overlap of the two curves, and therefore, a lower % area difference indicates a better correlation of two curves.

Equation 5 % Area difference

$$\% \text{ Area difference} = \frac{A_{nc}}{A_c + A_{nc}} * 100$$

A_{nc} = area that is not common between two curves

A_c = area that is common between two curves

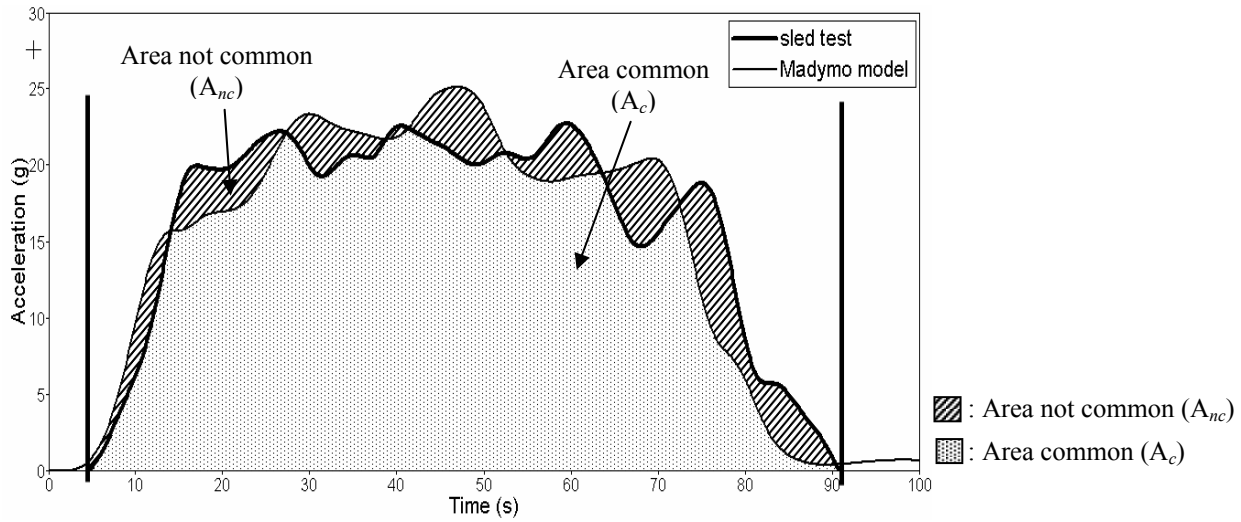

Figure 30 Representation of *common* and *not common* areas of a model vs. sled test

The % Area differences of the $VAR_{time\_history}$ for the model are shown in Table 14. The % Area differences was calculated using the time interval between two time points where the sled test time history crossed the horizontal axis, 0 Y-value (see Figure 30). The time increment used in the calculation was 0.1 ms. The % Area difference ranged from 15.8 % to 26.4 % with the average % Area difference of 20.5 %.

Table 14 Calculation of % Area difference

$VAR_{time\_history}$	Full_FE Belt (%)
WC CG x-acc	15.8
Rear_R tiedown F	19.7
Rear_L tiedown F	19.3
Shoulder belt F	19.0
Lap belt F	26.4
Head acc	22.8
Chest acc	20.6
Average % Area difference	**20.5**

2.4.4.5 Regression Analysis

To test whether a significant relationship exists between the peaks measured from the sled test and the peaks obtained from the model, linear regression analysis of the Full_FE Belt model versus the sled test was conducted. The null hypothesis was H_0: b=0, and the significance (alpha) level of 0.05 were used.

The results of the regression analysis are shown in Table 15. The correlation coefficient between the peaks measured from the sled test and the peaks obtained from the model was also calculated. r = 0.998 indicates strong linear relationship between the sled test peaks and the peaks generated from the model. r^2 of 0.996 indicates that 99.6 % of the sled test peaks is explained by the Full_FE Belt model peaks. Since $P = 0.000 < 0.05$, the H_0: b=0 is rejected. The results show that there is a linear relationship between the peaks measured from the sled test and the peaks obtained from the model.

Table 15 Regression analysis of the Full_FE Belt model versus the sled test

r	r^2	$y = a + bx$		T-statistic (P value)
		a	b	
0.998	0.996	6.075	0.937	43.508 ($P = 0.000$)

2.5 DISCUSSION

A MADYMO model representing a Zippie pediatric wheelchair with a seated Hybrid III 6-year-old ATD subjected to a 20g/48kph frontal crash was developed. The Full_FE Belt model (both shoulder and lap belts modeled with the FE belts) was developed through two preliminary steps; Step 1 – a Standard Belt model and Step 2 – an FE_Segment Belt model. The developed model was tuned by matching the trends and the peaks of time histories generated through the computer simulation to those of time histories measured during sled testing. Comparison of the time history profiles and peak values has typically been used to validate computer simulation models in the automotive industry [5] [15] [16] [17] [18] [19] [20]. In this study, after the comparison of the time history profiles, the model validation criteria, determined based on the previous crash simulation studies, were applied to evaluate the model. The model was found to comply with establish validation criteria.

Previous computer simulation studies which assessed the agreement between the computer simulation models and the experimental tests were reviewed [6] [21] [22] [23] [24] [30]. Table 16 shows the % Peak differences presented in the previous studies of adult wheelchair computer crash simulation models [6] [21] [22]. The average % Peak difference of the pediatric wheelchair model developed in this study, 8.1 %, falls within the range (4.1% to 15.6%) presented in the previous reviewed studies. The % Peak difference for individual variables (WC acceleration, rear tiedown forces, shoulder belt and lap belt forces, and ATD head and chest accelerations) of the pediatric wheelchair model, with a range of 1.5 to 15.8 %, also fall with in the range (0.6% to 28.1%) presented in the previous reviewed studies. This would indicate that the pediatric model developed in this study is a reasonable representation of a wheelchair crash simulation model.

Table 16 Comparison of the peak values between sled tests and computer models – adult wheelchairs (% Peak difference , %)

WC Model	SAE/ISO SurrogateWC [21]			Powerbase WC [6]		Manual WC w/ rigid seat [22]	Manual WC w/ sling seat [22]
Variable	UVA[1]	UMTRI[1]	MURSEL[1]	UMTRI	UVA	UMTRI	UMTRI
WC X acc	1.0	10.9	4.2	--	6.8	7.1	13.2
Head CG acc	10.7	3.0	5.8	1.4	7.7	7.5	15.7
Rear tiedown F	0.6	5.5	3.0	7.9	2.2	9.7	11.1
Shoulder belt F	4.8	11.8	9.4	8.4	8.5	11.2	28.1
Lap belt F	3.4	4.4	4.9	4.9	11.2	7.7	9.9
Average % Peak difference	**4.1**	**7.1**	**5.5**	**5.7**	**7.3**	**8.6**	**15.6**

The high % Peak difference of the wheelchair and ATD excursions shown in the Standard Belt model indicated that the model did not well represent the kinematics of the wheelchair and ATD of the sled test. Therefore, the occupant restraint belts were remodeled with the FE belts, which allowed the belts to slide over the ATD body surfaces, and the model was retuned using sled test data. The wheelchair and ATD kinematics were highly improved in the Full_FE Belt model (average % Peak difference of 11.3 %) compared to the Standard Belt model (average % Peak difference of 150.9 %).

Kinematics of the Full_FE Belt model were also evaluated by comparing the % Peak differences of the horizontal excursions resulting from this study to those reported in a recent TRL report, *The safety of wheelchair occupants in road passenger vehicles* [23]. The TRL study developed three adult wheelchair models; manual, electric, and surrogate [31] wheelchairs developed in MADYMO. In the TRL study, the models were validated through comparing the kinematics of the wheelchair and ATD resulting from the models to the sled test videos (see Table 17). The average % Peak difference of the Full_FE Belt model, 11.3 %, falls within the range presented in the TRL report, 6.4 % to 18.2 %. And the % Peak difference for three variables of the Full_FE Belt model (15.4 %, 7.7 %, and 10.7 %) also falls within the range

presented for the TRL models, 0 % to 23.7 %. Again, this provides further evidence of the developed pediatric FE Belt models meeting previously accepted standards of validation.

Table 17 Comparison of the peak horizontal excursions between TRL sled tests and computer models – adult wheelchairs [23]

Sled test	Manual wheelchair (mm)			Power wheelchair (mm)			Surrogate wheelchair (mm)		
	Test	Model	% Peak difference	Test	Model	% Peak difference	Test	Model	% Peak difference
Wheelchair excursion (mm)	91	111	22.0	123	109	11.4	156	153	1.9
Head excursion (mm)	485	528	8.9	639	639	0.0	541	479	11.5
Knee excursion (mm)	333	254	23.7	341	396	16.1	298	315	5.7
Average % Peak difference			**18.2**			**9.2**			**6.4**

The Pearson's correlation coefficient has previously been used to compare computer simulation results to experimental test results in previous computer simulation studies [24] [30]. The correlation coefficient across all $VAR_{time\_history}$ for the Full_FE Belt model ranged from 0.86 to 0.95 and fell with in the range deemed to meet validation criteria in previous studies ($r > 0.8$) [24]. General guidelines for interpreting the correlation coefficient (see Table 18), indicate that *r- values* above 0.8 are associated with "high" correlations between two compared groups [25]. The results presented in this study show that there are "high" correlations between the Full_FE Belt model and the sled test across all $VAR_{time\_history}$.

Table 18 Guidelines for interpreting correlation coefficient (*r*) [25]

Range of coefficients	Type of relationship
1.00 – 0.80	High
0.80 – 0.60	Moderate to High
0.60 – 0.40	Moderate
0.40 – 0.20	Low to Moderate
0.20 – 0	Low

In comparison of the time histories between the sled test the Full_FE Belt model, difference was observed in the trends of two shoulder belt force-time histories. The maximum shoulder belt force occurred earlier in sled testing (46 ms) than in the computer simulation model (73ms). The differences between the shoulder belt-ATD torso interaction in the model and sled testing may account for the differences between two force-time histories. During the sled testing, the shoulder belt was taped to the ATD's shirt, and the taped section of the shoulder belt was able to move with the shirt. Up to 46 ms (the first peak, 3862 N, in the sled test shoulder belt force-time history, Figure 23 – (d)), the shoulder belt was properly positioned and restrained the ATD's shoulder. At approximately 46 ms, while the ATD was still in the early phase of a frontal impact and in forward motion, the shoulder belt slid off the shoulder resulting in a decrease in belt force. After the shoulder belt slid off the shoulder, it restrained the upper arm of the ATD and reached the second peak (3300 N) in the force-time history (Figure 23 – (d)). In the model, a portion of the FE shoulder belt was attached to the ATD's upper torso. The attached part of the shoulder belt was fixed to the ATD's body and did not slide along the torso as in the sled test. Therefore, the shoulder belt restrained the ATD torso through out the impact without sliding off the shoulder reaching a peak force (3931 N) at 73ms (MADYMO shoulder belt force-time history, Figure 23 – (d)).

Differences between the sled test and the pediatric wheelchair model could also have resulted from the simplified wheelchair representation and estimations of contact characteristics. The wheelchair frame was represented in the model as one body; therefore, the model might not accurately represent the actual frame structure which could have absorbed more energy during impact. Moreover, the characteristics (contact characteristics and belt characteristics) used in the model were initially estimated based on the previous studies [22] [32]. If the load response

characteristics of the wheels, seat, seat back, and wheelchair tiedown straps could have been dynamically measured, then the model may more accurately represented the sled test. Another reason for differences can be that the model developed in this study used a Hybrid III 6-year-old anthromorphic model provided in MADYMO from TNO (TNO Automotive, Netherlands). Although the model has been calibrated and validated through component tests and sled tests, slight differences between the ATD responses of the computer model and ATD used in the sled test may exist.

The pediatric wheelchair model developed and validated in this study is the first computer crash simulation model representing a pediatric manual wheelchair with a seated Hybrid III 6-year-old ATD developed in MADYMO. Existing computer simulation models that have been developed and used in the field of wheelchair transportation safety represent only adult wheelchairs and adult occupants [6] [7] [8] [9] and have been developed using Articulated Total Body (ATB) simulation software. Compared to previous ATB models, MADYMO has more advanced capabilities, such as the ability to utilize both multi-body systems and finite element models. Moreover, MADYMO provides a variety of validated dummy models representing crash dummies available in the industry. The pediatric wheelchair model presented in this study will be a useful tool in studying the safety of pediatric wheelchair users in crashes and for manufacturers designing products for pediatric users seated in wheelchairs during transit.

2.6 CONCLUSION

In this study, the Full_FE Belt model was developed through two preliminary steps: Step 1 – a Standard Belt model and Step 2 – an FE_Segment Belt model. The Full_FE Belt model was validated using the model validation criteria which were determined based on the previous studies. Evaluation of the validated pediatric wheelchair model, including Adviser software,

regression analysis, etc., showed that the Full_FE Belt model provided a good representation of the sled test.

Studies conducted to-date on wheelchair transportation safety have primarily focused on adult wheelchair users and their wheelchairs, and there have been no previous studies published on children using wheelchairs in transit. The model developed and validated in this study, a manual pediatric wheelchair with a seated Hybrid III 6-year-old ATD subjected to a 20g/30mph frontal impact, provides a foundation for studying the response of a manual pediatric wheelchair in frontal crashes. The pediatric wheelchair model can also promote the study of injury risk associated with children traveling seated in their wheelchairs.

2.7 REFERENCES

1. Equal Employment Opportunity Commission and the U.S. Department of Justice. (1991). *Americans with Disabilities Act Handbook*. Washington: U.S Government Printing Office.
2. U.S. Department of Justice Civil-Rights Division. (May 2000). *A Guide to Disability Rights Laws*. Washington, DC.
3. McHenry, R. R., & Naab, K. N. (1966). Computer simulation of the crash victim - a validation study. *SAE, SAE Paper No. 660792*, 73-94.
4. Bartz, J. A. (1972). Development and validation of a computer simulation of a crash victim in three dimensions. *SAE, SAE Paper No. 720961*, 105-127.
5. Hou, J., Tomas, J., & Sparke, L. (1995). Optimization of driver-side airbag and restraint system by occupant dynamics simulation. *SAE, SAE Paper No. 952703*, 461-471.

6. Bertocci, G. E., Szobota, S., Hobson, D. A., & Digges, K. (1999). Computer Simulation and Sled Test Validation of a Powerbase Wheelchair and Occupant Subjected to Frontal Crash Conditions. *IEEE Transactions on Rehabilitation Engineering, 7*(2), 234-244.

7. Bertocci, G. E., Digges, K., & Hobson, D. (1996). Development of transportable wheelchair design criteria using computer crash simulation. *IEEE Transactions of Rehabilitation Engineering, 4*(3), 171-181.

8. Bertocci, G. E., Szobota, S., Ha, D., & vanRoosemalen, L. (2000). Development of Frontal Impact Crashworthy Wheelchair Seating Design Criteria Using Computer Simulation. *Journal of Rehab Research and Development, 37*(No. 5), 565-572.

9. Leary, A., & Bertocci, G. (2001). *Design Criteria for Manual Wheelchairs Used as Motor Vehicle Seats Using Computer Simulation.* Paper presented at the RESNA, Reno, Nevada.

10. Paskoff, G. (1995). *Transportation of Wheelchair Users - An Assessment of Neck Injury Risk During Rear Collisions.* Unpublished Masters thesis, University of Virginia, Virginia.

11. Arva, J. (September, 2002). Children's Specialized Hospital. Mountainside, NJ.

12. Wonsettler, T. (September, 2002.). The Children's Institute. Pittsburgh, PA.

13. ANSI/RESNA Subcommittee on Wheelchairs and Transportation (SOWHAT). (2000). *ANSI/RESNA WC/Vol 1: Section 19 Wheelchairs - Wheelchairs Used as Seats in Motor Vehicles*: ANSI/RESNA.

14. TNO Automotive. (2001). *MADYMO V6.0 Database Manual*. The Netherlands.

15. Jenkins, J., Ridella, S., & Ham, S. (2002). *Development of an Inflatable Knee bolster by using MADYMO and DOE.* Paper presented at the 9th International MADYMO User Conference.

16. Lee, W., & Feustel, J. R. (2002). *Use of Madymo DOE to Optimize D-ring Location.* Paper presented at the 9th International MADYMO User Conference.

17. Reed, S., Milosic, M., & Furtado, R. (2001). *Neck Injury Prevention in Automotive Seating Applications - Using MADYMO to Optimize Seat Parameters.* Paper presented at the 4th MADYMO User's Meeting of The America's.

18. Ridella, S. A., & Nayef, A. (2001). *Rollover: a methodology for restraint system development.* Paper presented at the 4th MADYMO User's Meeting of The America's.

19. Nieboer, J., Wismans, J., Versmissen, A., van Siagmaat, M., Kurawaki, I., & Ohara, N. (1993). Motorcycle Crash Test Modelling. *SAE Paper No. 933133*, 273-288.

20. Trella, T. J., Gabler, H. C., Kanianthra, J. N., & Wagner, J. J. (1991). Side Impact Crashworthiness Design: Evaluation of Padding Characterisitics through Mathmatical Simulations. *SAE Paper No. 912900*, 163-176.

21. Pilkey, W., Kang, W., & Shaw, G. (1994). *Crash Response of Wheelchair-occupant systems in transport.* Paper presented at the RESNA, Nashville, TN.

22. Leary, A. M. (2001). *Injury risk analysis and design criteria for manual wheelchairs in frontal impacts.* Unpublished Masters thesis, University of Pittsburgh, Pittsburgh.

23. Claire, M. L., Visvikis, C., Oakley, C., Savill, T., Edwards, M., & Cakebread, R. (2003). *The safety of wheelchair occupants in road passenger vehicles* (No. ISBN 0-9543339-1-9): TRL Limited.

24. Pipkorn, B., & Eriksson, M. (2003). *A Method to Evaluate the Validity of Mathematical Models.* Paper presented at the 4th European MADYMO Users Meeting, Brussels, Belgium.

25. Glasnapp, D. R., & Poggio, J. P. (1985). *Essentials of Statistical Analysis: for the Behavioral Sciences*. Columbus: Charles E. Merrill.

26. Portney, L. G., & Watkins, M. P. (2000). *Foundations of Clinical Research: Applications to Practive* (2nd ed.). Upper Saddle River: Prentice-Hall.

27. MECALOG Business Unit Safety. (October 2003 (Revision: 11/26/2003)). *Adviser V1.3.2 Reference Guide*.

28. Wismans, J. (October, 2003). TNO Automotive. The Netherlands.

29. Schmidt, R. A., & Lee, T. D. (1999). *Motor Control and Learning: a Behavioral Emphasis*. Champaign: Human Kinetics.

30. Gupta, S., van der Helm, F. C. T., Sterk, J. C., van Keulen, F., & Kaptein, B. L. (2004). Development and experimental validation of a three-dimentional finite element model of the human scapula. *Proceedings of the I MECH E Part H: Journal of Engineering in Medicine, 218*, 127-142.

31. International Standards Organization (ISO). (2001). *ISO 10542: Wheelchair Tiedown and Occupant Restraint Systems* (No. ISO 10542): ISO.

32. Ha, D. (2000). *Development of test methods for wheelchair seating systems used as motor vehicle seats and evaluation of wheelchair seating system crashworthiness.* Unpublished Masters thesis, University of Pittsburgh, Pittsburgh.

3 INJURY RISK ANALYSIS OF A 6 YEAR-OLD WHEELCHAIR-SEATED OCCUPANT IN A FRONTAL CRASH – SLED TEST DATA ANALYSIS

3.1 ABSTRACT

Children with disabilities are transported on a daily basis to schools and developmental facilities. When they travel, they often remain seated in their wheelchairs in vehicles. To study injury risks of pediatric wheelchair users in crashes, three pediatric manual wheelchairs were sled tested with a seated Hybrid III 6-year-old ATD using 20g/48kph frontal crash pulse. The sled test results were compared to injury criteria specified in the ANSI/RESNA WC-19, FMVSS 213 and FMVSS 208. All sled tests results fell below the injury criteria limits specified in the ANSI/RESNA WC-19 standard and FMVSS 213. All tests exceeded the N_{ij} limit of 1 specified in FMVSS 208, and one test exceeded the limit of peak neck tension force. Chest deflection resulting from one of three tests was at the limit specified in the regulation. Children with disabilities who remain seated in their wheelchairs in vehicles are at risk of injury to the neck and chest areas in a frontal impact motor vehicle crash. More research and regulations related to protection of children with disabilities in motor vehicle crashes are needed.

Keywords: pediatric wheelchair, 6-year-old Hybrid III ATD, injury risk, wheelchair transport safety

3.2 BACKGROUND

Injuries related to motor vehicle crashes (MVCs) are the leading cause of death for children over the age of one in the United States [1]. Therefore, to protect children from injuries and death in MVCs, extensive research has been conducted in the automotive industry, and federal and state laws related to child protection in MVCs have been established. Federal Motor Vehicle Safety Standard (FMVSS) 213 regulates the child restraint systems designed for children

weighing 50 lbs or less [2]. And recently, there has been an increase in concerns related to children who have outgrown booster seats but who have not yet reached adult stature. The result has been a proposal to extend the FMVSS 213 regulation to children weighing more than 50 lbs [3]. In June of 2003, National Highway Traffic Safety Administration (NHTSA) extended the FMVSS 213 to cover children weighing 50 to 65 lbs [4]. FMVSS 208 outlines the air bag deployment requirements in order to minimize the risk of injury resulting from deployment of an air bag [5]. The standard specifies injury criteria for different sized dummies, including child dummies (the 12-month-old CRABI dummy, the 3-year-old child dummy, and the 6-year-old child dummy).

Children with disabilities often cannot be seated in standard booster seats or automobile seats because of physical deformities or poor trunk and head control; they may differ anatomically from children who do not have disabilities or may lack sufficient balance while sitting due to trunk or head instability. The results of the survey study on transportation of children with disabilities conducted by Everly et al. indicated that a large percentage of children (44%) transported daily have poor head and trunk control and are therefore unable to sit upright without support [6]. Therefore, children with disabilities who must travel seated in their wheelchairs are often excluded from the protections dictated by the FMVSS 213, as well as by other laws relating to child protection in MVCs.

Federal laws such as the Americans with Disabilities Act (ADA) and the Individuals with Disabilities Education Act (IDEA), which prohibit discrimination against adults and children with disabilities, increase the number of disabled travelers [7] [8]. Children with disabilities are transported daily to schools and developmental educational facilities. The survey study conducted by Everly et al. shows that a majority of children using transportation services are

school aged children, 6 to 17 years old [6]. When children are transported, they often remain seated in their wheelchairs in vehicles, such as school buses and family vans.

Not only children with disabilities, but the overall number of disabled travelers seated in wheelchairs in public or private transportation has increased since the passage of the ADA. In order to improve the safety of wheelchair-seated travelers and other vehicle occupants, voluntary standards have been established by national and international organizations [9] [10] [11] [12]. However, with the exception of one standard, the American National Standards Institute (ANSI) / Rehabilitation Engineering and Assistive Technology Society of North America (RESNA) WC-19 *Wheelchairs for Use in Motor Vehicles*, test setup and performance requirements stated in the standards address only adult anthropomorphic test devices (ATDs) and adult wheelchairs.

The ANSI/RESNA WC-19 contains design and performance requirements as well as test procedures for wheelchairs used as forward-facing seats in motor vehicles. This standard applies to wheelchairs designed for adults and children with a body mass of 22 kg. It requires that a wheelchair be provided with two front and two rear securement points for attachment to a four-point, strap-type tiedown system. The standard also requires that the wheelchair, including wheelchair frame and seating systems, be sled-impact tested using a 20g/48kph (30mph) frontal crash pulse.

Research conducted to-date on wheelchair transportation safety has focused largely on adult wheelchair users. Therefore, studies on pediatric transit wheelchairs and the injury risks for pediatric wheelchair users in crashes are needed. In this study, the injury risks for manual pediatric wheelchair occupants in a frontal impact motor vehicle crash were assessed by analyzing frontal impact sled test data.

3.3 METHODS

Among pediatric manual wheelchairs available on the market, one with the transit option (transit wheelchair) was chosen for the study. A transit wheelchair is defined as a wheelchair that has been tested in accordance with the ANSI/RESNA WC-19 and provides four tiedown attachment points. Using the transit wheelchair would allow assessment of the injury risk for manual pediatric wheelchair occupants in a frontal impact motor vehicle crash independently from the injury due to the failure of the wheelchair. Sunrise Medical Zippie (Longmont, CO), one of the most commonly used transit pediatric manual wheelchairs, with the transit-tested standard conventional seating, which consisted of a padded solid seat and solid back, was used in the study.

Three Zippie wheelchairs having identical configuration (frame width and depth, caster size, rear wheel size, and seating systems) were sled tested with a seated Hybrid III 6-year-old ATD (Hybrid III 6). The pediatric wheelchair was placed on the sled platform, and the instrumented Hybrid III 6 was seated in the wheelchair (see Figure 31). The wheelchair was then secured to the sled platform using a surrogate four-point, strap-type tiedown, and the ATD was restrained with a surrogate, vehicle-anchored, three-point belt which includes a lap and shoulder belt. Sled tests were then conducted in accordance with the WC-19 standard, 48 km/h and 20-g average impact conditions. The deceleration pulses used for three sled tests with the pulse requirements stated in ANSI/RESNA WC-19 are shown in Figure 32.

The following variables were collected from the instrumented ATD during each sled test: head acceleration, chest acceleration, chest compression, and forces and moments at the dummy's upper neck. Data were collected at the rate of 10,000/sec. Moreover, the entire impact event was recorded using high-speed (1000 frames/sec) motion cameras positioned at the side of

the sled track to measure the wheelchair and the ATD excursions after the test. All signals were filtered following the requirements of SAE J211-2, instrumentation for impact testing.

The WC-19 standard requires the ATD to be kept in a seated posture in the wheelchair at the end of the test. It is determined by "the ATD torso being oriented at not more than 45 degrees to the vertical when viewed from any direction." [11] Posture of the ATD was examined at the end of each test.

Figure 31 Sled test setup

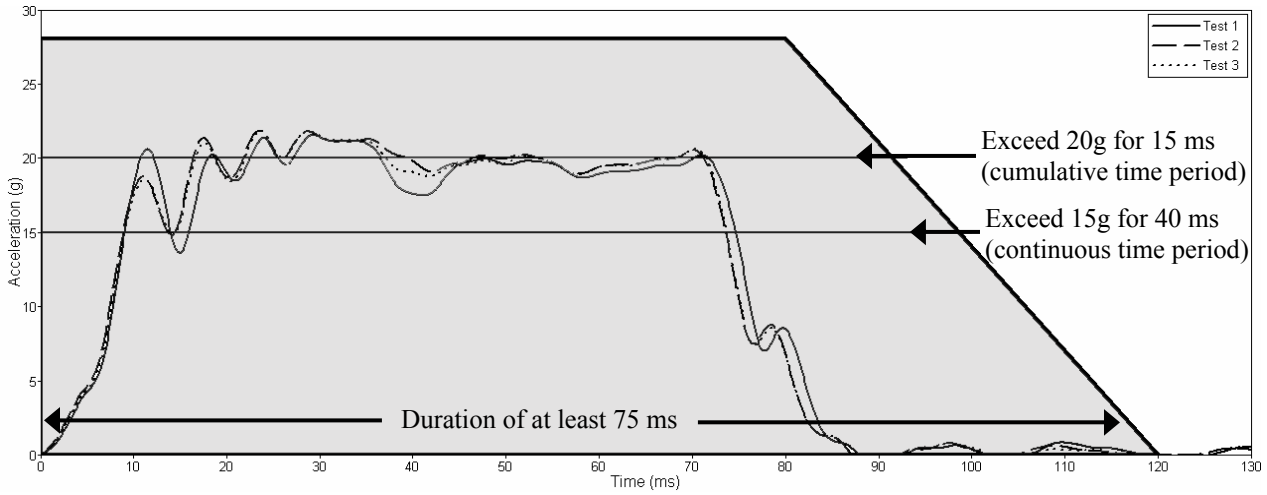

Figure 32 Sled deceleration pulses with ANSI/RESNA WC-19 corridor

Injury criteria and kinematic limits specified in the ANSI/RESNA WC-19 [11] and automotive regulations, FMVSS 213 [2] and FMVSS 208 [5], were applied to collected sled test data to determine the injury risk of a pediatric occupant in a wheelchair. The injury criteria and kinematic limits used for comparison with sled test data are shown in Table 19. FMVSS 213 injury criteria include a head injury criterion (HIC)* and a maximum resultant acceleration of the upper thorax sustained for three consecutive milliseconds (3ms clipped peak). Injury criteria for the Hybrid III 6-year-old ATD specified in FMVSS 208 include HIC_{15}, chest acceleration, chest compression deflection, N_{ij}, peak neck tension force, and peak neck compression force. HIC was calculated using Equation 6. N_{ij} was calculated using Equation 7.

Equation 6 Calculation of HIC

$$\mathrm{HIC} = \left[\frac{1}{(t_2 - t_1)} \int_{t_1}^{t_2} a_r \, dt \right]^{2.5} (t_2 - t_1)$$

$HIC_{unlimited}$: any two moments, t1 and t2, during the impact [2]

HIC_{36}: two moments, t1 and t2, separated by not more than 36 ms [4]

HIC_{15}: two moments, t1 and t2, separated by not more than 15 ms [5]

Equation 7 Calculation of Nij

$$Nij = \left(\frac{Fz}{Fzc} \right) + \left(\frac{Mocy}{Myc} \right)$$

Fz - axial force

Mocy - the occipital condyle bending moment

Fzc = 2800 N when Fz is in tension

Fzc = 2800 N when Fz is in compression

Myc = 93 Nm when a flexion moment exists at the occipital condyle

Myc = 37 Nm when an extension moment exists at the occipital condyle [5]

* On June 2003, $HIC_{umlimited}$ was replaced by HIC_{36} in FMVSS 213 [4]

Table 19 ANSI/RESNA WC-19, FMVSS 213, and FMVSS 208 injury criteria and kinematic limits of the 6-year-old ATD and a wheelchair

	ANSI/RESNA WC-19 [11]						FMVSS 213 [2] [4]			FMVSS 208 [5]				
	1	2	3	4	5	6								
	X_{wc} (mm)	X_{knee} (mm)	X_{headF} (mm)	X_{headR} (mm)	X_{knee}/X_{wc}	$(H_{pre}-H_{post})/H_{pre}$	$HIC_{unlimited}$	HIC_{36}	Chest acc (g)	HIC_{15}	Chest defl. (mm)	Nij	Neck tension (N)	Neck comp. (N)
Limit	150	300	450	-350	≥ 1.1	< 0.2	1000	1000	60	700	40	1	1490	1820

1 X_{wc} = the horizontal distance relative to the sled platform between the contrast target placed at or near point P on the test wheelchair at time t_0, to the point P target at the time of peak wheelchair excursion (point p = a wheelchair seat reference point located on the wheelchair reference plane approximately 50 mm above and 50 mm forward of the projected sideview intersection of the undepressed backrest and undepressed seat cushion) [11]

2 X_{knee} = the horizontal distance relative to the sled platform between the dummy knee-joint target at time t_0, to the knee joint target at the time of peak knee excursion [11]

3 X_{headF} = the horizontal distance relative to the sled platform between the most forward point on the dummy's head above the nose at time t_0, to the most forward point on the dummy's head at the time of peak forward head excursion [11]

4 X_{headR} = the horizontal distance relative to the sled platform between the most rearward point on the dummy's head at time t_0, to the most rearward point on the dummy's head at the time of peak rearward head excursion [11]

5 The wheelchair shall not impose forward loads on the ATD, which is considered to be achieved if the peak ATD knee excursion exceeds the peak wheelchair Point-P excursion by 10% [11]

6 The posttest height of the average of left and right ATD H-points relative to the wheelchair ground plane shall not decrease by more than 20% from the pretest height (H-point = A point located on the left and right sides of the buttock/pelvis region of a weighted manikin or ATD that represents the approximate human hip joint location relative to the back and bottom surfaces of the pelvic flesh) [11]

3.4 RESULTS

Figure 33 shows the post test pictures of the wheelchair and the ATD. In all three sled tests, the ATD was kept in a seated posture in the wheelchair as required in the ANSI/RESNA WC-19 standard. The ATD torso was kept within 45 degrees to the vertical when viewed from any direction. Table 20 shows the sled test results compared to ANSI/RESNA WC-19 horizontal excursion limits and injury criteria. The maximum horizontal excursions of the wheelchair and the ATD for all three tests were within the WC-19 limits. All tests complied with the limit, $X_{knee}/X_{wc} \geq 1.1$, which assures that the wheelchair did not load the ATD. And none of the three tests exceeded the $(H_{pre}-H_{post})/H_{pre}$ limit of 0.2, which evaluated integrity of seat surface and seat attachment hardware with the intent to prevent the occurrence of occupant submarining.

Table 20 Comparison between sled test results and ANSI/RESNA WC-19 injury criteria and kinematic limits

	ANSI/RESNA WC-19					
	X_{wc} (mm)	X_{knee} (mm)	X_{headF} (mm)	X_{headR} (mm)	X_{knee}/X_{wc}	$(H_{pre}-H_{post})/H_{pre}$ [1]
Limit	**150**	**300**	**450**	**-350**	**$\geq$ 1.1**	**< 0.2**
Test 1	17	56	283	-136	3.3	-0.05 (5% increase)
Test 2	13	57	230	-139	4.4	-0.03 (3% increase)
Test 3	13	65	252	-132	5.0	-0.03 (3% increase)

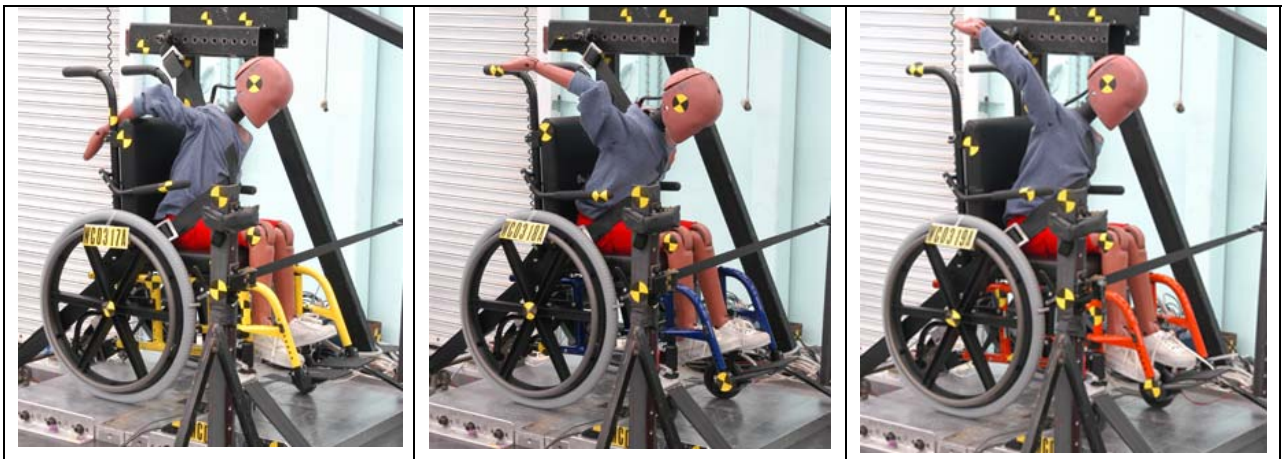

Test 1 | Test 2 | Test 3

Figure 33 Post sled tests

Table 21 shows the sled test results compared to FMVSS 213 and FMVSS 208 injury criteria. And Figure 34 shows the time histories of the head resultant acceleration of three sled tests which were used in the calculation of the HIC values. FMVSS 213 injury criteria assessed in this study included $HIC_{unlimited}$, HIC_{36}, and peak chest acceleration. In all tests, the $HIC_{unlimited}$ and HIC_{36} values remained below the limit of 1000. And no tests exceeded the maximum chest acceleration limit of 60 g. FMVSS 208 specifies injury criteria of HIC_{15}, chest deflection, neck tension, neck compression, and N_{ij}, neck injury criteria. All the HIC_{15} values resulting from the sled tests remained below the 700 limit. Chest deflection resulting from sled test 3 was at the limit specified in the regulation, which was 40 mm. Sled test 2 chest deflection value, 39.3 mm, also reached close to the 40 mm limit. Figure 35 shows the N_{ij} values for each sled test as compared to the limits specified in FMVSS 208. All tests exceeded the N_{ij} limit of 1 at the Tension Extension limit. The peak N_{ij} was observed at 52.8 ms in Test 1, 48.3 ms in Test 2, and 47.4 ms in Test 3 (see Figure 36). The peak neck tension force of Test 1, 1582 N, exceeded the

limit of 1490 N at 68.1 ms. Sled test 2 neck tension force, 1435 N, also reached close to the 1490 N limit. No tests exceeded the independent compressive neck force limits.

Table 21 Comparison between sled test results and FMVSS 213 and FMVSS 208 injury criteria

	FMVSS 213			FMVSS 208				
	$HIC_{unlimited}$	HIC_{36}	Chest acc (g)	HIC_{15}	Chest defl. (mm)	Nij	Neck ten. (N)	Neck comp. (N)
Limit	**1000**	**1000**	**60**	**700**	**40**	**1**	**1490**	**1820**
Test 1	520 (41-109 ms)	344 (55-91 ms)	52.0	208 (62-77 ms)	39.3	1.4*	1582	1128
Test 2	406 (35-109 ms)	276 (40-76 ms)	49.5	155 (62-77 ms)	37.0	1.4*	1435	669
Test 3	385 (34-95 ms)	275 (46-82 ms)	48.0	158 (64-79 ms)	40.0	1.3*	1231	241

* Tension extension
Note: Value exceeded the FMVSS limit was shaded in grey.

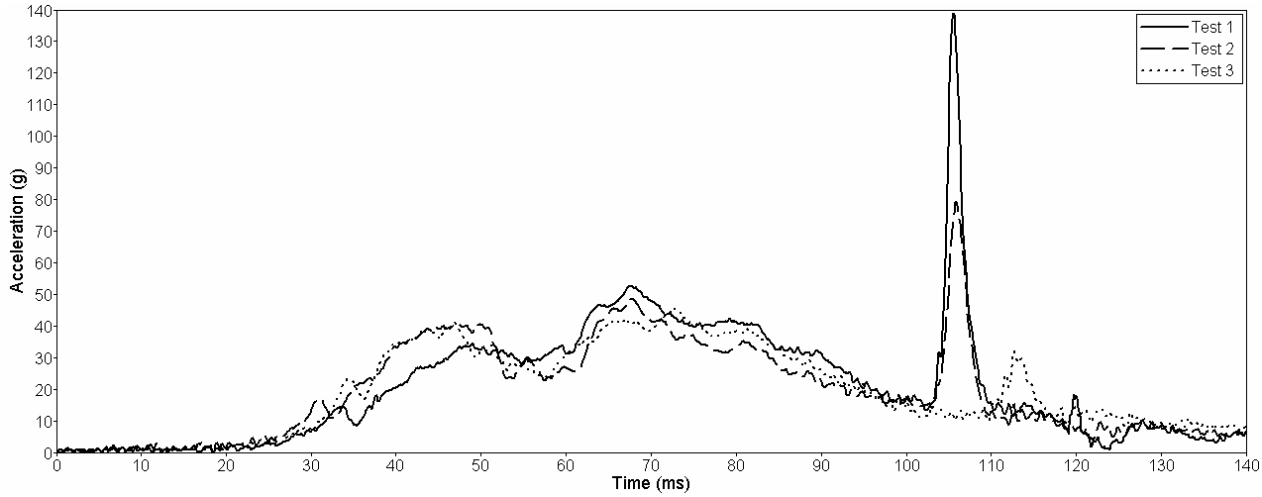

Figure 34 Head resultant acceleration

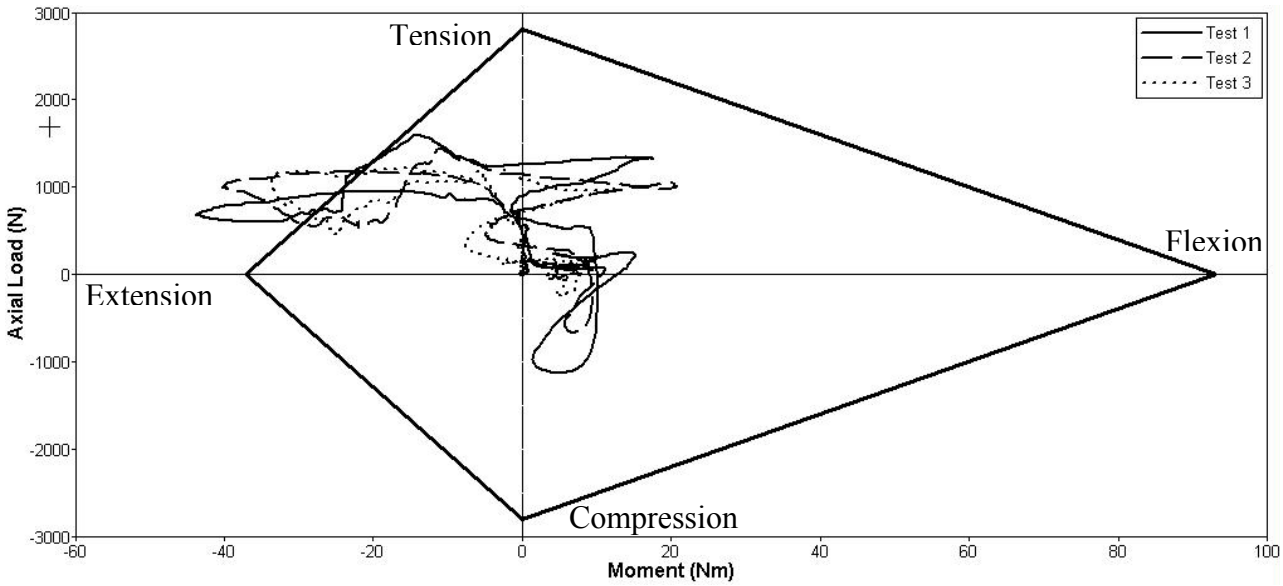

Figure 35 Nij – sled test results

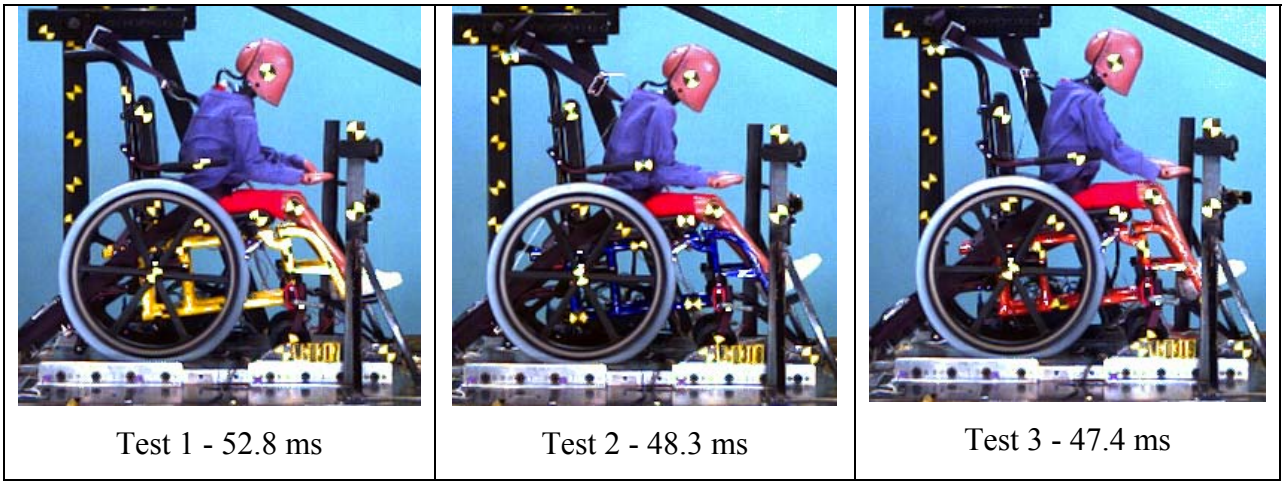

Figure 36 Sled test pictures at maximum Nij

3.5 DISCUSSION

To assess the injury risks of manual pediatric wheelchair occupants in a frontal impact motor vehicle crash, three pediatric manual wheelchairs, Zippie, were sled tested with a seated Hybrid III 6-year-old ATD in accordance with the ANSI/RESNA WC-19 standard. The sled test results were then compared to injury criteria specified in the ANSI/RESNA WC-19, FMVSS 213 and, FMVSS 208. FMVSS 208 requires measuring the chest deflection, neck forces, and neck

bending moments of the ATD in addition to the head and chest acceleration required in FMVSS 213. Therefore, FMVSS 208 requires using a Hybrid III 6-year-old ATD, which has more advanced instrumentation capabilities than a Hybrid II 6-year-old ATD, in compliance testing. A Hybrid II 6-year-old ATD can be equipped to measure head acceleration, chest acceleration, pelvis acceleration, and femur forces. With a Hybrid III 6-year-old ATD, chest deflection and neck forces and moments can also be measured in addition to the instrumentation available with a Hybrid II 6-year-old ATD.

The Hybrid III 6-year-old ATD was developed by the SAE Hybrid III Dummy Family Task Force, based on the information available on anthropometry and mass distribution characteristics of 6-year-old children in the United States [13] [14] [15] [16] [17] [18]. Because "there [was] virtually no literature dealing with biomechanical impact response of children," [19] biomechanical impact response requirements for head, neck, chest, and knees of 6-year-old ATD [20] were scaled from biomechanical response corridors of the mid size adult male, which were constructed from test data of human cadavers and volunteers [18] [21] [22] [23] [24] [25]. Replacement of Hybrid II 6-year-old ATD with Hybrid III 6-year-old ATD in FMVSS 213 was proposed by NHTSA to improve the evaluation of child restraint system performance in May, 2002 [3]. After the notice of proposed rulemaking (NPRM) was released [3], NHTSA received comments that expressed concerns about the biofidelity of the Hybrid III 6-year-old ATD's neck and upper chest areas. Several commenters stated that the Hybrid III 6-year-old ATD had more flexible neck and ribs than the Hybrid II 6-year-old ATD [4]. However, NHTSA stated in the Final Rule that "the neck of the HIII 6-year-old is currently performing within the specifications established by the Hybrid III Dummy Family Task Force of the Society of Automotive Engineers (SAE)," and the agency believed "the current neck on the HIII 6-year-old dummy [provided]

improved biofidelity over the current dummy, [Hybrid II 6-year-old dummy]." [4] As a result, the Hybrid III 6-year-old ATD was adopted into FMVSS 213 in the Final Rule in June, 2003.

Although a Hybrid III 6-year-old ATD provides improved biofidelity over that of a Hybrid II 6-year-old ATD, biofidelity of the Hybrid III 6-year-old ATD has not been confirmed by biomechanical impact response of child data. Hagedorn and Rhule conducted an accident reconstruction study to verify the injury criteria performance limits of child dummies in FMVSS 208 [26]. Reconstruction of incidents was chosen as an alternative approach to child cadaver testing, since "child cadaver availability [was] unknown, potentially very politically sensitive and of undetermined timeliness" [27]. Three accident cases were reconstructed in the study; one case involved a 7-year-old female child and two cases involved 5-month-old infants. The study focused on head and neck injuries to a child occupant. Three reconstruction tests were conducted for each case, and a Hybrid III 6-year-old ATD was used in the tests representing the accident involving a 7-year-old child. Based on the test results, the authors concluded that "the magnitude of [the loads measured from the neck load cell of a Hybrid III 6-year-old ATD] is consistent with the neck injuries received by the 7 year-old victim in this case who suffered transection of the spinal cord in the neck." [26] The N_{ij} values in the tests, which evaluate the potential for neck injury, were also well above the FMVSS 208 performance limit of 1. HIC values, which measure risk of head injury, were below the limit of 700 in all three tests. Authors stated that "[the results were] consistent with the minor head injuries of the case occupant, with the exception of the fractured left mandible. However, HIC is not expected to be a good predictor of mandibular injuries." [26]

Biofidelity of Hybrid III 6-year-old ATD was evaluated in the study conducted by Sherwood et al. [28]. 49 kph sled tests were conducted using a Hybrid III 6-year-old ATD, and

sled test results were compared to a 12-year-old cadaver test conducted at the University of Heidelberg (Heidelberg, Germany) [29]. The study focused on cervical spine injury risk for a 6-year-old child in frontal crashes. The authors concluded in the study that "the thoracic spine of the Hybrid III 6-year-old dummy is not biofidelic in restrained frontal crash tests" [28]. The authors also stated that "the stiff thoracic spine of the dummy results in high neck forces and moments that are not representative of the true injury potential" [28]. A limitation of this study was that the size of the 12-year-old cadaver was different from that of the Hybrid III 6-year-old ATD. The authors indicated in the study that "ideally comparisons to the dummy tests would be done with a cadaver of the same age and size, but this was not possible due to the small number of child cadaver tests available for comparison" [28]. A Hybrid III 6-year-old ATD was originally developed using the biomechanical impact response requirements derived from adult data. Therefore, verification of the performance of a Hybrid III 6-year-old ATD with the actual biomechanical impact response data of 6-year-old children is needed through such studies conducted by Hagedorn and Rhule [26] and Sherwood et al. [28], and if needed, then design changes should be made to a Hybrid III 6-year-old ATD to improve the biofidelity of the ATD.

In one of the comments that NHTSA received (in response to the NPRM), it was stated that due to the flexible neck of Hybrid III 6-year-old ATD, head-to-chest or head-to-knee contact was observed during sled tests and resulted in "unrealistic and unacceptably high HIC." [4]. NHTSA's response to the comment was that "none of the sled testing conducted with the HIII 6-year-old dummy [initiated or conducted by the agency had] indicated that head-to-chest or head-to-knee impacts [were] an issue. Such impacts [were] not typical." [4] The agency indicated that during one test, the shoulder portion of the occupant belt slipped off the ATD's shoulder and resulted in head-to-knee contact. Therefore, "NHTSA believes that if head-to-knee contact

occurs, there are likely design concerns with respect to the particular child restraint that should be addressed to eliminate such contact." [4] NHTSA also stated that if head-to-knee contact occurred during the sled test and resulted in a spike in head acceleration, then the spike needs to be included in the HIC computation.

Head-to-knee contact occurred in all three sled tests of a pediatric wheelchair with the Hybrid III 6-year-old ATD in this study. The spike in head acceleration was included in the calculation of the HIC value for each test, and all calculated HIC values remained below the limits specified in the standards. Similar to one of the sled tests conducted by NHTSA, the shoulder belt slipped off the ATD's shoulder during all three sled tests (see Figure 37). The occupant restraint system was setup in accordance with the WC-19 standard. In the frontal impact test method section of the standard, it is stated to "bolt the upper anchorage of the surrogate shoulder belt assembly to the rigid support structure at a location that provides a good fit of the shoulder belt to the ATD's chest and shoulder as illustrated in Figure." [11] However, the Figure provided in the WC-19 standard is for the midsize-male ATD, which might not be the proper position for an ATD other than the midsize-male. The misplacement of the shoulder belt during the tests might be due to the improper position of the shoulder belt upper anchor point. The preferred and optional zones for the shoulder belt upper vehicle anchor point for different sizes of occupants are provided in the Society of Automotive Engineers (SAE) Recommended Practice (RP) J2249, *Tiedowns and Occupant Restraint Systems* [9]. Use of the preferred zones for 6-year-old occupant size specified in the SAE PR J2249 in sled testing might prevent the shoulder belt from slipping off the ATD's shoulder during sled testing.

Figure 37 Post sled test should belt position

Chest deflection resulting from sled test 3 was at the limit specified in FMVSS 208, 40 mm. Sled test 1 and 2 chest deflections, 39.3 mm and 37 mm, also reached close to the limit. As stated previously, the occupant shoulder belt slipped off the ATD's shoulder during all three sled tests. The slippage of the shoulder belt moved the belt away from the chest deflection potentiometer as shown in Figure 37. The chest deflections could be higher if the shoulder belt did not slip off the shoulder.

To study the injury risks for manual pediatric wheelchair occupants in a frontal impact motor vehicle crash, a Hybrid III 6-year-old ATD was used in this study. Currently, a Hybrid III 6-year-old ATD, which represents the lower range of school aged children, is the largest child dummy available for the FMVSS compliance tests. In the automotive industry, because there has been an increase in concerns related to children who have outgrown booster seats but not yet reached adult stature, the Society of Automotive Engineers (SAE) began development of Hybrid

III 10-year-old ATD in 2000.[‡] "The 10-year-old was chosen because it is the transitional size at which [standard vehicle] belt fit and seat design may be adequate and a booster/safety seat may no longer be necessary."[§] To assess injury risks for children who travel seated in their wheelchairs in vehicles, testing of pediatric wheelchairs with a Hybrid III 10-year-old ATD is also needed in future studies.

3.6 CONCLUSION

When children with disabilities are transported to schools and developmental facilities, they often remain seated in their wheelchairs in vehicles, such as school buses and family vans. Children with disabilities who travel seated in their wheelchairs are often excluded from the protections dictated by the federal and state laws related to child protection in MVCs. To study the injury risks of manual pediatric wheelchair occupants in a frontal impact motor vehicle crash, three pediatric manual wheelchairs were sled tested with a seated Hybrid III 6-year-old ATD in accordance with the ANSI/RESNA WC-19 standard.

During three sled tests, the shoulder belt slipped off the ATD's shoulder, but the ATD was kept in a seated posture in the wheelchair as required in the ANSI/RESNA WC-19 standard. Injury criteria and kinematic limits specified in the ANSI/RESNA WC-19 standard, FMVSS 213 and, FMVSS 208 were applied to collected sled test data. All three tests complied with the criteria specified in the ANSI/RESNA WC-19 and FMVSS 213. Among injury criteria specified in FMVSS 208, all tests exceeded the N_{ij} injury criteria limit of 1 at the Tension Extension limit, and the peak neck tension force of Test 1 exceeded the limit of 1490 N. Chest deflection resulting from sled test 3 was at the 40 mm limit specified in the regulation.

[‡] http://www-nrd.nhtsa.dot.gov/vrtc/bio/child/hybIII10ysum.htm
[§] www.dentonatd.com/dentonatd/pdf/HIII10F.PDF

Study results presented in this paper show that children with disabilities who remain seated in their wheelchairs in vehicles are at risk of injury, especially to the neck and chest areas, in a frontal impact motor vehicle crash. The same level of safety and protection offered to children seated in OEM vehicle seats should be provided to children with disabilities seated in wheelchairs in vehicles. During all three sled tests, the N_{ij} (neck injury criterion) limit exceeded the Tension Extension limit. The risk of neck injury can be reduced by minimizing the rearward movement of the head and neck during motor vehicle crashes. Using a device that provides support at the head and neck areas and minimizes the head-neck rearward movement, such as head restraints, with a wheelchair in transit can reduce the risk of neck injury and also reduce the N_{ij} value, which measures the risk of neck injury. More research on the design and performance of head restraints used with transit wheelchairs is needed in the future.

Study results also showed that children with disabilities who remain seated in their wheelchairs in vehicles are at risk of chest injury in a frontal motor vehicle crash. For the pediatric population, three-point occupant restraint systems, which were used in this study, may not be the best occupant restraint system to provide protection during frontal crashes. Occupant restraint systems that allow the crash force to be distributed over larger contact areas can possibly reduce the risk of chest injury. Studies on designing of an occupant restraint system for children seated in wheelchairs in transit are also needed in the future.

3.7 REFERENCES

1. Centers for Disease Control and Prevention. Leading causes of death reports. *Available at: http://webapp.cdc.gov/sasweb/ncipc/leadcaus.html*, February 2003
2. National Highway Traffic Safety Administration (NHTSA). (1979). *FMVSS 213 Child Restraint Systems* (October, 2000 ed. Vol. 49 CFR 571.213).

3. National Highway Traffic Safety Administration (NHTSA). (2002). *Notice of proposed rulemaking (NPRM) on Federal Motor Vehicle Safety Standards; Child Restraint Systems* (Docket No. NHTSA-02-11707): NHTSA.

4. National Highway Traffic Safety Administration (NHTSA). (2003). *Final rule on Federal Motor Vehicle Safety Standards; Child Restraint Systems* (Docket No. NHTSA-03-15351): NHTSA.

5. National Highway Traffic Safety Administration (NHTSA). (1971). *FMVSS 208 Occupant Crash Protection* (October, 2000 ed. Vol. 49 CFR 571.208).

6. Everly, J. S., Bull, M. J., Stroup, K. B., Goldsmith, J. J., Doll, J. P., & Russell, R. (1993). A Survey of Transportation Services for Children with Disabilities. *The American Journal of Occupational Therapy, 47*(9), 804-810.

7. Equal Employment Opportunity Commission and the U.S. Department of Justice. (1991). *Americans with Disabilities Act Handbook*. Washington: U.S Government Printing Office.

8. U.S. Department of Justice-Civil Rights Division. (2000). *A Guide to Disability Rights Laws*. Washington, DC.

9. Society of Automotive Engineers (SAE). (1997). *SAE J2249: Wheelchair Tiedowns and Occupant Restraint Systems for Use in Motor Vehicles* (No. SAE J2249): SAE.

10. International Standards Organization (ISO). (2001). *ISO 10542: Wheelchair Tiedown and Occupant Restraint Systems* (No. ISO 10542): ISO.

11. ANSI/RESNA Subcommittee on Wheelchairs and Transportation (SOWHAT). (2000). *ANSI/RESNA WC/Vol 1: Section 19 Wheelchairs - Wheelchairs Used as Seats in Motor Vehicles*: ANSI/RESNA.

12. International Standards Organization (ISO). (2000). *ISO 7176-19: Wheelchairs Used as Seats in Motor Vehicles* (No. ISO 7176-19): ISO.

13. Weber, K., Lehman, R. J., & Schneider, L. W. (1985). *Child Anthropometry for Restraint System Design* (No. UMTRI-85-23). Ann Arbor, MI: University of Michigan.

14. Snyder, R. G., Schneider, L. W., Owings, C. L., Reynolds, H. M., Golumb, D. H., & Schork, M. A. (1977). *Anthropometry of infants, children and youths to age 18 for product safety design* (No. SP-450). Warrendale, PA: Society of Automotive Engineers.

15. Reynolds, H. M., Young, J. W., McConville, J. T., & Snyder, R. G. (1976). *Development and Evaluation of Masterbody Forms for Three-Year Old and Six-Year Old Child Dummies* (No. DOT HS-801-811). Ann Arbor, MI: University of Michigan.

16. *Anthropomorphic Test Dummy*. (No. DOT-HS-299-3-569)(December 1973). Final Report, Volume 1, NHTSA.

17. *Anthropometry of Motor Vehicle Occupants*. (No. DOT-HS-806-715)(April 1985). Final Report, Volume 1, NHTSA.

18. Hubbard, R. P., & McLeod, D. G. (1974). Definition and Development of a Crash Dummy Head. *SAE Paper No. 741193*.

19. National Highway Traffic Safety Administration (NHTSA). (June 1998). *Technical Report: Development and Evaluation of the Hybrid III type Six-Year-Old Child Dummy* (No. Docket 98-3972).

20. Irwin, A., & Mertz, H. J. (1997). Biomechanical Basis for the CRABI and Hybrid III Child Dummies. *SAE No. 973317*, 261-272.

21. Culver, C. C., Neathery, R. F., & Mertz, H. J. (1972). Mechanical Necks with Humanlike Responses. *SAE720959*.

22. Mertz, H. J., Neathery, R. F., & Culver, C. C. (1972). *Performance Requirements and Characteristics of Mechanical Necks*: General Motors Research Laboratories Symposium, Human Impact Response-Measurement and Simulation, Warren, MI.

23. Neathery, R. F. (1974). Analysis of Chest Impact Response Data and Scaled Performance Recommendations. *SAE74118*.

24. Horsch, J. D., & Patrick, L. M. (1976). Cadaver and Dummy Knee Impact Response. *SAE760799*.

25. Hodgson, V. R., & Tomas, L. M. (1971). Comparison of Head Acceleration Injury Indices in Cadaver Skull Fracture. *SAE 710854*.

26. Hagedorn, A. V., & Rhule, D. A. (June, 2001). Child injury tolerance through case reconstruction. *17th International Technical Conference on the Enhanced Safety of Vehicles, Paper No. 226*.

27. http://www-nrd.nhtsa.dot.gov/vrtc/bio/child/childinjurytol.htm.

28. Sherwood, C. P., Shaw, C. G., Van Rooij, R. W. K., Crandall, J. R., Orzechowski, K. M., Eichelberger, M. R., et al. (2003). Prediction of Cervical Spine Injury Risk for the 6-Year-Old Child in Frontal Crashes. *Traffic Injury Prevention, 2*, 206-213.

29. Kallieris, D., Schmidt, G., Barz, J., Mattern, R., & Schulz, F. (1978). *Response and Vulnerability of the Human Body at Different Impact Velocities in Simulated Three-Point Belted Cadaver Tests.* Paper presented at the 3rd IRCOBI Conference.

4 INVESTIGATION OF THE EFFECT OF DIFFERENT MANUAL WHEELCHAIR SETTINGS ON DYNAMIC RESPONSE OF A 6-YEAR-OLD WHEELCHAIR OCCUPANT AND OCCUPANT INJURY RISK DURING A FRONTAL MOTOR VEHICLE CRASH

4.1 ABSTRACT

To study injury risks of a 6-year-old wheelchair occupant in a frontal motor vehicle crash under different wheelchair setup scenarios (seat back angle, rear securement point vertical location with respect to wheelchair CG, and seat-to-back intersection horizontal location with respect to rear wheels), a parametric sensitivity analysis was conducted using a previously validated computer model. The model represents a Hybrid III 6-year-old ATD seated in a manual pediatric wheelchair subjected to a 20g/48kph frontal crash. Study results showed that altering wheelchair settings does have impact on kinematics and injury risk of a 6-year-old wheelchair occupant in a frontal motor vehicle crash. Results presented in this study also showed that a 6-year-old wheelchair seated occupant may be subjected to a risk of neck and chest injuries in a frontal impact motor vehicle crash. In order to improve the safety of pediatric wheelchair users in transit, additional studies are needed.

Keywords: computer simulation, pediatric wheelchair, injury risk, 6-year-old Hybrid III ATD, wheelchair transportation safety

4.2 BACKGROUND

To protect children from injuries and death in motor vehicle crashes (MVCs), extensive research has been conducted in the automotive industries, and federal and state laws related to child protection in MVCs have been established in the United States. Federal Motor Vehicle Safety Standard (FMVSS) 213 regulates child restraint systems [1], and all states have child passenger safety laws [2]. However, children with disabilities often cannot be seated in standard

booster seats or automobile seats because of physical deformities or poor trunk and head controls, and instead must be seated in their wheelchairs with specialized postural supports. The results of the survey study on transportation of children with disabilities conducted by Everly et al. indicated that a large percentage of children (44%) transported daily have poor head and trunk control and are therefore unable to sit upright without support [3]. Therefore, children with disabilities who must travel seated in their wheelchairs are often excluded from the protections dictated by FMVSS 213, as well as by other laws relating to child protection in MVCs.

Disability laws, such as Americans with Disabilities Act (ADA) and the Individuals with Disabilities Education Act (IDEA), prohibit discrimination of children with disabilities and promote disabled children obtaining education along with non-disabled children. Therefore, children with disabilities are transported on a daily basis to schools and developmental facilities. When children with disabilities are transported, they often remain seated in their wheelchairs in vehicles. In order to improve the safety of wheelchair-seated travelers, voluntary standards, which have not been mandated by state or federal laws, have been established by national and international organizations [4] [5] [6] [7]. Research conducted to-date on wheelchair transportation safety, including wheelchair occupant injuries in a crash, have focused largely on adult wheelchair users. It is likely that pediatric wheelchair occupants respond differently in crashes than adult occupants, and therefore, research related to injury risks associated with pediatric wheelchair users in crashes is needed.

Children can outgrow a wheelchair in a year or two yet many funding agencies only fund the purchase of a wheelchair every four to five years [8]. Therefore, many pediatric wheelchairs are design to ‘grow’ with children [9] [10]. The wheelchair frame and seating components can be adjusted to serve growing children. Previous studies on adult transit wheelchairs showed that

altering wheelchair settings and wheelchair tiedown position do have an impact on occupant kinematics and occupant injury risks [11] [12] [13]. In this study, the dynamic response and injury risk of a 6-year-old wheelchair occupant during a frontal motor vehicle crash under different wheelchair setup scenarios (seat back angle, rear securement point vertical location with respect to wheelchair center of gravity (CG), and seat-to-back intersection horizontal location with respect to rear wheels) were investigated using the previously validated computer crash simulation model (Chapter 2).

4.3 METHODS

A previously developed MADYMO (V6.01) computer simulation model representing a Hybrid III 6-year-old anthropomorphic test device (ATD) seated in a manual pediatric wheelchair (Sunrise Medical Zippie) subjected to a 20g/48kph (30 mph) was used in this study. In the model, the wheelchair was secured to the sled platform using a surrogate four-point, strap-type tiedown, and the ATD was restrained with a vehicle-anchored, three-point occupant restraint belts (see Figure 38). The model was validated using 20g/48kph frontal impact sled test data. The sled test setup conditions are shown in Table 22.

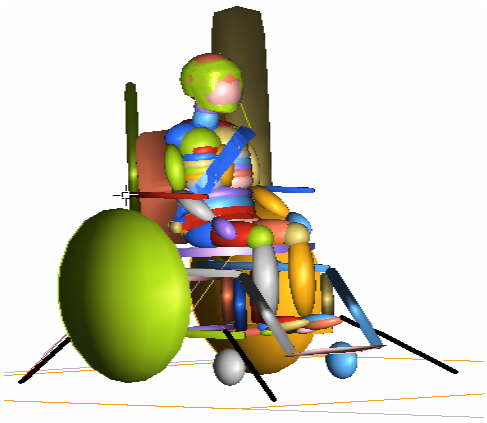

Figure 38 MADYMO model of a Hybrid III 6-year-old ATD seated in a pediatric manual WC

Table 22 Sled test setup (baseline) conditions

Wheelchair Type	Sunrise Medical Zippie
Wheelchair Securement	Surrogate 4-point strap-type tiedown
Occupant Restraint	Surrogate independent 3-point belt
Anthropomorphic Test Dummy	Hybrid III 6-year-old, 25kg
Target Impact Velocity (ΔV)	48 kph
Target Average Sled Deceleration	20g
Wheelchair	
Wheelchair Weight	18.6 kg
Wheelchair $CG_{vertical}$	359 mm above ground
Wheelchair $CG_{horizontal}$	188 mm front of rear hub
Wheelchair Rear Hub Height	280 mm above ground
Wheelchair Tiedown	
Front Securement Point	419 mm front of rear hub
	191 mm above ground/ 168 mm below CG_{WC}
Rear Securement Point to Rear Hub	105 mm behind rear hub
	315 mm above ground/ 44 mm below CG_{WC}
Wheelchair Seating System	
Seat Back Angle	4 º
Seat Pan Angle	3 º
Seat-to-back Intersection Location	23 mm front of rear hub

Note: Parameters investigated in the parametric sensitivity analysis are shaded in grey.

The axle positioning and seat back angle are adjustable on the Zippie pediatric manual wheelchair. Axle positioning can change the seating system location (seat-to-back intersection location) relative to the rear wheels, as well as the rear securement point vertical location. To study the effect of adjustable wheelchair features on dynamic response and injury risks of a 6-year-old wheelchair occupant during a frontal motor vehicle crash, a parametric sensitivity analysis was conducted. Each parameter (seat back angle, rear securement point vertical location, and seat-to-back intersection horizontal location) was varied independently while all other parameters remained at their baseline; baseline values were established from the sled test setup. Baseline conditions of the wheelchair model are described in Table 22. The seat back

angle (SBA) was varied from -5º to 35º (see Figure 39-a), the rear securement point (SP) vertical location was varied from 200 mm below the center of gravity of the wheelchair (-200 CG_{WC}) to 100 mm above the CG_{WC} (+100 CG_{WC}) (see Figure 39-b), and the seat-to-back intersection (STBI) horizontal position ranged from 100 mm behind the rear hub (R100) to 100 mm in front of the rear hub (F100) (see Figure 39-c).

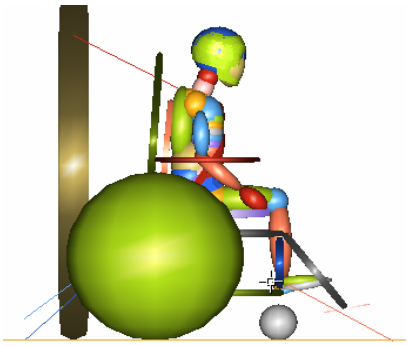

-5º seat back

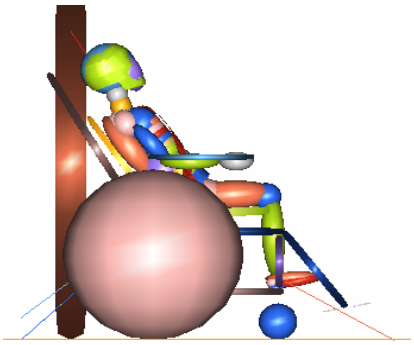

35º seat back

(a)

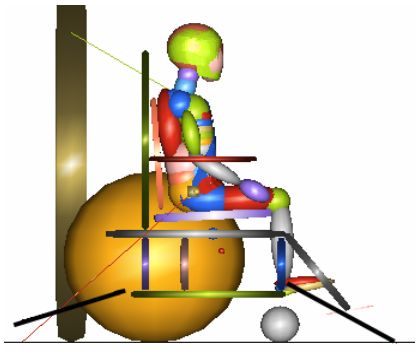

rear securement - 200 mm below CG_{WC}

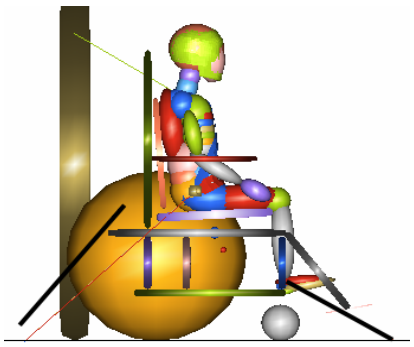

rear securement - 100 mm above CG_{WC}

(b)

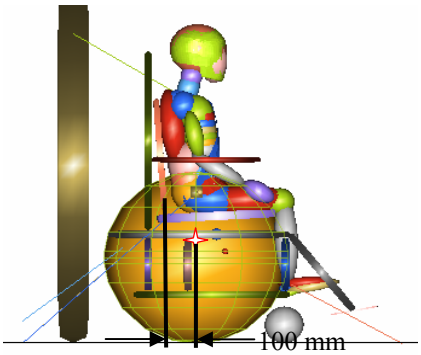

seat-to-back intersection - 100 mm behind the rear hub

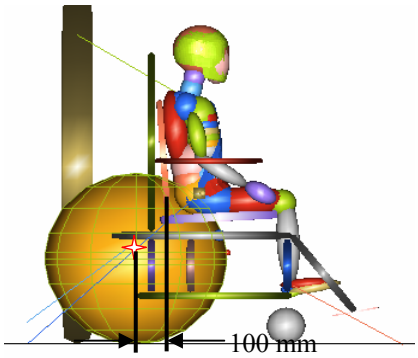

seat-to-back intersection - 100 mm behind the rear hub

(c)

Figure 39 Parameters varied in Parametric Sensitivity Analysis

Each model was programmed to generate ATD head acceleration, chest acceleration, chest compression, and upper neck forces and moments. The computer model was also programmed to generate time/history positions of the wheelchair, ATD knee, ATD head, and ATD H-point, representing the hip joint location. The model was run through 400 ms to capture a complete occupant rebound phase. The 'Time_Step' used in the model was 0.00002 s. Data was generated every 0.0001 s, and animation output was generated every 0.002 s.

Generated data were compared to the injury criteria and kinematic limits specified in the ANSI/RESNA WC-19 standard [6] and automotive regulations, FMVSS 213 [1] and FMVSS 208 [14], to determine injury risk. Horizontal excursion limits for pediatric wheelchair and 6-year-old occupant specified in the ANSI/RESNA WC-19 are shown in Table 23. The injury criteria for the Hybrid III 6-year-old ATD specified in FMVSS 213 and FMVSS 208 are provided in Table 24. FMVSS 213 injury criteria include the Head Injury Criterion (HIC)[**] and the maximum resultant acceleration of the upper thorax sustained for three consecutive milliseconds. Injury criteria specified in FMVSS 208 include HIC_{15}, chest acceleration, chest compression deflection, N_{ij}, peak neck tension force, and peak neck compression force.

[**] On June 2003, $HIC_{umlimited}$ was replaced by HIC_{36} in FMVSS 213 [15]

Table 23 ANSI/RESNA WC-19 horizontal excursion limits of the 6-year-old ATD and wheelchair [6]

	X_{wc} (mm)	X_{knee} (mm)	X_{headF} (mm)	X_{headR} (mm)	X_{knee}/X_{wc}
ANSI/RESNA WC-19 limit	150	300	450	-350	$\geq$ 1.1

X_{wc} = the horizontal distance relative to the sled platform between the contrast target placed at or near point P on the test wheelchair at time t_0, to the point P target at the time of peak wheelchair excursion (point p = a wheelchair seat reference point located on the wheelchair reference plane approximately 50 mm above and 50 mm forward of the projected sideview intersection of the undepressed backrest and undepressed seat cushion)

X_{knee} = the horizontal distance relative to the sled platform between the dummy knee-joint target at time t_0, to the knee joint target at the time of peak knee excursion

X_{headF} = the horizontal distance relative to the sled platform between the most forward point on the dummy's head above the nose at time t_0, to the most forward point on the dummy's head at the time of peak forward head excursion

X_{headR} = the horizontal distance relative to the sled platform between the most rearward point on the dummy's head at time t_0, to the most rearward point on the dummy's head at the time of peak rearward head excursion

X_{knee}/X_{wc} - The wheelchair shall not impose forward loads on the ATD, which is considered to be achieved if the peak ATD knee excursion exceeds the peak wheelchair Point-P excursion by 10% [6]

Table 24 FMVSS 213 and FMVSS 208 injury criteria of the 6-year-old ATD

	FMVSS 213 [1] [15]		FMVSS 208 [14]				
	HIC_{36}	Chest acceleration (g)	HIC_{15}	Chest deflection (mm)	N_{ij}	Neck tension (N)	Neck compression (N)
limit	1000	60	700	40	1	1490	1820

Except the peak rearward head excursion (X_{headR}), all data were analyzed up to 200 ms since the model and validating sled tests used a 0 to 200 ms time frame. Since the peak rearward head excursion was expected to occur during the occupant rebound phase, time/history excursion of ATD's head was analyzed up to 400 ms to capture the complete occupant rebound phase.

Animation output generated from the model were used to evaluate the dynamic response of the Hybrid III 6-year-old (occupant kinematics) in the 20g/48kph frontal impact under different setup conditions.

4.4 RESULTS

Figure 40 shows the 20g/48kph frontal crash response of the 6-year-old Hybrid III ATD and wheelchair for the baseline model with a 4° SBA, rear SP 44 mm below the CG_{WC} and a STBI at 23 mm forward of the rear hub (Table 22).

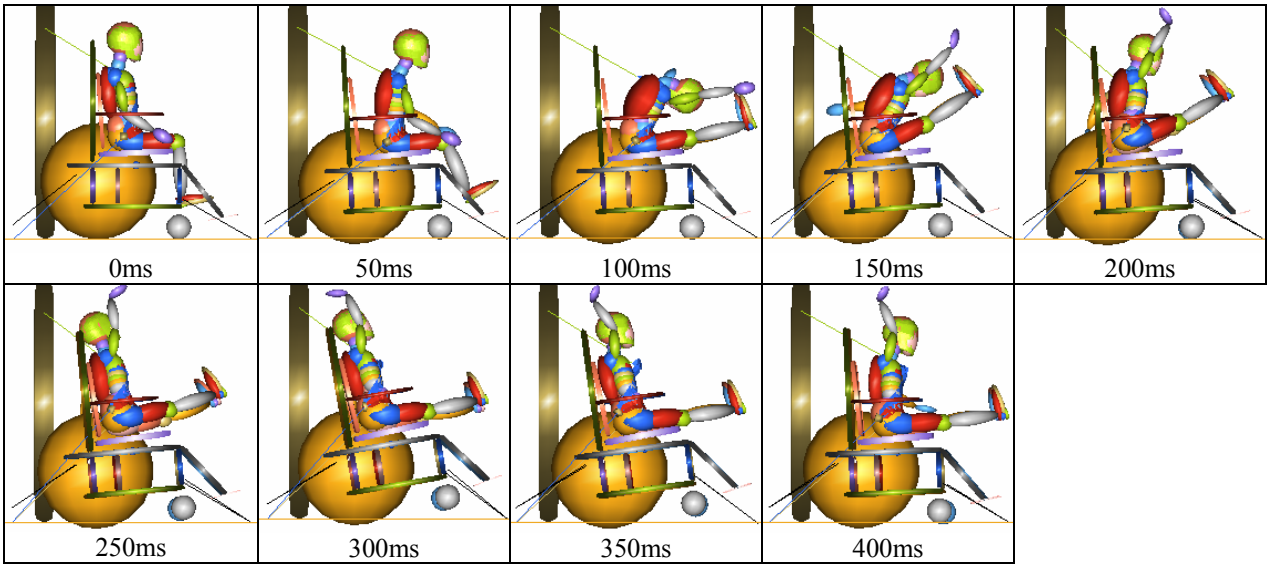

Figure 40 Crash response of the ATD and wheelchair: baseline model

4.4.1 Wheelchair Seatback Angle

The horizontal excursions resulted from the models with varied seat back angle were compared to the ANSI/RESNA WC-19 excursion limits (see Table 25). The maximum horizontal excursions of the wheelchair and the ATD for all models with different seat back angles were within WC-19 limits. All models complied with the conditions, $X_{knee}/X_{wc} \geq 1.1$, which assures that the wheelchair did not load the ATD. The peak forward head excursion increased from 209 mm to 363 mm as seat back angle increased from -5° to +35°.

Table 25 Comparison between computer model results and ANSI/RESNA WC-19 peak horizontal excursion limits: -5º to 35 º seat back angle

	X_{wc} (mm)	X_{knee} (mm)	X_{headF} (mm)	X_{headR} (mm)	X_{knee}/X_{wc}
WC-19 limit	**150**	**300**	**450**	**-350**	**≥ 1.1**
Seat Back Angle (º)					
-5	15	80	209	-117	5.4
Baseline (+4)	15	70	225	-121	4.7
+15	15	66	255	-119	4.3
+25	16	74	299	-115	4.6
+35	17	78	363	-73	4.5

Table 26 shows the comparison of the results of the models with varied SBA to the FMVSS 213 and FMVSS 208 injury criteria. FMVSS 213 injury criteria assessed in this study included HIC_{36} and peak chest acceleration. In all models, the HIC_{36} value and peak chest acceleration remained below the limits of 1000 and 60g, respectively. As seat back angle was increased from -5° to +35º, the HIC_{36} value increased and the peak chest acceleration decreased.

FMVSS 208 specifies injury criteria of HIC_{15}, chest deflection, neck tension, neck compression, and N_{ij} (neck injury criteria). All HIC_{15} values resulting from the models remained under the 700 limit (Table 26). All models exceeded the chest deflection limit of 40 mm and the N_{ij} injury criteria of 1 at the Tension Extension limit (Table 26). Figure 41 shows the N_{ij} values for the models, -5º, +15°, and +35° SBA, as compared to the limits specified in FMVSS 208. The peak neck tension of all models also exceeded the limit of 1490 N. The neck tension force increased from 1587 N to 1886 N as seat back angle increased from -5° to +35º. None of the models exceeded the independent compressive neck force limit of 1820 N.

Table 26 Comparison between computer model results and FMVSS injury criteria: -5º to 35 º seat back angle

	FMVSS 213		FMVSS 208				
	HIC_{36}	Chest acceleration (g)	HIC_{15}	Chest deflection (mm)	N_{ij}	Neck tension (N)	Neck compression (N)
FMVSS limit	**1000**	**60**	**700**	**40**	**1**	**1490**	**1820**
Seat Back Angle (º)							
-5	404	52	241	44	1.1	1587	24
Baseline (+4)	429	50	262	42	1.2	1662	36
+15	480	46	282	45	1.2	1718	115
+25	523	45	295	45	1.3	1717	356
+35	558	40	355	43	1.3	1886	543

Note: Value exceeded the FMVSS limit was shaded in grey.

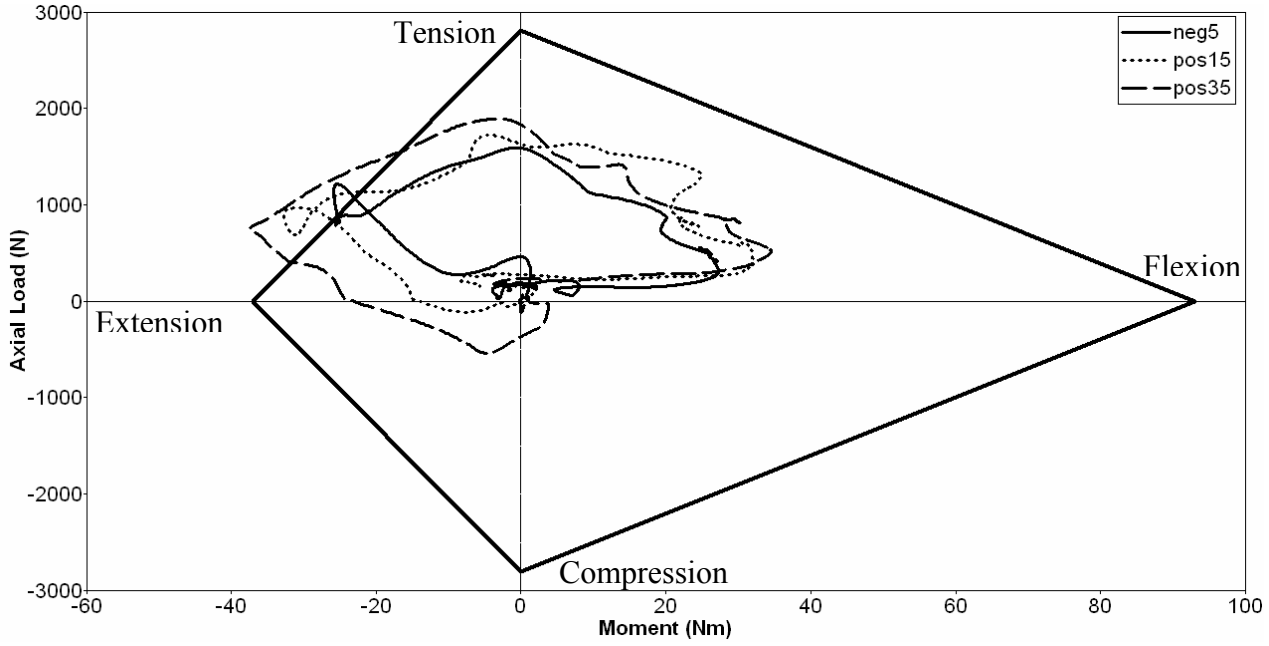

Figure 41 Nij: -5º, +15°, and +35° seat back angles

Figure 42 through Figure 45 show the crash response of the ATD and the wheelchair for each model with varying seat back angle. As the seat back angle increased, there was an

increased tendency of “ramping” (the ATD moved upward along the seat back surface) during the rebound phase. Head-neck extension increased as the seat back angle increased from -5° to +35°.

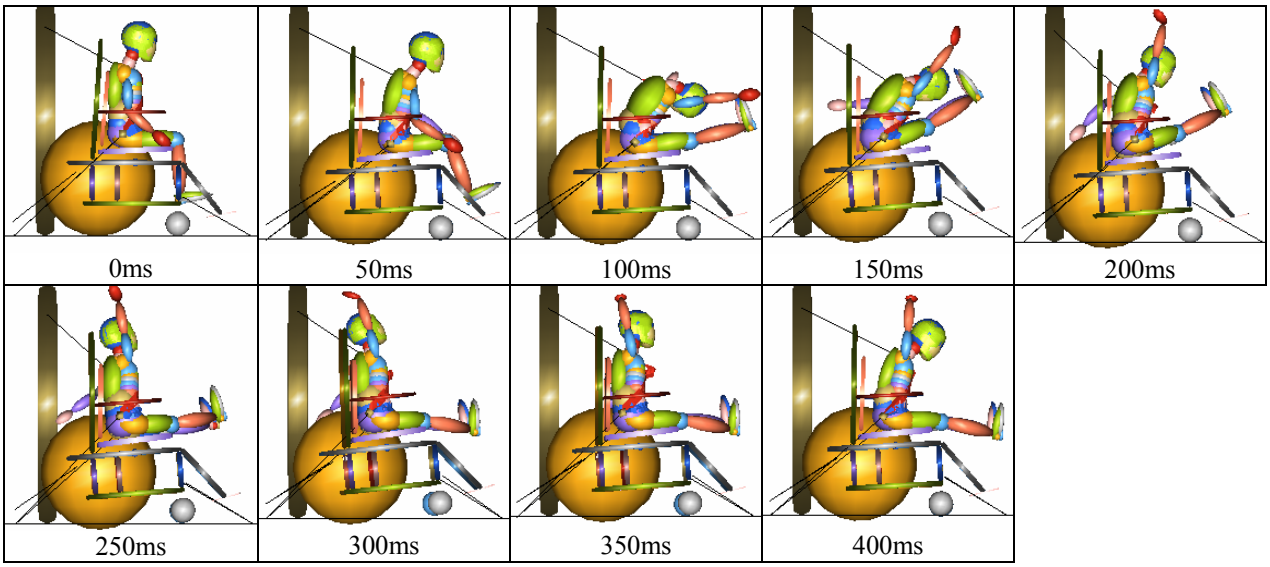

Figure 42 Crash response of the ATD and wheelchair: -5° seat back

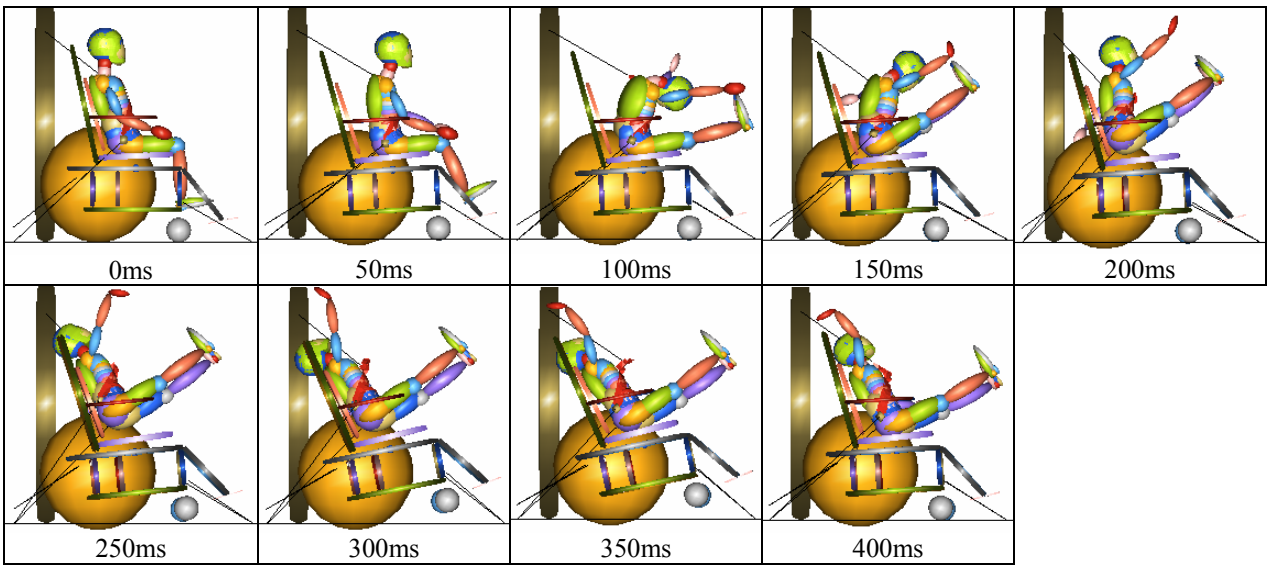

Figure 43 Crash response of the ATD and wheelchair: 15° seat back

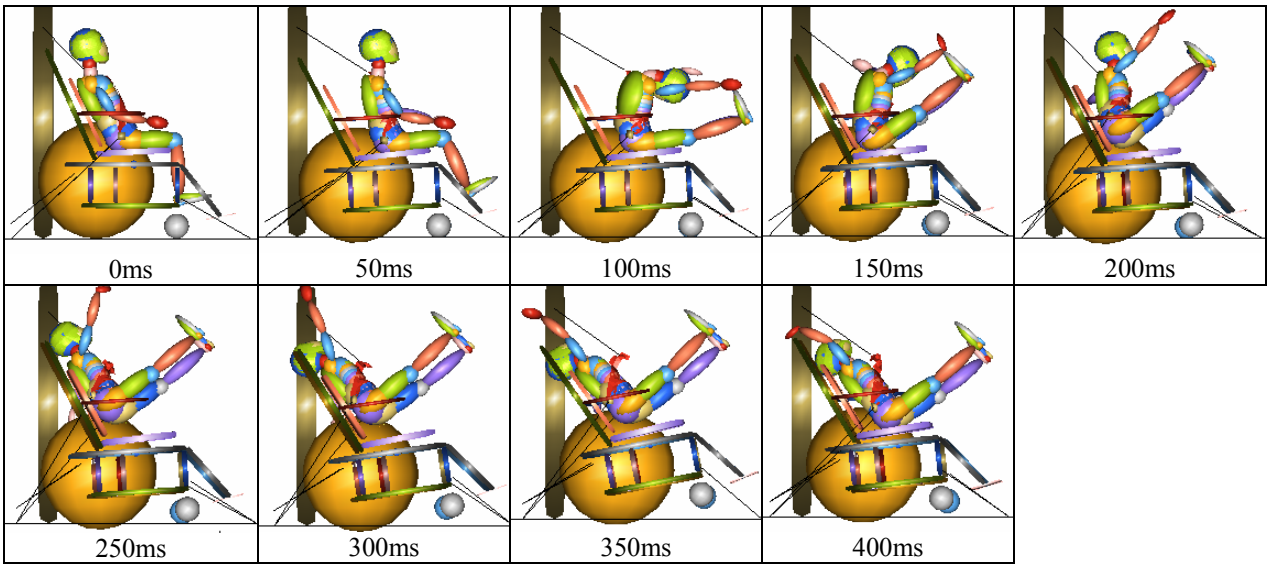

Figure 44 Crash response of the ATD and wheelchair: 25° seat back

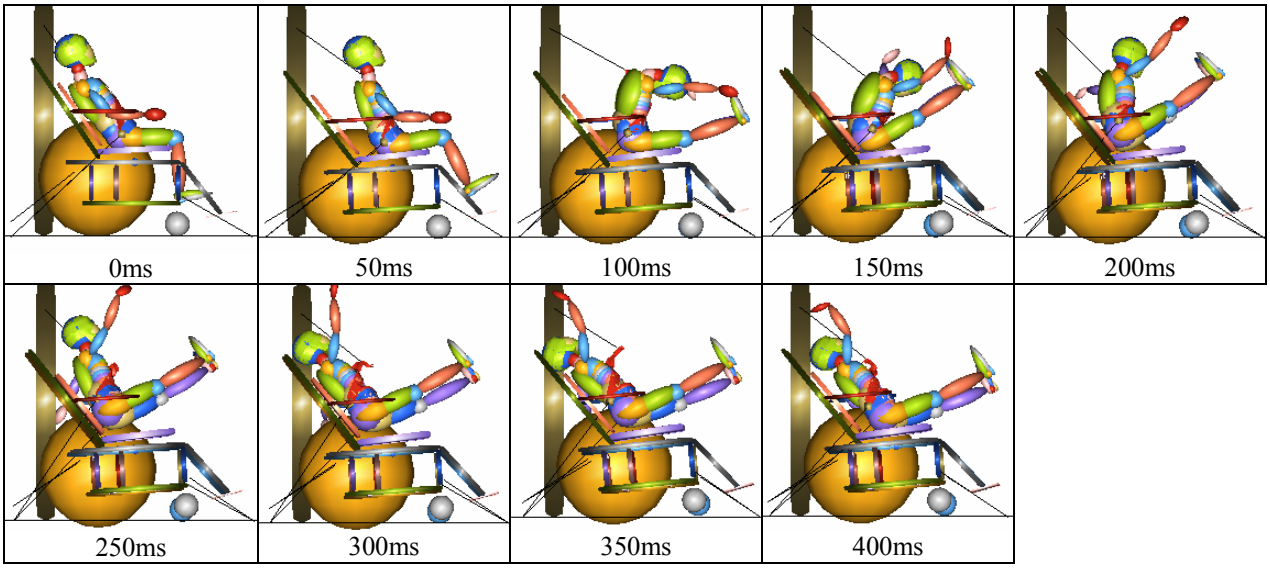

Figure 45 Crash response of the ATD and wheelchair: 35° seat back

4.4.2 Rear Securement Point Vertical Location

Horizontal excursions resulting from the models with varied rear SP location were compared to the ANSI/RESNA WC-19 limits (Table 27). The maximum horizontal excursions of the wheelchair and the ATD for all models with different rear SP location fell within the WC-

19 limits. Although all models complied with the limit, $X_{knee}/X_{wc} \geq 1.1$, when the rear SP was positioned 100 mm above the CG_{WC}, the X_{knee}/X_{wc} value (1.2) was very close to the limit of 1.1. The peak rearward head excursion increased from 58 mm to 222 mm as the rear SP was raised from -200 CG_{WC} to +100 CG_{WC}.

Table 27 Comparison between computer model results and ANSI/RESNA WC-19 horizontal excursion limits: rear SP positioned 200mm below CG_{WC} to 100mm above CG_{WC}

	X_{wc} (mm)	X_{knee} (mm)	X_{headF} (mm)	X_{headR} (mm)	X_{knee}/X_{wc}
WC-19 limit	**150**	**300**	**450**	**-350**	**≥ 1.1**
Rear SP position wrt CG_{WC} (mm)					
-200	13	66	228	-58	5.1
-100	8	68	226	-89	8.5
Baseline (-44)	15	70	225	-121	4.7
0 (at CG_{WC})	25	71	224	-155	2.8
+100	61	75	219	-222	**1.2**

Table 28 shows the results of the models with varied rear SP position compared to the FMVSS 213 and FMVSS 208 injury criteria. In all models, the HIC_{36} value and peak chest acceleration fell below the limit of 1000 and 60g, respectively. All HIC_{15} values resulting from the models also remained under the 700 limit. All models exceeded the chest deflection limit of 40 mm and the N_{ij} injury criteria of 1 at the Tension Extension limit. Figure 46 shows N_{ij} values for the models, -200 CG_{WC}, at CG_{WC}, and +100 CG_{WG}, as compared to the limits specified in FMVSS 208. The peak neck tension force of all models also exceeded the limit of 1490 N. The neck tension force increased from 1621 N to 1811 N as the rear SP was raised from -200 CG_{WC} to +100 CG_{WC}. None of the models exceeded the independent compressive neck force limit of 1820 N.

Table 28 Comparison between computer model results and FMVSS injury criteria: rear SP positioned 200mm below CG_{WC} to 100mm above CG_{WC}

	FMVSS 213		FMVSS 208				
	HIC_{36}	Chest acceleration (g)	HIC_{15}	Chest deflection (mm)	N_{ij}	Neck tension (N)	Neck compression (N)
FMVSS limit	**1000**	**60**	**700**	**40**	**1**	**1490**	**1820**
Rear SP position wrt CG_{WC} (mm)							
-200	460	50	260	43	1.2	1621	40
-100	436	50	254	42	1.2	1640	35
Baseline (-44)	429	50	262	42	1.2	1662	36
0 (at CG_{WC})	435	51	282	43	1.2	1683	38
+100	497	50	337	41	1.1	1811	42

Note: Value exceeded the FMVSS limit was shaded in grey.

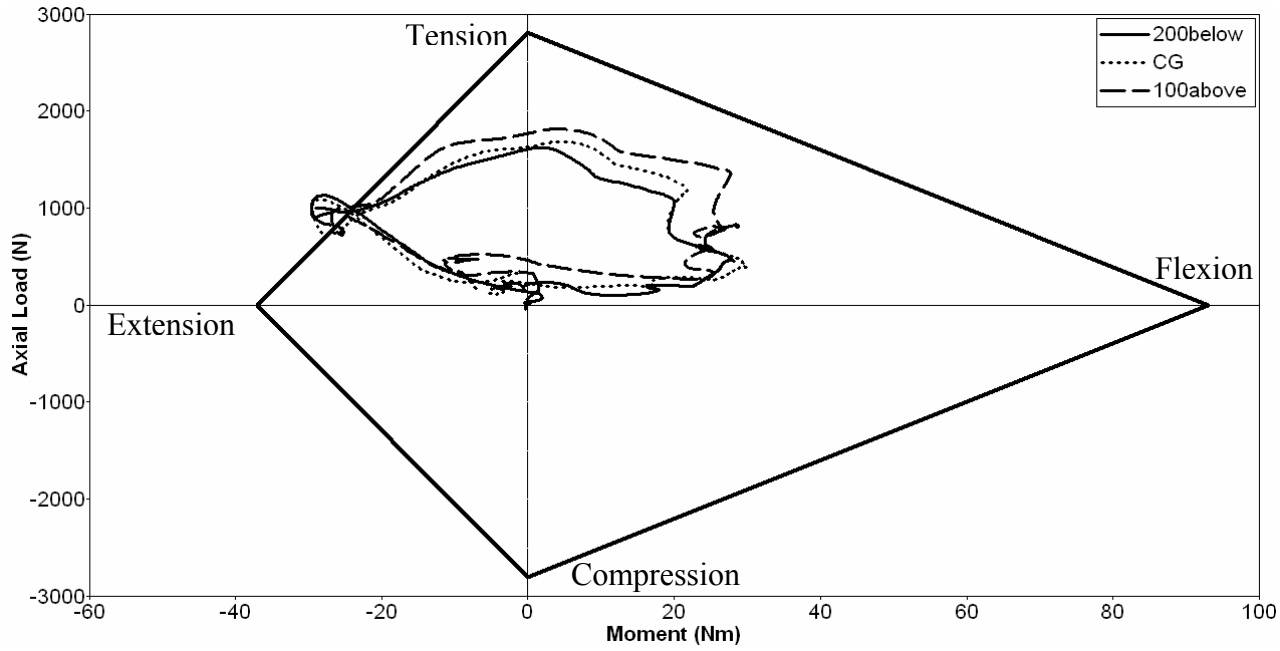

Figure 46 Nij: rear SP positioned 200mm below CG_{WC}, at CG_{WC}, and 100mm above CG_{WC}

Figure 47 through Figure 50 show the crash response of the ATD and the wheelchair for each model with varying rear SP location. When the rear SP was positioned 100 mm above the

CG_{WC}, the wheelchair rotated rearward during impact. In the +100 CG_{WC} model, severe head-neck extension of the ATD occurred along with ramping.

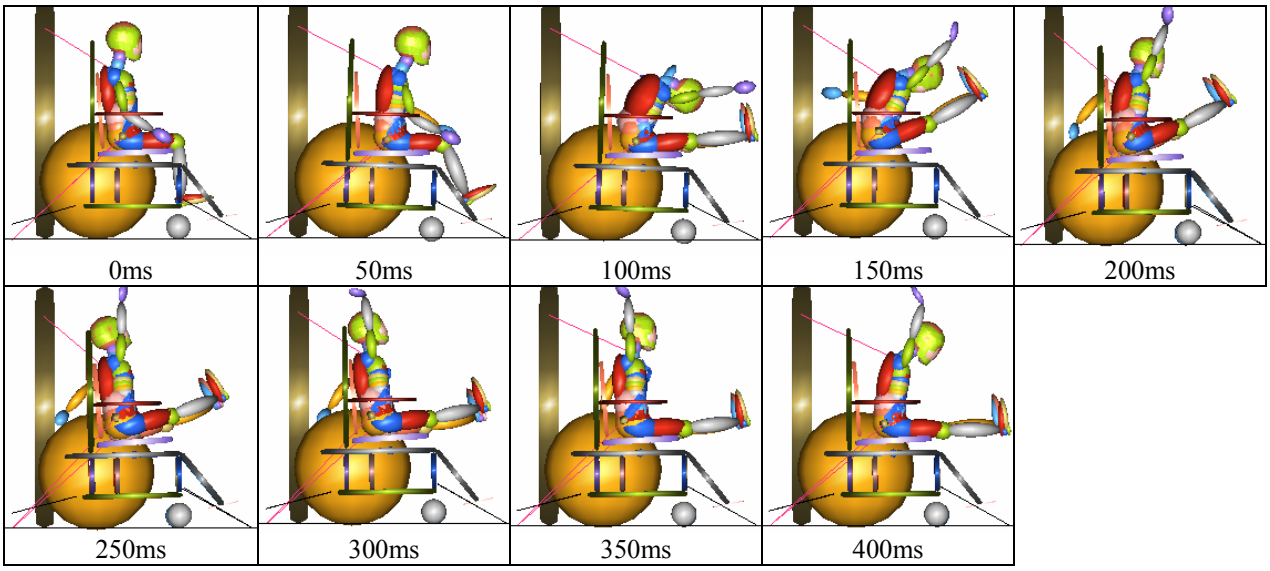

Figure 47 Crash response of the ATD and wheelchair: rear SP positioned 200 mm below CG_{WC}

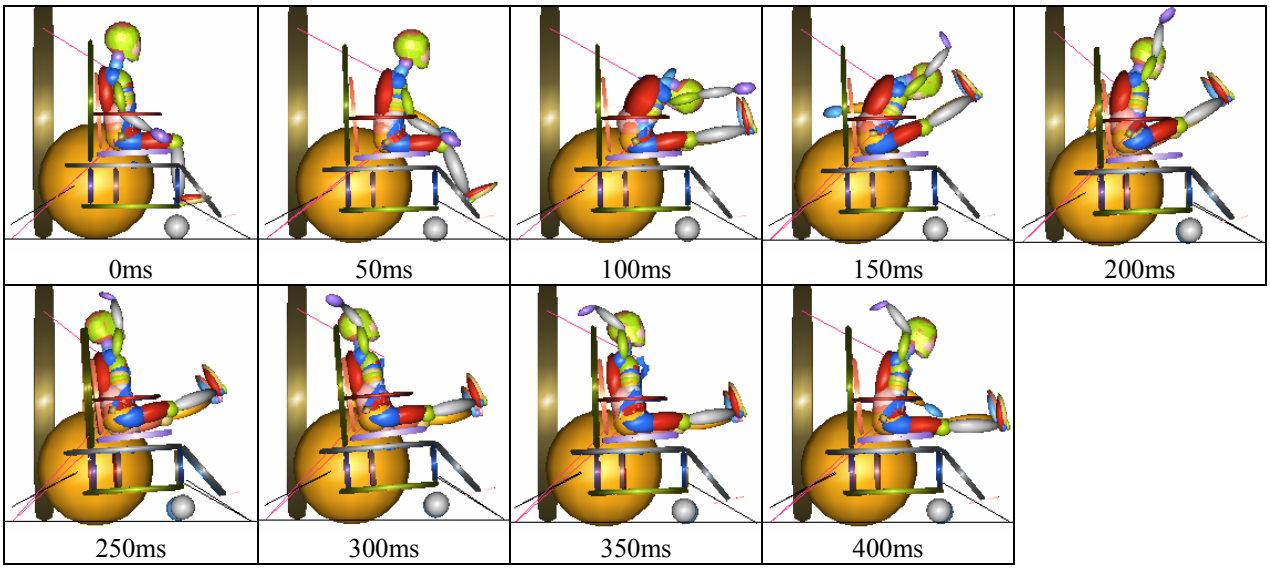

Figure 48 Crash response of the ATD and wheelchair: rear SP positioned 100 mm below CG_{WC}

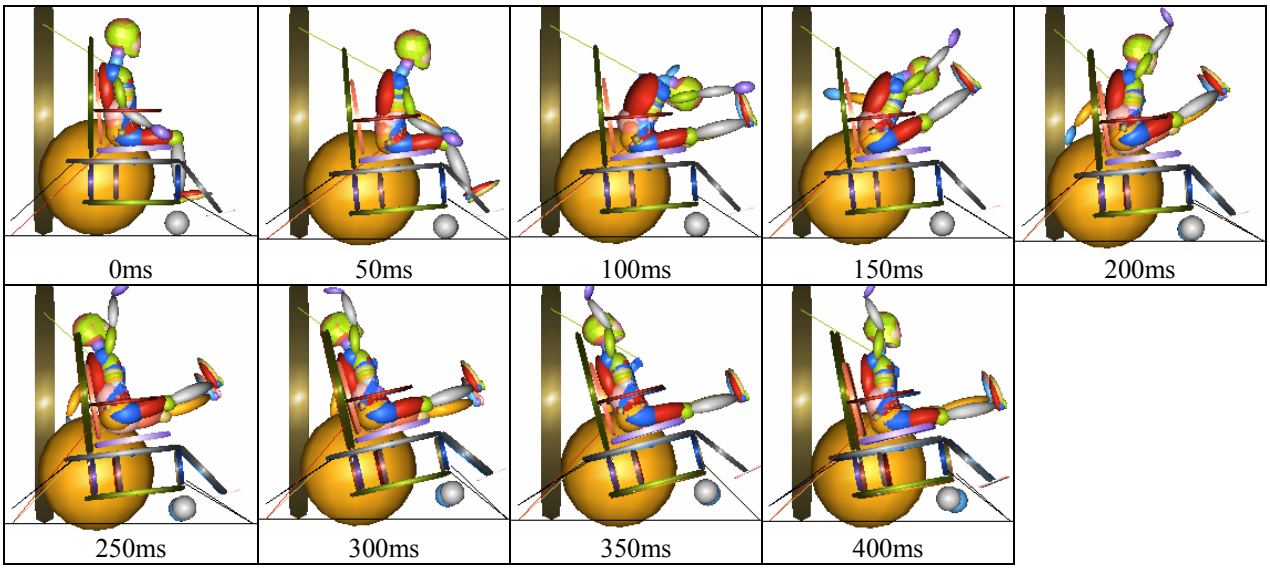

Figure 49 Crash response of the ATD and wheelchair: rear SP positioned at CG_{WC}

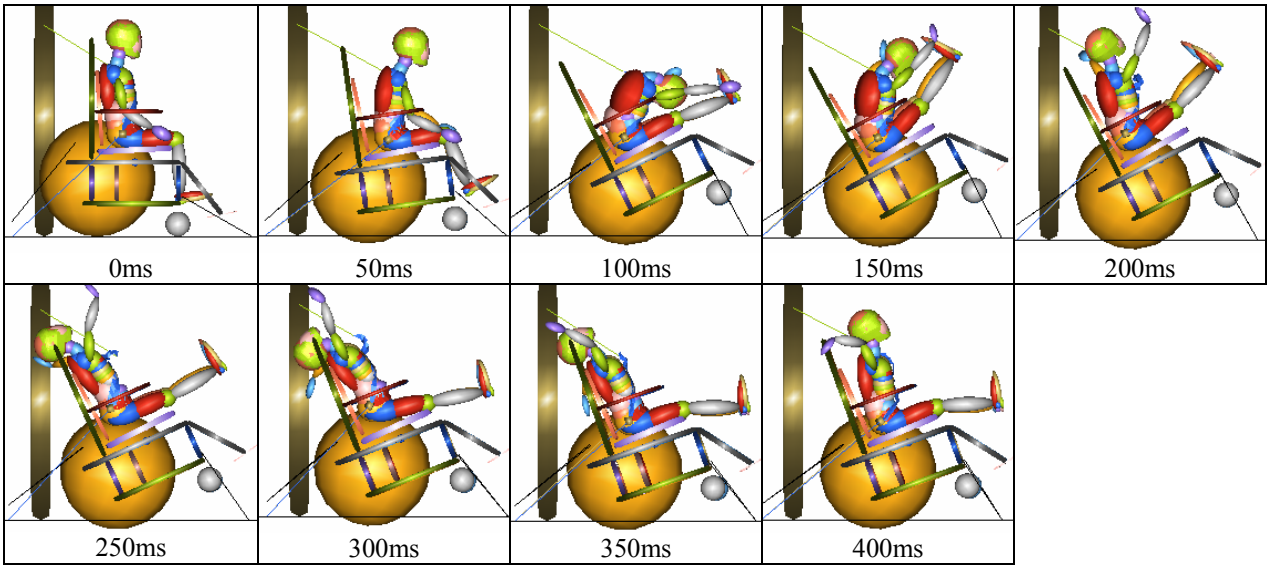

Figure 50 Crash response of the ATD and wheelchair: rear SP positioned 100 mm above CG_{WC}

4.4.3 Seat-to-back Intersection Horizontal Location

In Table 29, the horizontal excursions resulting from the models with varying STBI location were compared to the ANSI/RESNA WC-19 excursion limits. The maximum horizontal excursions of the wheelchair and the ATD for all models with different STBI location

were within the WC-19 limits. All models complied with the limit, $X_{knee}/X_{wc} \geq 1.1$. The peak rearward head excursion decreased from 242 mm to 84 mm as the STBI location was moved forward from R100 to F100.

Table 29 Comparison between computer model results and ANSI/RESNA WC-19 horizontal excursion limits: STBI located 100mm behind rear hub to 100mm in front of rear hub

	X_{wc} (mm)	X_{knee} (mm)	X_{headF} (mm)	X_{headR} (mm)	X_{knee}/X_{wc}
WC-19 limit	**150**	**300**	**450**	**-350**	**$\geq$ 1.1**
STBI location wrt rear hub (mm)					
R100	13	71	223	-242	5.5
R50	16	71	224	-179	4.4
0 (at rear hub)	15	70	225	-136	4.7
Baseline (F23)	15	70	225	-121	4.7
F50	15	69	225	-106	4.6
F100	14	69	226	-84	4.9

Table 30 shows the results of the models with varied STBI location compared to the FMVSS 213 and FMVSS 208 injury criteria. In all models, HIC_{36} value and peak chest acceleration remained under the limit of 1000 and 60g. All HIC_{15} values resulting from the models also remained under the 700 limit. All models exceeded the chest deflection limit of 40 mm and the N_{ij} injury criteria of 1 at the Tension Extension limit. Figure 51 shows N_{ij} values for the models, R100, at hub (0), and F100, as compared to the limits specified in FMVSS 208. The peak neck tension force of all models also exceeded the limit of 1490 N. The neck tension force decreased from 1732 N to 1644 N as the STBI location was moved forward from R100 to F100. None of the models exceeded the independent compressive neck force limit of 1820 N.

Table 30 Comparison between computer model results and FMVSS injury criteria: STBI located 100mm behind rear hub to 100mm in front of rear hub

	FMVSS 213		FMVSS 208				
	HIC_{36}	Chest acceleration (g)	HIC_{15}	Chest deflection (mm)	N_{ij}	Neck tension (N)	Neck compression (N)
FMVSS limit	**1000**	**60**	**700**	**40**	**1**	**1490**	**1820**
STBI location wrt rear hub (mm)							
R100	437	53	299	43	1.2	1732	36
R50	419	52	267	42	1.2	1676	36
0 (at rear hub)	427	51	263	42	1.2	1667	36
Baseline (F23)	429	50	262	42	1.2	1662	36
F50	431	50	259	42	1.2	1654	36
F100	432	50	278	42	1.2	1644	37

Note: Value exceeded the FMVSS limit was shaded in grey.

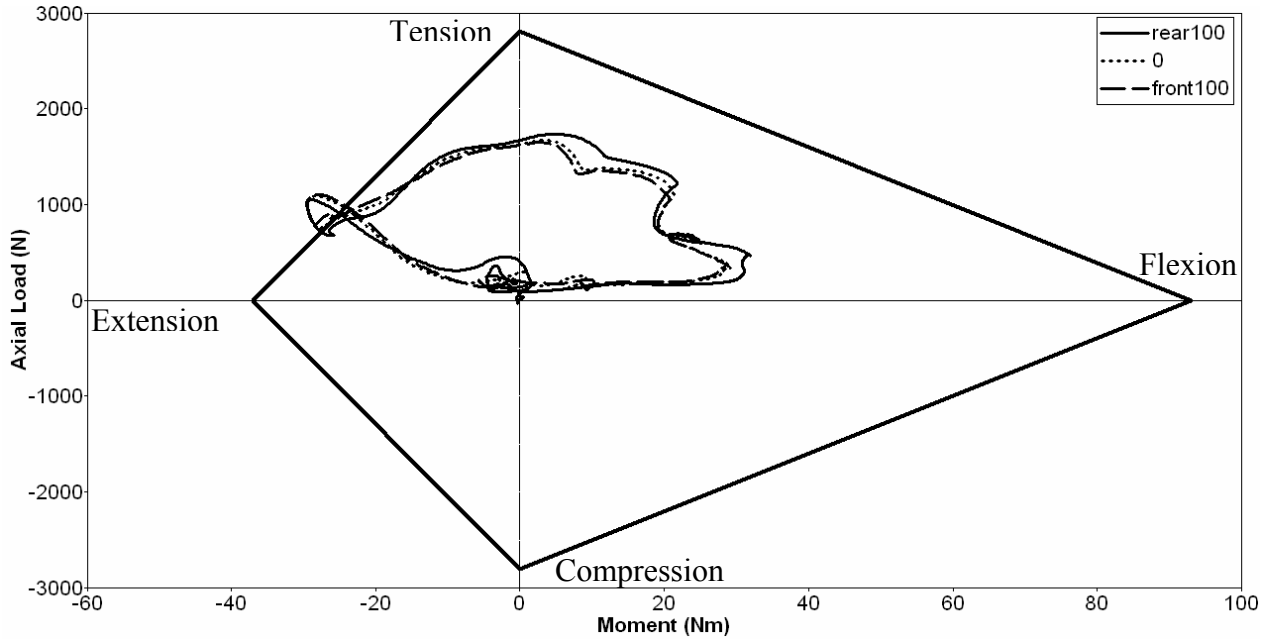

Figure 51 Nij: STBI located 100mm behind rear hub, at rear hub, and 100mm in front of rear hub

Figure 52 through Figure 56 show the crash response of the ATD and the wheelchair for each model with varied STBI location. Increased rearward rotation of the wheelchair was observed as the STBI location was moved horizontally toward the rear of the wheelchair. ATD

head-neck extension and ramping also increased as the STBI location was moved horizontally toward the rear of the wheelchair.

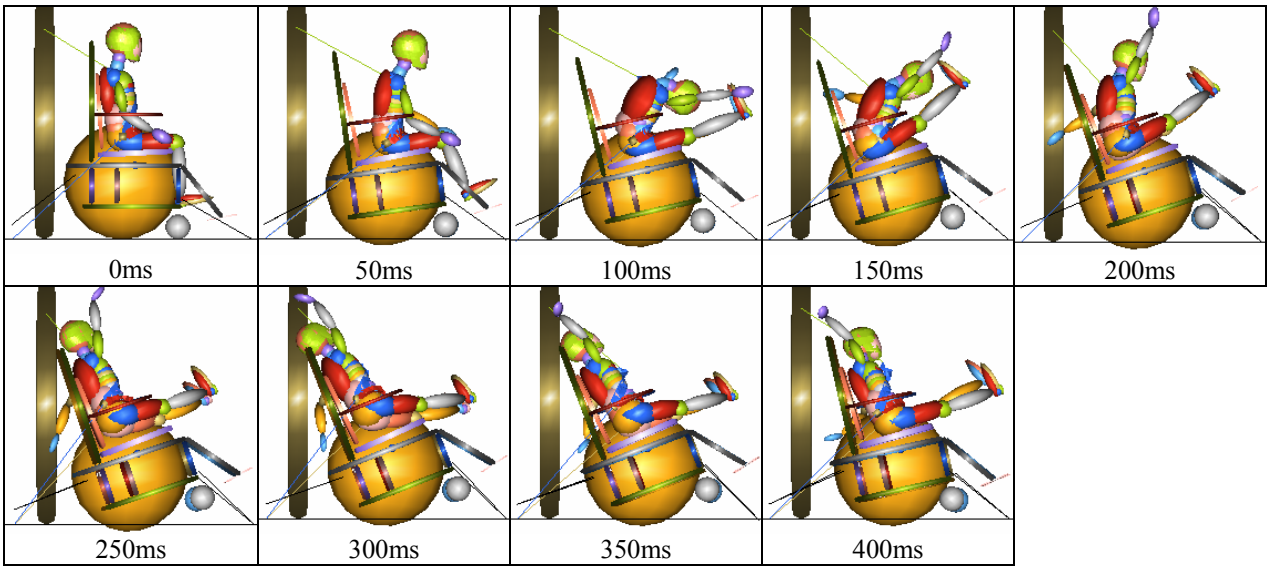

Figure 52 Crash response of the ATD and wheelchair: STBI located 100mm behind rear hub

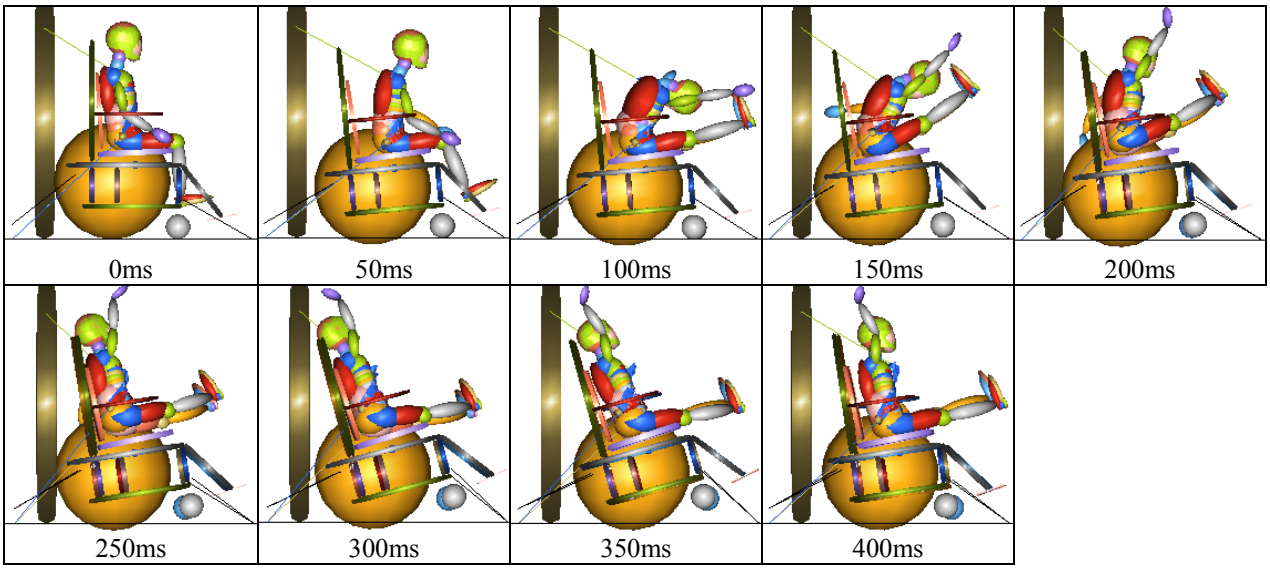

Figure 53 Crash response of the ATD and wheelchair: STBI located 50mm behind rear hub

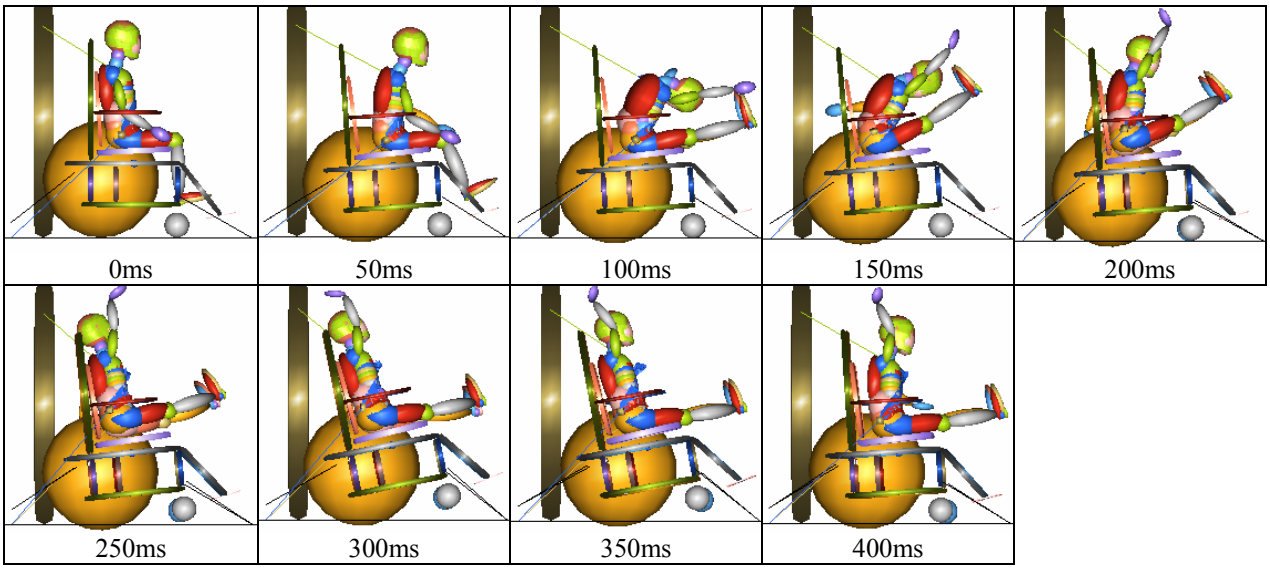

Figure 54 Crash response of the ATD and wheelchair: STBI located at rear hub

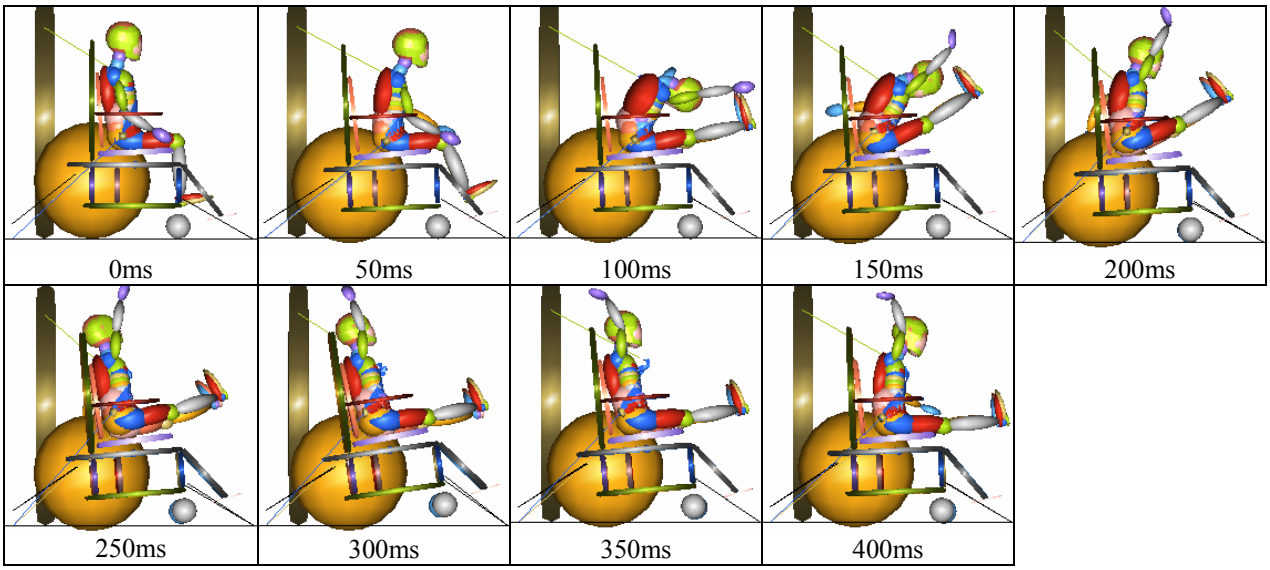

Figure 55 Crash response of the ATD and wheelchair: STBI located 50mm in front of rear hub

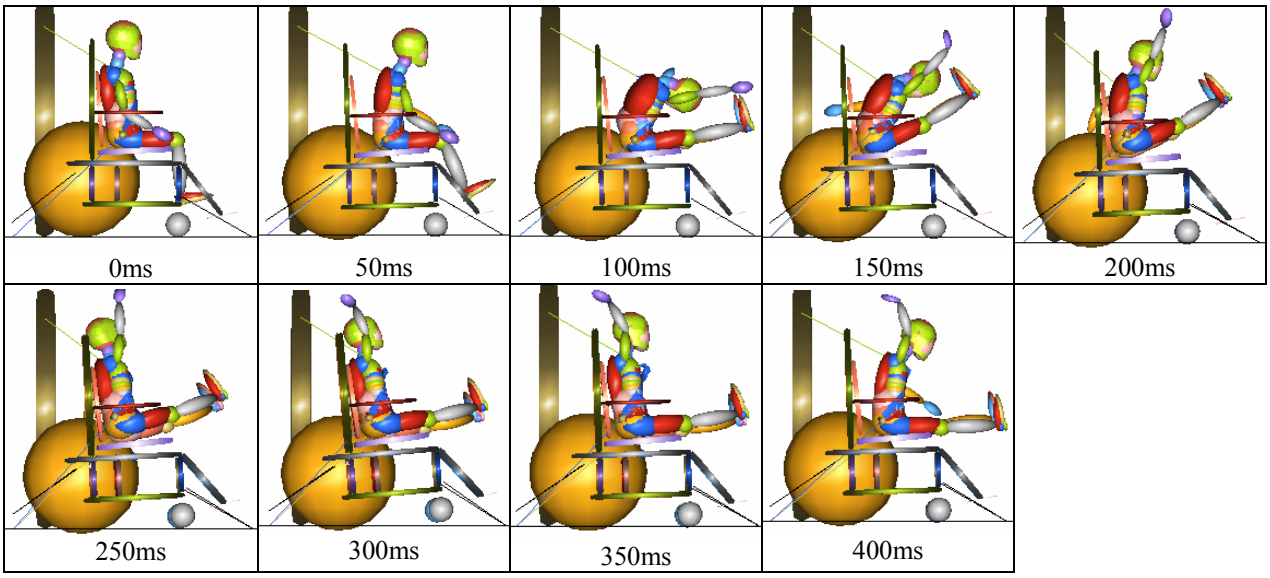

Figure 56 Crash response of the ATD and wheelchair: STBI located 100mm in front of rear hub

4.4.4 Results Summary

None of the models tested in this study exceeded the WC-19 horizontal excursion limits of the wheelchair, ATD head, and ATD knee. When the rear SP was positioned 100 mm above the CG_{WC}, the ratio of the maximum knee excursion to the maximum wheelchair excursion, X_{knee}/X_{wc}, was close to the limit of 1.1. All peak chest accelerations, HIC values, and peak neck compression forces remained below the limits specified in the FMVSS. All models exceeded the peak chest deflection limit of 40 mm and the N_{ij} injury criteria of 1 at the Tension Extension limit. Moreover, the peak neck tension force of all models also exceeded the limit of 1490 N.

4.5 Discussion

Injury risk of a 6-year-old wheelchair occupant during a frontal motor vehicle crash under different wheelchair setup scenarios was investigated in this study. In the automotive industry, the term "ramping" is used "to describe the motion of the occupant parallel to the seat back during a rear impact." [16] In this study, when the SBA was set to 25°, the rear SP was positioned 100 above CG_{WC}, and the STBI location was set to 100mm behind the rear hub,

significant occupant ramping was observed during the rebound phase of the frontal impact; especially in the model with 25° seat back angle, high occupant ramping was observed. "An occupant who ramps is potentially exposed to head and neck injury by contact with vehicle structures, [such as the roof structure, rear seat cushion, or vehicle windows]" [16]. The horizontal excursion limits specified in the ANSI/RESNA WC-19 standard [6] have been established to prevent contact between a wheelchair occupant and vehicle interior, and to prevent wheelchair loading of the wheelchair occupant. However, the WC-19 horizontal excursion limit will not be able to assess the vertical motion of an occupant and to prevent occupant contact with the roof structure.

When the rear SP was positioned 100 mm above the CG_{WC} and the STBI was located 100mm behind rear hub, the wheelchair rotated rearward from the beginning of the impact. An excessive wheelchair rearward rotation can lead to increased risk of head and neck injury via impact with interior vehicle surfaces. Although it is not observed in this study, excessive wheelchair forward rotation can also cause an occupant to impact vehicle structures positioned ahead of the wheelchair station and to be injured by the "secondary impact." To prevent the wheelchair occupants from injury resulting from "secondary impact" with interior vehicle structures, rotation of a wheelchair should be minimized. Wheelchair kinematics presented in this study (Figure 47 through Figure 50 and Figure 52 through Figure 56) showed that wheelchair rotation can be limited by positioning the rear SP 100 mm below the CG_{WC} and positioning the STBI near the rear hub.

In the study conducted by Bertocci et al., kinematics of the SAE/ISO surrogate wheelchair, which represents an 85 kg typical power wheelchair, subjected to a 20g/48 kph frontal crash at three different rear SP positions were reported [17]. The authors stated that

"controlling or limiting wheelchair rotation can be accomplished through positioning rear securement points at or near the same level as the wheelchair CG." In this study, although placing the rear SP at the CG_{WC} reduced wheelchair rotation more than placing the rear SP 100 mm above the CG_{WC}, the wheelchair rotation was minimal (among different rear SP positions) when the rear SP was positioned 100 mm below the CG_{WC}. The difference between results presented in the study done by Bertocci et al. and results of this study could be due to the position of the front securement point. The front SP on the SAE/ISO surrogate wheelchair was located 172 mm above the CG_{WC}. However, the front SP on the ZIPPIE pediatric wheelchair in this study was located 168 mm below the CG_{WC}. Although not investigated in this study, it is anticipated that the front SP location has an impact on the rotation of a wheelchair. Evaluation of this design parameter (the front SP location) in the future will provide more information on pediatric occupant injury risks.

One of the performance requirements specified in the WC-19 standard is that the pre- to posttest (20g/48 kph sled test) change in the ATD hip-point (H-pt) vertical position must not exceed 20 percent, $(H_{pre}-H_{post})/H_{pre} < 0.2$. This requirement evaluates crash integrity of seat surface and seat attachment hardware with the intent to prevent the occurrence of occupant submarining. (Submarining is defined as the lap belt slipping upward over the iliac crest and loading the soft abdominal tissues.) Occupant submarining can potentially lead to severe internal injuries of organs in the abdominal region as well as lumbar vertebrae fractures in severe cases [18] [19] [20]) However, it is important to note that submarining may occur without seat failure and such a scenario may not be detected by the WC-19 test criterion. In this study, the ATD visually appeared to have submarine-type kinematics when the seat back angle was set to higher than 25° (see Figure 57).

Viano and Arepally propose a downward pelvis excursion limit of 50 mm and forward pelvis excursion limit of 250 mm for use in assessing submarining risk during sled testing [21]. Previous studies on injury risks of adult wheelchair users in crashes compared the peak H-pt excursions to the Viano and Arepally limit to assess the risk of the wheelchair occupant submarining [11] [22]. The peak horizontal and vertical H-pt excursions of the 6-year-old ATD found in this study are shown in Table 31. Data were analyzed up to the point where the forward ATD motion was ended, approximately 75 ms. H-pt excursion data during the rebound phase of impact, where the ATD moved rearward, was excluded since submarining is related to the forward and downward motion sequence of the pelvis.

H-pt excursions resulting from all models tested in this study stayed below the horizontal H-pt peak excursion limit of 250 mm and the vertical H-pt peak excursion limit of 50 mm. However, it is important to note that the H-pt excursion limits recommended by the Viano and Arepally limit have been derived base on the studies conducted with adult ATDs [21]. Children have statures smaller than adults, and therefore the threshold of pelvic excursion would be lower for children than for adults. Research conducted in the automotive industry indicated that although seat belts, which were designed for adults, do reduce morbidity, "a school age child [who usually has smaller stature than a adult] may sustain abdominal or spinal injury as a result of wearing a seat belt." [23] [24]

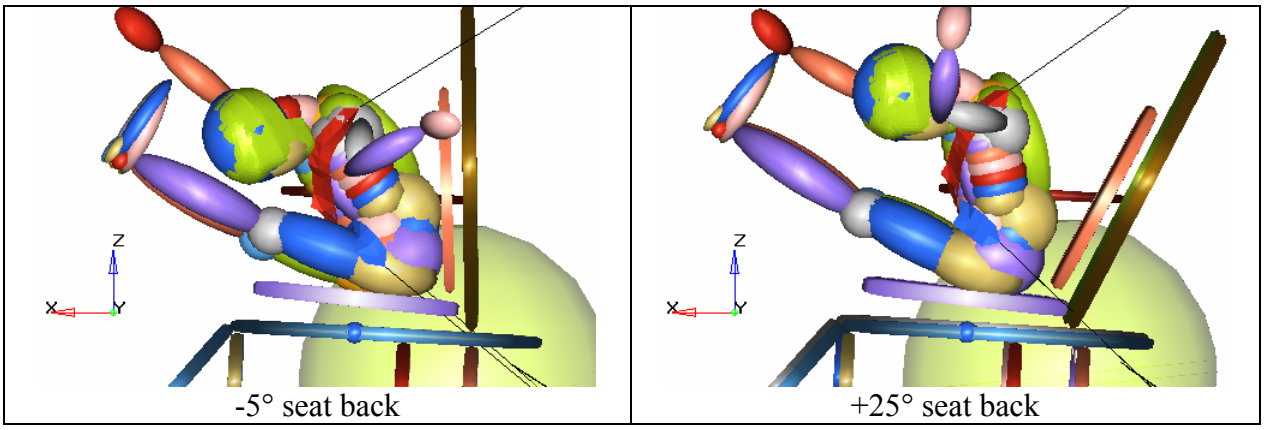

-5° seat back +25° seat back

Figure 57 Possible ATD submarining with 25° seat back angle

Table 31 Peak horizontal and vertical H-pt excursions of 6-year-old ATD

	Max H-pt downward vertical excursion (mm)	Max H-pt forward horizontal excursion (mm)
Seat Back Angle (°)		
-5	24	83
Baseline (+4)	20	71
+15	21	65
+25	23	73
+35	27	77
Rear SP position wrt CG_{WC} (mm)		
-200	15	69
-100	18	69
Baseline (-44)	20	71
0 (at CG_{WC})	23	72
+100	22	77
Seating location wrt rear hub (mm)		
R100	24	72
R50	24	72
0 (at rear hub)	21	71
Baseline (F23)	20	71
F50	20	70
F100	20	70

The results presented in this study showed that a 6-year-old wheelchair seated occupant may be at risk of neck injury during a frontal car crash. All models tested in this study exceeded

the N_{ij} injury criteria of 1 and the peak neck tension force limit of 1490 N. "Blood in the synovial fluid of the occipital condylar joint capsules was rated as an Abbreviated Injury Scale (AIS) = 3 neck injury and was defined as the threshold of undesirable neck trauma" [25]. Injury risk curves, representing probability of risk of injury at various injury measures, such as chest deflection and N_{ij}, are presented in *Proposed Amendment to FMVSS No 213 Frontal Test Procedure* released by NHTSA [26]. The probability that a vehicle occupant would receive a certain level of AIS injury [27] can be calculated using the injury risk curves. For a 6-year-old ATD, the N_{ij} limit of 1 is equivalent to a 22 percent risk of AIS $\geq$ 3.

The results also showed that a 6-year-old wheelchair seated occupant may have a risk of chest injury in a frontal impact motor vehicle crash. The peak chest deflection values of all models exceeded the FMVSS limit of 40 mm. "Thoracic injuries associated with peak sternal deflection are rib and sternal fractures, which are rated as AIS $\geq$ 2, and thoracic organ damage produced by crushing forces, which is rated as AIS $\geq$ 4" [25]. The chest deflection limit of 40 mm is equivalent to a 72 percent risk of AIS $\geq$ 2 and 11 percent risk of AIS $\geq$ 4 [26].

The results presented in this study need to be interpreted with caution since there are concerns regarding the biofidelity of the Hybrid III 6-year-old ATD's neck and chest areas [15] [28]. The Hybrid III 6-year-old ATD was developed by the SAE Hybrid III Dummy Family Task Force based on the information available on anthropometry and mass distribution characteristics of 6-year-old children in the United States [29] [30] [31] [32] [33] [34]. Because "there [was] virtually no literature dealing with biomechanical impact response of children," [35] biomechanical impact response requirements for head, neck, chest, and knees of 6-year-old ATD [36] were scaled from biomechanical response corridors of the mid size adult male, which were constructed from test data of human cadavers and volunteers [34] [37] [38] [39] [40] [41].

NHTSA received comments that expressed concerns about the biofidelity of the Hybrid III 6-year-old ATD's neck and upper chest areas after NHTSA released the Notice of Proposed Rulemaking (NPRM), which proposed replacement of a Hybrid II 6-year-old ATD with a Hybrid III 6-year-old ATD in FMVSS 213 [42]. Several commenters stated that the Hybrid III 6-year-old ATD had more flexible neck and ribs than the Hybrid II 6-year-old ATD [15]. However, NHTSA stated in the Final Rule that "the neck of the HIII 6-year-old is currently performing within the specifications established by the Hybrid III Dummy Family Task Force of the Society of Automotive Engineers (SAE)," and the agency believed "the current neck on the HIII 6-year-old dummy [provided] improved biofidelity over the current dummy, [Hybrid II 6-year-old dummy]." [15] As a result, the Hybrid III 6-year-old ATD was adopted into FMVSS 213 in the Final Rule in June, 2003.

Although a Hybrid III 6-year-old ATD provides improved biofidelity over than of a Hybrid II 6-year-old ATD, biofidelity of the Hybrid III 6-year-old ATD has not been confirmed by biomechanical impact response of child data. In a recent study conducted by Sherwood et al., biofidelity of the Hybrid III 6-year-old ATD was evaluated [28]. 49 kph sled tests were conducted using a Hybrid III 6-year-old ATD, and sled test results were compared to a 12-year-old cadaver test conducted at the University of Heidelberg (Heidelberg, Germany) [43]. The study focused on cervical spine injury risk for a 6-year-old child in frontal crashes. The authors concluded in the study that "the thoracic spine of the Hybrid III 6-year-old dummy is not biofidelic in restrained frontal crash tests" [28]. The authors also stated that "the stiff thoracic spine of the dummy results in high neck forces and moments that are not representative of the true injury potential" [28]. A limitation of this study was that the size of the 12-year-old cadaver was different from that of the Hybrid III 6-year-old ATD. The authors indicated in the study that

"ideally comparisons to the dummy tests would be done with a cadaver of the same age and size, but this was not possible due to the small number of child cadaver tests available for comparison" [28]. A Hybrid III 6-year-old ATD was originally developed using the biomechanical impact response requirements derived from adult data. Therefore, verification of the performance of a Hybrid III 6-year-old ATD with the actual biomechanical impact response data of 6-year-old children is needed through such studies conducted by Sherwood et al. [28], and if needed, then design changes should be made to a Hybrid III 6-year-old ATD to improve the biofidelity of the ATD.

Existing wheelchair standards do not currently address occupant neck or chest injury risk. They evaluate crash integrity of wheelchairs and WTORS but do not include injury criteria or limitations that address neck and chest injury risk during frontal impact. Adaptation of these additional occupant injury assessment measures, such as N_{ij} and/or peak chest deflection, into wheelchair standards could potentially improve wheelchair occupant protection in motor vehicle crashes.

4.6 CONCLUSION

Using computer simulation techniques, this study investigated injury risks of a 6-year-old wheelchair occupant in a frontal motor vehicle crash under different wheelchair setup scenarios (seat back angle, rear securement point vertical location with respect to wheelchair CG, and seat-to-back intersection horizontal location with respect to rear wheels). Study results showed that various achievable pediatric wheelchair settings can have an impact on crash kinematics and injury risk of a 6-year-old wheelchair occupant in a frontal motor vehicle crash. As the seat back angle increased, there was an increased tendency of "ramping" (an occupant moving upward along the seat back surface) during the rebound phase and severity of head-neck extension

increased. ATD head-neck extension and ramping also increased as the STBI location was moved horizontally toward the rear of the wheelchair. When the rear SP was positioned 100 mm above the CG_{WC}, the wheelchair rotated rearward from the beginning of the impact and severe head-neck extension of the ATD occurred along with ramping.

Study results show that a 6-year-old wheelchair seated occupant has a risk of neck and chest injuries in a frontal impact motor vehicle crash under all evaluated scenarios. Neck injury risk can be reduced by minimizing rearward movement of the head and neck during motor vehicle crashes. Using a device that provides a support at the head and neck areas and minimizes the head-neck rearward movement, such as head restraints, with a wheelchair in transit can reduce the risk of neck injury. More research on the design and performance of head restraints used with transit wheelchairs is needed in the future. To reduce chest injury risk, further studies on occupant restraint systems for children seated in wheelchairs in transit also need to be conducted. For the pediatric population, three-point occupant restraint systems, which were used in this study, may not be the best occupant restraint system to provide protection during frontal crashes. Occupant restraint systems that allow the crash force to be distributed over larger contact areas can possibly reduce the risk of chest injury.

Existing wheelchair standards do not currently address occupant head, neck, or chest injury risk. Adaptation of additional occupant injury assessment measures, such as HIC, N_{ij} and/or peak chest deflection, into wheelchair standards should be further explored to improve wheelchair occupant protection in motor vehicle crashes.

4.7 REFERENCES

1. National Highway Traffic Safety Administration (NHTSA). (1979). *FMVSS 213 Child Restraint Systems* (October, 2000 ed. Vol. 49 CFR 571.213).

2. National Highway Traffic Safety Administration (NHTSA). (April 2002). *State Legislative Fact Sheet*. Retrieved March, 2003

3. Everly, J. S., Bull, M. J., Stroup, K. B., Goldsmith, J. J., Doll, J. P., & Russell, R. (1993). A Survey of Transportation Services for Children with Disabilities. *The American Journal of Occupational Therapy, 47*(9), 804-810.

4. Society of Automotive Engineers (SAE). (1997). *SAE J2249: Wheelchair Tiedowns and Occupant Restraint Systems for Use in Motor Vehicles* (No. SAE J2249): SAE.

5. International Standards Organization (ISO). (2001). *ISO 10542: Wheelchair Tiedown and Occupant Restraint Systems* (No. ISO 10542): ISO.

6. ANSI/RESNA Subcommittee on Wheelchairs and Transportation (SOWHAT). (2000). *ANSI/RESNA WC/Vol 1: Section 19 Wheelchairs - Wheelchairs Used as Seats in Motor Vehicles*: ANSI/RESNA.

7. International Standards Organization (ISO). (2000). *ISO 7176-19: Wheelchairs Used as Seats in Motor Vehicles* (No. ISO 7176-19): ISO.

8. Weber, K. S. (1998). Choosing a wheeled manual mobility product. *Exceptional Parent, 28*(10), 46-47.

9. Sunrise Medical.*http://www.sunrisemedical.com*

10. Convaid.*http://www.convaid.com*

11. Leary, A. M. (2001). *Injury risk analysis and design criteria for manual wheelchairs in frontal impacts.* Unpublished Masters thesis, University of Pittsburgh, Pittsburgh.

12. Bertocci, G. E., Hobson, D. A., & Digges, K. H. (2000). Development of a wheelchair occupant injury risk assessment method and its application in the investigation of

wheelchair securement point influence on frontal crash safety. *IEEE Transactions on Rehabilitation Engineering, 8*(1), 126-139.

13. Bertocci, G. E., Digges, K. H., & Hobson, D. A. (1996). Shoulder belt anchor location influences on wheelchair occupant crash protection. *Journal of Rehab Research and Development, 33*(3), 279-289.

14. National Highway Traffic Safety Administration (NHTSA). (1971). *FMVSS 208 Occupant Crash Protection* (October, 2000 ed. Vol. 49 CFR 571.208).

15. National Highway Traffic Safety Administration (NHTSA). (2003). *Final rule on Federal Motor Vehicle Safety Standards; Child Restraint Systems* (No. Docket No. NHTSA-03-15351): NHTSA.

16. Warner, C., Stother, C., James, M., & Decker, R. (1991). *Occupant Protection in Rear End Collisions: The Role of Seat Back Deformation in Injury Reduction* (No. SAE Paper No. 912914): SAE.

17. Bertocci, G. E., Digges, K., & Hobson, D. (1996). Development of transportable wheelchair design criteria using computer crash simulation. *IEEE Transactions of Rehabilitation Engineering, 4*(3), 171-181.

18. Epstein, B., Epstein, J., & Jones, M. (1978). Lap-sash three point seat belt fractures of the cervical spine. *Spine, 3*, 189-193.

19. Leung, Y., Tarriere, C., Lestrelin, D., Hureau, J., Got, C., Guillon, F., et al. (1982). Submarining injuries of 3 point belted occupants in frontal crashes.

20. Dehner, J. (1971). Seat belt injuries of the spine and abdomen. *American Journal of Rontgenology, 111*, 833-843.

21. Viano, D. C., & Arepally, S. (1990). *Assessing the safety performance of occupant restraint systems* (No. SAE Paper No. 902328): Society of Automotive Engineers (SAE).

22. Bertocci, G. E., Souza, A. L., & Szobota, S. (2003). The effects of wheelchair-seating stiffness and energy absorption on occupant frontal impact kinematics and submarining risk using computer simulation. *Journal of Rehab Research and Development, 40*(2), 125-130.

23. Murphy, M. M. (1999). Pediatric Occupant Car Safety: Clinical Implications Based on Recent Literature. *Pediatric Nursing, 25*(2), 137-148.

24. Klinich, K. D., & Burton, R. W. (1993). *Injury Patterns of Older Children in Automotive Accidents* (No. SAE Paper No. 933082): SAE.

25. Mertz, H. J. (2002). *Accidental Injury - Biomechanics and Prevention* (Second Edition ed.). New York: Springer-Verlag.

26. National Highway Traffic Safety Administration (NHTSA). (2002). *Proposed Amendment to FMVSS 213 Frontal Test Procedure*: NHTSA.

27. States, J. D. (1969). Abbreviated and the comprehensive research injury scales. *SAE, SAE Paper No. 690810*.

28. Sherwood, C. P., Shaw, C. G., Van Rooij, R. W. K., Crandall, J. R., Orzechowski, K. M., Eichelberger, M. R., et al. (2003). Prediction of Cervical Spine Injury Risk for the 6-Year-Old Child in Frontal Crashes. *Traffic Injury Prevention, 2*, 206-213.

29. Weber, K., Lehman, R. J., & Schneider, L. W. (1985). *Child Anthropometry for Restraint System Design* (No. UMTRI-85-23). Ann Arbor, MI: University of Michigan.

30. Snyder, R. G., Schneider, L. W., Owings, C. L., Reynolds, H. M., Golumb, D. H., & Schork, M. A. (1977). *Anthropometry of infants, children and youths to age 18 for product safety design* (No. SP-450). Warrendale, PA: Society of Automotive Engineers.

31. Reynolds, H. M., Young, J. W., McConville, J. T., & Snyder, R. G. (1976). *Development and Evaluation of Masterbody Forms for Three-Year Old and Six-Year Old Child Dummies* (No. DOT HS-801-811). Ann Arbor, MI: University of Michigan.

32. *Anthropomorphic Test Dummy*. (No. DOT-HS-299-3-569)(December 1973). Final Report, Volume 1, NHTSA.

33. *Anthropometry of Motor Vehicle Occupants*. (No. DOT-HS-806-715)(April 1985). Final Report, Volume 1, NHTSA.

34. Hubbard, R. P., & McLeod, D. G. (1974). Definition and Development of a Crash Dummy Head. *SAE Paper No. 741193*.

35. National Highway Traffic Safety Administration (NHTSA). (June 1998). *Technical Report: Development and Evaluation of the Hybrid III type Six-Year-Old Child Dummy* (No. Docket 98-3972).

36. Irwin, A., & Mertz, H. J. (1997). Biomechanical Basis for the CRABI and Hybrid III Child Dummies. *SAE No. 973317*, 261-272.

37. Culver, C. C., Neathery, R. F., & Mertz, H. J. (1972). Mechanical Necks with Humanlike Responses. *SAE720959*.

38. Mertz, H. J., Neathery, R. F., & Culver, C. C. (1972). *Performance Requirements and Characteristics of Mechanical Necks*: General Motors Research Laboratories Symposium, Human Impact Response-Measurement and Simulation, Warren, MI.

39. Neathery, R. F. (1974). Analysis of Chest Impact Response Data and Scaled Performance Recommendations. *SAE74118*.

40. Horsch, J. D., & Patrick, L. M. (1976). Cadaver and Dummy Knee Impact Response. *SAE760799*.

41. Hodgson, V. R., & Tomas, L. M. (1971). Comparison of Head Acceleration Injury Indices in Cadaver Skull Fracture. *SAE 710854*.

42. National Highway Traffic Safety Administration (NHTSA). (2002). *Notice of proposed rulemaking (NPRM) on Federal Motor Vehicle Safety Standards; Child Restraint Systems* (No. Docket No. NHTSA-02-11707): NHTSA.

43. Kallieris, D., Schmidt, G., Barz, J., Mattern, R., & Schulz, F. (1978). *Response and Vulnerability of the Human Body at Different Impact Velocities in Simulated Three-Point Belted Cadaver Tests.* Paper presented at the 3rd IRCOBI Conference.

5 DEVELOPMENT OF MANUAL PEDIATRIC TRANSIT WHEELCHAIR DESIGN GUIDELINES USING COMPUTER SIMULATION

5.1 ABSTRACT

Many children must use their wheelchair as a seat while traveling in a motor vehicle. Under crash conditions these wheelchairs are subjected to higher loads than those experienced during normal mobility and warrant special design consideration. Using a previously validated pediatric wheelchair model, our study investigated wheelchair and occupant restraint loading under 20g/48kph frontal impact conditions with varying wheelchair characteristics. Our model utilized a four-point tiedown secured pediatric manual wheelchair with a seated Hybrid III 6-year-old ATD, restrained using a three-point occupant restraint. Rear securement point loads were found to be as high as 4355 N, with maximum seat pan loading of 1374 N and seat back loading of 1992 N. Maximum rear wheel loads were found to be 5098 N, with caster loading as high as 2013 N. Peak occupant restraint loads were found to be 4002 N for the shoulder belt and 2683 N for the pelvic belt. These findings which are different from those of adult wheelchairs should provide guidelines for manufacturers designing technologies for safe pediatric wheelchair transportation.

Keywords: pediatric transit wheelchair, computer crash simulation, wheelchair transportation safety

5.2 BACKGROUND

The Individuals with Disabilities Education Act (IDEA) (formerly called Education for all Handicapped Children Act of 1975) requires "public schools to make available to all eligible children with disabilities a free appropriate public education in the least restrictive environment appropriate to their individual needs" [1]. 1997 amendments of IDEA require states to

coordinate services and funding sources to provide early intervention services to infants and toddlers with disabilities. Through the New Freedom Initiative of 2001, funding for the IDEA has increased, so more students with disabilities have access to free appropriate public education [2]. Due to the disability laws, that prohibit discrimination of children with disabilities and promote equal education for disabled children, many children with disabilities now receive their education along with non-disabled children in the same mainstreamed schools. And more children with disabilities are transported on a daily basis to schools and developmental facilities.

When children with disabilities are transported, they often remain seated in their wheelchairs in vehicles. Because wheelchairs may not be designed to serve as vehicle seats, occupant protection can be compromised. To assure the safety of wheelchair-seated travelers, voluntary standards, which have not been mandated by state or federal laws, have been established by national organizations. The Society of Automotive Engineers (SAE) J2249 *Wheelchair Tiedowns and Occupant Restraint Systems* (WTORS) specifies design requirements, test methods, and performance requirements for WTORS [3]. American National Standards Institute (ANSI) / Rehabilitation Engineering and Assistive Technology Society of North America (RESNA) WC-19 *Wheelchairs for Use in Motor Vehicles* specifies design and performance requirements of wheelchairs used as seats in motor vehicles [4]. ANSI/RESNA WC19 also provides instruction to users and testing methods for both adult and pediatric transit wheelchairs. Test methods include a 20g/48kph frontal impact of the wheelchair with a seated, appropriately sized test dummy.

Most studies and research conducted to-date in the wheelchair transportation safety field on wheelchair tiedown and occupant restraint systems (WTORS), wheelchair and seating system crashworthiness, transit wheelchair design criteria, and wheelchair occupant injuries in a crash

have focused on adult wheelchair users [5] [6] [7] [8]. Wheelchair seated children might respond differently in crashes from adult occupants since they have statures smaller than adults. In addition, pediatric transit wheelchairs, which are seated by children who usually weigh less than the adults occupants, are subjected to different loading conditions in a crash than are adult transit wheelchairs. Studies investigating crash loading conditions on pediatric transit wheelchairs and the injury risks for pediatric wheelchair users in a crash are needed.

Due to the rapid growth of children, pediatric wheelchairs must be adoptable to accommodate for their growth as third party payers often only provide new wheelchairs every fourth or fifth years [9]. Wheelchair seats, seat backs, wheels, frames, and footrests are usually adjustable on most pediatric wheelchair models [10] [11]. Previous studies on adult transit wheelchairs have shown that changing of wheelchair settings, such as back angle, rear-wheel position, and rear securement point location, do have an effect on crash loads imposed upon a wheelchair [5] [6] [7] [12]. In this study, the loads imposed upon a pediatric manual wheelchair during a frontal motor vehicle crash under different wheelchair setup scenarios were investigated using a previously validated computer crash simulation model. Wheelchair design characteristics including seat back angle, rear tiedown point vertical location, and seat-to-back intersection location with respect to the rear wheel hub were varied to assess their effect on securement point, occupant restraint, wheel and seating system loading in a 20g/48kph frontal impact. Currently, no study exists that provides guidelines to the manufacturers designing pediatric transit wheelchairs. Wheelchair manufacturers have begun producing pediatric transit wheelchairs in compliance with the WC-19 standard. At last count, there were approximately nine manufacturers who produce pediatric transit wheelchairs, including transit stroller, with the

number continuously increasing. To promote the development of pediatric transit wheelchairs, guidelines aiding manufacturers in the design of these products would be useful.

5.3 METHODS

A previously developed MADYMO (V6.01) computer simulation model representing a Hybrid III 6-year-old ATD seated in a manual pediatric wheelchair (Sunrise Medical Zippie, Longmont, CO) and subjected to a 20g/48kph was used in this study [13]. The 20g frontal impact pulse is shown in Figure 58. In the model, the wheelchair was secured to the sled platform using a surrogate four-point, strap-type tiedown, and the ATD was restrained with vehicle-anchored, three-point occupant restraint belts (see Figure 59) [4]. The model was validated using data from three 20g/48kph frontal impact sled tests which complied with ANSI/RESNA WC-19 test methods (Figure 60). The sled test setup conditions are described in Table 32.

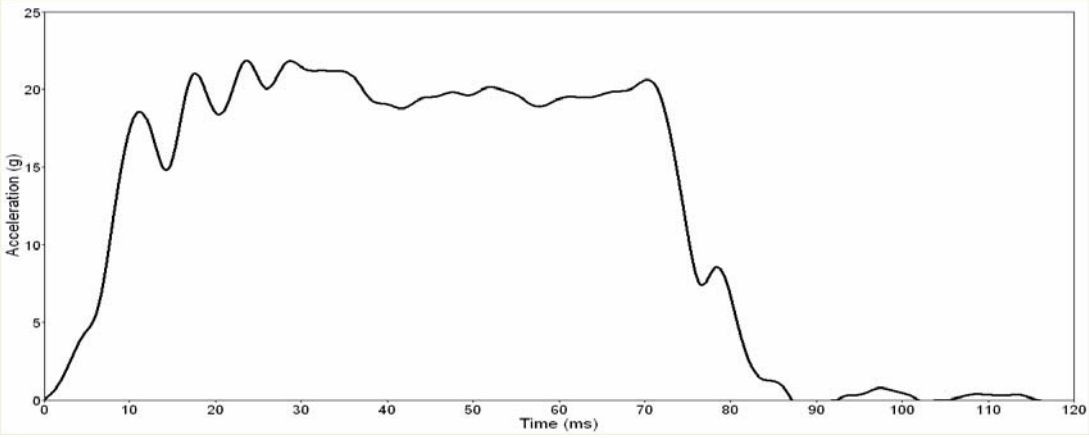

Figure 58 Sled deceleration pulse

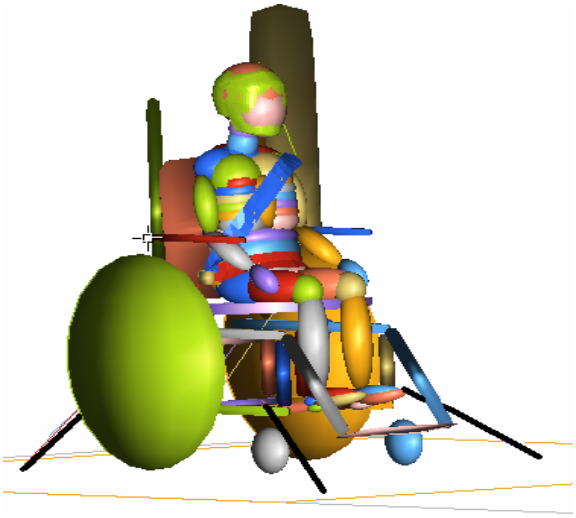

Figure 59 MADYMO model of a Hybrid III 6-year-old ATD seated in a pediatric manual WC

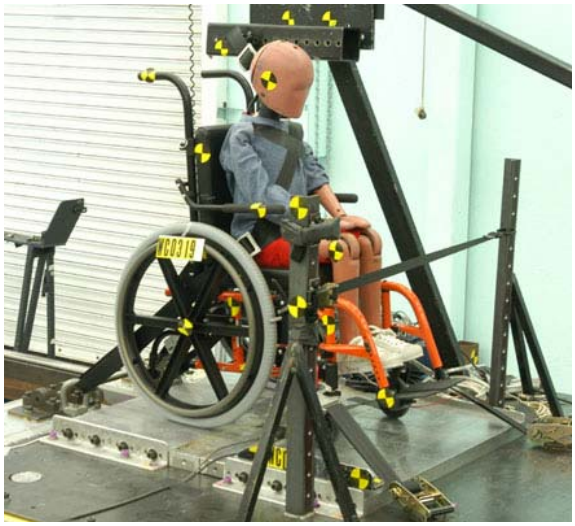

Figure 60 Sled test setup

Table 32 Sled test setup (baseline) conditions

Wheelchair Type	Sunrise Medical Zippie
Wheelchair Securement	Surrogate 4-point strap-type tiedown
Occupant Restraint	Surrogate independent vehicle mounted 3-point belt
Anthropomorphic Test Dummy	Hybrid III 6-year-old, 25kg
Target Impact Velocity (ΔV)	48 kph
Target Average Sled Deceleration	20g
Wheelchair	
Wheelchair Weight	18.6 kg
Wheelchair $CG_{vertical}$	359 mm above ground
Wheelchair $CG_{horizontal}$	188 mm front of rear hub
Wheelchair Rear Hub Height	280 mm above ground
Wheelchair Tiedown	
Front Securement Point	419 mm forward of rear hub
	191 mm above ground/ 168 mm below CG_{WC}
Rear Securement Point to Rear Hub	105 mm behind rear hub
	315 mm above ground/ 44 mm below CG_{WC}
Wheelchair Seating System	
Seat pan depth	380 mm
Seat pan width	310 mm
Seat back height	380 mm
Seat back width	310 mm
Seat Back Angle	4 º
Seat Pan Angle	3 º
Seat-to-Back Intersection Location	23 mm forward of rear hub

Note: Parameters included in the sensitivity analysis are shaded in grey.

The rear axle positioning and seat back angle are adjustable with the Zippie pediatric manual wheelchair. Adjusting the rear axle positioning can change the seat-to-back intersection location relative to the rear hub, as well as the rear securement point vertical location. To study the effect of adjustable features on loads imposed upon the wheelchair and occupant restraint system (ORS), a parametric sensitivity analysis was conducted. Each parameter (seat back angle, rear tiedown point vertical location, and seat-to-back intersection horizontal location) was varied independently while all other parameters remained at their baseline. Baseline conditions of the wheelchair model are described in Table 32. The seat back angle (SBA) was varied from -

5º to 35º in 10° increments (see Figure 61-a), the rear securement point (SP) vertical location was varied from 200 mm below the CG_{WC} to 100 mm above the CG_{WC} in 100 mm increments (see Figure 61-b), and the seat-to-back intersection (STBI) horizontal location was varied from 100 mm behind the rear hub to 100 mm in front of the rear hub in 50 mm increments (see Figure 61-c).

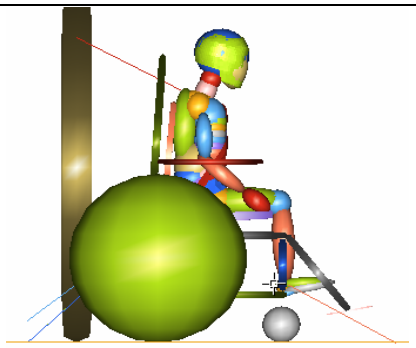

-5º seat back

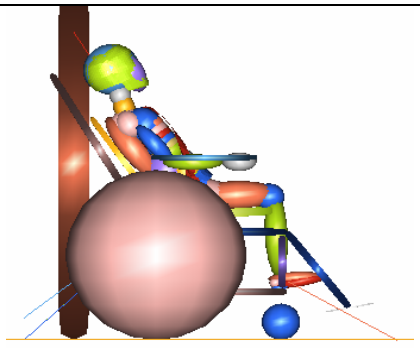

35º seat back

(a)

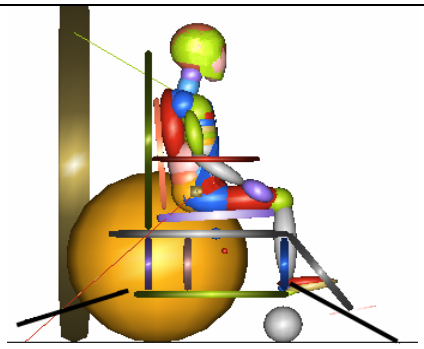

rear securement point - 200 mm below CG_{WC}

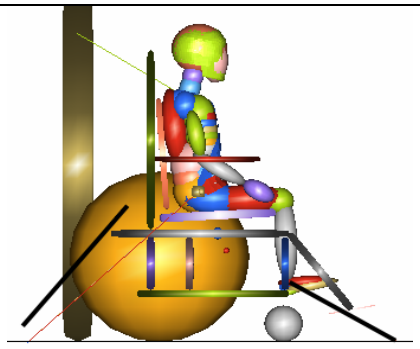

rear securement point - 100 mm above CG_{WC}

(b)

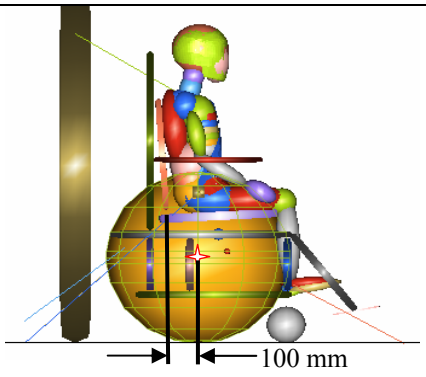

seat-to-back intersection - 100 mm behind rear hub

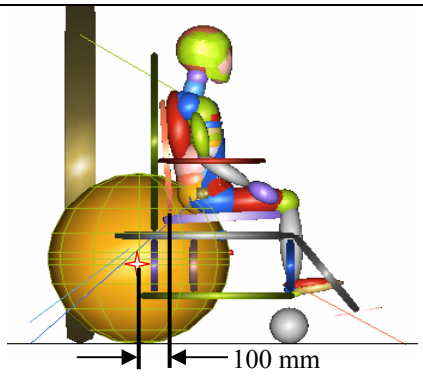

seat-to-back intersection - 100 mm in front of rear hub

(c)

Figure 61 Parameter end ranges used in Sensitivity Analysis

The MADYMO model was programmed to calculate the forces on the ORS (occupant shoulder belt and lap belt), wheelchair seating system (seat pan and seat back), securement points

(front and rear), and wheels (front and rear) during the simulation. The 'Time_Step' used in the model calculation was 0.00002 s. Data was generated every 0.0001 s, and animation output was generated every 0.002 s.

Except for the forces on the seat back and the front securement points, all data was analyzed up to 200 ms. In the sled tests, data was collected up to 200 ms, and therefore, the model was validated using data collected during the 0 to 200 ms time interval. However, the maximum seat back force and the maximum front securement point force were expected to occur during the occupant rebound phase which exceed the 200 ms time frame; therefore, seat back force and front securement force model data was analyzed through 400 ms, which would include the complete occupant rebound phase.

5.4 RESULTS

Baseline Model

Time histories of the forces on the ORS and wheelchair components during the baseline model simulation are shown in Figure 62. For the occupant restraint belts, the maximum lap belt forces occurred first, around 40 ms, followed by the maximum shoulder belt forces, around 70 ms. For the forces on the seating system, the maximum seat pan force occurred during the early phase of the frontal impact (around 40 ms), and the maximum seat back force occurred during the rebound phase of the frontal impact (near 120 ms). The maximum rear securement point forces occurred during the early phase of the impact (around 40 ms) followed by the maximum front securement point forces, which occurred during the rebound phase of the frontal impact (around 160 ms). The maximum wheel forces also occurred during the early phase of the impact (around 50 ms).

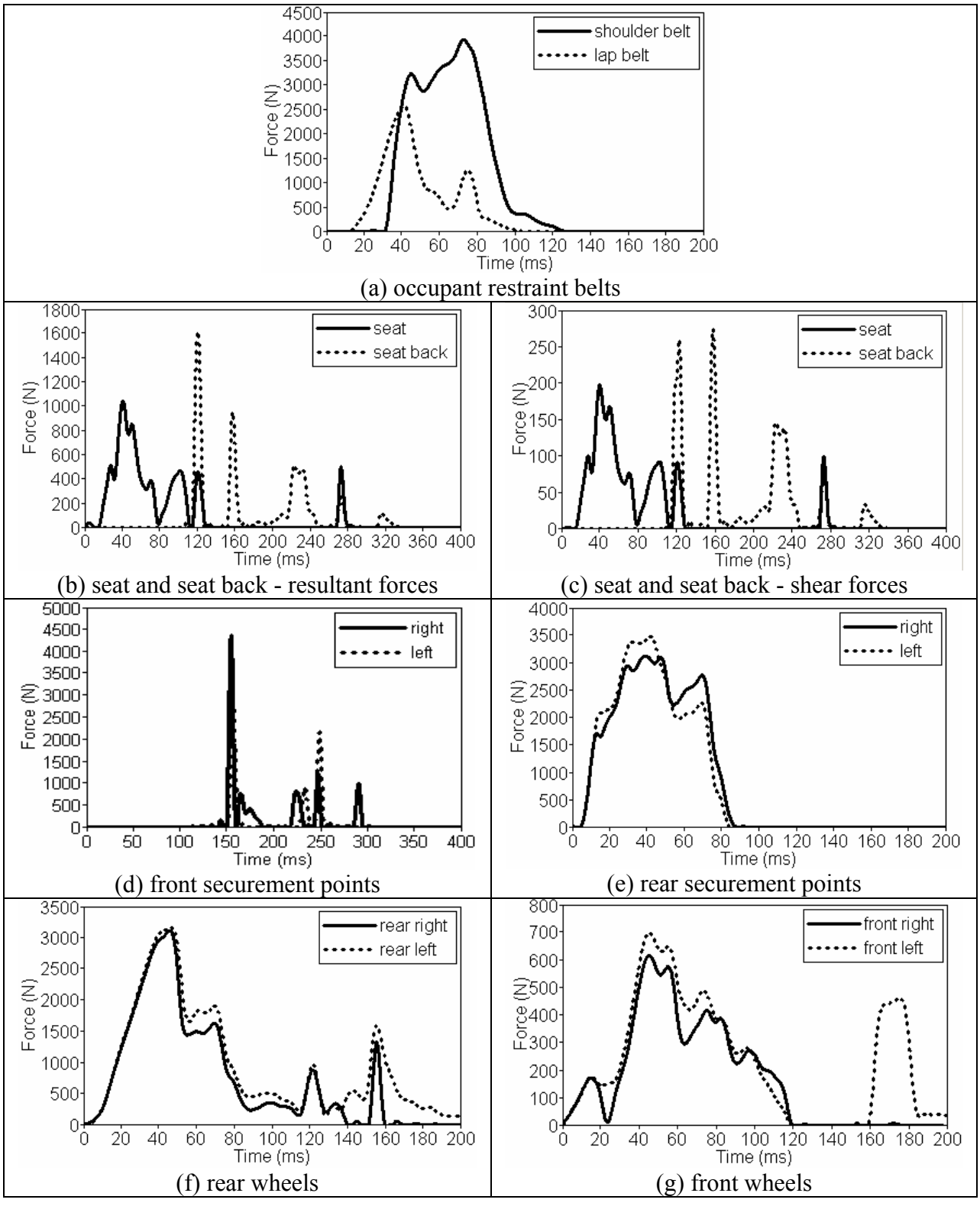

Figure 62 Force time histories of ORS and wheelchair components–baseline model

5.4.1 Wheelchair Seatback Angle

Figure 63 shows the crash response of the ATD and the wheelchair at -5° and +25° seat back angles. As the SBA increased, the tendency of ATD slide upward along the seat back surface during the rebound phase was increased. In the +25° SBA model, the dummy moved toward the upper shoulder belt anchor point during the rebound phase and caused the wheelchair to both tilt and rotate to the left.

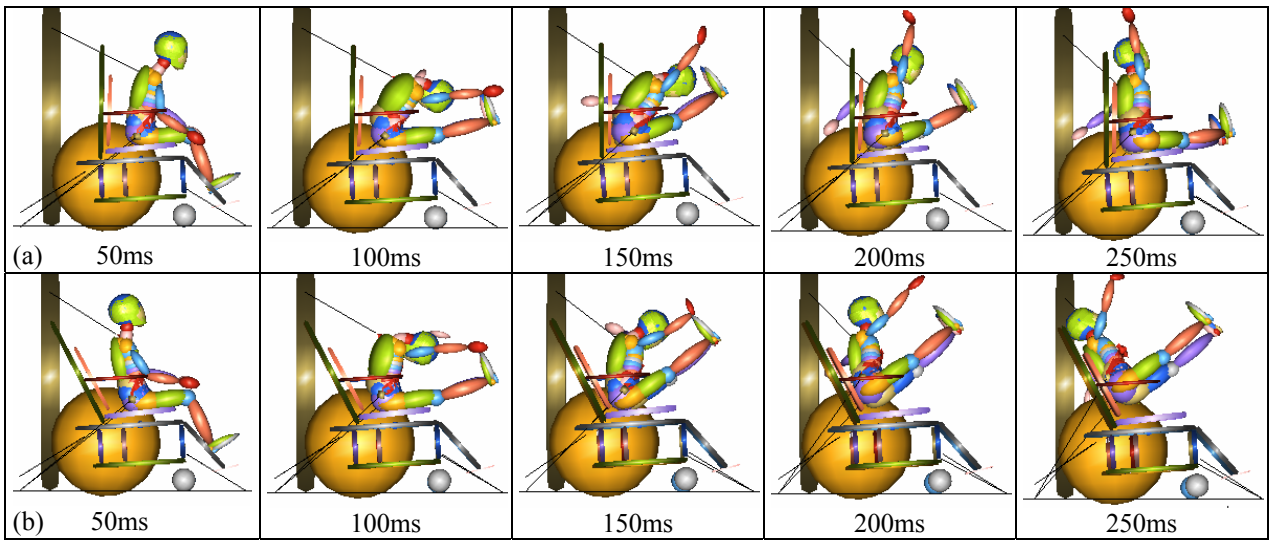

Figure 63 Crash response of the wheelchair and ATD: (a) -5° seat back and (b) +25° seat back

Table 33 shows the maximum force on the ORS and time that the maximum force occurred when the SBA was varied from -5º to 35º. The greatest difference between any two scenario was expressed as $(Force_{max}-Force_{min})/(Force_{max})*100$. The maximum % difference of the shoulder belt force and the lap belt force was 9 %.

Table 33 Maximum force on ORS: -5º to 35 º seat back angle

	Shoulder belt		Lap belt	
Seat Back Angle (º)	Time (ms)	Force (N)	Time (ms)	Force (N)
-5	75	3650	43	2683
Baseline (+4)	73	3931	42	2558
+15	77	4002	42	2442
+25	75	3820	43	2559
+35	74	3882	45	2624
Max. % difference		**9**		**9**

Note: % difference was calculated as ($Force_{max}$-$Force_{min}$)/($Force_{max}$) *100

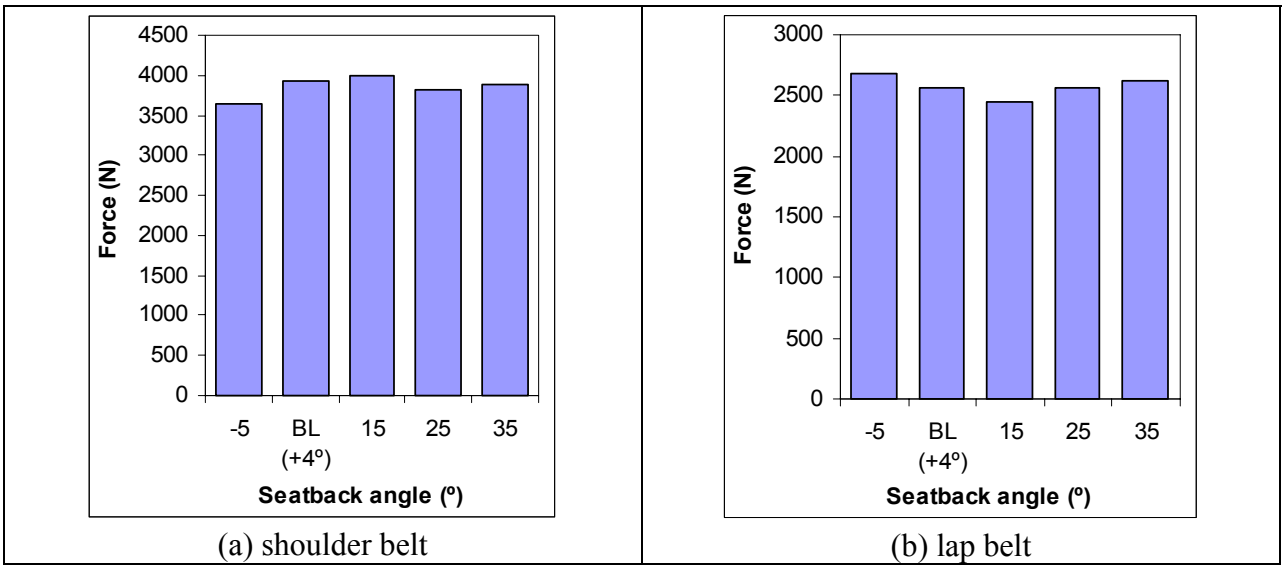

(a) shoulder belt (b) lap belt

Figure 64 Maximum force on ORS vs. seat back angle (BL = baseline)

Table 34 shows the maximum force on the wheelchair components (seating system, securement points, and wheels), and the time when the maximum force occurred while varying the SBA from -5º to 35º. Except for the 15° and 25° seat back models, the maximum force on wheelchair seat back occurred between 100ms and 200 ms. The maximum force on the wheelchair seat back for the 15º and 25º models occurred later in time than other models (after 200 ms). The SBA had considerable influence on seat back loads (both resultant and shear loads). When the SBA was positioned in between the range (15° and 25°), lower seat back loads resulted than when the SBA was positioned at the extremes (-5° and -35°). (See Figure 65-

(c) and (d)) For the seat loads, when the SBA was changed from 35° to 25°, the seat resultant load decreased from 1301 N to 1046 N (20 % decrease) and the seat shear load decreased from 252 N to 191 N (24 % decrease).

The SBA had more influence on the front securement point load than the rear securement point load. (See Figure 65-(e) through (h)) The front left securement point load decreased from 3097 N to 0 N (100 % decrease) when the SBA was changed from -5° to 25°. In the +25° SBA model, no force was imposed on the front left securement point. In the model, the wheelchair and ATD rotated to the left during the rebound phase (phase when the front tiedown belts resisted wheelchair movement), and the rotation of the wheelchair created tension on the front right tiedown belt and slack on the front left tiedown belt (see Figure 66).

The load on the rear wheels increased as the SBA increased from -5° to 35° (see Figure 65-(i) and (j)). The front wheel loads were also affected by the SBA: as the SBA changed from 35º to the baseline (4º), the front wheel loads were decreased 38 % for the right wheel and 32 % for the left wheel.

Table 34 Maximum force on wheelchair components: -5º to 35 º seat back angle

(a) wheelchair seat pan and seat back

	Seat Pan				Seat back			
Seat Back Angle (º)	Time (ms)	Resultant (N)	Time (ms)	Shear (N)	Time (ms)	Resultant (N)	Time (ms)	Shear (N)
SB -5	51	1038	51	204	126	1859	125	463
Baseline (+4)	41	1039	40	196	121	1609	158	273
SB +15	44	1166	43	203	229	1028	229	302
SB +25	45	1046	42	191	246	1028	250	213
SB +35	47	1301	44	252	134	1992	134	587
Max. % diff.		**20**		**24**		**48**		**64**

(b) wheelchair securement points

	Front Right SP		Front Left SP		Rear Right SP		Rear Left SP	
Seat Back Angle (º)	Time (ms)	Force (N)	Time (ms)	Force (N)	Time (ms)	Force (N)	Time (ms)	Force (N)
-5	158	4993	159	3097	48	3060	43	3503
Baseline (+4)	155	4340	156	3012	39	3115	42	3470
+15	137	4203	138	1300	49	3323	43	3648
+25	128	4674	NA	0	43	3283	45	3772
+35	121	4575	147	1897	45	3387	49	4171
Max. % diff.		**16**		**100**		**10**		**17**

(c) wheelchair wheels

	Rear Right Wheel		Rear Left Wheel		Front Right Wheel		Front Left Wheel	
Seat Back Angle (º)	Time (ms)	Force (N)	Time (ms)	Force (N)	Time (ms)	Force (N)	Time (ms)	Force (N)
SB -5	47	2986	47	3052	57	694	57	772
Baseline (+4)	46	3105	47	3150	45	615	45	696
SB +15	47	3316	47	3311	45	666	138	711
SB +25	48	3482	49	3465	45	821	131	954
SB +35	50	3697	50	3678	48	994	47	1023
Max. % diff.		**19**		**17**		**38**		**32**

Note: % difference was calculated as $(Force_{max}-Force_{min})/(Force_{max}) *100$
SP =Securement Point

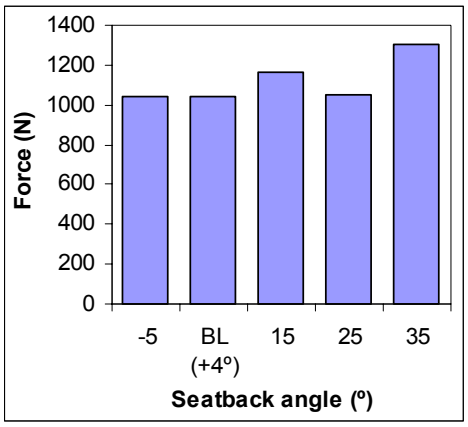

(a) wheelchair seat – resultant force

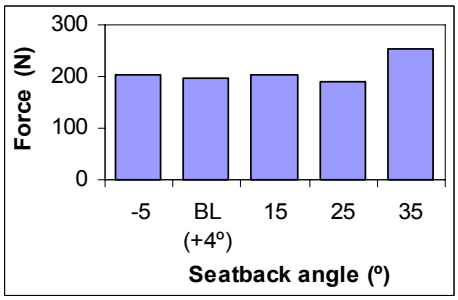

(b) wheelchair seat – shear force

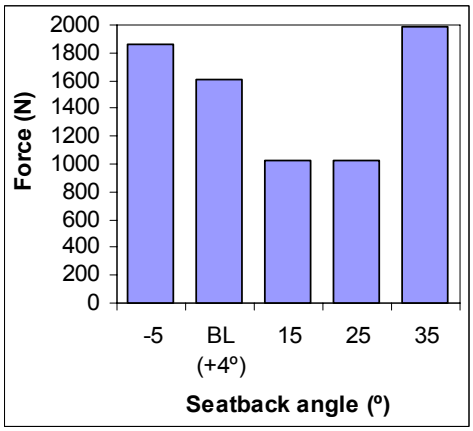

(c) wheelchair seat back – resultant force

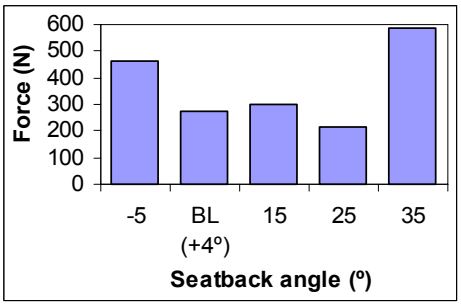

(d) wheelchair seat back – shear force

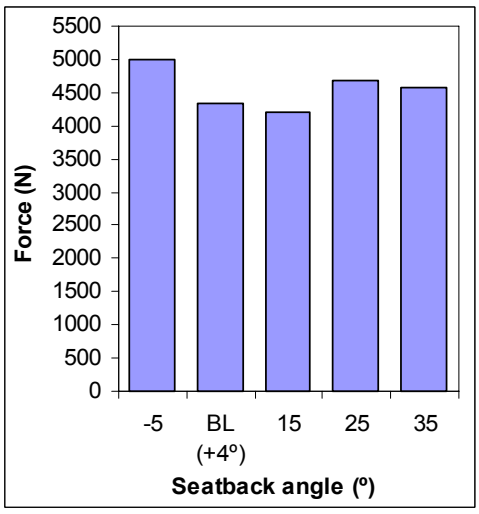

(e) front right securement point

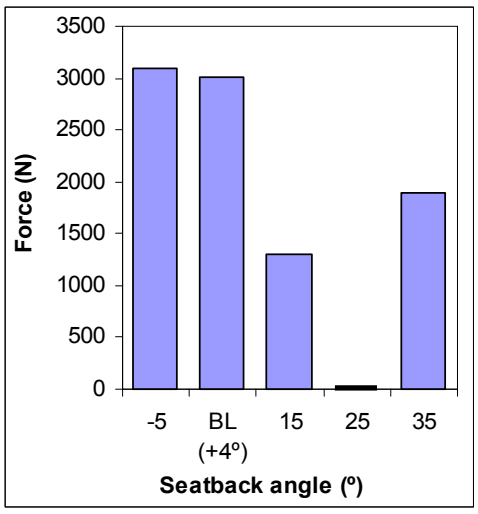

(f) front left securement point

(Continue)

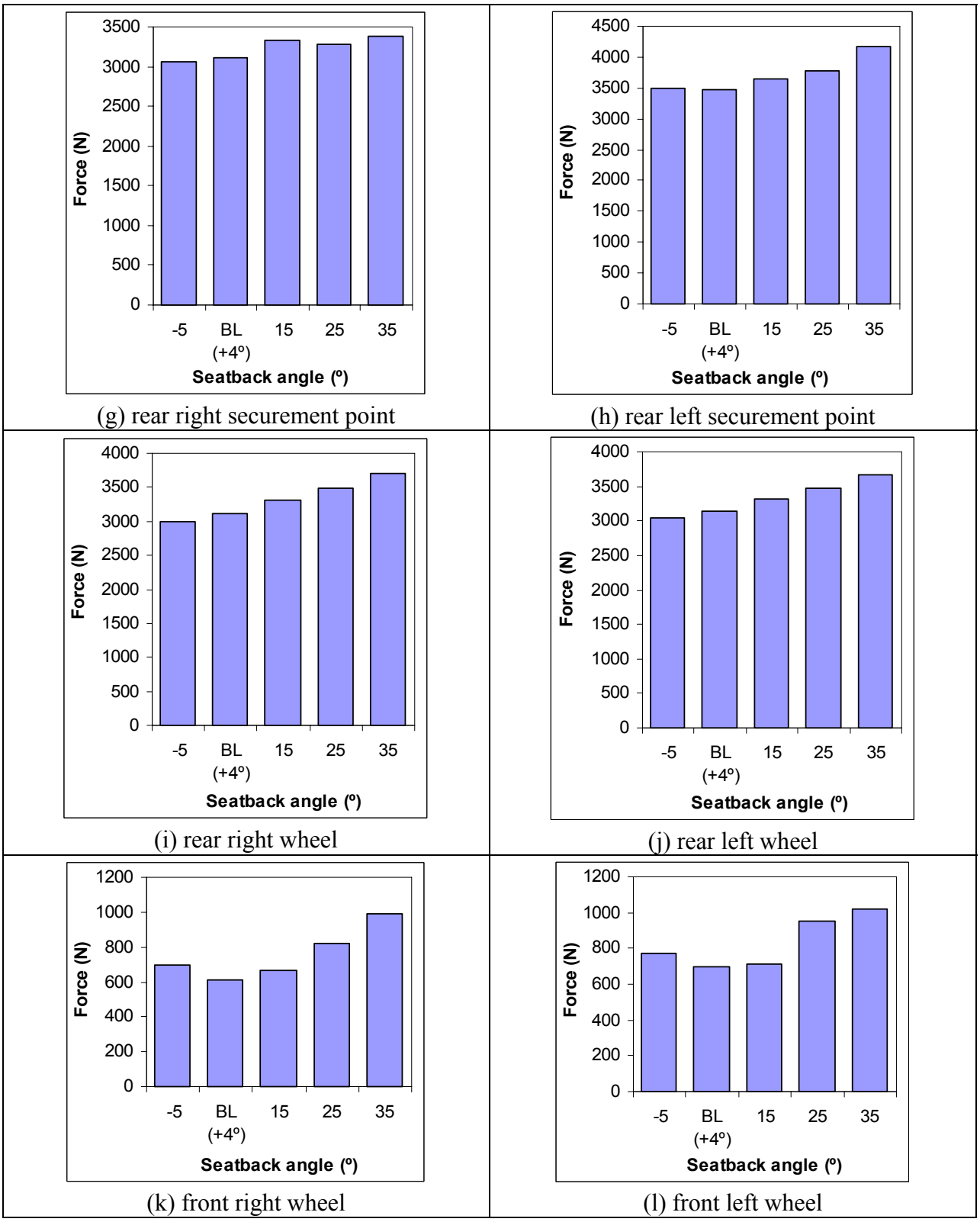

Figure 65 Maximum force on wheelchair components vs. seat back angle (BL = baseline)

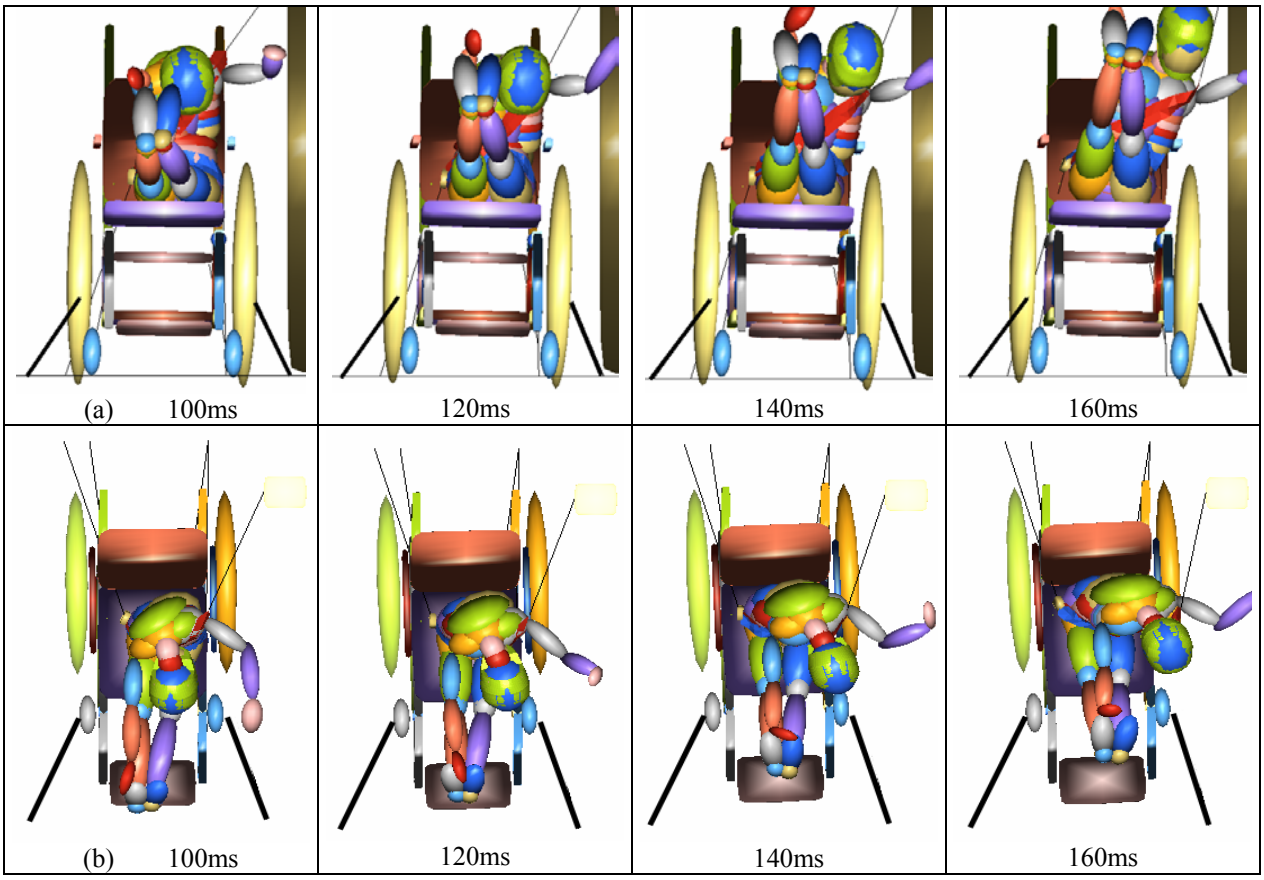

Figure 66 (a) Front view and (b) top view of the +25° SBA model in rebound phase

5.4.2 Rear Securement Point Vertical Location

The crash response of the ATD and the wheelchair with the rear tiedown at the -200CG_{WC} SP position and +100CG_{WC} SP position are shown in Figure 67. As the rear SP position was raised from 200mm below the CG_{WC} to 100mm above the CG_{WC}, the wheelchair had an increased tendency of rotating rearward at the rear wheel axle point. When the rear SP was located 100mm above the CG_{WC}, severe rearward rotation of the wheelchair occurred.

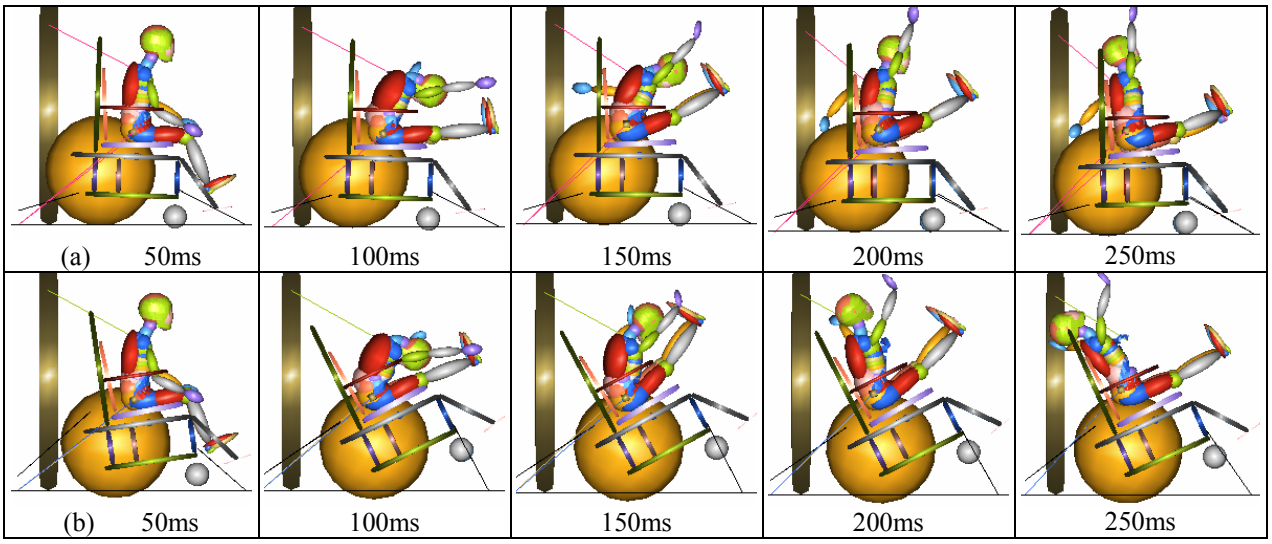

Figure 67 Crash response of the wheelchair and ATD: (a) -200CG_{WC} rear SP position and (b) +100CG_{WC} rear SP position

The maximum force measured on ORS and time the maximum force occurred when the wheelchair rear SP position was varied from 200mm below (-200) the CG_{WC} to 100mm above (+100) the CG_{WC} are presented in Table 35. The shoulder belt force decreased from 4151 N to 3365 N (19 % decrease) while the rear SP position moved from CG_{WC} to +100 CG_{WC}. The rear SP position did not have much impact on the lap belt force.

Table 35 Maximum force on ORS: 200mm below CG_{WC} to 100mm above CG_{WC}

	Shoulder belt		Lap belt	
Rear SP position wrt CG_{WC} (mm)	Time (ms)	Force (N)	Time (ms)	Force (N)
-200	75	4010	42	2636
-100	73	3901	42	2582
Baseline (-44)	73	3931	42	2558
0 (at CG_{WC})	76	4151	42	2539
+100	74	3365	44	2610
Max. % difference		**19**		**4**

Note: % difference was calculated as ($Force_{max}$-$Force_{min}$)/($Force_{max}$) *100
SP =Securement Point

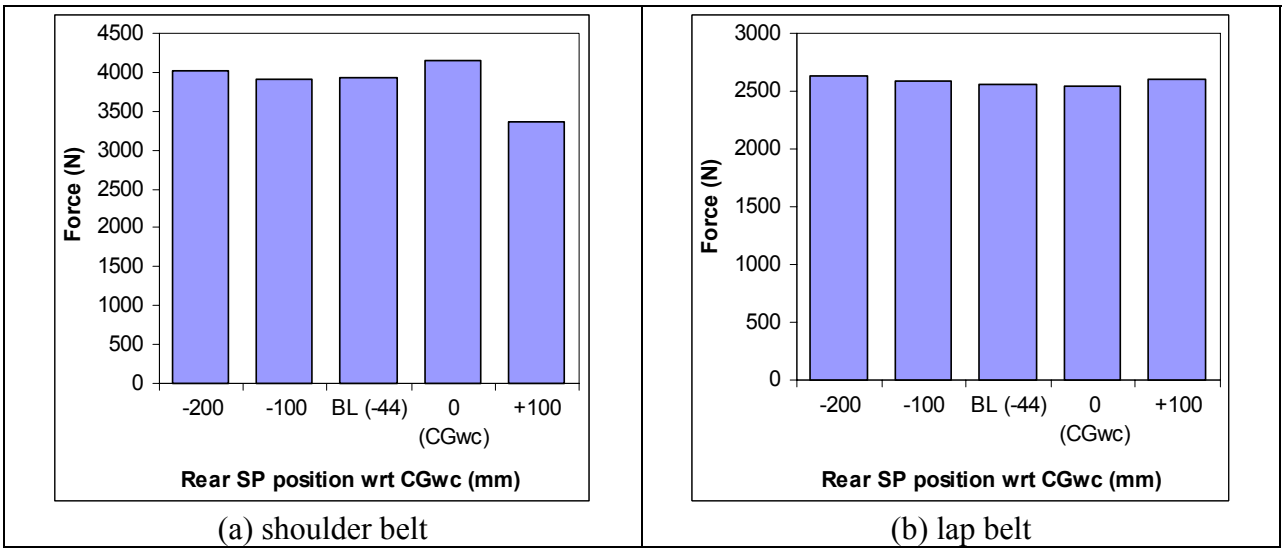

(a) shoulder belt (b) lap belt

Figure 68 Maximum force on ORS vs. rear tiedown position (BL = baseline)

The maximum force on the wheelchair components (seating system, securement points, and wheels) and time the maximum force occurred while varying the wheelchair rear SP from 200mm below the CG_{WC} (-200) to 100mm above the CG_{WC} (+100) are presented in Table 36. The seat pan loads (both resultant and shear loads) were found to increase as the rear tiedown point was raised from -200 CG_{WC} to +100 CG_{WC} (see Figure 69-(a) and (b)). The seat pan resultant force had a 32% change and the seat pan shear force had a 36% change when the rear SP was moved from -200 CG_{WC} to +100 CG_{WC}. The rear SP position had more influence on the seat back shear force than the seat back resultant force (see Table 36).

Among four securement points (two front and two rear securement points), the highest force occurred at the front right securement point. When the rear SP position was located 100mm above CG_{WC} (+100 CG_{WC}), 6988 N force was measured at the front right securement point.

The loads on wheelchair wheels were greatly affected by the rear SP position (see Figure 69-(i) through (l)). As the rear SP position was lowered from +100 CG_{WC} to -200 CG_{WC}, the rear

right wheel load was decreased from 5098 N to 1064 N (79 % change), the rear left wheel load was decreased from 4964 N to 914 N (82 % change), the front right wheel load was increased from 97 N to 1961 N (95 % change), and the front left wheel load was increased from 95 N to 2013 N (95 % change).

Table 36 Maximum force on wheelchair components: 200mm below CG_{WC} to 100mm above CG_{WC}

(a) wheelchair seat pan and seat back

	Seat Pan				Seat Back			
Rear SP position wrt CG_{WC} (mm)	Time (ms)	Resultant (N)	Time (ms)	Shear (N)	Time (ms)	Resultant (N)	Time (ms)	Shear (N)
-200	50	931	50	183	122	1560	122	448
-100	40	1017	40	196	146	1538	127	236
Baseline (-44)	41	1039	40	196	121	1609	158	273
0 (at CG_{WC})	53	1123	53	220	115	1929	115	349
+100	54	1374	54	284	114	1901	115	549
Max. % diff.		**32**		**36**		**20**		**57**

(b) wheelchair securement points

	Front Right SP		Front Left SP		Rear Right SP		Rear Left SP	
Rear SP position wrt CG_{WC} (mm)	Time (ms)	Force (N)	Time (ms)	Force (N)	Time (ms)	Force (N)	Time (ms)	Force (N)
-200	131	4540	134	2939	35	2319	40	2780
-100	144	4607	145	3319	35	2860	40	3135
Baseline (-44)	155	4340	156	3012	39	3115	42	3470
0 (at CG_{WC})	162	5075	251	2228	51	3443	43	4069
+100	108	6988	113	1759	62	4355	52	3904
Max. % diff.		**38**		**47**		**47**		**32**

(c) wheelchair wheels

	Rear Right Wheel		Rear Left Wheel		Front Right Wheel		Front Left Wheel	
Rear SP position wrt CG_{WC} (mm)	Time (ms)	Force (N)	Time (ms)	Force (N)	Time (ms)	Force (N)	Time (ms)	Force (N)
-200	134	1064	137	914	48	1961	45	2013
-100	44	2106	44	2158	45	1163	45	1240
Baseline (-44)	46	3105	47	3150	45	615	45	696
0 (at CG_{WC})	50	3804	51	3925	89	237	180	703
+100	110	5098	70	4964	10	97	11	95
Max. % diff.		**79**		**82**		**95**		**95**

Note: % difference was calculated as $(Force_{max}-Force_{min})/(Force_{max}) *100$
SP =Securement Point

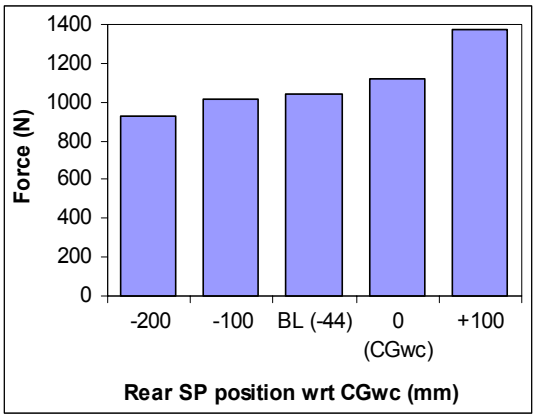

(a) wheelchair seat pan – resultant force

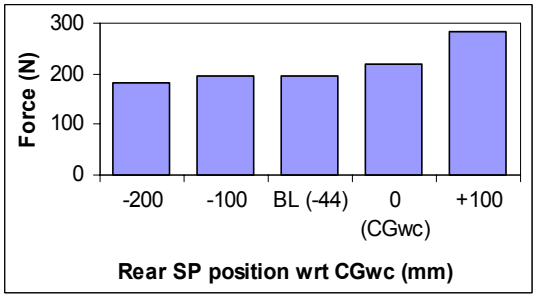

(b) wheelchair seat pan – shear force

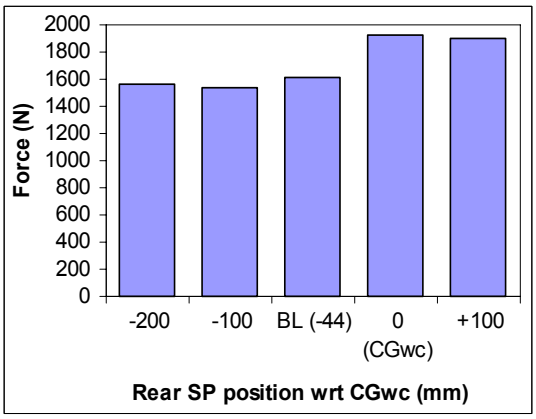

(c) wheelchair seat back – resultant force

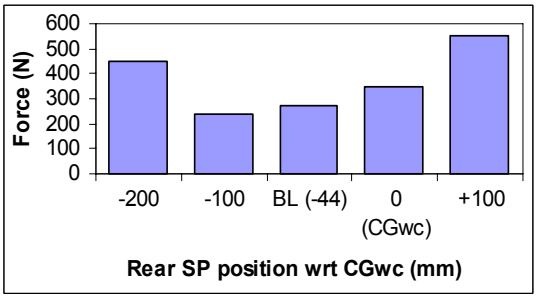

(d) wheelchair seat back – shear force

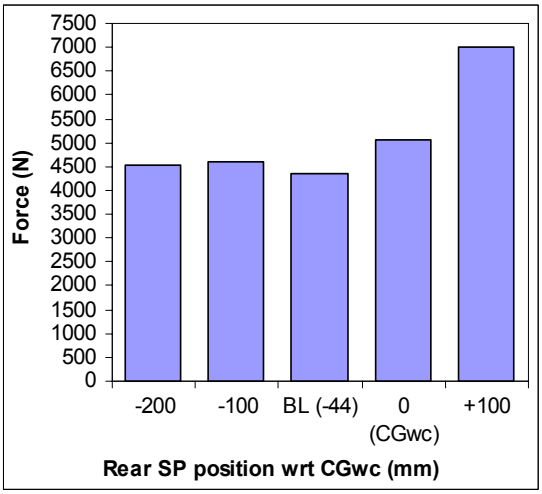

(e) front right securement point

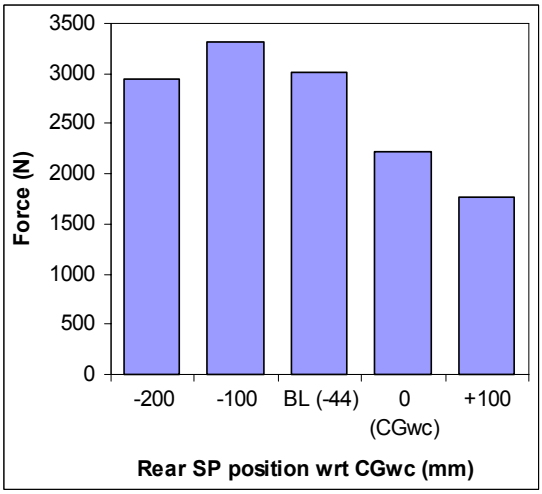

(f) front left securement point

(Continue)

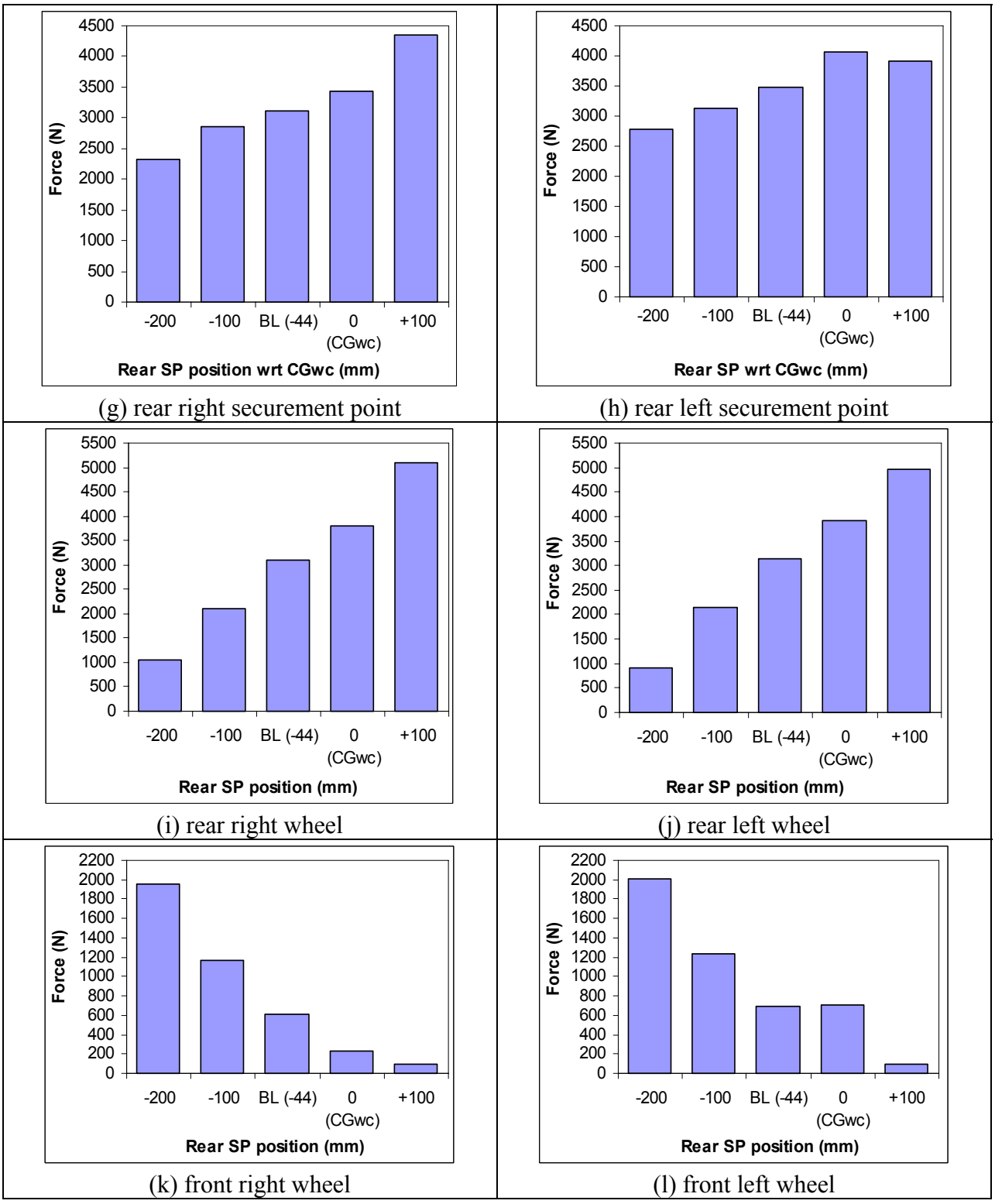

(g) rear right securement point

(h) rear left securement point

(i) rear right wheel

(j) rear left wheel

(k) front right wheel

(l) front left wheel

Figure 69 Maximum force on wheelchair components vs. rear tiedown position (BL = baseline)

5.4.3 Seat-to-back Intersection Horizontal Location

Figure 70 shows the crash response of the ATD and the wheelchair when STBI was located 100mm behind rear hub and STBI was located 100mm in front of rear hub. As the STBI location was moved horizontally toward the rear of the wheelchair, increased rearward rotation of the wheelchair was occurred.

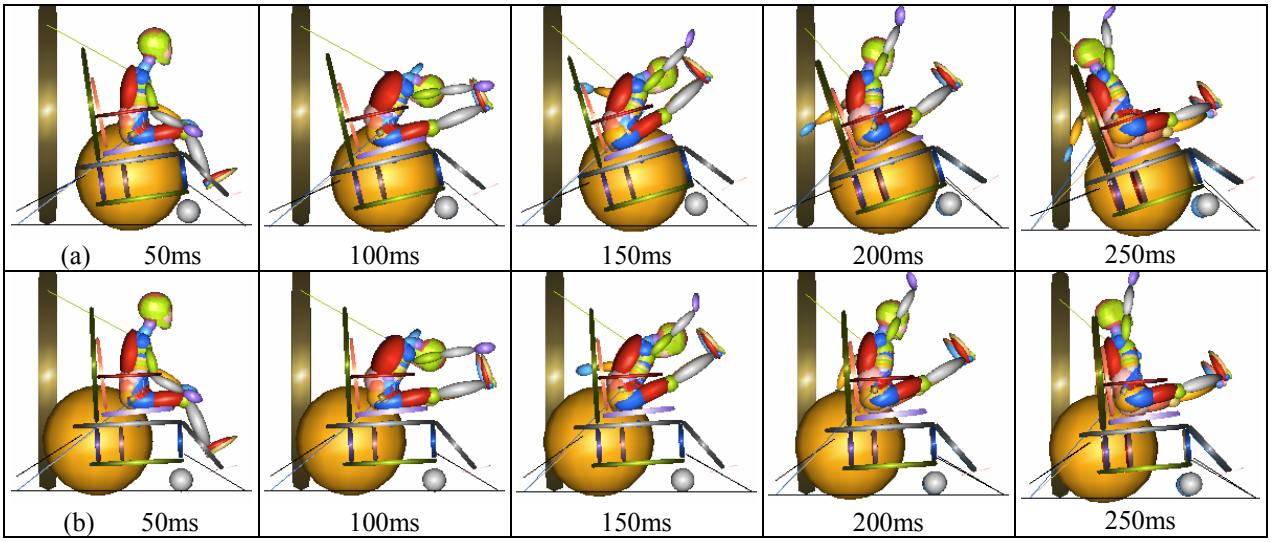

Figure 70 Crash response of the wheelchair and ATD: (a) STBI 100mm behind rear hub and (b) STBI 100mm in front of rear hub

The maximum force measured on ORS and the time when the maximum force occurred as the STBI horizontal location varied from 100 mm behind the rear hub (R100) to 100 mm in front of the rear hub (F100) are presented in Table 37. The STBI location had almost no impact on the occupant restraint belt loads (see Figure 71).

Table 37 Maximum force on ORS: STBI 100mm behind rear hub to 100mm in front of rear hub

	Shoulder belt		Lap belt	
Seating location wrt rear hub	Time (ms)	Force (N)	Time (ms)	Force (N)
R100	76	3939	42	2513
R50	73	3976	42	2537
0	73	3937	42	2552
Baseline (F23)	73	3931	42	2558
F50	73	3920	42	2560
F100	73	3921	42	2569
Max. % difference		**1**		**2**

Note: % difference was calculated as $(Force_{max}-Force_{min})/(Force_{max}) *100$

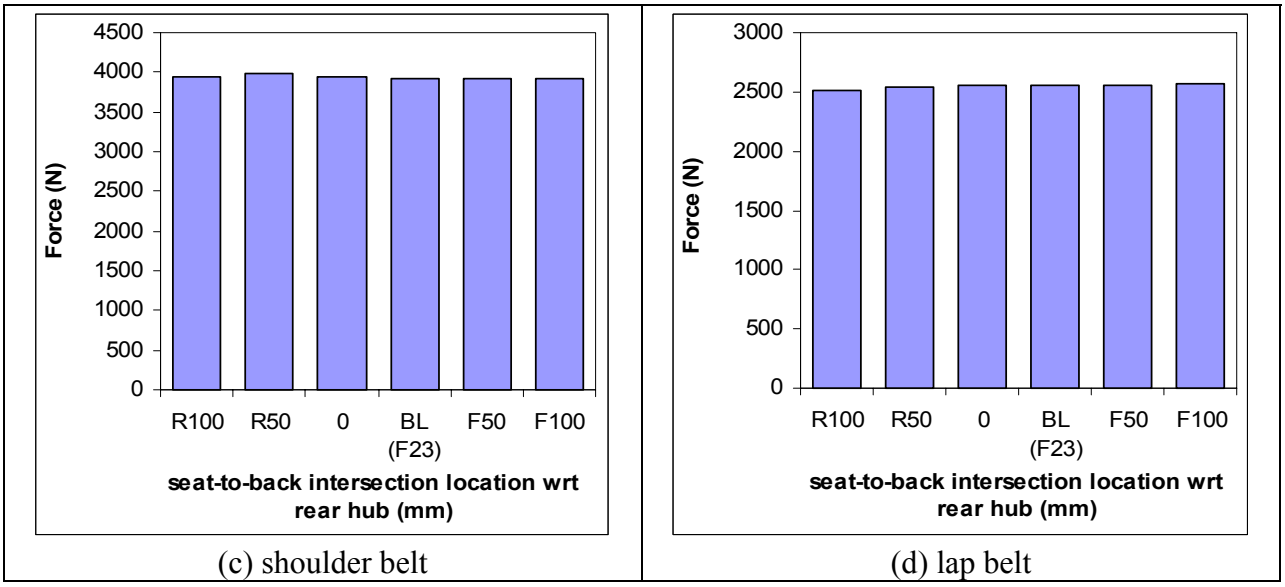

(c) shoulder belt (d) lap belt

Figure 71 Maximum force on ORS vs. seat-to-back intersection location (BL = baseline)

Table 38 shows the maximum force on wheelchair components (seating system, securement points, and wheels) and the time when the maximum force occurred as the STBI horizontal location was varied from 100 mm behind the rear hub (R100) to 100 mm in front of the rear hub (F100). When the STBI was located between 50 mm behind the rear hub (R50) to 100 mm in front of the rear hub (F100), the maximum force on the seating systems was not much influenced by the STBI location. When the STBI location was moved from 50 mm behind the

rear hub (R50) to 100 mm behind the rear hub (R100), the seat pan resultant load was increased from 1086 N to 1311 N (17 % change) and the seat back shear force was increased from 254 N to 450 N (44 % change). (See Figure 72-(a) through (d))

The STBI location had more influence on the front securement point force than the rear securement point force. The highest force occurred at the front right securement point among four securement points.

As the seat-to-back intersection location was moved forward from R100 to F100, the rear right wheel load was decreased from 3450 N to 2675 N (22 % change) and the rear left wheel load was decreased from 3639 N to 2708 N (26 % change). (See Figure 72-(i) and (j)) The loads on the front wheels were greatly affected by the wheelchair seating position. As the seat-to-back intersection location was moved forward from R100 to F100, the front right wheel load was increased from 131 N to 1141 N (89 % change) and the front left wheel load was increased from 129 N to 1197 N (89 % change).

Table 38 Maximum force on wheelchair components: STBI 100mm behind rear hub to 100mm in front of rear hub

(a) wheelchair seat pan and seat back

	Seat Pan				Seat Back			
Seating location wrt rear hub	Time (ms)	Resultant (N)	Time (ms)	Shear (N)	Time (ms)	Resultant (N)	Time (ms)	Shear (N)
R100	52	1311	51	253	125	1709	126	450
R50	52	1086	52	213	120	1535	123	254
0	41	1044	41	198	120	1576	123	266
Baseline (F23)	41	1039	40	196	121	1609	158	273
F50	41	1034	40	195	121	1631	155	273
F100	41	1036	40	194	121	1674	152	287
Max. % diff.		**21**		**23**		**10**		**44**

(b) wheelchair securement points

	Front Right SP		Front Left SP		Rear Right SP		Rear Left SP	
Seating location wrt rear hub	Time (ms)	Force (N)	Time (ms)	Force (N)	Time (ms)	Force (N)	Time (ms)	Force (N)
R100	161	5493	275	2397	53	3025	45	3869
R50	162	5122	259.9	2021	51	3039	43	3742
0	157	4557	250	2968	48	3126	42	3518
Baseline (F23)	155	4340	156	3012	39	3115	42	3470
F50	153	4316	154	2994	39	3183	42	3436
F100	150	4561	150	3174	39	3211	42	3371
Max. % diff.		**21**		**36**		**6**		**13**

(c) wheelchair wheels

	Rear Right Wheel		Rear Left Wheel		Front Right Wheel		Front Left Wheel	
Seating location wrt rear hub	Time (ms)	Force (N)	Time (ms)	Force (N)	Time (ms)	Force (N)	Time (ms)	Force (N)
R100	51	3450	48	3639	13	131	13	129
R50	50	3441	46	3604	90	257	89	464
0	47	3218	48	3284	45	451	45	526
Baseline (F23)	46	3105	47	3150	45	615	45	696
F50	45	2955	46	2995	45	813	46	883
F100	44	2675	44	2708	45	1141	46	1197
Max. % diff.		**22**		**26**		**89**		**89**

Note: % difference was calculated as $(Force_{max}-Force_{min})/(Force_{max}) *100$
SP =Securement Point

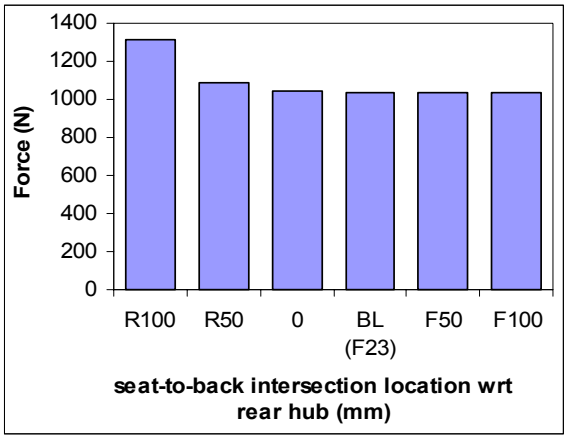

(a) wheelchair seat pan – resultant force

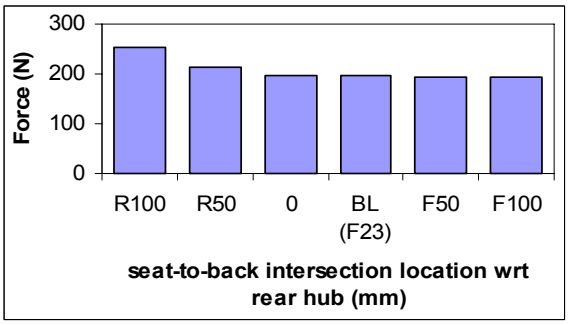

(b) wheelchair seat pan – shear force

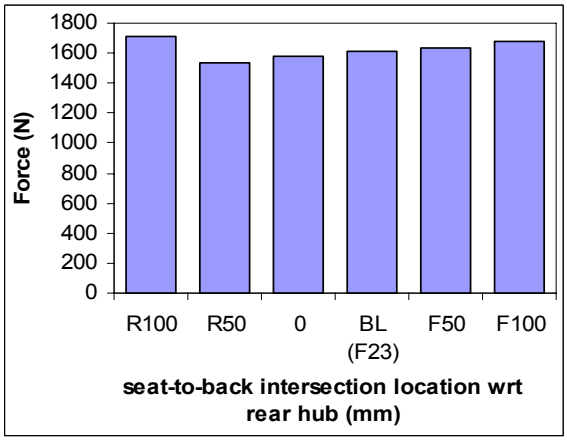

(c) wheelchair seat back – resultant force

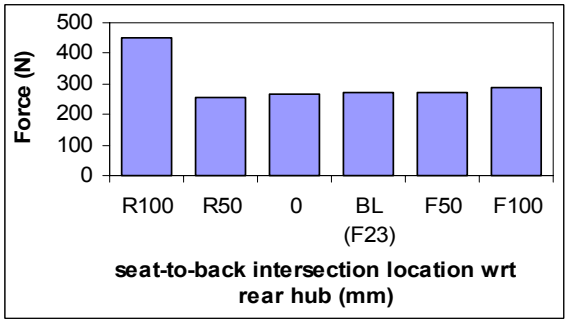

(d) wheelchair seat back – shear force

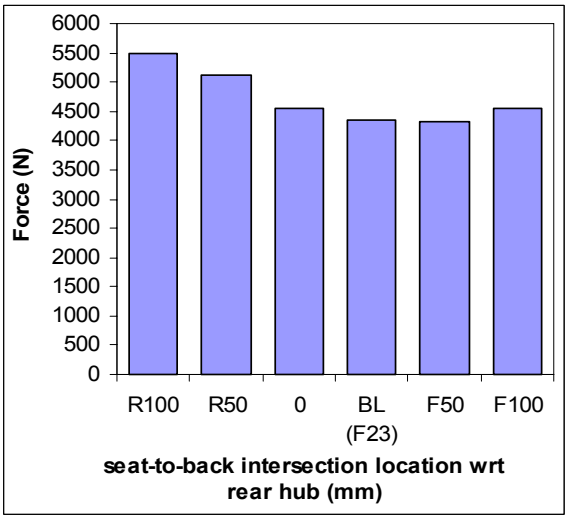

(e)front right securement point

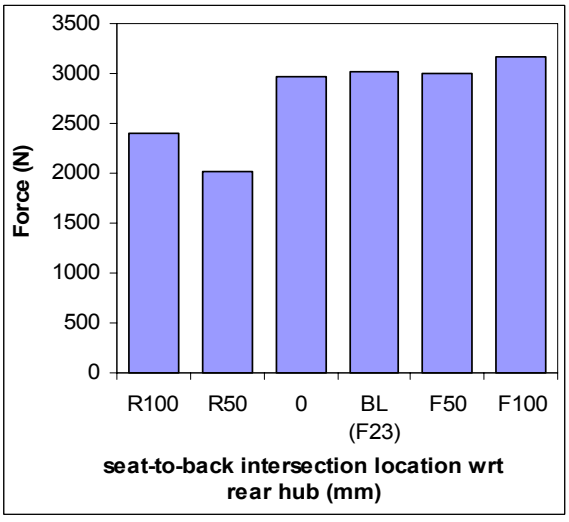

(f) front left securement point

(Continue)

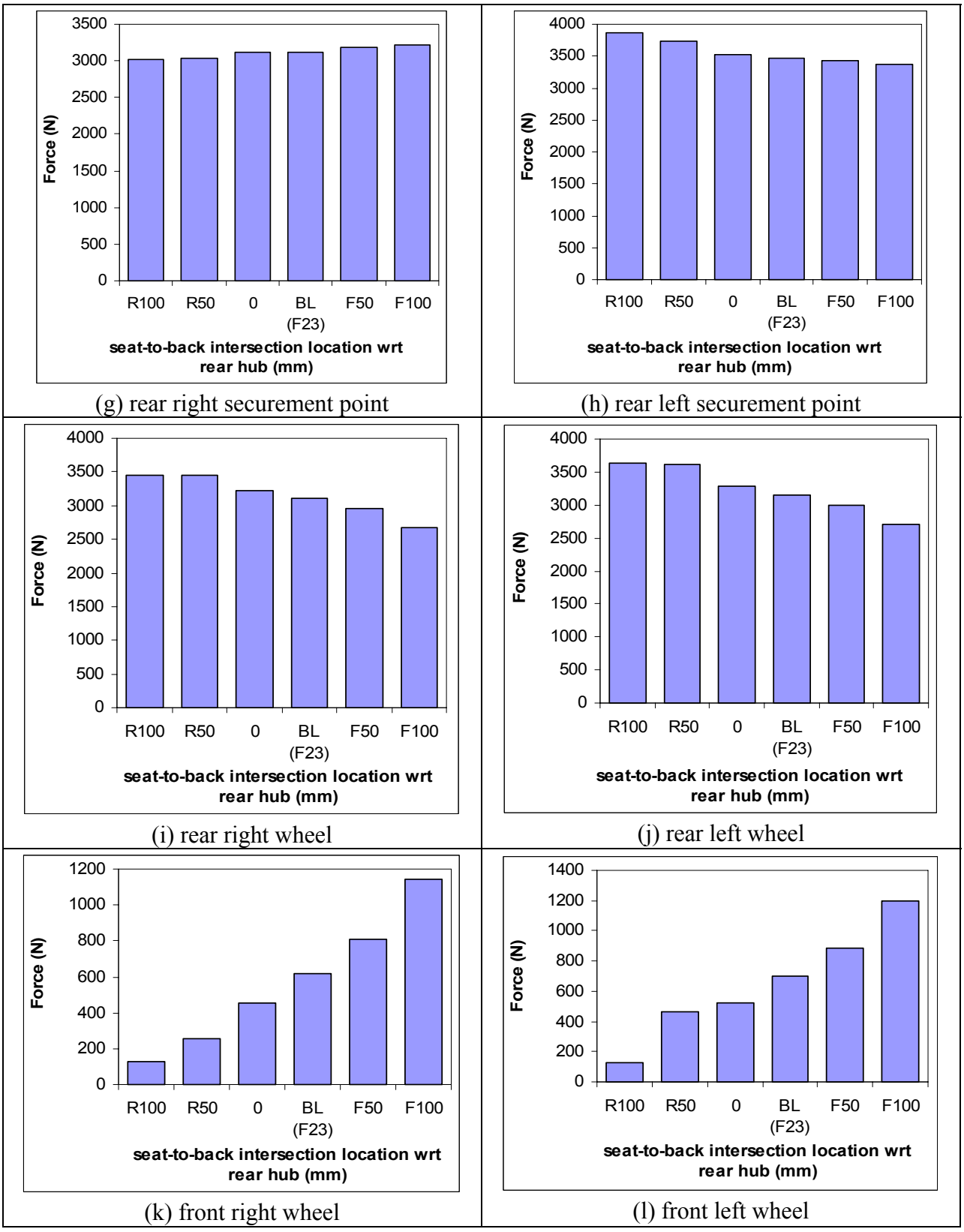

Figure 72 Maximum force on wheelchair components vs. seat-to-back intersection location (BL = baseline)

Among different wheelchair setup scenarios, the seat pan force was influenced the most by the wheelchair rear SP location: the seat pan resultant force ranged from 931 N to 1374 N (32 % difference), and the seat pan shear force ranged from 183 N to 284 N (36 % difference). The seat back force was influenced the most by the SBA changes: the resultant force ranged from 1028 N to1992 N (48 % difference), and the shear force ranged from 213 N to 587 N (64 % difference) with changes in SBA. The greatest SP forces (both front SP and rear SP) occurred when the rear SP was positioned 100mm above the CG_{WC}. The rear tiedown locations also had a substantial impact on wheelchair wheel forces (both rear wheels and front casters): force on the rear right wheel ranged from 1064 N to 5098 N (79 % difference) and force on the front left wheel ranged from 95 N to 2013 N (95 % difference).

Based on the results found in this study, the maximum loads a manual pediatric wheelchair and ORS experience during a 20g/48kph frontal impact when a 6-year-old occupant is seated in the wheelchair is presented in Table 39.

Table 39 Maximum force on a manual pediatric wheelchair and WTORS

ORS and WC components	Force (N)
Shoulder belt	4002
Lap belt	2683
Front SP	6988
Rear SP	4355
Seat pan	1374
Seat back	1992
Rear wheel	5098
Front wheel	2013

5.5 DISCUSSION

The results of this study showed that changing of wheelchair settings do have impact on the loads imposed upon wheelchair components. Seat back force was influenced the most by the

SBA of the wheelchair. Increased in the SBA between -5° and +25° tends to decrease seat back loading because the ATD slid along the seat back surface in rebound phase (see Figure 63). In 35° SBA model, the ATD's pelvis imposed high load on the seat back before it slid along the seat back. In general, the dummy kinematics showed that the contact between the dummy's pelvis and the seat back occurred first followed by the contact between the dummy's upper torso and the seat back (see Figure 63). The maximum force on seat back for 15° and 25° SBA models occurred later in time (after 200 ms) than the other models because the maximum force occurred due to the contact between the upper torso of the dummy (not the pelvis like other models) and the seat back (see Figure 73).

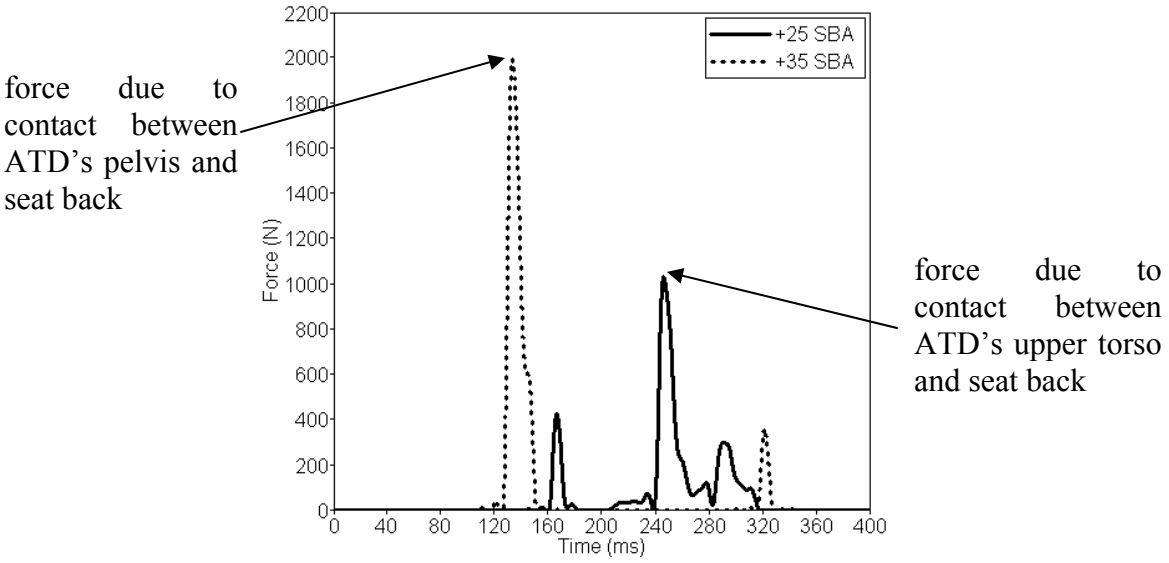

Figure 73 Seat back force time histories of +25° and +35° SBA models

The rear SP position had significant affect on the forces on several wheelchair components. As the rear SP position was raised from 200 mm below the CG_{WC} (-200 CG_{WC}) to 100 mm above the CG_{WC} (+100 CG_{WC}), increased wheelchair rearward rotation was occurred.

The increased rearward rotation of the wheelchair, combined with the forward momentum of the occupant, increased the loading on seat pan as the rear SP position was raised.

The effect of rear SP position was more profound on wheelchair wheel forces than seat pan force. Rearward rotation of the wheelchair required the rear wheels to carry the entire load of the wheelchair and occupant during an impact. The highest rear wheel force (5098 N) among various wheelchair setups was occurred at the +100CG_{WC} model, which had severe rearward wheelchair rotation during an impact (see Figure 67-(b)). Conversely, the highest front wheelchair force (2013 N) was occurred when the rear SP was positioned 200 below CG_{WC}. In -200 CG_{WC} model, the wheelchair was slightly rotated forward (see 100ms in Figure 67-(a)). This forward rotation imposed higher force on the front wheels than the rear wheels during an impact.

The largest front and the rear securement point forces occurred when the rear SP was positioned 100 above CG_{WC}. The movement of a wheelchair is limited by wheelchair tiedown, and more extensive rotation or movement of a wheelchair generally leads to greater forces on the securement points where the tiedown were attached. In +100CG_{WC} model, the rear SP force reached 4355 N during the early phase of the impact and the front SP force reached 6988 N during the rebound phase of the impact due to extensive rearward rotation of the wheelchair (see Figure 67-(b)).

Loads on wheelchair parts and WTORS under different wheelchair setup conditions have been studied previously using computer models representing adult wheelchairs and adult occupants (mostly 50^{th} percentile male ATD weighing 76.3kg). In the study done by Bertocci et al., wheelchair rear SP position was varied from 190 mm below the wheelchair CG to 190 mm above wheelchair CG, and loads on ORS and wheelchair components were evaluated [7]. The

wheelchair and ATD model used in the study were a SAE/ISO surrogate wheelchair (85kg) and a Hybrid III 50th percentile male ATD. Similar to the results found in this pediatric wheelchair study, the rear SP load and the seat pan load increased (18815 N to 31150 N for the rear SP load and 12696 N to 19158 N for the seat pan load) as the rear SP position was raised from -190mm CG_{WC} to +190mm CG_{WC} (see Table 40). Similar to our results, the loads on wheelchair wheels were greatly affected by the rear SP position in the surrogate wheelchair study. As the rear SP position was lowered from +190mm CG_{WC} to -190mm CG_{WC}, the rear right wheel load decreased from 33865 N to 320 N (99 % change), and the front left wheel load increased from 525 N to 8002 N (95 % change).

Table 40 Influence of rear securement point position: SAE/ISO surrogate WC (85kg) and Hybrid III 50th percentile male ATD [7]

Rear SP position wrt CG_{WC} (mm)	Rear SP (N)	Lap belt (N)	Seat pan – resultant (N)	Rear wheel (N)	Front wheel (N)
-190	18815	8649	12696	320	8002
0	21033	8273	16680	7990	5695
190	31150	5821	19158	33865	525
Max. % difference	**40**	**33**	**34**	**99**	**93**

Influence of surface stiffness of wheelchair seating surfaces (seat pan and seat back) and seat back angle on wheelchair seat pan and seat back loading was evaluated using a validated computer model representing a 116 kg powerbase wheelchair and 50th percentile Hybrid III male ATD [6]. Similarly to our results, although changing the seat back angle impacted both seat pan and seat back loads, the change of seat back angle influenced seat back load more than seat pan load. As the seat back angle increased, the seat back load decreased. (See Table 41)

Table 41 Influence of wheelchair seat back angle: powerbase WC (116kg) and Hybrid III 50th percentile male ATD [6]

Seat back angle (º)	Seat pan (N)	Seat back (N)
0	13762	11970
10	10035	10866
20	9554	10239
30	11205	6347
Max. % difference	**31**	**47**

Influence of different wheelchair setup scenarios on wheelchair components and ORS loading has also previously been evaluated for the adult manual wheelchair [5] [8]. Previously conducted studies on an adult manual wheelchair used a validated model representing a 21kg manual wheelchair and a 50th percentile Hybrid III male ATD. The results presented in this adult manual wheelchair study also showed that the rear securement point loads and wheelchair wheel loads are influenced considerably by the rear SP position (see Table 42). As the rear SP position was raised from -184mm CG_{WC} to +121mm CG_{WC}, the rear SP load increased (from 4657 N to 7534 N), the rear wheel load increased (from 3883 to 12338 N), and the front left wheel load decreased (from 8764 N to 5287 N).

Table 42 Influence of wheelchair setup conditions on ORS and wheelchair components: adult manual WC (21kg) and Hybrid III 50th percentile male ATD [8]

	Rear left SP (N)	Rear right SP (N)	Shldr belt (N)	Lap belt (N)	Rear wheel (N)	Front wheel (N)
Seat back angle						
0º	6192	6177	10201	13799	5569	6244
10º	6296	6301	10460	14247	5854	6507
20º	6233	6236	10543	14000	5939	6574
30º	6196	6195	11496	13704	5394	5712
Max. % diff.	**2**	**2**	**11**	**4**	**9**	**13**
Rear Tiedown position wrt CG_{wc}						
-7.25" (-184 mm)	4657	4665	10649	14225	3883	8764
-5.25" (-133 mm)	5095	5108	10534	14069	4882	7750
-1.25" (-32 mm)	6296	6301	10460	14247	5854	6507
2.75" (70 mm)	7347	7287	10205	14189	10873	5969
4.75" (121 mm)	7534	7224	10170	14160	12338	5287
Max. % diff.	**38**	**36**	**4**	**1**	**69**	**40**

The study conducted using the adult manual wheelchair model with a 50th percentile male ATD showed that the seat pan load was slightly affected by the wheelchair setup conditions while the seat back load was significantly influenced by all setup conditions (seat back angle, rear SP vertical location, and seat-to-back intersection horizontal location) (see Table 43) [5]. Among different setup conditions, changing of the seat back angle had the most influence on the seat back load. Our study results also showed that the wheelchair seat back force was influenced the most by the seat back angle changes. However, different from the adult wheelchair study, seat pan load was influenced considerably by all setup conditions in our study. In our pediatric wheelchair study, changing the rear tiedown vertical location and changing the seating system horizontal location had even more influence on seat pan load than the seat back load.

Table 43 Influence of wheelchair setup conditions on seat pan and seat back loads: adult manual WC (21kg) and Hybrid III 50th percentile male ATD [5]

Seat Back Angle	Seat pan loading (N)	Seat back Loading (N)
0º	16640	34846
10º	16898	34677
20º	16987	22485
30º	17014	2086
Max. % difference	**0.02**	**0.94**
Rear SP position wrt CG_{wc}		
-7.25"	16004	30607
-4.25"	16266	32777
-1.25"	16898	34677
1.75"	16538	42478
4.75"	17014	49889
Max. % difference	**0.06**	**0.39**
Seating location wrt rear hub		
-2”	16898	34677
0”	16338	32257
4”	15274	21969
8”	14073	13722
Max. % difference	**0.17**	**0.60**

The magnitude and types of forces that can be imposed upon a pediatric manual wheelchair and ORS in a frontal crash are evaluated in this study. However, it is important to note that these loads are defined for a simulated pediatric manual wheelchair weighing 18.6kg with a Hybrid III 6-year-old ATD weighing 25 kg seated in the wheelchair. Pediatric power wheelchairs which are heavier in weight will produce SP loads and wheel loads that are higher than those found in this study. As shown in the Table 44, the maximum rear SP load and rear wheel load are significantly higher in adult power wheelchair model weighing 116 kg than the adult manual wheelchair weighing 21 kg.

When designing a wheelchair or ORS, occupant size should also be considered. As shown in Table 44, the maximum loads found in this study are much less than those found in the previous studies which used a 50th percentile male ATD weighing 76.3 kg. % difference

between the forces resulting from an adult WC model and those resulting from the pediatric model were calculated using, % difference $= \frac{\left|Force_{adult\_WC} - Force_{pediatric\_WC}\right|}{Force_{adult\_WC}} * 100$, and presented in Table 44. Ha and Bertocci reviewed thirty-six frontal impact sled test reports which included different sizes of test dummies (6-year-old, 5th percentile female, and 50th percentile male ATDs) seated in various manual wheelchairs [14]. The study results showed that the average peak lap-belt and shoulder-belt loads were 2538N and 3913N for the 6-year-old ATD, 3801N and 7018N for the 5th %-tile female ATD, and 6086N and 9634N for the 50th %-tile male ATD. Therefore, the loads higher than those found in this study should be considered when a product is design for a children weighing more than 25 kg, usually older than 6-year-old.

Table 44 Comparison of maximum force on wheelchair components and ORS – adult wheelchairs vs pediatric wheelchair

	Adult power WC 50th % male wc anc. lap belt [6] [7]	Adult manual WC 50th % male vehicle anc. lap belt [5] [8]	Pediatric manual WC 6-year-old vehicle anc. lap belt		
	Force (N)	Force (N)	Force (N)	Adult WC vs Pediatric WC (% difference)	
				power WC	manual WC
Shoulder belt	NA	11496+	4002	NA	65.2
Lap belt	8649*	14247+	2683	69.0	81.2
Front SP	26575*	NA	6988	73.7	NA
Rear SP	31150*	7534+	4355	86.0	42.2
Seat pan	13762**	17087+	1374	90.0	92.0
Seat back	11970**	49889++	1992	83.4	96.0
Rear wheel	33865*	12338+	5098	84.9	58.7
Front wheel	8002*	8764+	2013	74.8	77.0
Ave. % diff.				**80.3**	**73.2**

Note: * Parameters varied – rear SP position
** Parameters varied – seat back angle
+ Parameters varied – seat back angle and rear SP position
++ Parameters varied – seat back angle, rear SP position, and seating location

The occupant restraint type (vehicle anchored lap belt vs wheelchair anchored lap belt) will also make difference on wheelchair component loads. The ATD in the adult power wheelchair studies was restrained with a lap belt which was anchored to the wheelchair, called integrated lap belt [6] [7]. And, in the adult manual wheelchair studies, the ATD was restrained with a lap belt which was anchored to the vehicle floor, called independent lap belt [5] [8]. When the lap belt anchor points are located on a wheelchair, the force generated by an occupant during an impact is transferred to the wheelchair. Therefore, compared to the wheelchair with the independent lap belt, larger force is imposed to the wheels of the wheelchair with the integrated lap belt. The integrated lap belt also increases SP forces since tiedowns are required to secure both the wheelchair and the occupant. When the independent lap belt is used, the tiedowns need to resist only the wheelchair load. The 6-year-old ATD in this study was restrained with the independent lap belt. SP load and wheel load that are higher than those found in this study will be resulted if the ATD is restrained with the integrated lap belt.

It is important to note that although the forces imposed on the wheelchair seating system (seat pan and seat back), front securement points, and wheels (front and rear) were evaluated in this study, the forces resulting on these wheelchair variables were not measured during sled testing and therefore were not compared to the sled test data in the model validation process. Comparison between sled test data and computer model results as a part of the model validation process showed that there was an 8.1 % average differences between the peak values resulting from sled test and those resulting from the computer model (see 2.4.2.3). Therefore, slight differences will exist between the forces reported in this study and the forces that resulted from the sled test.

5.6 CONCLUSION

Influence of changing wheelchair settings on the loads imposed upon wheelchair components and ORS was investigated in this study. Using the previously validated computer crash simulation model representing a Hybrid III 6-year-old ATD seated in a manual pediatric wheelchair, the loads imposed upon ORS and a pediatric manual wheelchair under different wheelchair setup scenarios (seat back angle, rear securement point vertical location with respect to wheelchair CG, and seat-to-back intersection horizontal location with respect to rear wheels) were evaluated.

Among different wheelchair setups, the wheelchair rear SP location had the greatest impact on the rear SP forces and the seat forces. Changes on the seat back angle and seating location also had influence on the seat forces. Wheelchair seat back force was influenced the most by the seat back angle changes. The rear SP location and the wheelchair seating location had great influence on the wheel loads. The maximum forces found in this study was 6988 N for the front SP, 4355 N for the rear SP, 4002 N for the shoulder belt, 2683 N for the lap belt, 1374 N for the seat pan, 1992 N for the seat back, 5098 N for the rear wheel, and 2013 N for the front (caster) wheel.

Compared to the loads found in the previous studies on adult wheelchairs with adult occupants, loads presented in this study for a manual pediatric wheelchair seated with a 6-year-old occupant were much lower: in average, the loads resulting from the pediatric wheelchair model were 80.3 % lower than those resulting from the adult power wheelchair model and 73.2 % lower than those resulting from the adult manual wheelchair model. Designing a pediatric transit wheelchair or other products for pediatric wheelchair transit might be easier to achieve than those designed for adults since the loads expected to be imposed on a product during a frontal impact are much lower for a pediatric wheelchair.

This is the first study to evaluate pediatric wheelchair loading associated with a frontal impact crash. Although the results presented in this study were derived based on the mathematical modeling techniques, the study results will provide wheelchair, seating, and ORS manufacturers designing products for pediatric population with insight as to the magnitude and types of forces that can be imposed upon their products in a frontal crash.

5.7 REFERENCES

1. U.S. Department of Justice Civil-Rights Division. (May 2000). *A Guide to Disability Rights Laws*. Washington, DC.
2. White House Domestic Policy Council. (March 2004). *New Freedom Initiative: a progress report*: http://www.whitehouse.gov/infocus/newfreedom/newfreedom-report-2004.pdf.
3. Society of Automotive Engineers (SAE). (1997). *SAE J2249: Wheelchair Tiedowns and Occupant Restraint Systems for Use in Motor Vehicles* (No. SAE J2249): SAE.
4. ANSI/RESNA Subcommittee on Wheelchairs and Transportation (SOWHAT). (April 2000). *ANSI/RESNA WC/Vol 1: Section 19 Wheelchairs - Wheelchairs Used as Seats in Motor Vehicles*: ANSI/RESNA.
5. Ha, D., & Bertocci, G. E. (2003). *An Investigation of Manual Wheelchair Seat Pan and Seat Back Loading Associated with Various Wheelchair Design Parameters Using Computer Crash Simulation.* Paper presented at the RESNA, Atlanta, GA.
6. Bertocci, G. E., Szobota, S., Ha, D., & vanRoosemalen, L. (2000). Development of Frontal Impact Crashworthy Wheelchair Seating Design Criteria Using Computer Simulation. *Journal of Rehab Research and Development, 37*(No. 5), 565-572.

7. Bertocci, G. E., Digges, K., & Hobson, D. (1996). Development of transportable wheelchair design criteria using computer crash simulation. *IEEE Transactions of Rehabilitation Engineering, 4*(3), 171-181.

8. Leary, A. M. (2001). *Injury risk analysis and design criteria for manual wheelchairs in frontal impacts.* Unpublished Masters thesis, University of Pittsburgh, Pittsburgh.

9. Weber, K. S. (1998). Choosing a wheeled manual mobility product. *Exceptional Parent, 28*(10), 46-47.

10. Sunrise Medical.*http://www.sunrisemedical.com*

11. Convaid.*http://www.convaid.com*

12. Leary, A., & Bertocci, G. (2001). *Design Criteria for Manual Wheelchairs Used as Motor Vehicle Seats Using Computer Simulation.* Paper presented at the RESNA, Reno, Nevada.

13. Ha, D., Bertocci, G. E., & Jategaonkar, R. (2004). *Development and Validation of a Frontal Impact 6-year-old Wheelchair-seated Occupant Computer Model.* Paper presented at the RESNA, Orlando, FL.

14. Ha, D., & Bertocci, G. (2002). *Wheelchair Tiedown Loads and Occupant Restraint Loads Associated with Various Occupant Sizes in Frontal Impact Testing.* Paper presented at the RESNA, Minneapolis, MN.

6 FRONTAL CRASH INJURY RISKS ASSOCIATED WITH CHILDREN IN WHEELCHAIRS RIDING IN SCHOOL BUSES

6.1 ABSTRACT

Children with disabilities who travel seated in their wheelchairs in school buses are excluded from the protections provided by compartmentalization (passive restraint system) and by other legislation relating to child protection in school buses. Injury risks associated with children seated in wheelchairs riding in school buses in a frontal crash were studied using a previously validated computer crash simulation model representing a 6-year-old Hybrid III ATD seated in a pediatric manual wheelchair and restrained with a 3-point occupant restraint system (ORS). A 13.5g/60.5kph frontal crash pulse, which was used in the *School Bus Safety* study conducted by NHTSA, was applied to the computer model of a manual wheelchair secured in a motor vehicle. Injury assessment measurements (HIC_{15}, Chest G and N_{ij}) obtained from the computer model were compared to those of Hybrid III 6 year-old ATD seated in OEM bus seats with and without a 3-point ORS, as reported in the *School Bus Safety* study. With an assumption that a wheelchair is able to tolerate crash level forces, the results of this study show that if a 6-year-old occupant is properly restrained with a 3-point ORS while traveling in his/her wheelchair in a school bus, then the wheelchair user is protected at a similar or higher level to that of 6-year-old occupants seated in OEM bus seats and restrained with 3-point ORS. The results also showed that in the event of a frontal crash, a 6-year-old wheelchair occupant restrained with a 3-point ORS is protected at a higher level than 6-year-old occupants seated in OEM bus seats utilizing compartmentalization as ORS in a school bus.

Keywords: pediatric wheelchair, 6-year-old Hybrid III ATD, injury risk, wheelchair transport safety, school bus

6.2 BACKGROUND

Approximately 13.2 million children, ranging in age from kindergarten to 12th grade, use school buses for school transportation [1]. Because of the US Department of Transportation's requirements for compartmentalization on large school buses and the inherent safety associated with larger vehicles, children seated in original equipment manufacturer (OEM) vehicle seats are approximately eight times safer in school buses than in their parents' cars [2]. The *Report Card on School Bus Safety* in the U.S reported that "600 school-age children are killed annually in non-school bus motor vehicles during school hours and during the school week to and from school. By comparison, approximately 15 school age children are killed annually while riding in yellow school buses. [1]" To protect children from injuries and death in school bus crashes, federal and state laws related to child protection in school buses have been established. Among the 60 Federal Motor Vehicle Safety Standards (FMVSS), 37 of them apply to school buses [3]. The following standards were developed specifically for school buses: FMVSS 131 *School Bus Pedestrian Safety Devices*, FMVSS 220 *School Bus Rollover Protection*, FMVSS 221 *School Bus Body Joint Strength*, and FMVSS 222 *School Bus Passenger Seating and Crash Protection* [4] [5] [6] [7].

FMVSS 222 was developed to reduce the number of deaths and the severity of injuries to school bus occupants in crashes and maneuvers [7]. The standard specifies design and performance requirements of seating (e.g. seat height and seat back force/deflection), restraining barriers, and occupant impact zones in school buses. Research has been conducted to increase protection of bus occupants, and a concept of compartmentalization has been used in the standard. Compartmentalization "provides a protective envelope consisting of strong, closely spaced seats that have energy-absorbing seat backs." [2] Compartmentalization is considered as a 'passive restraint system' since "active participation is not required by the passenger to engage

the restraint system." [2] However, children with disabilities who are seated in their wheelchairs while riding school buses do not benefit from compartmentalization.

FMVSS 222 includes requirements for wheelchair users in school buses, including wheelchair securement devices and their anchorages and wheelchair occupant restraints and their anchorages. The standard states that a school bus should be equipped so that a wheelchair can be secured in a forward-facing position with at least two front and two rear securement straps. Moreover, a wheelchair occupant restraint system, including both pelvic and upper torso restraints, should be provided at each wheelchair location. Although FMVSS 222 states that the movement of the wheelchair should be limited, the standard does not specify the excursion limits of the wheelchair and the occupant.

To protect children from injuries and death in school bus crashes, extensive research also has been conducted on school bus safety. In 1976, a study was conducted to develop new design concepts for school buses which provided occupant protection for school bus passengers [8]. The study included frontal, rear, and side impacts of school buses, and the study results provided the basis for the occupant protection requirement specified in FMVSS 222 [2]. Various OEM school bus seats were evaluated by NHTSA in 1978 [9]. Seat spacing, test speed, dummy size, and use of lap belts varied in the tests. Transport Canada conducted a comparison study of lap belt versus compartmentalization in three different sized school buses [10]. The study results showed that lap belts increased head injury (evaluated by HIC_{36}) for the 5^{th} percentile female ATDs by approximately three times over compartmentalization.

To develop "the next generation of school bus occupant protection," a *School Bus Safety* study was conducted by NHTSA [2]. A full scale crash test and sled tests simulating frontal crashes were conducted using various sized anthropomorphic test devices (ATDs) (Hybrid III 6-

year-old ATD, 5th percentile female ATD, and 50th percentile male ATD), which represented different age groups of children. The study evaluated different types of restraint systems (compartmentalization, 2-point lap belt, and 3-point shoulder/lap belts) and various types of seating. The occupant injury assessment measurement (OIAM) values (HIC_{15}, N_{ij}, and chest acceleration) and dummy motion were compared in the results. OIAM values reported in NHTSA's study were used in this study to assess whether wheelchair seated children are as safe as the children seated in OEM bus seats in school buses.

Children with disabilities often cannot be seated in standard OEM vehicle seats because of physical deformities or poor trunk and head controls. A study conducted by Everly et al., *A Survey of Transportation Services for Children with Disabilities,* showed that a large percentage of children (44%) transported daily have poor head and trunk control and are therefore unable to sit upright without support [11]. Thus, these children with disabilities often remain seated in their wheelchairs in vehicles when they are transported to and from schools, community agencies, and rehabilitation facilities. According to the study, the majority of children (61%) using transportation services are school aged children, six to 17 years old, and the majority of them (53%) are transported by 66-passenger school buses (Figure 74 and Figure 75) [11]. Children with disabilities who must travel seated in their wheelchairs in school buses will be excluded from the protections provided by compartmentalization and by other laws relating to child protection in school buses.

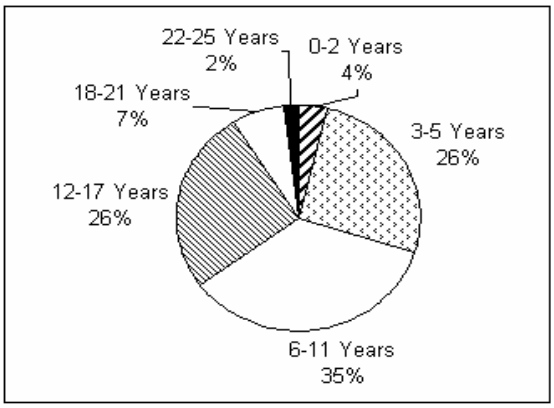

Figure 74 Age categories of children transported [11]

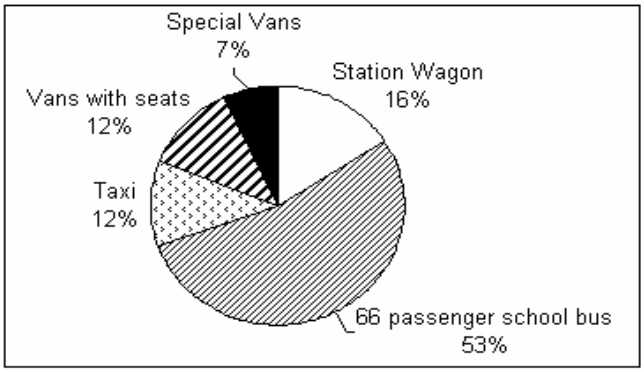

Figure 75 Vehicle types used by respondents to transport children [11]

There have been no studies published on the injury risks of children seated in wheelchairs riding in school buses that encounter a crash. In vehicle crashes and emergency maneuvers, children seated in wheelchairs riding in school buses should be protected at the same level as children seated in OEM bus seats. The safety of children in wheelchairs riding in school buses was studied in this paper by using computer simulation to assess injury risks associated with a frontal crash.

6.3 METHODS

The MADYMO (V6.01) computer simulation model representing a Hybrid III 6-year-old ATD (25 kg) seated in a Zippie manual pediatric wheelchair (Sunrise Medical, Longmont, CO) was used in the study (Chapter 2). The ATD was restrained by a three-point occupant restraint system (ORS), and the wheelchair was secured to the sled platform by a four-point tiedown system (Figure 76). The model was validated using 20g/48kph (30mph) frontal impact sled test data. Wheelchair configuration is described in Table 45.

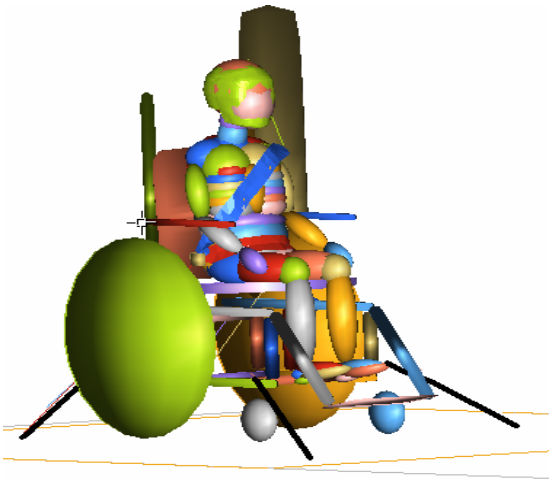

Figure 76 Pediatric manual wheelchair and Hybrid III 6-year-old ATD model in MADYMO

Table 45 Pediatric manual wheelchair configuration

Wheelchair Weight	18.6 kg
Wheelchair $CG_{vertical}$	359 mm above ground
Wheelchair $CG_{horizontal}$	188 mm front of rear hub
Wheelchair Rear Hub Height	280 mm above ground
Front Securement Point	419 mm front of rear hub
	191 mm above ground/ 89 mm below rear hub
Rear Securement Point to Rear Hub	105 mm behind rear hub
	315 mm above ground/ 35 mm above rear hub
Seat Back Angle	4 º
Seat Pan Angle	3 º

A 13.5g/60.5kph (37.8mph) frontal crash pulse, which was used in the *School Bus Safety* study [2], was applied to the validated computer model (Chapter 2). In the *School Bus Safety* study, the 13.5g/60.5kph crash pulse was established through a rigid barrier frontal crash test conducted with a large school bus (Class C[††]) (see Figure 77) [2]. The deceleration pulse applied to the model is shown in Figure 78.

Figure 77 Pre-crash photograph of frontal school bus test [2]

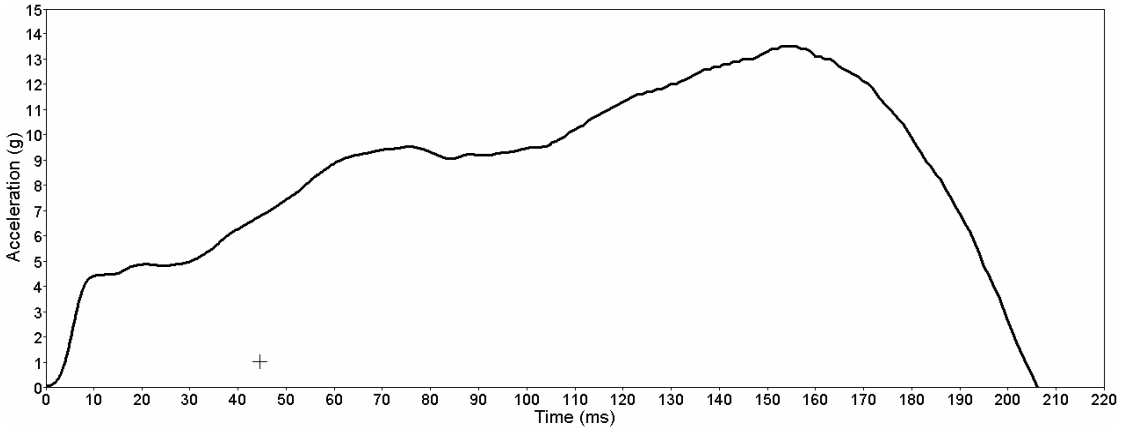

Figure 78 13.5g/60.5kph frontal crash deceleration pulse

[††] **Class C** school bus "is a body installed upon a flat-back cowl chassis with a gross vehicle weight rating (G.V.W.R) of more than 10,000 pounds, designed for carrying more than 10 persons. [The entire] engine is in front of the windshield and the entrance door is behind the front wheels."
[http://www.stnonline.com/stn/operations/schoolbusfaqs/]

The MADYMO model was programmed to generate time histories of head CG acceleration, upper thorax acceleration, and upper neck forces and moments. HIC_{15} and N_{ij} were calculated using equations (a) and (b), and 3-ms chest peak acceleration (chest G) was obtained from MADYMO output. HIC_{15}, N_{ij}, and chest G values are used in FMVSS 208 to predict injury risk of an occupant in frontal crashes [12]. HIC_{15} is a measure of risk of head injury, N_{ij} is a measure of neck injury risk, and chest G is a measure of risk of chest injury. The OIAM values (HIC_{15}, N_{ij}, and chest G) calculated from the computer simulation model were compared to injury criteria limits for a 6-year-old ATD specified in FMVSS 208 (700 for HIC_{15}, 1 for N_{ij}, and 60 for chest G) [12]. The OIAM values obtained from the computer model were also compared to those of Hybrid III 6 year-old ATD seated in OEM bus seats with and without a 3-point ORS as described in the aforementioned *School Bus Safety* study [2].

(a) $$HIC_{15} = \left[\frac{1}{(t_2 - t_1)} \int_{t_1}^{t_2} a_r dt \right]^{2.5} (t_2 - t_1)$$ [12]

HIC_{15}: two times, t1 and t2, separated by not more than 15 ms

(b) $$Nij = \left(\frac{Fz}{Fzc} \right) + \left(\frac{Mocy}{Myc} \right)$$ [12]

Fz - axial force

Mocy - the occipital condyle bending moment

Fzc = 2800 N when Fz is in tension

Fzc = 2800 N when Fz is in compression

Myc = 93 Nm when a flexion moment exists at the occipital condyle

Myc = 37 Nm when an extension moment exists at the occipital condyle

The model was also programmed to generate excursion time histories of a wheelchair, ATD knee, and ATD head. ATD excursions were not reported in the *School Bus Safety* study. Therefore, to assess injury risk of a 6-year-old wheelchair occupant in a school bus frontal crash,

the peak horizontal excursions of the wheelchair and ATD, determined from excursion time histories, were compared to the peak horizontal excursion limits specified in the American National Standards Institute (ANSI)/Rehabilitation Engineering and Assistive Technology Society of North America (RESNA) WC-19, *Wheelchairs for Use in Motor Vehicles*, standard [13].

6.4 RESULTS

Gross motions of the 6-year-old ATD in the wheelchair during a 13.5g/60.5kph frontal crash are shown in Figure 79. The maximum forward horizontal head excursion occurred at time 196 ms, and the maximum rearward horizontal head excursion occurred at time 518 ms.

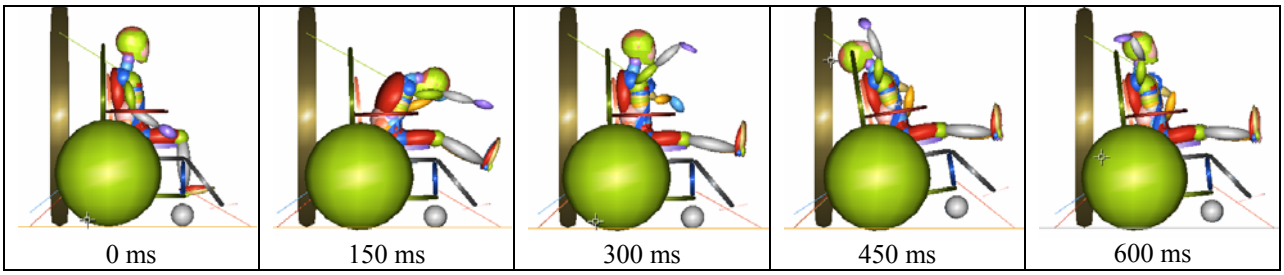

Figure 79 Gross motions of the WC occupant during a 13.5g/60.5kph frontal crash

Among 25 sled tests conducted by NHTSA (each test included one to six dummies), those including 6-year-old ATD and using compartmentalization and a 3-point belt as an ORS were selected from the report [2]. Table 46 shows HIC_{15}, Chest G, and N_{ij} values resulting from the selected sled tests. For the compartmentalization system tests, the mean HIC_{15}, Chest G, and N_{ij} were 328, 31.8g, and 1.08 with the range of 107-528 for HIC_{15}, 26.7-38.3g for Chest G, and 0.86-1.36 for N_{ij}. The test results of the OEM seated 6-year-old ATD with a 3-point ORS (henceforth, abbreviated as 'OEM-6ATD-3ORS') showed lower mean OIAM values than those

of the compartmentalization system; 96.1 HIC_{15} with the range of 59-185, 21.7 Chest G with the range of 17.9-25.0, and 0.62 N_{ij} with the range of 0.46-0.99.

Table 47 shows the OIAM values resulting from the computer simulation of the 6-year-old ATD seated in a manual wheelchair subjected to the same 13.5g/60.5kph frontal crash pulse. The ATD was restrained by the 3-point occupant restraint system. The injury criteria limits for a 6-year-old ATD specified in FMVSS 208, *Occupant Crash Protection*, is also shown in Table 47 [12].

The OIAM values resulting from the computer simulation were compared to the mean OIAM values resulting from the *School Bus Safety* study (see Figure 80). HIC_{15}, Chest G, and N_{ij} resulting from the wheelchair model were lower than those resulting from the OEM-6ATD-3ORS tests. All OIAM values resulting from both the wheelchair model and the OEM-6ATD-3ORS tests were found to be well below FMVSS 208 limits. Wheelchair model OIAM values were also lower than the mean OIAM values measured in the compartmentalization system tests. The mean Nij of the compartmentalization system tests (1.08) exceeded the FMVSS limit of 1.

Table 46 Occupant injury measures resulting from sled tests of OEM seated 6-year-old ATD - School Bus Safety study [2]

Compartmentalization				**3-point lap/shoulder belt system**			
Test No	HIC_{15}	Chest G	N_{ij}	Test No	HIC_{15}	Chest G	N_{ij}
VAL 01	107	31.5	0.93	VAL 06	88	23.1	0.46
VAL 02	528	30.4	0.86	VAL 07	185	20.4	0.63
VAL 03	369	30.6	1.24	VAL 08	85	25.0	0.53
VAL 09	417	33.1	0.96	VAL 08	89	21.4	0.65
VAL 15	294	38.3	1.12	VAL 10	81	19.8	0.53
VAL 16	250	26.7	1.36	VAL 11	90	23.7	0.99
				VAL 19	92	17.9	0.50
				VAL 20	59	21.9	0.70
Mean	328	31.8	1.08	**Mean**	96	21.7	0.62

Table 47 Occupant injury measures resulting from computer simulation of wheelchair seated 6-year-old ATD as compared to FMVSS 208 injury criteria

	HIC_{15}	Chest G	N_{ij}
FMVSS 208 limit – 6-year-old ATD	700	60	1
WC simulation: 3-point ORS	34.7	16.4	0.49

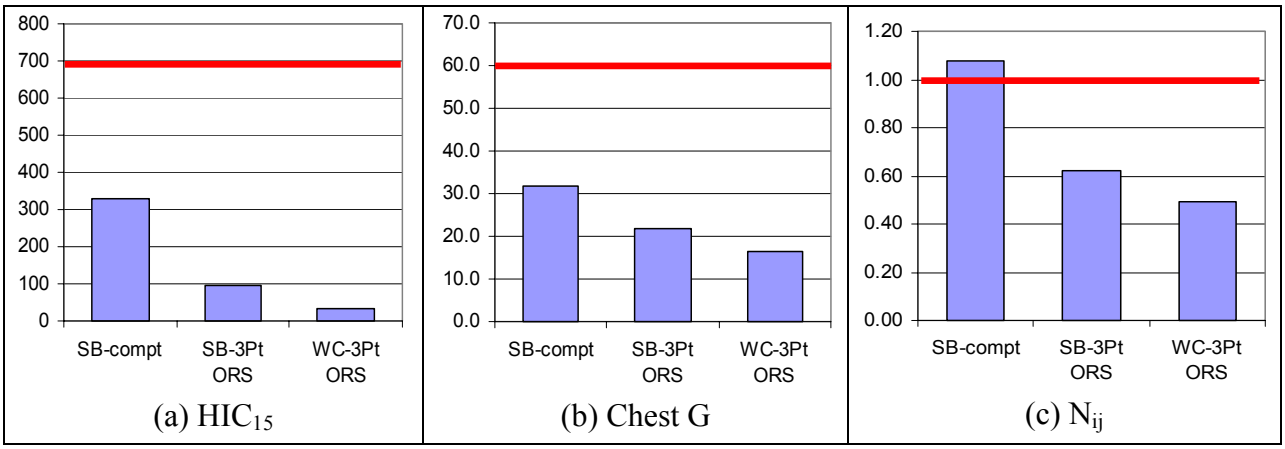

Note: Bold lines indicate FMVSS 208 limits

Figure 80 Comparison of occupant injury measures: a) HIC_{15}, b) Chest G, and c) N_{ij}

The ANSI/RESNA WC-19 horizontal excursion limits for a wheelchair and a 6-year-old ATD are shown in Table 48 and compared to the computer simulation results. The maximum horizontal excursions of the manual pediatric wheelchair and the 6-year-old ATD were well below the WC-19 limits.

Table 48 Comparison between computer simulation results and ANSI/RESNA WC-19 excursion limits [13]

	X_{wc} (mm)	X_{knee} (mm)	X_{headF} (mm)	X_{headR} (mm)	X_{knee}/X_{wc}
ANSI/RESNA WC-19 limit	150	300	450	-350	≥ 1.1
WC-3pt belt	8	43	183	-135	5.4

X_{wc} = the horizontal distance relative to the sled platform between the contrast target placed at or near point P on the test wheelchair at time t_0, to the point P target at the time of peak wheelchair excursion (point p = a wheelchair seat reference point located on the wheelchair reference plane approximately 50 mm above and 50 mm forward of the projected sideview intersection of the undepressed backrest and undepressed seat cushion)

X_{knee} = the horizontal distance relative to the sled platform between the dummy knee-joint target at time t_0, to the knee joint target at the time of peak knee excursion

X_{headF} = the horizontal distance relative to the sled platform between the most forward point on the dummy's head above the nose at time t_0, to the most forward point on the dummy's head at the time of peak forward head excursion

X_{headR} = the horizontal distance relative to the sled platform between the most rearward point on the dummy's head at time t_0, to the most rearward point on the dummy's head at the time of peak rearward head excursion

X_{knee}/X_{wc} - The wheelchair shall not impose forward loads on the ATD, which is considered to be achieved if the peak ATD knee excursion exceeds the peak wheelchair Point-P excursion by 10%

6.5 DISCUSSION

A 13.5g/60.5kph frontal crash pulse, used in the *School Bus Safety* study [2], was applied to the validated computer model representing a Hybrid III 6-year-old ATD seated in a manual wheelchair restrained with a 3-point ORS. The OIAM values obtained from the model were 34.7 HIC_{15}, 16.4 Chest G, and 0.49 N_{ij}. Injury risk curves, representing probability of risk of injury at various HIC_{15}, Chest G, and N_{ij} values, are presented in *Proposed Amendment to FMVSS No 213 Frontal Test Procedure* released by NHTSA [14]. The probability that a vehicle occupant would receive a certain level of Abbreviated Injury Scale (AIS) injury [15] can be calculated using the injury risk curves. For a 6-year-old ATD, HIC_{15} of 34.7 is equivalent to a 0.07 percent risk of a serious head injury (Abbreviated Injury Scale (AIS) ≥ 3), Chest G of 16.4 is equivalent to an 11 percent risk of serious chest injury (AIS ≥ 3), and N_{ij} of 0.49 is equivalent to a 9 percent risk of serious neck injury (AIS ≥ 3) [14].

The OIAM values resulting from the computer simulation were lower than those resulting from the OEM-6ATD-3ORS tests. Wheelchair model OIAM values were also lower than the mean OIAM values measured in the compartmentalization system tests. However, it is important to note that the compartmentalization system used in a school bus is a 'passive restraint system' [2]. "Since active participation is not required by the passenger to engage the restraint system, [compartmentalization] is considered a passive restraint system." [2] ORS is not required in school buses over 10,000 lbs gross vehicle weight rating (G.V.W.R) [7] because "the federal government concluded from available research that compartmentalization is a better safety measure [than other types of ORS]." [16] One of the arguments favoring compartmentalization is that "compartmentalization is more manageable. The protection exists and is in force without depending on any action by the children or any extra special supervision by drivers or monitors." [16] Although a passenger seated in the compartmentalization bus seat does not "actively participate" to engage an occupant restraint system, the passenger is protected by a specially designed seat that is regulated by FMVSS 222.

In this study, the wheelchair occupant (a 6-year-old ATD) was restrained by a 3-point occupant restraint system. If the wheelchair occupant is not restrained like the passenger seated in the compartmentalization bus seat, then the wheelchair occupant will be ejected out of the wheelchair without being protected by a passive restraint system during frontal impact (see Figure 81). Wheelchair seated occupants in motor vehicles often face a risk of injuries even during common evasive maneuvers, such as braking and turns [17] [18] [19]. Several studies on wheelchair occupant risks in motor vehicles have shown that most wheelchair occupant injuries result not from collisions but from abrupt vehicle maneuvers [17] [18] [19]. And in many cases, the wheelchair occupants were injured because they fell from their wheelchairs during the

incidents. A 3-point occupant restraint system would provide additional postural stability to wheelchair seated occupants, not only during a frontal crash but also during evasive vehicle maneuvers.

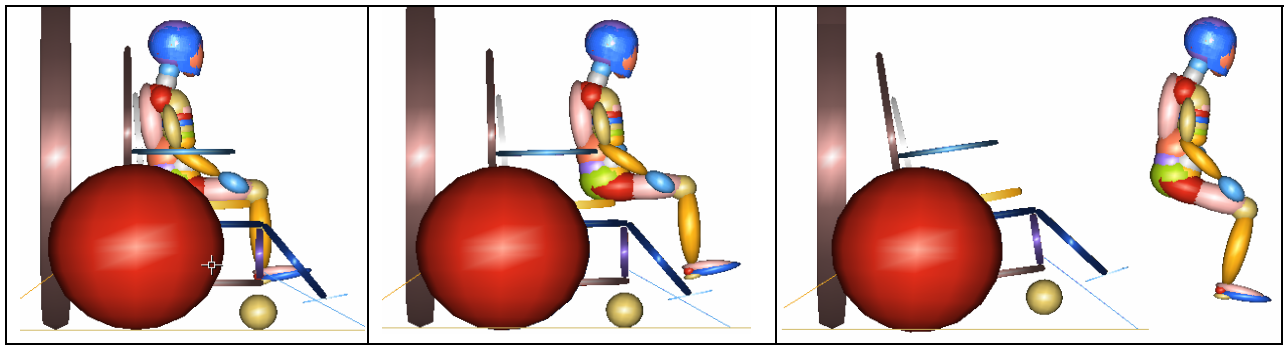

Figure 81 Wheelchair occupant without 3-point ORS during a frontal crash

The peak horizontal excursion of the wheelchair and ATD obtained from computer simulation were compared to the peak horizontal excursion limits specified in the ANSI/RESNA WC-19 [13]. Although several voluntary standards have been established by national and international organizations to improve the safety of wheelchair-seated travelers [13] [20] [21] [22], the ANSI/RESNA WC-19 standard is the only transit wheelchair standard which specifies the excursion limits of a 6-year-old occupant in a frontal impact test [13]. The International Standard Organization (ISO)-Working Group (WG) on Wheelchair Tiedown and Occupant Restraint (WTORS) and Transportable Wheelchairs is currently working towards including children (22kg and larger) in the ISO 7176-19 *Wheeled Mobility Devices for Use in Motor Vehicles* standard. The excursion limits specified in the ANSI/RESNA WC-19 standard and proposed in the ISO 7176-19 standard have been established to prevent contact between wheelchair occupants and the vehicle interior, and to prevent the wheelchair from loading the occupant. Although the deceleration pulse used in this study is lower than that of the WC-19

frontal impact test, the horizontal excursion limits specified in the WC-19 standard can still be used in this study to assess injury risk of a 6-year-old wheelchair occupant in a school bus frontal crash.

In this study, the maximum forward horizontal head excursion of the WC occupant occurred at time 196 ms, and the maximum rearward horizontal head excursion occurred at time 518 ms. Compared to previous studies on wheelchair occupant risks in motor vehicles, the peak horizontal excursions of the ATD observed in this study occurred later in time due to the protracted deceleration pulse. Most of the previously conducted studies on wheelchair transportation safety used a 20g/48kph frontal crash pulse associated with a private passenger vehicle, and specified in the ANSI/RESNA WC-19 standard. Figure 82 shows the deceleration pulse of the previously conducted WC-19 sled test and the deceleration pulse used in this study. The time duration of the pulse used in this study (approximately 210 ms) is more than twice as long as that of the WC-19 test pulse (approximately 90 ms). The injury severity is inversely related to the acceleration duration [23]. Therefore, if a wheelchair is able to tolerate crash level forces, then a wheelchair occupant faces lower risk of injury in a school bus, which has a long deceleration duration, than in a smaller vehicle such as family van.

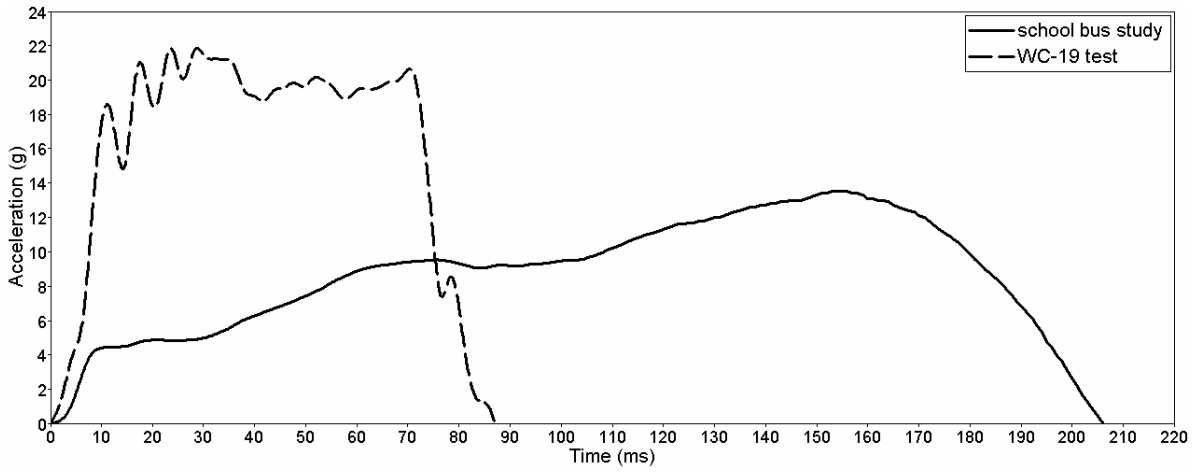

Figure 82 Comparison of the WC-19 deceleration pulse and school bus deceleration pulse

The results of this study show that if a 6-year-old occupant is properly restrained with a 3-point ORS while traveling in his/her wheelchair in a school bus, then the wheelchair user is protected at a similar or higher level to that of 6-year-old occupants seated in OEM bus seats and restrained with 3-point ORS. The results also showed that, in the event of a frontal crash, a 6-year-old wheelchair occupant restrained with a 3-point ORS is protected at a higher level than 6-year-old occupants seated in OEM bus seats utilizing compartmentalization as ORS in a school bus. It is important to note that the manual pediatric wheelchair model used in this study was developed using sled test data of a Zippie transit pediatric wheelchair. A transit wheelchair is defined as a wheelchair that has been tested in accordance with the ANSI/RESNA WC-19 standard, which requires a 20g/48kph (30 mph) frontal impact sled test [13]. This means that the integrity of the wheelchair has been tested by the WC-19 standard. Therefore, the results of this study should be interpreted under the assumption that a wheelchair is able to tolerate crash level forces.

Several limitations are associated with this study. First, the model used in this study has been initially developed and validated using data of 20g/30mph frontal impact sled test. The

model has not been validated to represent 13.5g/60.5kph frontal crash sled test. Therefore, differences might exist between the results reported in this study and the results measured in 13.5g/60.5kph frontal impact sled test.

Second, this study used a Hybrid III 6-year-old ATD computer model provided from TNO (TNO Automotive, Netherlands). Although the model has been calibrated and validated through component tests and sled tests, differences between the computer model ATD response and the actual ATD response may exist.

Lastly, the wheelchair model used in this study represents one kind of pediatric transit manual wheelchair (Zippie transit wheelchair). A 6-year-old child seated in a different type of wheelchair may respond different from the results presented in this study.

6.6 CONCLUSION

To study front injury risks associated with children in wheelchairs riding in school buses, a previously developed computer model representing a Hybrid III 6-year-old ATD seated in a manual pediatric wheelchair restrained by the three-point occupant restraint system was used. A 13.5g/60.5kph frontal crash pulse, which was used in the *School Bus Safety* study, was applied to the manual wheelchair computer model. The OIAM values (HIC_{15}, N_{ij}, and chest acceleration) resulting from the computer model were compared to those of Hybrid III 6 year-old ATD seated in OEM bus seats with and without a 3-piont ORS reported in the *School Bus Safety* study. Occupant and wheelchair excursions were also compared to the horizontal excursion limits specified in the ANSI/RESNA WC-19 standard.

Assuming that a wheelchair is able to tolerate crash level forces, the results of this study show that if a 6-year-old occupant is properly restrained with a 3-point ORS while traveling in his/her wheelchair in a school bus, then the wheelchair user is protected at a similar or higher

level to that of 6-year-old occupants seated in OEM bus seats and restrained with 3-point ORS. The results also showed that in the event of a frontal crash, a 6-year-old wheelchair occupant restrained with a 3-point ORS is protected at a higher level than that of 6-year-old occupants seated in OEM bus seats utilizing compartmentalization as ORS in a school bus.

The compartmentalization system used in a school bus is a 'passive restraint system.' If the wheelchair occupant is not restrained like the passenger seated in a large bus seat, then the wheelchair occupant will be ejected out of the wheelchair without being protected by a passive restraint system during frontal impact. Additional studies in the development of passive restraint system for children in wheelchairs in school buses should be conducted in the future. Children with disabilities often have less trunk or head stability than children without disabilities. Therefore, compartmentalization systems used in school buses will not provide the same protection of children with disabilities in frontal crashes as it does for children without disabilities who have normal muscle tone and balance. For children with disabilities, a passive restraint system which is designed to protect children not only in collisions, but also in abrupt vehicle maneuvers, such as braking and turns, is needed.

6.7 REFERENCES

1. http://www.stnonline.com/stn/schoolbussafety/annualreportcard/index.htm.
2. Hinch, J., McCray, L., Prasad, A., Sullivan, L., Willke, D., Hott, C., et al. (2002). *School Bus Safety: Crashworthiness Research*: National Highway Traffic Safety Administration.
3. http://www.stnonline.com/stn/government/fmvssregulations/index.htm.
4. National Highway Traffic Safety Administration (NHTSA). (1991). *FMVSS 131 School bus pedestrian safety devices* (October, 2003 ed. Vol. 49CFR571.131).

5. National Highway Traffic Safety Administration (NHTSA). (1976). *FMVSS 220 School bus rollover protection* (October, 2003 ed. Vol. 49CFR571.220).

6. National Highway Traffic Safety Administration (NHTSA). (1976). *FMVSS 221 School bus body joint strength* (October 1, 2003 ed. Vol. 49CFR571.221).

7. National Highway Traffic Safety Administration (NHTSA). (1976). *FMVSS 222 School bus passenger seating and crash protection* (October, 2003 ed. Vol. 49CFR571.222).

8. National Highway Traffic Safety Administration. (1976). *Development of a Unitized School Bus, Volume 1 - Summary Report* (No. DOT-HS-802-004). Washington, D.C: U.S. Department of Transportation.

9. National Highway Traffic Safety Administration. (1978). *School Bus Passenger Seat and Lap Belt Sled Tests* (No. DOT HS-804-985). Washington, D.C.: U.S. Department of Transportation.

10. Farr, G. N. (1985). *School Bus Safety Study - Volume I* (No. TP6222(E)). Quebec City: Transport Canada.

11. Everly, J. S., Bull, M. J., Stroup, K. B., Goldsmith, J. J., Doll, J. P., & Russell, R. (1993). A Survey of Transportation Services for Children with Disabilities. *The American Journal of Occupational Therapy, 47*(9), 804-810.

12. National Highway Traffic Safety Administration (NHTSA). (1971). *FMVSS 208 Occupant Crash Protection* (October, 2000 ed. Vol. 49 CFR 571.208).

13. ANSI/RESNA Subcommittee on Wheelchairs and Transportation (SOWHAT). (2000). *ANSI/RESNA WC/Vol 1: Section 19 Wheelchairs - Wheelchairs Used as Seats in Motor Vehicles*: ANSI/RESNA.

14. National Highway Traffic Safety Administration (NHTSA). (2002). *Proposed Amendment to FMVSS 213 Frontal Test Procedure*: NHTSA.

15. States, J. D. (1969). Abbreviated and the comprehensive research injury scales. *SAE, SAE Paper No. 690810*.

16. http://www.stnonline.com/stn/occupantrestraint/seatbeltfaqs/index.htm.

17. Shaw, G. (2000). Wheelchair rider risk in motor vehicles: A technical note. *Journal of Rehabilitation Research and Development, 37*(1), 89-100.

18. Shaw, G., & Gillispie, T. (2003). Appropriate protection for wheelchair riders on public transit buses. *Journal of Rehabilitation Research and Development, 40*(4), 309-320.

19. Kirby, R., & MacLeod, D. (2001, June 22-26). *Wheelchair-related injuries reported to the national electronic injury surveillance system.* Paper presented at the RESNA annual conference, Orlando, FL.

20. Society of Automotive Engineers (SAE). (1997). *SAE J2249: Wheelchair Tiedowns and Occupant Restraint Systems for Use in Motor Vehicles* (No. SAE J2249): SAE.

21. International Standards Organization (ISO). (2001). *ISO 10542: Wheelchair Tiedown and Occupant Restraint Systems* (No. ISO 10542): ISO.

22. International Standards Organization (ISO). (2000). *ISO 7176-19: Wheelchairs Used as Seats in Motor Vehicles* (No. ISO 7176-19): ISO.

23. Ghista, D. N. (1982). *Human body dynamics : impact, occupational, and athletic aspects* (Vol. 4). New York: Oxford : Clarendon Press.

7 CONCLUSIONS

7.1 STUDY CONCLUSIONS

The safety of children in wheelchairs in transit was investigated in this dissertation, mainly using computer simulation model. Three Sunrise Medical Zippie pediatric wheelchairs (Sunrise Medical Zippie, Longmont, CO) were tested with a Hybrid III 6-year-old ATD in accordance with the ANSI/RESNA WC-19 standard [1]. Using the measurements taken from the sled test, a computer model representing a Zippie wheelchair seated with a Hybrid III 6-year-old ATD subjected to a 20g/48kph frontal crash was developed in MADYMO (Chapter 2). The model was validated using the "model validation criteria" which were determined based on the previous crash simulation studies as well as accepted statistical assumptions [2] [3] [4] [5] [6] [7]. Evaluation of the validated pediatric wheelchair model, including Adviser software (TNO Automotive, Netherlands) and regression analysis, showed that the pediatric wheelchair model provided good representation of the sled test.

To study the injury risks of a 6-year-old wheelchair occupant in a frontal impact motor vehicle crash, injury criteria and kinematic limits specified in the ANSI/RESNA WC-19 standard [1], FMVSS 213 [8], and FMVSS 208 [9] were applied to collected sled test data (Chapter 3). The results showed that 6-year-old children with disabilities who remain seated in their wheelchairs in vehicles may be subjected to a risk of neck and chest injuries in a frontal impact motor vehicle crash. Similar results were found in the study investigating injury risks of a 6-year-old wheelchair occupant in a frontal motor vehicle crash under different wheelchair setup scenarios (Chapter 4).

Using the validated model developed in Chapter 2, the effect of adjustable features (seat back angle, rear securement point vertical location, and seat-to-back intersection horizontal

location) on the injury risks of a 6-year-old wheelchair occupant and occupant kinematics during a frontal impact was studied in Chapter 4. The results showed that altering wheelchair settings does have impact on kinematics and injury risk of a 6-year-old wheelchair occupant in a frontal motor vehicle crash. As the seat back angle increased, and as the STBI location was moved horizontally toward the rear of the wheelchair, ATD head-neck extension and tendency of ramping increased. Positioning the rear SP at 100 mm above the CG_{WC} also caused severe ATD head-neck extension along with ramping.

In Chapter 5, the loads imposed on wheelchair (seat back, seat pan, securement points and wheels) and occupant restraint (shoulder and lap belt) under 20g/48kph frontal impact conditions with varying wheelchair characteristics was investigated using the pediatric wheelchair model. Compared to the loads found in previous studies on adult wheelchairs with adult occupants, the loads found for a manual pediatric wheelchair seated with a 6-year-old occupant were much lower. The study results should provide guidelines for the manufacturers designing technologies for safe pediatric wheelchair transportation.

Lastly, the safety of children in wheelchairs riding in school buses was studied by assessing injury risks associated with them in a frontal crash (Chapter 6). A 13.5g/60.5kph frontal crash pulse, which was established through a rigid barrier frontal crash test conducted with a large school bus [10], was applied to the pediatric wheelchair model. Injury assessment measurements (HIC, N_{ij}, chest G) resulting from the computer model were compared to those obtained from the school bus safety study [10]. Assuming that a wheelchair was able to tolerate crash level forces, the study results showed that if a 6-year-old occupant is properly restrained with a 3-point occupant restraint system while traveling in his/her wheelchair in a school bus, then the wheelchair user is protected at a similar or higher level to that of 6-year-old occupants

seated in OEM bus seats and restrained with 3-point ORS. The results also showed that in the event of a frontal crash, a 6-year-old wheelchair occupant restrained with a 3-point ORS is protected at a higher level than that of 6-year-old occupants seated in OEM bus seats utilizing compartmentalization as ORS in a school bus.

7.2 STUDY LIMITATIONS

This study provides a preliminary assessment of injury risk for a 6-year-old child using a manual wheelchair as a seat in motor vehicles. Also, this study provides guidelines for wheelchair, seating, and ORS manufacturers who design products for pediatric population by providing the magnitude and types of forces that can be imposed upon them in a frontal crash. However, several limitations are associated with this study, as follow:

1. A Hybrid III 6-year-old ATD (Hybrid III6) was used in this study, and occupant injury risk was measured from the Hybrid III6. The Hybrid III6 was originally developed using data derived through the scaling procedures from adult data, and biofidelity of the Hybrid III6 has not been confirmed by biomechanical impact response of child data. The results presented in this study need to be interpreted in caution since there are concerns regarding the biofidelity of the Hybrid III6 [11] [12].
2. A Hybrid III 6-year-old ATD represents an average 6-year-old child (23.4 kg). Child occupants having anthropometric and inertial characteristics differing from that of a Hybrid III 6-year-old ATD would likely lead outcomes that vary from those reported in this study.
3. In the sled test, a piece of tape was used to attach the shoulder belt to the upper torso of the test dummy since WC-19 requires 75mm of shoulder belt slack simulating the belt pay out with a retractor [1]. Due to the slack, the shoulder belt was likely to slide off the ATD's shoulder. Therefore, tape was used to retain the shoulder belt in place during initial phase of

the sled test. Since people do not use a tape in the real world when they wear an occupant restraint system in motor vehicles, using a piece of tape during the sled testing may not well represent the real world occupant shoulder belt.

4. In the sled test (and also in the model), the 6-year-old ATD's feet were not supported by the footrest of the wheelchair because the length of the footrest was greater than that of the ATD's leg. However, it was believed that the ATD's feet not being supported by the footrest represented a worse case scenario than the feet being placed on the footrest. (If wheelchair occupant's feet are not placed on the footrest, no friction between the feet and the footrest exists. Therefore, greater leg extension will result if the wheelchair occupant's feet are not supported by the footrest than if the occupant's feet rest on the footrest.)
5. The computer model developed in this study used a Hybrid III 6-year-old anthromorphic model provided in MADYMO from TNO (TNO Automotive, Netherlands). Although the model has been calibrated and validated through component tests and sled tests, slight differences between the ATD responses of the computer model and ATD used in the sled test may exist.
6. In development of the models, a portion of the shoulder belt was attached to the dummy's upper chest in order to simulate the taped section of the shoulder belt in sled testing. During the sled tests, because the shoulder belt was taped to the dummy's shirt, the taped section of the shoulder belt was able to move with the shirt. However, in the models, the attached part of the shoulder belt was fixed to the dummy's body and did not move as it did in the actual test. Therefore, there would be differences between the shoulder belt-ATD torso interaction in the model and sled testing.

7. The wheelchair model developed in this study represents one type of manual pediatric wheelchair (Zippie). Inertial and geometric characteristics can be found to vary greatly across different types of wheelchair, especially power wheelchairs, and can have an effect on wheelchair response to impact. Therefore, the results presented in this study do not represent all the pediatric transit wheelchairs available in the market. However, it should be noted that the Sunrise Medical Zippie is one of the most commonly used transit pediatric manual wheelchairs. And, it is a good representation of manual pediatric wheelchairs currently available on the market.
8. The manual wheelchair model developed and used in this study is a simplified representation of the actual wheelchair. For example, the wheelchair frame is represented with one body in the model. Therefore, the model might not accurately represent the actual frame structure which could have absorbed more energy during impact. The simplifications may cause the differences between the sled test and the models.
9. The characteristics (contact characteristics and belt characteristics) used in the model were initially estimated based on the previous studies [4] [13]. If the load response characteristics of the wheels, seat, seat back, and wheelchair tiedown straps could have been dynamically measured, then the model may more accurately represented the sled test.
10. The FMVSS injury criteria used in this study were developed to assess the injury risk of non-disabled children, who have normal muscle tone and balance, in motor vehicle crashes. Because children with disabilities often have less trunk or head stability than that of an average 6-year-old child without disabilities, children with disabilities seated in wheelchairs may be more susceptible to severe and fatal injuries in circumstances that would not be

injurious to children without disabilities. Therefore, the injury risks presented in this study may be underestimated when considering disabled children.

7.3 FUTURE WORK

Based on the results found in this dissertation, several areas of future work are suggested:

1. In all three sled tests, the shoulder belt slipped off the six-year-old ATD's shoulder and ATD head-to-knee contact occurred. The three-point occupant restraint system was setup in accordance with the WC-19 standard [1]. In the frontal impact test method section of the standard, it is stated to "bolt the upper anchorage of the surrogate shoulder belt assembly to the rigid support structure at a location that provides a good fit of the shoulder belt to the ATD's chest and shoulder as illustrated in Figure" [1]. However, the Figure provided in the WC-19 standard is for the midsize-male ATD, and the test setup of the shoulder belt upper anchorage point for an ATD other than the midsize-male is not specified in the standard. The shoulder belt upper anchorage point specified in the WC19 standard is likely not the optimal position for pediatric ATDs.

   Shoulder belt slack required in the WC19 standard could also have caused the shoulder belt slippage during the sled tests. WC-19 requires 75mm of shoulder belt slack (simulating the belt pay out with a retractor) in the frontal impact sled test. Compared to the adult ATDs, the Hybrid III 6-year-old ATD has very narrow shoulders (see Figure 83). Although the requirement of shoulder belt slack works well with the adult ATDs in sled tests, it might not be an appropriate requirement for the pediatric ATDs. Investigation of the occupant restraint system setup, including shoulder belt anchor point location and shoulder belt slack, for the pediatric population is needed in the future.

Figure 83 Narrow shoulders of Hybrid III 6-year-old ATD

2. In this study, the computer model was validated using data from the sled tests representing one specific wheelchair setup. To further extend the usefulness and predictive power of the model, a sled test with a slightly different wheelchair setup (such as different wheelchair back angles) should be conducted and compared to the model with the same setup modifications in the future.
3. Study results showed that 6-year-old children with disabilities who remain seated in their wheelchairs in vehicles are at risk of neck injury in a frontal motor vehicle crash. The risk of neck injury can be reduced by minimizing rearward movement of the head and neck during motor vehicle crashes. Using a device that provides support for the head and neck and minimizes head-neck rearward movement, such as head restraints, with a wheelchair in transit can reduce the risk of neck injury. More research on the design and performance of head restraints used with transit wheelchairs is needed in the future.
4. Study results also showed that 6-year-old wheelchair seated occupants are subjected to a risk of chest injury in a frontal impact motor vehicle crash. For the pediatric population, three-point occupant restraint systems, which were used in this study, may not be the best occupant

restraint system to provide protection during frontal crashes. Occupant restraint systems that allow the crash force to be distributed over larger contact areas can possibly reduce the risk of chest injury. Studies on designing of an occupant restraint system for children seated in wheelchairs in transit are also needed in the future.

5. Existing wheelchair standards do not currently address occupant head, neck or chest injury risk. Adaptation of additional occupant injury assessment measures, such as HIC, N_{ij} and/or peak chest deflection, into wheelchair standards should be considered to improve wheelchair occupant protection in motor vehicle crashes. Unfortunately, this will likely increase the cost of sled impact testing.
6. Although not investigated in this dissertation study, the results of the recently conducted preliminary study showed that the location of front SP position had an impact on the movement of a wheelchair and an occupant. Evaluation of this design parameter (front SP position) in the future will provide more information on pediatric occupant injury risks and possible loads on the wheelchair components and ORS.
7. Currently, comparison of the time history profiles is the most typical way to validate computer simulation models in research involving computer simulation. Therefore, the quality of validation is a subjective opinion and varies with each individual. Evaluating one's model using a software product which provides a quality rating for a numerical model, such as Adviser (TNO Automotive, Netherlands), will allow an individual to compare a quality rating of his/her model to that of the others in the future.
8. Compartmentalization is a 'passive restraint system' used in large school buses to protect children seated in OEM seats from injuries in crashes. A passive restraint system is not available for children with disabilities who remain seated in their wheelchairs in school

buses. Additional studies in the development of passive restraint system for children in wheelchairs in school buses should be conducted in the future. Children with disabilities often have less trunk or head stability than children without disabilities. Therefore, compartmentalization systems used in school buses will not provide the same protections of children with disabilities in frontal crashes as it does for children without disabilities who have normal muscle tone and balance. For children with disabilities, a passive restraint system which is design to protect children not only in collisions but also in abrupt vehicle maneuvers, such as braking and turns, is needed.

To date, no study has been published that evaluates the injury risks of pediatric wheelchair users in motor vehicle crashes. The pediatric wheelchair model developed and validated in this study will provide a foundation for studying the response of a manual pediatric wheelchair and a child occupant in crashes. Moreover, the model will promote the study of associated pediatric wheelchair user injury risks in motor vehicle crashes. The study results presented in this dissertation will provide guidelines to manufacturers designing pediatric transit wheelchairs, seating, and ORS.

7.4 REFERENCES

1. ANSI/RESNA Subcommittee on Wheelchairs and Transportation (SOWHAT). (2000). *ANSI/RESNA WC/Vol 1: Section 19 Wheelchairs - Wheelchairs Used as Seats in Motor Vehicles*: ANSI/RESNA.
2. Bertocci, G. E., Szobota, S., Hobson, D. A., & Digges, K. (1999). Computer Simulation and Sled Test Validation of a Powerbase Wheelchair and Occupant Subjected to Frontal Crash Conditions. *IEEE Transactions on Rehabilitation Engineering, 7*(2), 234-244.

3. Pilkey, W., Kang, W., & Shaw, G. (1994). *Crash Response of Wheelchair-occupant systems in transport.* Paper presented at the RESNA, Nashville, TN.

4. Leary, A. M. (2001). *Injury risk analysis and design criteria for manual wheelchairs in frontal impacts.* Unpublished Masters thesis, University of Pittsburgh, Pittsburgh.

5. Claire, M. L., Visvikis, C., Oakley, C., Savill, T., Edwards, M., & Cakebread, R. (2003). *The safety of wheelchair occupants in road passenger vehicles* (No. ISBN 0-9543339-1-9): TRL Limited.

6. Pipkorn, B., & Eriksson, M. (2003). *A Method to Evaluate the Validity of Mathematical Models.* Paper presented at the 4th European MADYMO Users Meeting, Brussels, Belgium.

7. Glasnapp, D. R., & Poggio, J. P. (1985). *Essentials of Statistical Analysis: for the Behavioral Sciences*. Columbus: Charles E. Merrill.

8. National Highway Traffic Safety Administration (NHTSA). (1979). *FMVSS 213 Child Restraint Systems* (October, 2000 ed. Vol. 49 CFR 571.213).

9. National Highway Traffic Safety Administration (NHTSA). (1971). *FMVSS 208 Occupant Crash Protection* (October, 2000 ed. Vol. 49 CFR 571.208).

10. Hinch, J., McCray, L., Prasad, A., Sullivan, L., Willke, D., Hott, C., et al. (2002). *School Bus Safety: Crashworthiness Research*: National Highway Traffic Safety Administration.

11. National Highway Traffic Safety Administration (NHTSA). (2003). *Final rule on Federal Motor Vehicle Safety Standards; Child Restraint Systems* (Docket No. NHTSA-03-15351): NHTSA.

12. Sherwood, C. P., Shaw, C. G., Van Rooij, R. W. K., Crandall, J. R., Orzechowski, K. M., Eichelberger, M. R., et al. (2003). Prediction of Cervical Spine Injury Risk for the 6-Year-Old Child in Frontal Crashes. *Traffic Injury Prevention, 2*, 206-213.

13. Ha, D. (2000). *Development of test methods for wheelchair seating systems used as motor vehicle seats and evaluation of wheelchair seating system crashworthiness.* Unpublished Masters thesis, University of Pittsburgh, Pittsburgh.

APPENDIX A

Hybrid II and Hybrid III 6 Year Old ATDs

Hybrid II 6-year-old Child [*]

Weights	Pounds	Kilograms
Head	**6.0**	**2.72**
Neck	**1.4**	**0.64**
Upper Torso	**11.5**	**5.22**
Lower Torso	**8.4**	**3.81**
Arm	**4.2**	**1.91**
Upper Leg	**9.8**	**4.44**
Lower Leg	**6.0**	**2.72**
Total Weight	47.3	21.46

Dimensions	Inches	Centimeters
Head Circumference	**21.6**	**54.9**
Head Length	**7.0**	**17.8**
Buttock to Knee	**15.1**	**38.4**
Knee to Floor	**14.4**	**36.6**
Hip Joint Height	**1.5**	**3.8**
Hip Joint To Seatback	**3.0**	**7.6**
Sitting Height	25.4	65.0
Standing Height	47.3	120.1

Possible Instrumentation
Head x, y, z accelerometers
Thorax CG x, y, z accelerometers
Pelvis x, y, z accelerometers
Femur x 2, z force or x, y, z forces and moments

Hybrid III 6-year-old Child [**]

Weights	Pounds	Kilograms
Head	**7.66**	**3.47**
Neck	**1.20**	**0.54**
Upper Torso	**12.25**	**5.57**
Lower Torso	**13.75**	**6.24**
Upper Arm	**1.05**	**0.48**
Lower Arm w/hand	**1.37**	**0.62**
Upper Leg	**3.20**	**1.45**
Lower Leg and Foot	**2.75**	**1.25**
Total Weight	51.60	23.41

Dimensions	Inches	Centimeters
Head Circumference	**20.50**	**52.07**
Head Breadth	**5.60**	**14.22**
Head Depth	**6.80**	**17.27**
Knee Pivot Height	**12.40**	**31.50**
Buttock to Knee Pivot	**13.90**	**35.31**
Hip Pivot Height	**2.7**	**6.86**
Hip Pivot From Backline	**3.7**	**9.40**
Sitting Height	25.00	63.50

Possible Instrumentation [2]
Head x, y, z accelerometers
T04 x, y, z accelerometers
Upper Sternum x accelerometer
Lower Sternum x accelerometer
Upper Spine Box x accelerometer
Lower Spine Box x accelerometer
Pelvis x, y, z accelerometers
Thorax x displacement
Upper Neck x, y, z forces and moments
Lower Neck x, y, z forces and moments
Lumbar x, y, z forces and moments
Anterior Superior Iliac Spine x 2, x forces and moments
Femur x 2, z force or x, y, z forces and moments

[*] http://www.dentonatd.com/dentonatd/anthropomorphic.html
[**] http://www-nrd.nhtsa.dot.gov/vrtc/bio/child/hybIII6ydat.htm

APPENDIX B

Conversion from Dynaman Input File to ATB3^{I} Input File

1. If the Dynaman file has joint torque functions, delete the Card F.5 and the NJNTF variable on Card D.1. Then insert a line beginning with the number 999 at the end of Cards E.7. (By putting a number > 50 for the joint ID number field, the joint functions are terminated.) The joint torque functions are assigned to the joints in the B.4 cards by putting the negative of the joint function ID number in the first field of the card for the corresponding joint (release note).
2. If HIC values are computed in Dynaman, replace Card H.11 with a blank card and reenter the numbers in ATB 3^I (release note).
3. Change function numbers in Dynaman to numbers <= 50.
4. In the ATB 3^I preprocessor, change Coulomb Friction Angular Velocity found in *Body* → *Edit* → *Joint* to non-zero values. For the Euler joint, in addition to the Coulomb Friction Angular Velocity, change Nutation Coulomb Angular Velocity and Spin Coulomb Angular Velocity to non-zero values.
5. In the ATB 3^I preprocessor, limit the number of plane/segment contacts to <=5 for each plane.

APPENDIX C

Test Setup Measurements for Computer Modeling

Date:

Test # (color of WC):

Weight of WC:

ATD H-point height:

View	Description	Number	Measurement, (mm) (deg)
Side	Ht: Rear Hub	1	
	Ht: Front Hub	2	
	Ht: General Anchor Pt.	3	
	Dist: Front and Rear Hub	4	
	Dist: F-hub to F-tiedown pt.	5	
	Dist: Sled R-edge to R-hub	6	
	Dist: Sled R-edge to R-tiedown pt. on platform	7	
	Dist: R-hub to R-tiedown pt. on WC	8	
	Ht: R-hub to R-tiedown pt. on WC	9	
	Dist: R-hub to F-tiedown pt. on WC	10	
	Ht: R-hub to F-tiedown pt. on WC	11	
	Dist: Sled R-edge to Pelvic belt anchor pt.	12	
	Dist: Sled R-edge to Shoulder belt anchor pt.	13	
	Ht: Platform to Shoulder belt anchor pt.	14	
	Dist: R-hub to WC seat(middle)	15	
	Ht: Platform to WC seat(middle)	16	
	Dist: R-hub to WC back(middle)	17	
	Ht: Platform to WC back(middle)	18	
	Dist: F-hub to Footrest(middle)	19	
	Ht: Platform to Footrest(middle)	20	
	Dist: R-hub to WC CG	21	
	Ht: R-hub to WC CG	22	
	Dist: R-hub to Tie-point	23	
	Ht: R-hub to Tie-point	24	
Top	Dist: Between F-tiedown points	25	
	Dist: Between R-tiedown points	26	
	Dist: Between Pelvic belt anchor points	27	
	Dist: Sled Side-edge to R-hub	28	
	Dist: R-hub to R-tiedown pt. on WC	29	
	Dist: R-hub to F-tiedown pt. on WC	30	
Front	Dist: Sled Side-edge to Shoulder belt anc. pt.	31	

Note: R – rear
F – front

(Continue)

Item	Description	Number	Measurement, (mm) (deg)
Occupant Restraint Angle	Pelvic belt - side view	32	
	Shoulder belt - side view	33	
	Shoulder belt - front view	34	
Platform	Platform Length	35	
	Platform Width	36	
Footrest	Length		
	Width		
	Angle - side view		
WC Seat	Depth		
	Width		
	Angle - side view		
WC Back	Height		
	Width		
	Angle - side view		

Side View

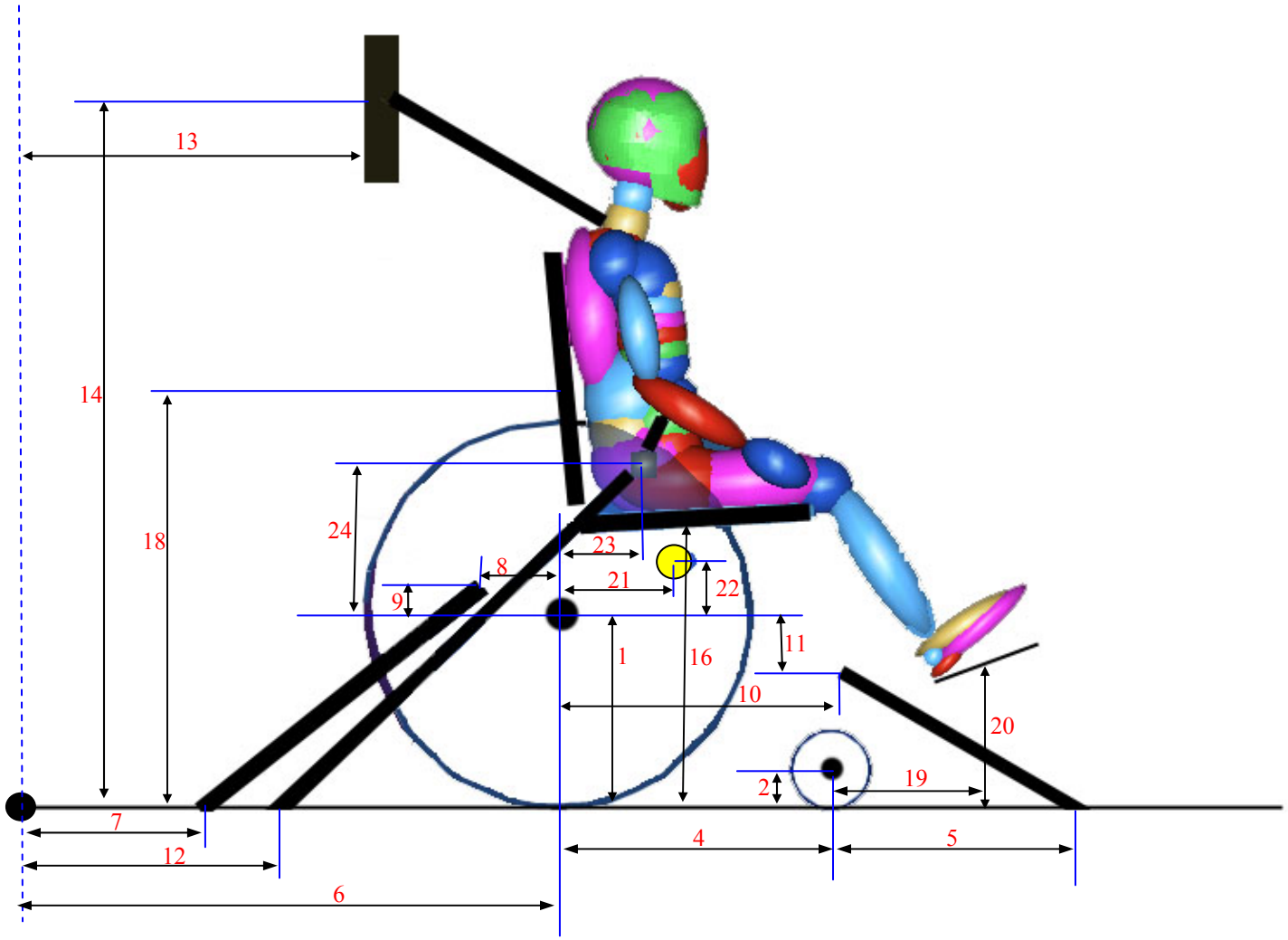

● : Rear edge of the sled platform

Top View

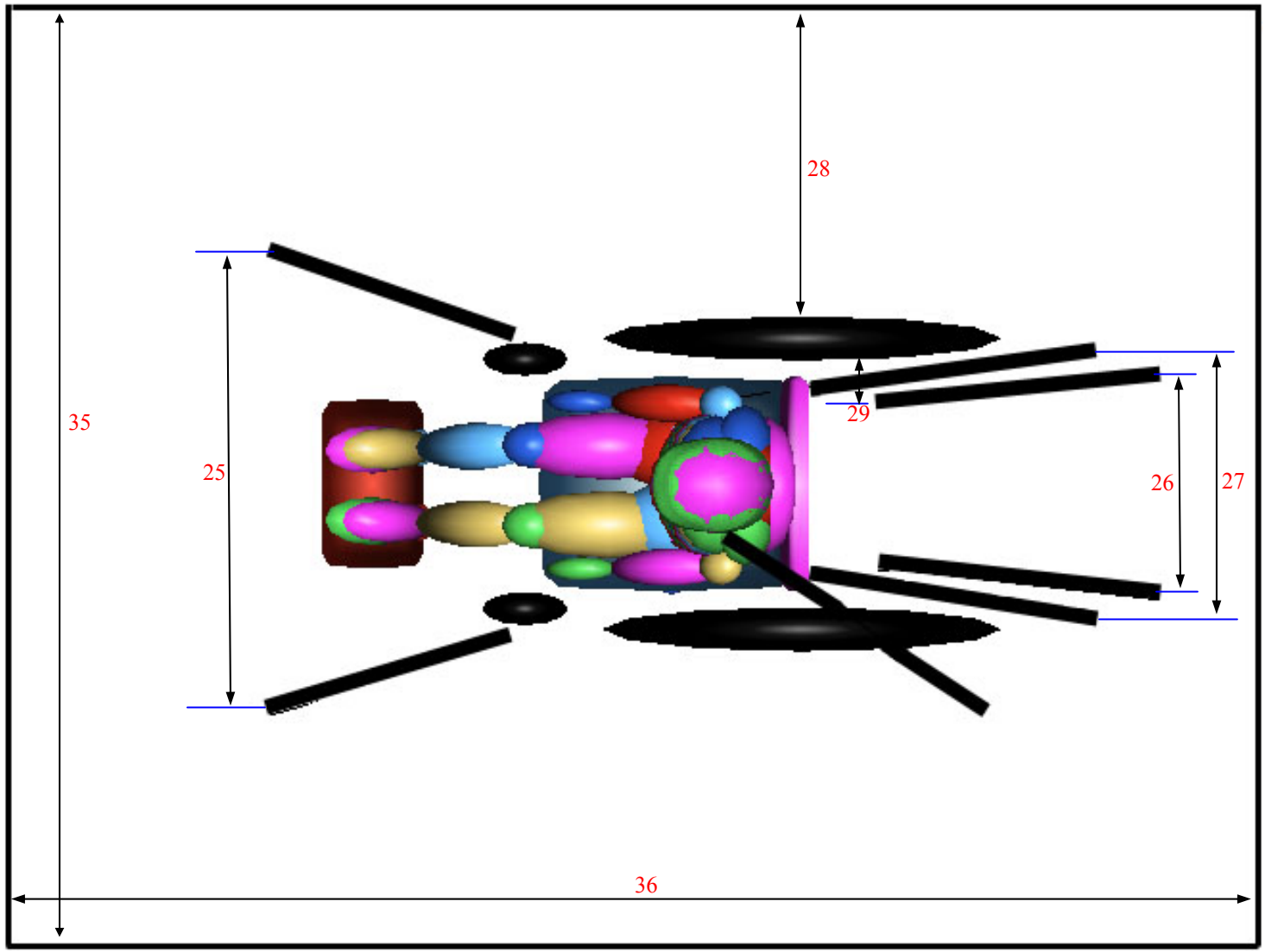

Front View

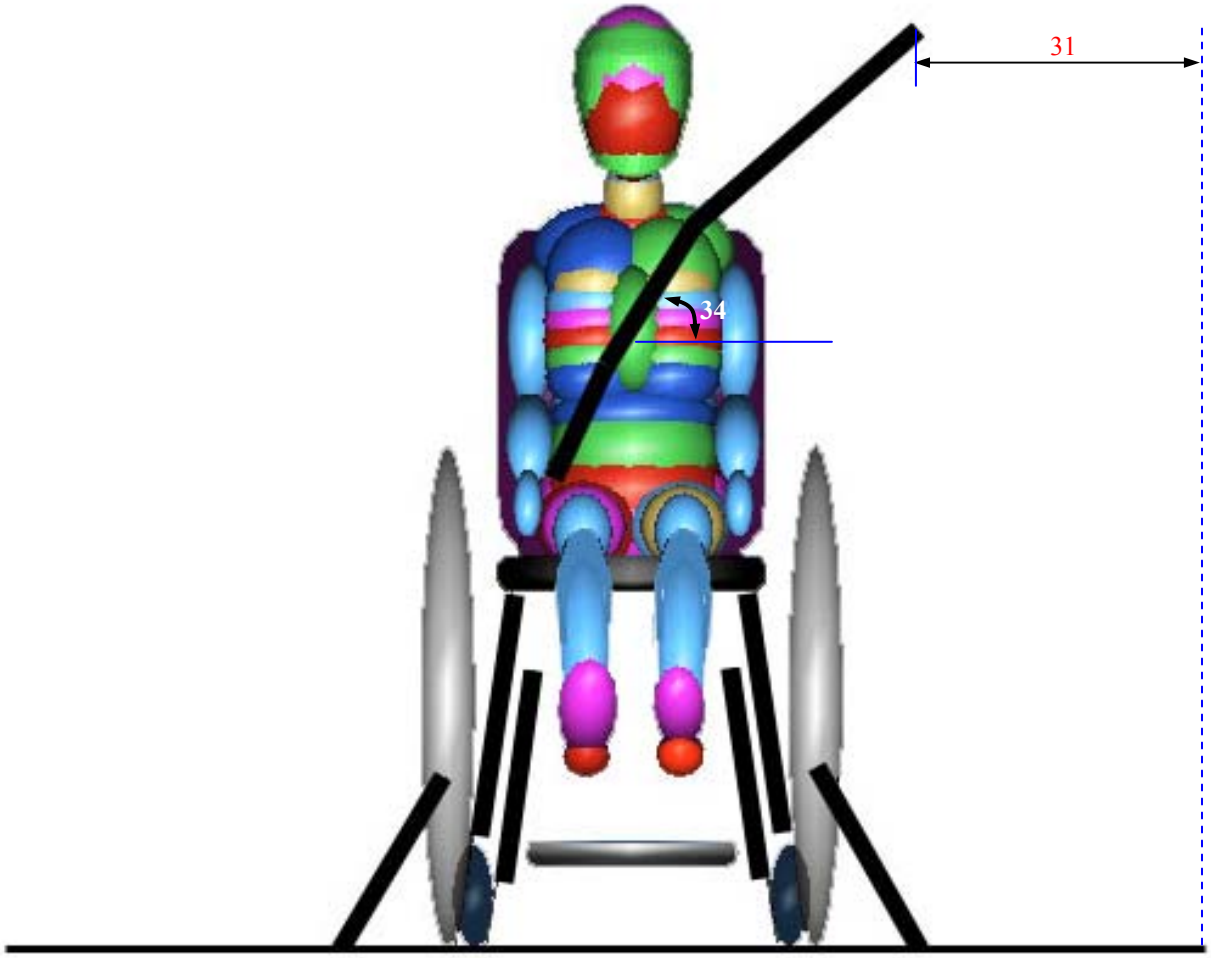

APPENDIX D

Moment of Inertia of Wheelchair Frame Structure

The moment of inertia of wheelchair frame structure was estimated as follow (see Figure D-1):

1. The moment of inertia of each piece of frame was calculated (Ix', Iy', and Iz' in Table D-1).

   Frame material: Aluminum 6061 Tubing (Density = 2700 kg/m^3)

   Frame part: 1-3, 5, 7-10

   OD = 25.4 mm (1"); ID = 20.64 mm (13/16")

   Frame part: 4 and 6

   OD = 25.4 mm (1"); ID = 19.05 mm (3/4")

2. x, y, and z distances from the center of each frame piece to the CG of entire WC frame structure were measured (x, y, and z in Table D-1).

   Note: The CG of whole wheelchair frame structure was obtained by hanging the structure at three different points while a piece of thread was dropped from each hanging point. The point where three pieces of thread were crossed was the CG of whole WC frame structure.

3. Using the Parallel-Axis Theorem shown below, the moment of inertia of entire WC frame structure was calculated.

$$Ix = \bar{I}x' + m(\bar{y}^2 + \bar{z}^2);\ Iy = \bar{I}y' + m(\bar{z}^2 + \bar{x}^2);\ Iz = \bar{I}z' + m(\bar{x}^2 + \bar{y}^2)$$

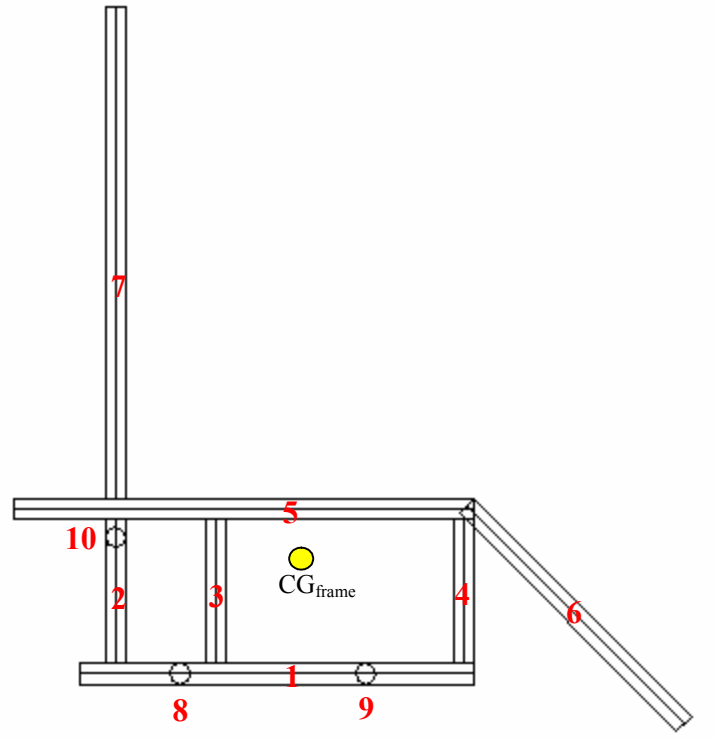

Figure D-1 Simplified Zippie wheelchair frame structure

Table D-1 Moment of inertia of Zippie wheelchair frame with respect to CG of entire frame.

Part	Ix' (kg m^2)	Iy' (kg m^2)	Iz' (kg m^2)	mass (kg)	x (m)	y (m)	z (m)	Ix (kg m^2)	Iy (kg m^2)	Iz (kg m^2)
1	0.000031	0.004574	0.004574	0.227822	0.0430	0.1402	0.1460	0.018700	0.015129	0.014373
2	0.000224	0.000224	0.000011	0.082760	0.2430	0.1402	0.0443	0.003802	0.010323	0.013038
3	0.000224	0.000224	0.000011	0.082760	0.1180	0.1402	0.0443	0.003802	0.002854	0.005569
4	0.000288	0.000288	0.000013	0.106542	0.1893	0.1402	0.0443	0.004895	0.008342	0.011837
5	0.000036	0.007269	0.007269	0.265948	0.0840	0.1402	0.0574	0.012243	0.012775	0.021477
6	0.001390	0.002751	0.001390	0.880000	0.3274	0.1402	0.0732	0.045415	0.200837	0.224640
7	0.008813	0.008813	0.000038	0.283616	0.2430	0.1402	0.3501	0.089488	0.111833	0.044682
8	0.000863	0.000017	0.000863	0.130370	0.1630	0.0000	0.1460	0.003642	0.006260	0.004327
9	0.000863	0.000017	0.000863	0.130370	0.0670	0.0000	0.1460	0.003642	0.003381	0.001448
10	0.000863	0.000017	0.000863	0.130370	0.2430	0.0000	0.0227	0.000930	0.007782	0.008561
							Total =	**0.186560**	**0.379515**	**0.349953**

Note: In calculation of Ix, Iy and Iz for frame part 1 through 7, values were multiplied by 2 since two frame parts exited in symmetry. (For example, $Ix = 2*[\bar{I}x'+m(\bar{y}^2+\bar{z}^2)]$.)

APPENDIX E

MADYMO XML Input file – Full_FE Belt model

```
<?xml version="1.0" encoding="UTF-8"?>
<?xml-stylesheet href="file://localhost/C:/Morphon XML-Editor/madymo.css" type="text/css"?>
<!DOCTYPE MADYMO SYSTEM "mtd_3d.dtd">
<MADYMO DESCRIPTION="Template input file" RELEASE="R6.0.1">
 <TYPEDEFS>
  <INCLUDE
   FILE = "typedefs.xml"/>
 </TYPEDEFS>
 <RUNID>
<![CDATA[
Zippie Wheelchair with Hybrid III 6 year-old ATD
by DongRan Ha   2004
For Madymo v.6.0.1
  ]]>
  </RUNID>
 <CONTROL_ALLOCATION/>
 <CONTROL_ANALYSIS.TIME
  INT_MTH          = "EULER"
  TIME_END         = "0.4"
  TIME_STEP        = "2.000000E-005"
 />
 <CONTROL_OUTPUT
  TIME_STEP            = "1.000000E-004"
  TIME_STEP_KIN        = "0.002"
  WRITE_KIN            = "EXTENDED"
 >
  <TIME_HISTORY_CONTACT
   CONTACT_OUTPUT_LIST     = "ALL"
  />
  <TIME_HISTORY_MB
   BELT_OUTPUT_LIST             = "ALL"
   BODY_OUTPUT_LIST             = "ALL"
   BODY_REL_OUTPUT_LIST         = "ALL"
  />
  <TIME_HISTORY_MB
   BODY_OUTPUT_LIST             = "Pelvis_acc     ThoraxT4_acc     HeadCG_acc"
   BODY_REL_OUTPUT_LIST         = "ChestDeflection_dis"
   DESCRIPTION              = "Output signals Hybrid III 6 year old ellipsoid dummy  model"
   JOINT_CONSTRAINT_OUTPUT_LIST                    =    "NeckUp_lce_F_CFC1000
NeckUp_lce_F_CFC600     NeckUp_lce_T"
   SYSTEM                   = "/Hybrid_III_6_year_old"
  >
   <COMMENT>
<![CDATA[
Available output signals
```

```
      BODY_OUTPUT_LIST
Pelvis_acc
ThoraxT4_acc
HeadCG_acc
SternumUp_acc
SternumLow_acc
ThoraxT1_acc
ThoraxUp_acc
ThoraxLow_acc
      BODY_REL_OUTPUT_LIST
ChestDeflection_dis
ChestDeflection_vel_CFC180
ChestDeflection_vel_CFC600

    JOINT_CONSTRAINT_OUTPUT_LIST
LumbarSpineLow_lce_F
LumbarSpineLow_lce_T
NeckLow_lce_F
NeckLow_lce_T
NeckUp_lce_F_CFC600
NeckUp_lce_F_CFC1000
NeckUp_lce_T
FemurL_lce_F
FemurL_lce_T
FemurR_lce_F
FemurR_lce_T
        ]>
        </COMMENT>
   </TIME_HISTORY_MB>
  </CONTROL_OUTPUT>
  <SYSTEM.REF_SPACE
   ID           = "1"
   NAME         = "sled_track"
  >
   <SURFACE.PLANE
    ID          = "1"
    NAME        = "track_surface"
    POINT_1     = "0.0         0.0         0.0"
    POINT_2     = "4.0         0.0         0.0"
    POINT_3     = "4.0         1.88         0.0"
   />
  </SYSTEM.REF_SPACE>
  <SYSTEM.MODEL
   ID           = "2"
   NAME         = "moving_sled"
  >
```

```
<BODY.RIGID
 CENTRE_OF_GRAVITY     = "1.07        0.94        0.0"
 ID                    = "1"
 INERTIA               = "500.0       1.000000E+003 1.000000E+003 0.0         0.0         0.0"
 MASS                  = "300.0"
 NAME                  = "sled_body"
/>
<SURFACE.PLANE
 BODY        = "sled_body"
 ID          = "1"
 NAME        = "sled_surface"
 POINT_1     = "0.0         0.0         0.0"
 POINT_2     = "2.14        0.0         0.0"
 POINT_3     = "2.14        1.88        0.0"
/>
<SURFACE.ELLIPSOID
 DEGREE          = "8"
 ID              = "2"
 NAME            = "sled_pole"
 SEMI_AXIS       = "0.05        0.06        0.6"
>
 <CRDSYS_OBJECT_1
  BODY       = "sled_body"
  POS        = "0.41        1.335       0.6"
 />
</SURFACE.ELLIPSOID>
<JOINT.TRAN
 ID       = "1"
 NAME     = "sled_joint"
>
 <CRDSYS_OBJECT_1
  POS        = "0.0         0.0         0.0"
 />
 <CRDSYS_OBJECT_2
  BODY       = "sled_body"
  POS        = "0.0         0.0         0.0"
 />
</JOINT.TRAN>
<INITIAL.JOINT_VEL
 JOINT      = "sled_joint"
 V1         = "13.444"
/>
<INITIAL.FE_MODEL
 BODY          = "/Hybrid_III_6_year_old/AbdomenInsert_bod"
 FE_MODEL      = "lap_FE"
/>
```

```
<INITIAL.FE_MODEL
 BODY          = "/Hybrid_III_6_year_old/Sternum_bod"
 FE_MODEL      = "shoulder_FE"
/>
<MOTION.JOINT_ACC
 A1_FUNC       = "/sled_pulse"
 JOINT         = "sled_joint"
>
 <FUNC_USAGE
  FUNC         = "/sled_pulse"
  Y_SCALE      = "9.81"
 />
</MOTION.JOINT_ACC>
<GROUP_MB
 ID               = "1"
 NAME             = "sled_group"
 SURFACE_LIST     = "sled_surface"
 SYSTEM           = "/moving_sled"
/>
<FE_MODEL
 ID       = "2"
 NAME     = "lap_FE"
>
 <CONTROL_FE_MODEL/>
 <CONTROL_FE_TIME_STEP/>
 <TABLE
  TYPE = "COORDINATE.CARTESIAN"
 >
     |   ID         X               Y               Z       |
          1    -4.0180568E-002    -1.3048837E-001    -1.4506770E-002
          2    -1.7538618E-002    -1.1592145E-001    -5.9377180E-003
          3    -1.0497045E-002    -1.1563981E-001    -2.9946104E-002
          4    -3.1716866E-002    -1.2980000E-001    -3.8020423E-002
          5     5.4814044E-003    -1.0198546E-001     2.6931445E-003
          6     1.0725760E-002    -1.0149093E-001    -2.1858648E-002
          7     2.8349816E-002    -8.7371861E-002     1.0512951E-002
          8     3.0765040E-002    -8.5639580E-002    -1.4272013E-002
          9     4.6018057E-002    -6.6376533E-002     1.5703983E-002
         10     4.4588653E-002    -6.3482012E-002    -9.0211017E-003
         11     5.6159601E-002    -4.0270478E-002     1.8709833E-002
         12     5.2759230E-002    -3.8250075E-002    -5.8953359E-003
         13     6.0786717E-002    -1.2508755E-002     2.0151462E-002
         14     5.6507087E-002    -1.1834762E-002    -4.4571357E-003
         15     6.0451919E-002     1.5703217E-002     2.0117375E-002
         16     5.6296911E-002     1.4890739E-002    -4.4059174E-003
         17     5.5343584E-002     4.3375519E-002     1.8623118E-002
```

18	5.1964432E-002	4.1213708E-002	-5.8757689E-003
19	4.4358263E-002	6.9105656E-002	1.5489385E-002
20	4.3247397E-002	6.6238408E-002	-9.1734957E-003
21	2.5940821E-002	8.9418909E-002	1.0203826E-002
22	2.8620997E-002	8.7772347E-002	-1.4655860E-002
23	2.2906906E-003	1.0255228E-001	2.0635236E-003
24	8.0878910E-003	1.0291769E-001	-2.2411815E-002
25	-2.1386994E-002	1.1517835E-001	-6.8006559E-003
26	-1.3958288E-002	1.1559140E-001	-3.0718691E-002
27	-4.4947693E-002	1.2801639E-001	-1.5670180E-002
28	-3.6214704E-002	1.2785845E-001	-3.9094738E-002
29	-2.1772801E-002	-1.3170113E-001	-6.0878710E-002
30	1.3650292E-003	-1.1788087E-001	-5.1891209E-002
31	2.5182828E-002	-1.0582004E-001	-4.2016143E-002
32	4.7122183E-002	-9.0867879E-002	-3.2186427E-002
33	6.2789549E-002	-6.8606862E-002	-2.5226966E-002
34	6.8577891E-002	-4.0961736E-002	-2.4851163E-002
35	6.9490440E-002	-1.2535333E-002	-2.5725346E-002
36	6.9384126E-002	1.5930203E-002	-2.5651034E-002
37	6.8059940E-002	4.4329929E-002	-2.4669548E-002
38	6.1034317E-002	7.1539356E-002	-2.5717599E-002
39	4.4630032E-002	9.3142705E-002	-3.3039910E-002
40	2.1885952E-002	1.0679043E-001	-4.3033516E-002
41	-2.5804214E-003	1.1744395E-001	-5.2940618E-002
42	-2.6636255E-002	1.2949818E-001	-6.2128726E-002

</TABLE>

<TABLE
TYPE = "ELEMENT.TRIAD3"
>

	ID	PART	N1	N2	N3	
	3	1	2	5	6	
	4	1	2	6	3	
	5	1	5	7	8	
	6	1	5	8	6	
	7	1	7	9	10	
	8	1	7	10	8	
	9	1	9	11	12	
	10	1	9	12	10	
	11	1	11	13	14	
	12	1	11	14	12	
	13	1	13	15	16	
	14	1	13	16	14	
	15	1	15	17	18	
	16	1	15	18	16	
	17	1	17	19	20	
	18	1	17	20	18	

```
          19       1       19       21       22
          20       1       19       22       20
          21       1       21       23       24
          22       1       21       24       22
          23       1       23       25       26
          24       1       23       26       24
          26       1       25       28       26
          29       1       30        3        6
          30       1        6       31       30
          31       1       31        6        8
          32       1        8       32       31
          33       1       32        8       10
          34       1       10       33       32
          35       1       33       10       12
          36       1       12       34       33
          37       1       34       12       14
          38       1       14       35       34
          39       1       35       14       16
          40       1       16       36       35
          41       1       36       16       18
          42       1       18       37       36
          43       1       37       18       20
          44       1       20       38       37
          45       1       38       20       22
          46       1       22       39       38
          47       1       39       22       24
          48       1       24       40       39
          49       1       40       24       26
          50       1       26       41       40
          51       1       41       26       28
        1820       1        4        3       30
        1821       1        2        3        4
   </TABLE>
<MATERIAL.HYSISO
 CHAR               = "belt_mat_char"
 DENSITY              = "800.0"
 ID                 = "1"
 NAME                 = "FEbeltmat"
 >
<CHARACTERISTIC.MATERIAL
 ELAS_LIMIT       = "0.0"
 HYS_MODEL        = "1"
 HYS_SLOPE        = "6.000000E+009"
 ID             = "10"
 LOAD_FUNC        = "mat_Load"
 NAME           = "belt_mat_char"
```

```
  UNLOAD_FUNC      = "mat_unload"
 />
 <PART
  ID          = "1"
  MATERIAL      = "FEbeltmat"
  NAME         = "PART_4"
  PROPERTY      = "propforlap"
 />
 <PROPERTY.MEM3
  ID            = "1"
  NAME           = "propforlap"
  THICK          = "1.000000E-003"
 />
 <SUPPORT
  BODY           = "/wheelchair/tiepoint_body"
  DOF_ALL         = "ON"
  NODE_LIST       = "4"
 />
 <FUNCTION.XY
  ID       = "100"
  NAME     = "mat_Load"
 >
  <TABLE
   TYPE = "XY_PAIR"
  >
|      XI                YI       |
 0.00000000E+000      0.00000000E+000
 2.10000000E-002      2.00000000E+007
 3.00000000E-002      5.90000000E+007
 4.00000000E-002      8.00000000E+007
 5.00000000E-002      9.40000000E+007
 6.00000000E-002      1.10000000E+008
 7.00000000E-002      1.20000000E+008
 8.00000000E-002      1.30000000E+008
 9.00000000E-002      1.40000000E+008
 1.00000000E-001      1.60000000E+008
 1.10000000E-001      1.70000000E+008
 1.20000000E-001      1.90000000E+008
 1.25000000E-001      2.00000000E+008
      </TABLE>
 </FUNCTION.XY>
 <FUNCTION.XY
  ID       = "101"
  NAME     = "mat_unload"
 >
  <TABLE
```

```
    TYPE = "XY_PAIR">
|      XI              YI      |
 0.00000000E+000     0.00000000E+000
 1.00000000E-001     2.00000000E+007
      </TABLE>
 </FUNCTION.XY>
</FE_MODEL>
<FE_MODEL
 ID       = "3"
 NAME     = "shoulder_FE"
>
 <CONTROL_FE_MODEL/>
 <CONTROL_FE_TIME_STEP/>
 <TABLE
  TYPE = "COORDINATE.CARTESIAN"
 >
      |   ID        X               Y               Z       |
          1    -4.6226349E-002    1.5608866E-001    9.8231343E-002
          2    -3.0790487E-002    1.3801742E-001    9.2331710E-002
          3    -4.0473235E-002    1.2297812E-001    1.0991427E-001
          4    -5.6421222E-002    1.4160853E-001    1.1587759E-001
          5    -1.8545823E-002    1.1852082E-001    8.3966722E-002
          6    -2.4461900E-002    1.0445196E-001    1.0380595E-001
          7    -6.0851766E-003    9.8835002E-002    7.6403463E-002
          8    -8.4774224E-003    8.5833444E-002    9.7898028E-002
          9    6.6228779E-003     7.9298332E-002    6.9003281E-002
         10     7.0836192E-003    6.7228103E-002    9.1096284E-002
         11     1.6656672E-002    6.1254800E-002    5.6362570E-002
         12     1.6430753E-002    4.8035772E-002    7.8091651E-002
         13     2.1649315E-002    4.4211549E-002    3.9688083E-002
         14     1.9014658E-002    2.9984952E-002    6.0697140E-002
         15     2.2881613E-002    2.7411601E-002    2.1956247E-002
         16     1.9964014E-002    1.2649281E-002    4.2403030E-002
         17     2.2916625E-002    1.0785070E-002    3.9676974E-003
         18     2.0792444E-002    -4.5682163E-003    2.3970507E-002
         19     2.2940146E-002    -5.7270925E-003    -1.4126076E-002
         20     2.1072240E-002    -2.1618546E-002    5.3769980E-003
         21     2.2944882E-002    -2.2153288E-002    -3.2297961E-002
         22     2.1238404E-002    -3.8575641E-002    -1.3312924E-002
         23     2.2741568E-002    -3.7966050E-002    -5.0998252E-002
         24     2.0477386E-002    -5.4928039E-002    -3.2477368E-002
         25     1.9114565E-002    -5.1890902E-002    -7.0736227E-002
         26     1.6522103E-002    -6.9552333E-002    -5.2654241E-002
         27     1.4869528E-002    -6.4442511E-002    -9.1336857E-002
         28     5.7758312E-003    -7.9497418E-002    -7.3030117E-002
         29     7.2838568E-003    -7.6284988E-002    -1.1136266E-001
```

```
        30    -5.7921155E-003    -8.8503382E-002    -9.3558335E-002
        31    -6.1842940E-003    -8.2257166E-002    -1.3073050E-001
        32    -1.8067462E-002    -9.6793925E-002    -1.1397729E-001
        33    -1.8381649E-002    -8.9997053E-002    -1.5051329E-001
        34    -3.0378818E-002    -1.0505223E-001    -1.3440109E-001
        35    -3.0581883E-002    -9.7740598E-002    -1.7029288E-001
        36    -4.2677742E-002    -1.1330105E-001    -1.5483804E-001
        37    -4.2782022E-002    -1.0549066E-001    -1.9006996E-001
        38    -5.4978432E-002    -1.2155071E-001    -1.7527360E-001
        39    -5.4970273E-002    -1.1325811E-001    -2.0984756E-001
        40    -6.7278346E-002    -1.2980000E-001    -1.9570977E-001
        41    -6.7568554E-002     1.2663837E-001     1.3250983E-001
        42    -5.0975867E-002     1.0761538E-001     1.2648522E-001
        43    -3.2523304E-002     8.9798787E-002     1.2244961E-001
        44    -1.4333486E-002     7.1888685E-002     1.1771297E-001
        45     2.3744364E-003     5.3467730E-002     1.1113182E-001
        46     1.3082382E-002     3.3600703E-002     9.8598462E-002
        47     1.6738951E-002     1.4846535E-002     8.1031716E-002
        48     1.8922964E-002    -3.0245608E-003     6.2320547E-002
        49     2.1007032E-002    -2.0710534E-002     4.3423477E-002
        50     2.2326498E-002    -3.8213682E-002     2.4311094E-002
        51     2.1101988E-002    -5.5581084E-002     5.1039753E-003
        52     1.6534278E-002    -7.1904821E-002    -1.4456508E-002
        53     8.1718605E-003    -8.5473253E-002    -3.4779359E-002
        54    -3.3158331E-003    -9.5687579E-002    -5.5639003E-002
        55    -1.6031724E-002    -1.0421204E-001    -7.6610903E-002
        56    -2.9823660E-002    -1.1156898E-001    -9.7318365E-002
        57    -4.2452481E-002    -1.2007900E-001    -1.1832874E-001
        58    -5.4825451E-002    -1.2884508E-001    -1.3940782E-001
        59    -6.7197376E-002    -1.3760481E-001    -1.6049015E-001
        60    -7.9583133E-002    -1.4634482E-001    -1.8157254E-001
   </TABLE>
<TABLE
  TYPE = "ELEMENT.TRIAD3"
>
     |   ID     PART      N1       N2       N3  |
         3      1      2      5      6
         4      1      2      6      3
         5      1      5      7      8
         6      1      5      8      6
         7      1      7      9     10
         8      1      7     10      8
         9      1      9     11     12
        10      1      9     12     10
        11      1     11     13     14
        12      1     11     14     12
```

13	1	13	15	16
14	1	13	16	14
15	1	15	17	18
16	1	15	18	16
17	1	17	19	20
18	1	17	20	18
19	1	19	21	22
20	1	19	22	20
21	1	21	23	24
22	1	21	24	22
23	1	23	25	26
24	1	23	26	24
25	1	25	27	28
26	1	25	28	26
27	1	27	29	30
28	1	27	30	28
29	1	29	31	32
30	1	29	32	30
31	1	31	33	34
32	1	31	34	32
33	1	33	35	36
34	1	33	36	34
35	1	35	37	38
36	1	35	38	36
38	1	37	40	38
41	1	42	3	6
42	1	6	43	42
43	1	43	6	8
44	1	8	44	43
45	1	44	8	10
46	1	10	45	44
47	1	45	10	12
48	1	12	46	45
49	1	46	12	14
50	1	14	47	46
51	1	47	14	16
52	1	16	48	47
53	1	48	16	18
54	1	18	49	48
55	1	49	18	20
56	1	20	50	49
57	1	50	20	22
58	1	22	51	50
59	1	51	22	24
60	1	24	52	51
61	1	52	24	26

```
          62       1      26      53      52
          63       1      53      26      28
          64       1      28      54      53
          65       1      54      28      30
          66       1      30      55      54
          67       1      55      30      32
          68       1      32      56      55
          69       1      56      32      34
          70       1      34      57      56
          71       1      57      34      36
          72       1      36      58      57
          73       1      58      36      38
          74       1      38      59      58
          75       1      59      38      40
      301748       1       2       3       4
      301751       1       4       3      42
   </TABLE>
<MATERIAL.HYSISO
  CHAR               = "belt_mat_char"
  DENSITY              = "800.0"
  ID                 = "1"
  NAME               = "FEbeltmat"
/>
<CHARACTERISTIC.MATERIAL
  ELAS_LIMIT       = "0.0"
  HYS_MODEL        = "1"
  HYS_SLOPE        = "6.000000E+009"
  ID             = "10"
  LOAD_FUNC        = "mat_Load"
  NAME           = "belt_mat_char"
  UNLOAD_FUNC      = "mat_unload"
/>
<PART
  ID           = "1"
  MATERIAL      = "FEbeltmat"
  NAME         = "PART_3"
  PROPERTY      = "propforshldr"
/>
<PROPERTY.MEM3
  ID             = "1"
  NAME           = "propforshldr"
  THICK          = "1.000000E-003"
/>
<!-- **R Support for end of the belt -->
<SUPPORT
  BODY           = "/wheelchair/tiepoint_body"
```

```
    DOF_ALL         = "ON"
    NODE_LIST       = "40"
   />
   <FUNCTION.XY
    ID        = "100"
    NAME      = "mat_Load"
   >
    <TABLE
     TYPE = "XY_PAIR"
    >
|      XI                YI       |
  0.00000000E+000      0.00000000E+000
  2.10000000E-002      2.00000000E+007
  3.00000000E-002      5.90000000E+007
  4.00000000E-002      8.00000000E+007
  5.00000000E-002      9.40000000E+007
  6.00000000E-002      1.10000000E+008
  7.00000000E-002      1.20000000E+008
  8.00000000E-002      1.30000000E+008
  9.00000000E-002      1.40000000E+008
  1.00000000E-001      1.60000000E+008
  1.10000000E-001      1.70000000E+008
  1.20000000E-001      1.90000000E+008
  1.25000000E-001      2.00000000E+008
        </TABLE>
   </FUNCTION.XY>
   <FUNCTION.XY
    ID        = "101"
    NAME      = "mat_unload"
   >
    <TABLE
     TYPE = "XY_PAIR"
    >
|      XI                YI       |
  0.00000000E+000      0.00000000E+000
  1.00000000E-001      2.00000000E+007
        </TABLE>
   <FUNCTION.XY>
  </FE_MODEL>
</SYSTEM.MODEL>
<SYSTEM.MODEL
  ID            = "3"
  NAME          = "wheelchair"
>
  <BODY.RIGID
   ID                  = "1"
```

```
 INERTIA          = "0.045937    0.091873    0.045937    0.0         0.0         0.0"
 MASS             = "2.2"
 NAME             = "rrwh_body"
/>
<BODY.RIGID
 ID               = "2"
 INERTIA          = "0.045937    0.091873    0.045937    0.0         0.0         0.0"
 MASS             = "2.2"
 NAME             = "rlwh_body"
/>
<BODY.RIGID
 ID               = "3"
 INERTIA          = "2.880000E-004 5.770000E-004 2.880000E-004 0.0         0.0         0.0"
 MASS             = "0.3"
 NAME             = "frwh_body"
/>
<BODY.RIGID
 ID               = "4"
 INERTIA          = "2.880000E-004 5.770000E-004 2.880000E-004 0.0         0.0         0.0"
 MASS             = "0.3"
 NAME             = "flwh_body"
/>
<BODY.RIGID
 ID               = "5"
 INERTIA          = "0.18656     0.379515    0.349953    0.0         0.0         0.0"
 MASS             = "9.6"
 NAME             = "frame_cg_body"
/>
<BODY.RIGID
 ID               = "6"
 INERTIA          = "0.01922     0.02888     0.0481      0.0         0.0         0.0"
 MASS             = "2.4"
 NAME             = "wcseat_body"
/>
<BODY.RIGID
 ID               = "7"
 INERTIA          = "0.044092    0.026473    0.017618    0.0         0.0         0.0"
 MASS             = "2.2"
 NAME             = "wcback_body"
/>
<BODY.RIGID
 ID               = "8"
 INERTIA          = "1.000000E-003 1.000000E-003 1.000000E-003 0.0         0.0         0.0"
 MASS             = "0.8"
 NAME             = "accelerometer"
/>
```

```
<BODY.RIGID
 ID                = "9"
 INERTIA             = "1.000000E-004 1.000000E-004 1.000000E-004 0.0         0.0         0.0"
 MASS              = "0.3"
 NAME               = "tiepoint_body"
/>
<BODY.RIGID
 ID                = "10"
 MASS              = "1.000000E-005"
 NAME               = "p_point"
/>
<SURFACE.ELLIPSOID
 CHAR          = "rwh_contact"
 DEGREE         = "2"
 ID            = "1"
 NAME          = "rrwh_surface"
 SEMI_AXIS     = "0.289       0.032       0.289"
>
 <CRDSYS_OBJECT_1
  BODY       = "rrwh_body"
  POS        = "0.0         0.0         0.0"
 />
</SURFACE.ELLIPSOID>
<SURFACE.ELLIPSOID
 CHAR          = "rwh_contact"
 DEGREE         = "2"
 ID            = "2"
 NAME          = "rlwh_surface"
 SEMI_AXIS     = "0.289       0.032       0.289"
>
 <CRDSYS_OBJECT_1
  BODY       = "rlwh_body"
  POS        = "0.0         0.0         0.0"
 />
</SURFACE.ELLIPSOID>
<SURFACE.ELLIPSOID
 CHAR          = "fwh_contact"
 DEGREE         = "2"
 ID            = "3"
 NAME          = "frwh_surface"
 SEMI_AXIS     = "0.062       0.024       0.062"
>
 <CRDSYS_OBJECT_1
  BODY       = "frwh_body"
  POS        = "0.0         0.0         0.0"
 />
```

```
</SURFACE.ELLIPSOID>
<SURFACE.ELLIPSOID
 CHAR          = "fwh_contact"
 DEGREE        = "2"
 ID            = "4"
 NAME          = "flwh_surface"
 SEMI_AXIS     = "0.062      0.024      0.062"
>
 <CRDSYS_OBJECT_1
  BODY      = "flwh_body"
  POS       = "0.0        0.0        0.0"
 />
</SURFACE.ELLIPSOID>
<SURFACE.ELLIPSOID
 CHAR          = "wcseat_contact"
 DEGREE        = "8"
 ID            = "5"
 NAME          = "wcseat_surface"
 SEMI_AXIS     = "0.19       0.155      0.015"
>
 <CRDSYS_OBJECT_1
  BODY      = "wcseat_body"
  POS       = "0.0        0.0        0.0"
 />
</SURFACE.ELLIPSOID>
<SURFACE.ELLIPSOID
 CHAR          = "wcback_contact"
 DEGREE        = "8"
 ID            = "6"
 NAME          = "wcback_surface"
 SEMI_AXIS     = "0.01       0.155      0.19"
>
 <CRDSYS_OBJECT_1
  BODY      = "wcback_body"
  POS       = "0.0        0.0        0.0"
 />
</SURFACE.ELLIPSOID>
<SURFACE.ELLIPSOID
 CHAR          = "footrest_contact"
 DEGREE        = "8"
 ID            = "7"
 NAME          = "footrest_surface"
 SEMI_AXIS     = "0.076      0.1225     0.0025"
>
 <CRDSYS_OBJECT_1
  BODY      = "frame_cg_body"
```

```
   ORIENT      = "foot_ori"
   POS         = "0.405        0.0          -0.2"
  />
</SURFACE.ELLIPSOID>
<SURFACE.ELLIPSOID
  DEGREE          = "2"
  ID              = "8"
  NAME            = "frame_cg_surface"
  SEMI_AXIS       = "0.01         0.01         0.01"
>
  <CRDSYS_OBJECT_1
   BODY        = "frame_cg_body"
   POS         = "0.0          0.0          0.0"
  />
</SURFACE.ELLIPSOID>
<SURFACE.ELLIPSOID
  DEGREE          = "2"
  ID              = "9"
  NAME            = "total_cg_surface"
  SEMI_AXIS       = "0.02         0.02         0.02"
>
  <CRDSYS_OBJECT_1
   BODY        = "accelerometer"
   POS         = "0.0          0.0          0.0"
  />
</SURFACE.ELLIPSOID>
<SURFACE.ELLIPSOID
  CHAR            = "tiepoint_contact"
  DEGREE          = "10"
  ID              = "10"
  NAME            = "tiepoint_surface"
  SEMI_AXIS       = "0.02         0.008        0.02"
>
  <CRDSYS_OBJECT_1
   BODY        = "tiepoint_body"
   POS         = "0.0          0.0          0.0"
  />
</SURFACE.ELLIPSOID>
<SURFACE.ELLIPSOID
  DEGREE          = "8"
  ID              = "50"
  NAME            = "r_hor1"
  SEMI_AXIS       = "0.245        0.0127       0.0127"
>
  <CRDSYS_OBJECT_1
   BODY        = "frame_cg_body"
```

```
   POS        = "-0.043       -0.1402       -0.146"
  />
</SURFACE.ELLIPSOID>
<SURFACE.ELLIPSOID
  DEGREE         = "8"
  ID             = "51"
  NAME           = "l_hor1"
  SEMI_AXIS      = "0.245       0.0127       0.0127"
>
  <CRDSYS_OBJECT_1
    BODY       = "frame_cg_body"
    POS        = "-0.043       0.1402       -0.146"
  />
</SURFACE.ELLIPSOID>
<SURFACE.ELLIPSOID
  DEGREE         = "8"
  ID             = "52"
  NAME           = "r_hor2"
  SEMI_AXIS      = "0.286       0.0127       0.0127"
>
  <CRDSYS_OBJECT_1
    BODY       = "frame_cg_body"
    POS        = "-0.084       -0.1402       0.0574"
  />
</SURFACE.ELLIPSOID>
<SURFACE.ELLIPSOID
  DEGREE         = "8"
  ID             = "53"
  NAME           = "l_hor2"
  SEMI_AXIS      = "0.286       0.0127       0.0127"
>
  <CRDSYS_OBJECT_1
    BODY       = "frame_cg_body"
    POS        = "-0.084       0.1402       0.0574"
  />
</SURFACE.ELLIPSOID>
<SURFACE.ELLIPSOID
  DEGREE         = "8"
  ID             = "54"
  NAME           = "r_ver1"
  SEMI_AXIS      = "0.0127       0.0127       0.089"
>
  <CRDSYS_OBJECT_1
    BODY       = "frame_cg_body"
    POS        = "-0.243       -0.1402       -0.0443"
  />
```

```
</SURFACE.ELLIPSOID>
<SURFACE.ELLIPSOID
 DEGREE         = "8"
 ID             = "55"
 NAME           = "l_ver1"
 SEMI_AXIS      = "0.0127      0.0127      0.089"
>
 <CRDSYS_OBJECT_1
  BODY       = "frame_cg_body"
  POS        = "-0.243       0.1402      -0.0443"
 />
</SURFACE.ELLIPSOID>
<SURFACE.ELLIPSOID
 DEGREE         = "8"
 ID             = "56"
 NAME           = "r_ver2"
 SEMI_AXIS      = "0.0127      0.0127      0.089"
>
 <CRDSYS_OBJECT_1
  BODY       = "frame_cg_body"
  POS        = "-0.118       -0.1402      -0.0443"
 />
</SURFACE.ELLIPSOID>
<SURFACE.ELLIPSOID
 DEGREE         = "8"
 ID             = "57"
 NAME           = "l_ver2"
 SEMI_AXIS      = "0.0127      0.0127      0.089"
>
 <CRDSYS_OBJECT_1
  BODY       = "frame_cg_body"
  POS        = "-0.118       0.1402      -0.0443"
 />
</SURFACE.ELLIPSOID>
<SURFACE.ELLIPSOID
 DEGREE         = "8"
 ID             = "58"
 NAME           = "r_ver3"
 SEMI_AXIS      = "0.0127      0.0127      0.089"
>
 <CRDSYS_OBJECT_1
  BODY       = "frame_cg_body"
  POS        = "0.1893      -0.1402      -0.0443"
 />
</SURFACE.ELLIPSOID>
<SURFACE.ELLIPSOID
```

```
 DEGREE         = "8"
 ID             = "59"
 NAME           = "l_ver3"
 SEMI_AXIS      = "0.0127      0.0127      0.089"
>
 <CRDSYS_OBJECT_1
  BODY       = "frame_cg_body"
  POS        = "0.1893      0.1402      -0.0443"
 />
</SURFACE.ELLIPSOID>
<SURFACE.ELLIPSOID
 DEGREE         = "8"
 ID             = "60"
 NAME           = "r_ver4"
 SEMI_AXIS      = "0.0127      0.0127      0.305"
>
 <CRDSYS_OBJECT_1
  BODY       = "frame_cg_body"
  POS        = "-0.243       -0.1402      0.3751"
 />
</SURFACE.ELLIPSOID>
<SURFACE.ELLIPSOID
 DEGREE         = "8"
 ID             = "61"
 NAME           = "l_ver4"
 SEMI_AXIS      = "0.0127      0.0127      0.305"
>
 <CRDSYS_OBJECT_1
  BODY       = "frame_cg_body"
  POS        = "-0.243       0.1402      0.3751"
 />
</SURFACE.ELLIPSOID>
<SURFACE.ELLIPSOID
 DEGREE         = "8"
 ID             = "62"
 NAME           = "r_leg"
 SEMI_AXIS      = "0.0127      0.0127      0.1639"
>
 <CRDSYS_OBJECT_1
  BODY       = "frame_cg_body"
  ORIENT     = "leg_ori"
  POS        = "0.3035      -0.1402      -0.0713"
 />
</SURFACE.ELLIPSOID>
<SURFACE.ELLIPSOID
 DEGREE         = "8"
```

```
 ID             = "63"
 NAME           = "l_leg"
 SEMI_AXIS      = "0.0127       0.0127       0.1639"
>
 <CRDSYS_OBJECT_1
  BODY       = "frame_cg_body"
  ORIENT     = "leg_ori"
  POS        = "0.3035       0.1402       -0.0713"
 />
</SURFACE.ELLIPSOID>
<SURFACE.ELLIPSOID
 DEGREE         = "8"
 ID             = "64"
 NAME           = "mid1"
 SEMI_AXIS      = "0.0127       0.128        0.0127"
>
 <CRDSYS_OBJECT_1
  BODY       = "frame_cg_body"
  POS        = "-0.163        0.0          -0.146"
 />
</SURFACE.ELLIPSOID>
<SURFACE.ELLIPSOID
 DEGREE         = "8"
 ID             = "65"
 NAME           = "mid2"
 SEMI_AXIS      = "0.0127       0.128        0.0127"
>
 <CRDSYS_OBJECT_1
  BODY       = "frame_cg_body"
  POS        = "0.067        0.0          -0.146"
 />
</SURFACE.ELLIPSOID>
<SURFACE.ELLIPSOID
 DEGREE         = "8"
 ID             = "66"
 NAME           = "mid3"
 SEMI_AXIS      = "0.0127       0.128        0.0127"
>
 <CRDSYS_OBJECT_1
  BODY       = "frame_cg_body"
  POS        = "-0.243        0.0          0.0227"
 />
</SURFACE.ELLIPSOID>
<SURFACE.ELLIPSOID
 CHAR           = "armrest_contact"
 DEGREE         = "8"
```

```
 ID            = "67"
 NAME          = "r_arm"
 SEMI_AXIS     = "0.17        0.0095      0.0095"
>
 <CRDSYS_OBJECT_1
  BODY       = "frame_cg_body"
  POS        = "-0.0603      -0.1702      0.3101"
 />
</SURFACE.ELLIPSOID>
<SURFACE.ELLIPSOID
 CHAR          = "armrest_contact"
 DEGREE        = "8"
 ID            = "68"
 NAME          = "l_arm"
 SEMI_AXIS     = "0.17        0.0095      0.0095"
>
 <CRDSYS_OBJECT_1
  BODY       = "frame_cg_body"
  POS        = "-0.0603      0.1702      0.3101"
 />
</SURFACE.ELLIPSOID>
<SURFACE.ELLIPSOID
 DEGREE        = "2"
 ID            = "69"
 NAME          = "p_point_surface"
 SEMI_AXIS     = "0.01        5.000000E-004 0.01"
>
 <CRDSYS_OBJECT_1
  BODY       = "p_point"
  POS        = "0.0         0.0         0.0"
 >
</SURFACE.ELLIPSOID>
<JOINT.FREE
 ID        = "1"
 NAME      = "hub_ref_joint"
>
 <CRDSYS_OBJECT_1
  POS        = "0.0         0.0         0.0"
 />
 <CRDSYS_OBJECT_2
  BODY       = "rrwh_body"
  POS        = "0.0         0.0         0.0"
 />
</JOINT.FREE>
<JOINT.FREE
 ID        = "4"
```

```
 NAME       = "accelerometer_joint"
 STATUS     = "LOCK"
>
 <CRDSYS_OBJECT_1
  BODY       = "frame_cg_body"
  POS        = "-0.027       0.1402       0.058"
 />
 <CRDSYS_OBJECT_2
  BODY       = "accelerometer"
  POS        = "0.0          0.0          0.0"
 />
</JOINT.FREE>
<JOINT.FREE
 ID         = "5"
 NAME       = "tiepoint_joint"
>
 <CRDSYS_OBJECT_1
  BODY       = "frame_cg_body"
  POS        = "-0.09        -0.128       0.199"
 />
 <CRDSYS_OBJECT_2
  BODY       = "tiepoint_body"
  POS        = "0.0          0.0          0.0"
 />
</JOINT.FREE>
</JOINT.FREE
 ID         = "10"
 NAME       = "p_point_joint"
 STATUS     = "LOCK"
>
 <CRDSYS_OBJECT_1
  BODY       = "frame_cg_body"
  POS        = "-0.08        -0.15        0.2"
 />
 <CRDSYS_OBJECT_2
  BODY       = "p_point"
  POS        = "0.0          0.0          0.0"
 />
</JOINT.FREE>
<JOINT.REVO
 ID       = "7"
 NAME     = "rlwh_joint"
>
 <CRDSYS_OBJECT_1
  BODY       = "frame_cg_body"
  ORIENT     = "wheel_ori"
```

```
   POS        = "-0.215       0.2102       -0.021"
  />
  <CRDSYS_OBJECT_2
   BODY       = "rlwh_body"
   ORIENT     = "wheel_ori"
   POS        = "0.0          0.0          0.0"
  />
</JOINT.REVO>
<JOINT.REVO
 ID       = "8"
 NAME     = "frwh_joint"
>
  <CRDSYS_OBJECT_1
   BODY       = "frame_cg_body"
   ORIENT     = "wheel_ori"
   POS        = "0.185        -0.1802       -0.248"
  />
  <CRDSYS_OBJECT_2
   BODY       = "frwh_body"
   ORIENT     = "wheel_ori"
   POS        = "0.0          0.0          0.0"
  />
</JOINT.REVO>
<JOINT.REVO
 ID       = "9"
 NAME     = "flwh_joint"
>
  <CRDSYS_OBJECT_1
   BODY       = "frame_cg_body"
   ORIENT     = "wheel_ori"
   POS        = "0.185        0.1802       -0.248"
  />
  <CRDSYS_OBJECT_2
   BODY       = "flwh_body"
   ORIENT     = "wheel_ori"
   POS        = "0.0          0.0          0.0"
  />
</JOINT.REVO>
<JOINT.REVO
 ID       = "6"
 NAME     = "rrwh_joint"
>
  <CRDSYS_OBJECT_1
   BODY       = "rrwh_body"
   ORIENT     = "wheel_ori"
   POS        = "0.0          0.0          0.0"
```

```
 />
 <CRDSYS_OBJECT_2
  BODY       = "frame_cg_body"
  ORIENT     = "wheel_ori"
  POS        = "-0.215       -0.2102       -0.021"
 />
</JOINT.REVO>
<JOINT.BRAC
 ID       = "2"
 NAME     = "wcseat_joint"
>
 <CRDSYS_OBJECT_1
  BODY       = "frame_cg_body"
  ORIENT     = "seat_ori"
  POS        = "-0.025       0.0         0.12"
 />
 <CRDSYS_OBJECT_2
  BODY       = "wcseat_body"
  POS        = "0.0          0.0         0.0"
 />
</JOINT.BRAC>
<JOINT.BRAC
 ID       = "3"
 NAME     = "wcback_joint"
>
 <CRDSYS_OBJECT_1
  BODY       = "frame_cg_body"
  ORIENT     = "back_ori"
  POS        = "-0.205       0.0         0.328"
 />
 <CRDSYS_OBJECT_2
  BODY       = "wcback_body"
  POS        = "0.0          0.0         0.0"
 />
<JOINT.BRAC>
<INITIAL.JOINT_POS
 D1         = "0.673"
 D2         = "0.74"
 D3         = "0.289"
 JOINT      = "hub_ref_joint"
/>
</ORIENTATION.SUCCESSIVE_ROT
 AXIS_1   = "Z"
 ID       = "1"
 NAME     = "wheel_ori"
 R1       = "-1.5708"
```

```
/>
<ORIENTATION.SUCCESSIVE_ROT
 AXIS_1    = "Y"
 ID        = "2"
 NAME      = "leg_ori"
 R1        = "-0.6632"
/>
<ORIENTATION.SUCCESSIVE_ROT
 AXIS_1    = "Y"
 ID        = "3"
 NAME      = "foot_ori"
 R1        = "-0.19199"
/>
<ORIENTATION.SUCCESSIVE_ROT
 AXIS_1    = "Y"
 ID        = "4"
 NAME      = "seat_ori"
 R1        = "-0.05236"
/>
<ORIENTATION.SUCCESSIVE_ROT
 AXIS_1    = "Y"
 ID        = "5"
 NAME      = "back_ori"
 R1        = "-0.06981"
/>
<INITIAL.JOINT_VEL
 JOINT     = "hub_ref_joint"
 V1        = "13.444"
/>
<CHARACTERISTIC.CONTACT
 CONTACT_MODEL     = "FORCE"
 ID                = "1"
 LOAD_FUNC         = "rwh_load"
 NAME              = "rwh_contact"
/>
<CHARACTERISTIC.CONTACT
 CONTACT_MODEL     = "FORCE"
 ID                = "2"
 LOAD_FUNC         = "fwh_load"
 NAME              = "fwh_contact"
/>
<CHARACTERISTIC.CONTACT
 CONTACT_MODEL     = "FORCE"
 ID                = "3"
 LOAD_FUNC         = "wcseat_load"
 NAME              = "wcseat_contact"
```

```
  />
  <CHARACTERISTIC.CONTACT
   CONTACT_MODEL     = "FORCE"
   ID                = "4"
   LOAD_FUNC         = "wcback_load"
   NAME              = "wcback_contact"
  />
  <CHARACTERISTIC.CONTACT
   CONTACT_MODEL     = "FORCE"
   ID                = "5"
   LOAD_FUNC         = "footrest_load"
   NAME              = "footrest_contact"
  />
  <CHARACTERISTIC.CONTACT
   CONTACT_MODEL     = "FORCE"
   ID                = "6"
   LOAD_FUNC         = "armrest_load"
   NAME              = "armrest_contact"
  />
  <CHARACTERISTIC.CONTACT
   CONTACT_MODEL     = "FORCE"
   ID                = "7"
   LOAD_FUNC         = "tiepoint_load"
   NAME              = "tiepoint_contact"
  />
  <FUNCTION.XY
   ID       = "1"
   NAME     = "rwh_load"
  >
   <TABLE
    TYPE = "XY_PAIR"
   >
< [CDATA[
  |      XI               YI      |
   0.00000000E+000     0.00000000E+000
   6.00000000E-002     2.00000000E+004
      ]]>
      </TABLE>
  </FUNCTION.XY>
  <FUNCTION.XY
   ID       = "2"
   NAME     = "fwh_load"
  >
   <TABLE
    TYPE = "XY_PAIR"
   >
```

```
<![CDATA[
   |      XI               YI       |
     0.00000000E+000      0.00000000E+000
     5.00000000E-002      2.00000000E+004
        ]]>
        </TABLE>
   </FUNCTION.XY>
   <FUNCTION.XY
     ID       = "3"
     NAME     = "wcseat_load"
   >
     <TABLE
       TYPE = "XY_PAIR"
     >
<![CDATA[
   |      XI               YI       |
     0.00000000E+000      0.00000000E+000
     2.30000000E-002      1.23000000E+003
     3.00000000E-002      2.16900000E+003
     1.00000000E-001      1.85040000E+004
        ]]>
        </TABLE>
   </FUNCTION.XY>
   <FUNCTION.XY
     ID       = "4"
     NAME     = "wcback_load"
   >
     <TABLE
       TYPE = "XY_PAIR"
     >
<![CDATA[
   |      XI               YI       |
     0.00000000E+000      0.00000000E+000
     1.60000000E-002      5.25000000E+002
     2.00000000E-002      1.05200000E+003
     1.00000000E-001      1.21690000E+004
        ]]>
        </TABLE>
   </FUNCTION.XY>
   <FUNCTION.XY
     ID       = "5"
     NAME     = "footrest_load"
   >
     <TABLE
       TYPE = "XY_PAIR"
     >
```

```
<![CDATA[
   |      XI               YI       |
     0.00000000E+000      0.00000000E+000
     1.00000000E-001      2.00000000E+004
        ]]>
        </TABLE>
   </FUNCTION.XY>
   <FUNCTION.XY
     ID       = "6"
     NAME     = "armrest_load"
   >
     <TABLE
       TYPE = "XY_PAIR"
     >
<![CDATA[
   |      XI               YI       |
     0.00000000E+000      0.00000000E+000
     1.50000000E-001      1.00000000E+004
        ]]>
        </TABLE>
   </FUNCTION.XY>
   <FUNCTION.XY
     ID       = "7"
     NAME     = "tiepoint_load"
   >
     <TABLE
       TYPE = "XY_PAIR"
     >
<![CDATA
   |      XI               YI       |
     0.00000000E+000      0.00000000E+000
     1.00000000E-002      2.00000000E+004
        ]]>
        </TABLE>
   </FUNCTION.XY>
   <GROUP_MB
     ID               = "1"
     NAME             = "rrwh_surface"
     SURFACE_LIST       = "rrwh_surface"
     SYSTEM             = "/wheelchair"
   />
   <GROUP_MB
     ID               = "11"
     NAME             = "rlwh_surface"
     SURFACE_LIST       = "rlwh_surface"
     SYSTEM             = "/wheelchair"
```

```
 />
 <GROUP_MB
  ID              = "2"
  NAME            = "frwh_surface"
  SURFACE_LIST    = "frwh_surface"
  SYSTEM          = "/wheelchair"
 />
 <GROUP_MB
  ID              = "22"
  NAME            = "flwh_surface"
  SURFACE_LIST    = "flwh_surface"
  SYSTEM          = "/wheelchair"
 />
 <GROUP_MB
  ID              = "3"
  NAME            = "wcseat_contact_surface"
  SURFACE_LIST    = "wcseat_surface"
  SYSTEM          = "/wheelchair"
 />
 <GROUP_MB
  ID              = "4"
  NAME            = "wcback_contact_surface"
  SURFACE_LIST    = "wcback_surface"
  SYSTEM          = "/wheelchair"
 />
 <GROUP_MB
  ID              = "5"
  NAME            = "footrest_contact_surface"
  SURFACE_LIST    = "footrest_surface"
  SYSTEM          = "/wheelchair"
 />
 <GROUP_MB
  ID              = "6"
  NAME            = "armrest_surfaces"
  SURFACE_LIST    = "r_arm     l_arm"
  SYSTEM          = "/wheelchair"
 />
 <GROUP_MB
  ID              = "7"
  NAME            = "tiepoint_contact_surface"
  SURFACE_LIST    = "ALL"
  SYSTEM          = "/wheelchair"
 />
</SYSTEM.MODEL>
<SYSTEM.MODEL
 ID          = "4"
```

```
  NAME          = "Hybrid_III_6_year_old"
>
  <INCLUDE
   FILE = "d_hyb36yel_inc.xml"
  />
  <CRDSYS_OBJECT
   ID          = "1"
   NAME        = "Dummy_Attachment"
   ORIENT      = "Dummy_Attachment_ori"
   POS         = "0.0          0.0          0.0"
  />
  <ORIENTATION.SUCCESSIVE_ROT
   AXIS_1    = "Y"
   ID        = "15"
   NAME      = "Dummy_Attachment_ori"
   R1        = "0.0"
  />
  <ORIENTATION.SUCCESSIVE_ROT
   AXIS_1    = "Y"
   ID        = "71"
   NAME      = "Dummy_ori"
   R1        = "-0.12217"
  />
  <ORIENTATION.SUCCESSIVE_ROT
   AXIS_1    = "Y"
   ID        = "72"
   NAME      = "LumbarSpine_ori"
   R1        = "0.061"
  />
  <ORIENTATION.SUCCESSIVE_ROT
   AXIS_1    = "X"
   ID        = "74"
   NAME      = "NeckPivotLow_ori"
   R1        = "0.0"
  />
  <ORIENTATION.SUCCESSIVE_ROT
   AXIS_1    = "X"
   ID        = "75"
   NAME      = "NeckPivotUp_ori"
   R1        = "0.0"
  />
  <ORIENTATION.SUCCESSIVE_ROT
   AXIS_1    = "X"
   ID        = "76"
   NAME      = "HipL_ori"
   R1        = "0.06981"
```

```
/>
<ORIENTATION.SUCCESSIVE_ROT
 AXIS_1    = "X"
 ID        = "77"
 NAME      = "HipR_ori"
 R1        = "0.06981"
/>
<ORIENTATION.SUCCESSIVE_ROT
 AXIS_1    = "X"
 ID        = "78"
 NAME      = "AnkleL_ori"
 R1        = "0.0"
/>
<ORIENTATION.SUCCESSIVE_ROT
 AXIS_1    = "X"
 ID        = "79"
 NAME      = "AnkleR_ori"
 R1        = "0.0"
/>
<RESTRAINT.JOINT
 DYNAMIC_FRIC_COEF      = "0.004"
 DYNAMIC_FRIC_LOAD      = "12.0"
 ID                     = "22"
 JOINT                  = "HipL_jnt"
 NAME                   = "HipL_joi"
 STATIC_FRIC_COEF       = "0.004"
 STATIC_FRIC_LOAD       = "12.0"
/>
<RESTRAINT.JOINT
 DYNAMIC_FRIC_COEF      = "0.004"
 DYNAMIC_FRIC_LOAD      = "12.0"
 ID                     = "23"
 JOINT                  = "HipR_jnt"
 NAME                   = "HipR_joi"
 STATIC_FRIC_COEF       = "0.004"
 STATIC_FRIC_LOAD       = "12.0"
/>
<RESTRAINT.JOINT
 DYNAMIC_FRIC_COEF      = "0.00159824"
 DYNAMIC_FRIC_LOAD      = "23.6257"
 ID                     = "26"
 JOINT                  = "AnkleL_jnt"
 NAME                   = "AnkleL_joi"
 STATIC_FRIC_COEF       = "0.00159824"
 STATIC_FRIC_LOAD       = "23.6257"
/>
```

```
<RESTRAINT.JOINT
 DYNAMIC_FRIC_COEF      = "0.00159824"
 DYNAMIC_FRIC_LOAD      = "23.6257"
 ID                     = "27"
 JOINT                  = "AnkleR_jnt"
 NAME                   = "AnkleR_joi"
 STATIC_FRIC_COEF       = "0.00159824"
 STATIC_FRIC_LOAD       = "23.6257"
/>
<INITIAL.JOINT_POS
 JOINT      = "Dummy_jnt"
 ORIENT     = "Dummy_ori"
 Q5         = "0.823"
 Q6         = "0.952"
 Q7         = "0.5"
/>
<INITIAL.JOINT_POS
 JOINT      = "LumbarSpine_jnt"
 ORIENT     = "LumbarSpine_ori"
/>
<INITIAL.JOINT_POS
 JOINT      = "NeckPivotLow_jnt"
 ORIENT     = "NeckPivotLow_ori"
/>
<INITIAL.JOINT_POS
 JOINT      = "NeckPivotMid_jnt"
/>
<INITIAL.JOINT_POS
 JOINT      = "NeckPivotUp_jnt"
 ORIENT     = "NeckPivotUp_ori"
/>
<INITIAL.JOINT_POS
 JOINT      = "ShoulderL_jnt"
 Q2         = "0.06"
/>
<INITIAL.JOINT_POS
 JOINT      = "ShoulderR_jnt"
 Q2         = "-0.06"
/>
<INITIAL.JOINT_POS
 JOINT      = "ElbowL_jnt"
 Q2         = "-0.837776"
/>
<INITIAL.JOINT_POS
 JOINT      = "ElbowR_jnt"
 Q2         = "-0.837776"
```

```
/>
<INITIAL.JOINT_POS
 JOINT      = "WristL_jnt"
/>
<INITIAL.JOINT_POS
 JOINT      = "WristR_jnt"
/>
<INITIAL.JOINT_POS
 JOINT      = "HipL_jnt"
 ORIENT     = "HipL_ori"
/>
<INITIAL.JOINT_POS
 JOINT      = "HipR_jnt"
 ORIENT     = "HipR_ori"
/>
<INITIAL.JOINT_POS
 JOINT      = "KneeL_jnt"
/>
<INITIAL.JOINT_POS
 JOINT      = "KneeR_jnt"
/>
<INITIAL.JOINT_POS
 JOINT      = "AnkleL_jnt"
 ORIENT     = "AnkleL_ori"
/>
<INITIAL.JOINT_POS
 JOINT      = "AnkleR_jnt"
 ORIENT     = "AnkleR_ori"
/>
<INITIAL.JOINT_VEL
 JOINT     = "Dummy_jnt"
 QD4       = "13.444"
/>
<INITIAL.JOINT_VEL
 JOINT     = "LumbarSpine_jnt"
/>
<INITIAL.JOINT_VEL
 JOINT     = "NeckPivotLow_jnt"
/>
<INITIAL.JOINT_VEL
 JOINT     = "NeckPivotMid_jnt"
/>
<INITIAL.JOINT_VEL
 JOINT     = "NeckPivotUp_jnt"
/>
<INITIAL.JOINT_VEL
```

```
 JOINT      = "ShoulderL_jnt"
/>
<INITIAL.JOINT_VEL
 JOINT      = "ShoulderR_jnt"
/>
<INITIAL.JOINT_VEL
 JOINT      = "ElbowL_jnt"
/>
<INITIAL.JOINT_VEL
 JOINT      = "ElbowR_jnt"
/>
<INITIAL.JOINT_VEL
 JOINT      = "WristL_jnt"
/>
<INITIAL.JOINT_VEL
 JOINT      = "WristR_jnt"
/>
<INITIAL.JOINT_VEL
 JOINT      = "HipL_jnt"
/>
<INITIAL.JOINT_VEL
 JOINT      = "HipR_jnt"
/>
<INITIAL.JOINT_VEL
 JOINT      = "KneeL_jnt"
/>
<INITIAL.JOINT_VEL
 JOINT      = "KneeR_jnt"
/>
<INITIAL.JOINT_VEL
 JOINT      = "AnkleL_jnt"
/>
<INITIAL.JOINT_VEL
 JOINT      = "AnkleR_jnt"
/>
<GROUP_MB
 ID             = "50"
 NAME           = "dummy_back_surface1"
 SURFACE_LIST       = "ThoracicBackPlate_ell"
 SYSTEM         = "/Hybrid_III_6_year_old"
/>
<GROUP_MB
 ID             = "51"
 NAME           = "dummy_back_surface2"
 SURFACE_LIST       = "LumbarSpineLow_ell "
 SYSTEM         = "/Hybrid_III_6_year_old"
```

```
  />
  <GROUP_MB
   ID               = "52"
   NAME             = "dummy_back_surface3"
   SURFACE_LIST     = " LumbarSpineUp_ell"
   SYSTEM           = "/Hybrid_III_6_year_old"
  />
  <!-- Additional Ellipsoid for contact -->
  <SURFACE.ELLIPSOID
   DEGREE         = "2"
   ID             = "52"
   NAME           = "ClavicleL_bod_Ellip_52"
   SEMI_AXIS      = "0.05        0.06        0.05"
  >
   <CRDSYS_OBJECT_1
    BODY       = "ClavicleL_bod"
    ORIENT     = "OrientSuccessive_209"
    POS        = "0.0058      0.0407      0.0084"
   />
  </SURFACE.ELLIPSOID>
  <ORIENTATION.SUCCESSIVE_ROT
   AXIS_1    = "X"
   AXIS_2    = "Y"
   AXIS_3    = "Z"
   ID       = "209"
   NAME     = "OrientSuccessive_209"
   R1       = "-1.3672658746"
   R2       = "0.13866896862"
   R3       = "-0.0086156889173"
  />
  <DISABLE>
<![CDATA[
<!--Pre-defined contact definitions using stress functions-->
    <GROUP_FE
      ID       = "1"
      NAME     = "UserFEGroup1_gfe"
      FE_MODEL  = "/USER_DEFINED_SYSTEM/USER_DEFINED_FE_MODEL"
      NODE_LIST = "USER_DEFINED_NODE_LIST">
    </GROUP_FE>

    <CONTACT.MB_FE
      ID           = "101"
      MASTER_SURFACE = "Sternum_gmb"
      SLAVE_SURFACE  = "UserFEGroup1_gfe"
      SURFACE_THICK  = "0.011">
      <CONTACT_FORCE.CHAR
```

```
    CONTACT_TYPE = "USER_MASTER"
    USER_CHAR    = "Sternum_Airbag_con"
    FRIC_FUNC    = "Friction1_fun"
    CONTACT_AREA = "0.0">
  </CONTACT_FORCE.CHAR>

</CONTACT.MB_FE>

<CONTACT.MB_FE
  ID           = "102"
  MASTER_SURFACE = "Ribs_gmb"
  SLAVE_SURFACE  = "UserFEGroup1_gfe"
  SURFACE_THICK  = "0.011">
  <CONTACT_FORCE.CHAR
    CONTACT_TYPE = "USER_MASTER"
    USER_CHAR    = "Ribs_Airbag_con"
    FRIC_FUNC    = "Friction1_fun"
    CONTACT_AREA = "0.0">
  </CONTACT_FORCE.CHAR>

</CONTACT.MB_FE>

<CONTACT.MB_FE
  ID           = "103"
  MASTER_SURFACE = "Abdomen_gmb"
  SLAVE_SURFACE  = "UserFEGroup1_gfe"
  SURFACE_THICK  = "0.077">
  <CONTACT_FORCE.CHAR
    CONTACT_TYPE = "USER_MASTER"
    USER_CHAR    = "Abdomen_Airbag_con"
    FRIC_FUNC    = "Friction1_fun"
    CONTACT_AREA = "0.0">
  </CONTACT_FORCE.CHAR>

</CONTACT.MB_FE>

<CONTACT.MB_FE
  ID           = "104"
  MASTER_SURFACE = "Head_gmb"
  SLAVE_SURFACE  = "UserFEGroup1_gfe"
  SURFACE_THICK  = "0.011">
  <CONTACT_FORCE.CHAR
    CONTACT_TYPE = "USER_MASTER"
    USER_CHAR    = "Head_Airbag_con"
    FRIC_FUNC    = "Friction2_fun"
    CONTACT_AREA = "0.0">
```

```
  </CONTACT_FORCE.CHAR>

</CONTACT.MB_FE>

<CONTACT.MB_FE
  ID           = "105"
  MASTER_SURFACE = "Neck_gmb"
  SLAVE_SURFACE  = "UserFEGroup1_gfe"
  SURFACE_THICK  = "0.005">
  <CONTACT_FORCE.CHAR
    CONTACT_TYPE = "USER_MASTER"
    USER_CHAR    = "Neck_Airbag_con"
    FRIC_FUNC    = "Friction2_fun"
    CONTACT_AREA = "0.0">
  </CONTACT_FORCE.CHAR>

</CONTACT.MB_FE>

<CONTACT.MB_FE
  ID           = "106"
  MASTER_SURFACE = "Shoulder_gmb"
  SLAVE_SURFACE  = "UserFEGroup1_gfe"
  SURFACE_THICK  = "0.011">
  <CONTACT_FORCE.CHAR
    CONTACT_TYPE = "USER_MASTER"
    USER_CHAR    = "Shoulder_Airbag_con"
    FRIC_FUNC    = "Friction1_fun"
    CONTACT_AREA = "0.0">
  </CONTACT_FORCE.CHAR>

</CONTACT.MB_FE>

<CHARACTERISTIC.CONTACT
  ID           = "101"
  NAME         = "Sternum_Airbag_con"
  CONTACT_MODEL = "STRESS"
  LOAD_FUNC     = "Sternum_Airbag_flo"
  DAMP_AMP_FUNC = "Sternum_Airbag_fda"
  DAMP_COEF     = "500"
  HYS_MODEL     = "NONE">
</CHARACTERISTIC.CONTACT>

<CHARACTERISTIC.CONTACT
  ID           = "102"
  NAME         = "Ribs_Airbag_con"
  CONTACT_MODEL = "STRESS"
```

```
  LOAD_FUNC     = "Ribs_Airbag_flo"
  DAMP_AMP_FUNC = "Ribs_Airbag_fda"
  DAMP_COEF     = "0.1375"
  HYS_MODEL     = "NONE">
</CHARACTERISTIC.CONTACT>

<CHARACTERISTIC.CONTACT
  ID          = "103"
  NAME        = "Abdomen_Airbag_con"
  CONTACT_MODEL = "STRESS"
  LOAD_FUNC     = "Abdomen_Airbag_flo"
  DAMP_AMP_FUNC = "Abdomen_Airbag_fda"
  DAMP_COEF     = "300.0"
  HYS_MODEL     = "NONE">
</CHARACTERISTIC.CONTACT>

<CHARACTERISTIC.CONTACT
  ID          = "104"
  NAME        = "Head_Airbag_con"
  CONTACT_MODEL = "STRESS"
  LOAD_FUNC     = "Head_Airbag_flo"
  UNLOAD_FUNC   = "Head_Airbag_ful"
  DAMP_AMP_FUNC = "Head_Airbag_fda"
  DAMP_COEF     = "1.0E+05"
  HYS_MODEL     = "1"
  HYS_SLOPE     = "2.50E+08">
</CHARACTERISTIC.CONTACT>

<CHARACTERISTIC.CONTACT
  ID          = "105"
  NAME        = "Neck_Airbag_con"
  CONTACT_MODEL = "STRESS"
  LOAD_FUNC     = "Neck_Airbag_flo"
  DAMP_AMP_FUNC = "Neck_Airbag_fda"
  DAMP_COEF     = "1.0E+05"
  HYS_MODEL     = "NONE">
</CHARACTERISTIC.CONTACT>

<CHARACTERISTIC.CONTACT
  ID          = "106"
  NAME        = "Shoulders_Airbag_con"
  CONTACT_MODEL = "STRESS"
  LOAD_FUNC     = "Shoulders_Airbag_flo"
  DAMP_AMP_FUNC = "Shoulders_Airbag_fda"
  DAMP_COEF     = "500"
  HYS_MODEL     = "NONE">
```

```
</CHARACTERISTIC.CONTACT>

<FUNCTION.XY ID = "101" NAME = "Sternum_Airbag_flo">
  <TABLE TYPE = "XY_PAIR">
  |      XI              YI      |
    0.00000000E+00     0.00000000E+00
    4.40457000E-01     3.51270000E+04
    6.77627000E-01     7.33535000E+04
    8.13153000E-01     1.45329000E+05
    9.48673000E-01     4.07705000E+06
    1.05032000E+00     8.94405000E+06
  </TABLE>

</FUNCTION.XY>

<FUNCTION.XY ID = "102" NAME = "Sternum_Airbag_fda">
  <TABLE TYPE = "XY_PAIR">
  |      XI              YI      |
    0.00000000E+00     0.00000000E+00
    3.00000000E+04     8.00000000E-01
    8.94405000E+05     1.00000000E+00
  </TABLE>

</FUNCTION.XY>

<FUNCTION.XY ID = "103" NAME = "Ribs_Airbag_flo">
  <TABLE TYPE = "XY_PAIR">
  |      XI              YI      |
    0.00000000E+00     0.00000000E+00
    4.40457000E-01     3.51399000E+04
    6.77627000E-01     7.33405000E+04
    8.13153000E-01     1.45325000E+05
    9.48673000E-01     4.07718000E+05
    1.05032000E+00     8.81505000E+05
  </TABLE>

</FUNCTION.XY>

<FUNCTION.XY ID = "104" NAME = "Ribs_Airbag_fda">
  <TABLE TYPE = "XY_PAIR">
  |      XI              YI      |
    0.00000000E+00     0.00000000E+00
    1.04758000E+05     6.08000000E+01
    2.18641000E+05     1.77600000E+02
    4.33241000E+05     2.76100000E+02
    1.21548000E+06     8.03000000E+02
```

```
    2.62794000E+06      2.64850000E+03
  </TABLE>

</FUNCTION.XY>

<FUNCTION.XY ID = "105" NAME = "Abdomen_Airbag_flo">
  <TABLE TYPE = "XY_PAIR">
  |      XI               YI      |
    0.00000000E+00      0.00000000E+00
    4.40457000E-01      3.51270000E+04
    6.77627000E-01      7.33535000E+04
    8.13153000E-01      1.45329000E+05
    9.48673000E-01      4.07705000E+05
    1.05032000E+00      8.94405000E+05
  </TABLE>

</FUNCTION.XY>

<FUNCTION.XY ID = "106" NAME = "Abdomen_Airbag_fda">
  <TABLE TYPE = "XY_PAIR">
  |      XI               YI      |
    0.00000000E+00      0.00000000E+00
    3.00000000E+04      8.00000000E-01
    8.94405000E+05      1.00000000E+00
  </TABLE>

</FUNCTION.XY>

<FUNCTION.XY ID = "107" NAME = "Head_Airbag_flo">
  <TABLE TYPE = "XY_PAIR">
  |      XI               YI      |
    0.00000000E+00      0.00000000E+00
    1.00000000E-01      1.13945000E+06
    2.00000000E-01      3.52265000E+06
    3.00000000E-01      8.71314000E+06
    3.50000000E-01      1.21207000E+07
    4.00000000E-01      1.66505000E+07
    4.50000000E-01      2.22784000E+07
    5.00000000E-01      2.89159000E+07
    5.50000000E-01      3.63497000E+07
  </TABLE>

</FUNCTION.XY>

<FUNCTION.XY ID = "108" NAME = "Head_Airbag_ful">
  <TABLE TYPE = "XY_PAIR">
```

```
  |      XI              YI      |
    0.00000000E+00     0.00000000E+00
    1.00000000E-01     2.78710000E+05
    2.00000000E-01     7.35480000E+05
    3.00000000E-01     1.50190000E+06
    3.50000000E-01     2.01290000E+06
    4.00000000E-01     2.74840000E+06
    4.50000000E-01     3.67740000E+06
    5.00000000E-01     4.77290000E+06
    5.50000000E-01     6.00000000E+06
  </TABLE>

</FUNCTION.XY>

<FUNCTION.XY ID = "109" NAME = "Head_Airbag_fda">
  <TABLE TYPE = "XY_PAIR">
  |      XI              YI      |
    0.00000000E+00     0.00000000E+00
    7.00000000E+06     3.14779000E-01
    3.00000000E+07     1.02000000E+00
  </TABLE>

</FUNCTION.XY>

<FUNCTION.XY ID = "110" NAME = "Neck_Airbag_flo">
  <TABLE TYPE = "XY_PAIR">
  |      XI              YI      |
    0.00000000E+00     0.00000000E+00
    1.00000000E-01     1.13945000E+06
    2.00000000E-01     3.52265000E+06
    3.00000000E-01     8.71314000E+06
    3.50000000E-01     1.21207000E+07
    4.00000000E-01     1.66505000E+07
    4.50000000E-01     2.22784000E+07
    5.00000000E-01     2.89159000E+07
    5.50000000E-01     3.63497000E+07
  </TABLE>

</FUNCTION.XY>

<FUNCTION.XY ID = "111" NAME = "Neck_Airbag_fda">
  <TABLE TYPE = "XY_PAIR">
  |      XI              YI      |
    0.00000000E+00     0.00000000E+00
    7.00000000E+06     3.14779000E-01
    3.00000000E+07     1.02000000E+00
```

```
  </TABLE>

</FUNCTION.XY>

<FUNCTION.XY ID = "112" NAME = "Shoulders_Airbag_flo">
  <TABLE TYPE = "XY_PAIR">
  |      XI              YI      |
    0.00000000E+00     0.00000000E+00
    4.40457000E-01     3.51270000E+05
    6.77627000E-01     7.33535000E+05
    8.13153000E-01     1.45329000E+06
    9.48673000E-01     4.07705000E+06
    1.05032000E+00     8.94405000E+06
  </TABLE>

</FUNCTION.XY>

<FUNCTION.XY ID = "113" NAME = "Shoulders_Airbag_fda">
  <TABLE TYPE = "XY_PAIR">
  |      XI              YI      |
    0.00000000E+00     0.00000000E+00
    3.00000000E+04     8.00000000E-01
    8.94405000E+05     1.00000000E+00
  </TABLE>

</FUNCTION.XY>

<FUNCTION.XY ID = "114" NAME = "Friction1_fun">
  <TABLE TYPE = "XY_PAIR">
  |      XI              YI      |
    0.00000000E+00     0.00000000E+00
    1.00000000E-02     0.00000000E+00
    2.00000000E-02     2.50000000E-01
    1.00000000E+02     2.50000000E-01
  </TABLE>

</FUNCTION.XY>

<FUNCTION.XY ID = "115" NAME = "Friction2_fun">
  <TABLE TYPE = "XY_PAIR">
  |      XI              YI      |
    0.00000000E+00     0.00000000E+00
    5.00000000E-02     4.00000000E-01
    1.00000000E+00     4.00000000E-01
  </TABLE>
```

```
   </FUNCTION.XY>
    ]]>
    </DISABLE>
</SYSTEM.MODEL>
<POINT_OBJECT
  BODY         = "/moving_sled/sled_body"
  ID           = "1"
  NAME         = "an_rrfl"
  POS          = "0.25        0.7827       0.075"
/>
<POINT_OBJECT
  BODY         = "/wheelchair/frame_cg_body"
  ID           = "2"
  NAME         = "an_rrwc"
  POS          = "-0.32        -0.13        0.014"
/>
<POINT_OBJECT
  BODY         = "/moving_sled/sled_body"
  ID           = "3"
  NAME         = "an_rlfl"
  POS          = "0.25        1.1177       0.075"
/>
<POINT_OBJECT
  BODY         = "/wheelchair/frame_cg_body"
  ID           = "4"
  NAME         = "an_rlwc"
  POS          = "-0.32        0.1198       0.014"
/>
<POINT_OBJECT
  BODY         = "/moving_sled/sled_body"
  ID           = "5"
  NAME         = "an_frfl"
  POS          = "1.443       0.6152       0.0"
/>
<POINT_OBJECT
  BODY         = "/wheelchair/frame_cg_body"
  ID           = "6"
  NAME         = "an_frwc"
  POS          = "0.204       -0.2102       -0.11"
/>
<POINT_OBJECT
  BODY         = "/moving_sled/sled_body"
  ID           = "7"
  NAME         = "an_flfl"
  POS          = "1.443       1.2852       0.0"
/>
```

```
<POINT_OBJECT
  BODY         = "/wheelchair/frame_cg_body"
  ID           = "8"
  NAME         = "an_flwc"
  POS          = "0.204       0.2348       -0.11"
/>
<POINT_OBJECT
  BODY         = "/moving_sled/sled_body"
  ID           = "9"
  NAME         = "shoulder_anc"
  POS          = "0.41        1.275        1.045"
/>
<POINT_OBJECT
  BODY         = "/Hybrid_III_6_year_old/ClavicleL_bod"
  ID           = "10"
  NAME         = "clavicleL"
  POS          = "0.0144      0.0337       0.0714"
/>
<POINT_OBJECT
  BODY         = "/Hybrid_III_6_year_old/Sternum_bod"
  ID           = "11"
  NAME         = "sternum_UpL"
  POS          = "0.013       0.0244       0.0432"
/>
<POINT_OBJECT
  BODY         = "/Hybrid_III_6_year_old/Sternum_bod"
  ID           = "12"
  NAME         = "sternum_LowL"
  POS          = "0.015       -0.024       -0.042"
/>
<POINT_OBJECT
  BODY         = "/wheelchair/tiepoint_body"
  ID           = "13"
  NAME         = "tie_point"
  POS          = "0.0         0.0          0.0"
/>
<POINT_OBJECT
  BODY         = "/wheelchair/tiepoint_body"
  ID           = "113"
  NAME         = "tie_point1"
  POS          = "0.0         0.0          0.0"
/>
<POINT_OBJECT
  BODY         = "/moving_sled/sled_body"
  ID           = "14"
  NAME         = "pelvic_ancR"
```

```
  POS          = "0.25         0.7477       0.0"
/>
<POINT_OBJECT
  BODY         = "/moving_sled/sled_body"
  ID           = "15"
  NAME         = "pelvic_ancL"
  POS          = "0.25         1.1177       0.0"
/>
<POINT_OBJECT
  BODY         = "/Hybrid_III_6_year_old/AbdomenInsert_bod"
  ID           = "16"
  NAME         = "abdomenL"
  POS          = "0.0332       0.082        -0.0161"
/>
<POINT_OBJECT
  BODY         = "/Hybrid_III_6_year_old/AbdomenInsert_bod"
  ID           = "17"
  NAME         = "abdomenR"
  POS          = "0.0332       -0.082       -0.0161"
/>
<POINT_OBJECT
  ID           = "114"
  NAME         = "PointObj_114"
  POS          = "0.6974       1.09678      0.8911"
/>
<POINT_OBJECT
  BODY         = "/moving_sled/sled_body"
  ID           = "115"
  NAME         = "pillar_point"
  POS          = "0.41         1.275        1.045"
/>
<POINT_OBJECT
  ID           = "116"
  NAME         = "UshoulderFE_node"
  POS          = "0.0          0.0          0.0"
/>
<POINT_OBJECT
  BODY         = "/wheelchair/tiepoint_body"
  ID           = "117"
  NAME         = "tiepoint1"
  POS          = "0.0          0.0          0.0"
/>
<POINT_OBJECT
  BODY         = "/Hybrid_III_6_year_old/Sternum_bod"
  ID           = "119"
  NAME         = "PointObj_119"
```

```
  POS          = "0.018082089101 0.0          0.027641211532"
/>
<POINT_OBJECT
  ID           = "120"
  NAME         = "PointObj_120"
  POS          = "0.0          0.0          0.0"
/>
<POINT_OBJECT
  BODY         = "/wheelchair/tiepoint_body"
  ID           = "130"
  NAME         = "tiepoint2"
  POS          = "0.0          0.0          0.0"
/>
<POINT_OBJECT
  ID           = "151"
  NAME         = "PointObj_151"
  POS          = "0.0          0.0          0.0"
/>
<POINT_OBJECT
  BODY         = "/moving_sled/sled_body"
  ID           = "152"
  NAME         = "Lfloor"
  POS          = "0.25         0.71         0.0"
/>
<POINT_OBJECT
  FE_MODEL     = "/moving_sled/lap_FE"
  ID           = "153"
  NAME         = "PointObj_153"
  NODE         = "4"
/>
<POINT_OBJECT
  ID           = "154"
  NAME         = "PointObj_154"
  POS          = "-9.649950E-004 1.4634088368 0.094725418903"
/>
<POINT_OBJECT
  ID           = "155"
  NAME         = "PointObj_155"
  POS          = "0.78183913654 1.0340730509 0.49815028332"
/>
<POINT_OBJECT
  BODY         = "/Hybrid_III_6_year_old/AbdomenInsert_bod"
  ID           = "156"
  NAME         = "PointObj_156"
  POS          = "0.055684666577 -0.0017545042728 -0.0061894221325"
/>
```

```
<POINT_OBJECT
  FE_MODEL      = "/moving_sled/lap_FE"
  ID            = "157"
  NAME          = "PointObj_157"
  NODE          = "28"
/>
<POINT_OBJECT
  ID            = "227"
  NAME          = "PointObj_227"
  POS           = "0.0          0.0          0.0"
/>
<POINT_OBJECT
  FE_MODEL      = "/moving_sled/lap_FE"
  ID            = "228"
  NAME          = "LlapFE_node"
  NODE          = "28"
/>
<POINT_OBJECT
  BODY          = "/moving_sled/sled_body"
  ID            = "229"
  NAME          = "Rfloor"
  POS           = "0.25         1.1177       0.0"
/>
<POINT_OBJECT
  BODY          = "/moving_sled/sled_body"
  ID            = "297"
  NAME          = "PointObj_297"
  POS           = "0.41         1.275        1.045"
/>
<POINT_OBJECT
  ID            = "298"
  NAME          = "PointObj_298"
  POS           = "0.782891018  1.0954099632 0.8120456835"
/>
<POINT_OBJECT
  ID            = "299"
  NAME          = "PointObj_299"
  POS           = "0.0          0.0          0.0"
/>
<POINT_OBJECT
  BODY          = "/moving_sled/sled_body"
  ID            = "300"
  NAME          = "PointObj_300"
  POS           = "0.41         1.275        1.045"
/>
<POINT_OBJECT
```

```
  FE_MODEL      = "/moving_sled/shoulder_FE"
  ID            = "301"
  NAME          = "UshdrFE"
  NODE          = "4"
/>
<POINT_OBJECT
  BODY          = "/Hybrid_III_6_year_old/Sternum_bod"
  ID            = "302"
  NAME          = "PointObj_302"
  POS           = "0.018107829273 0.0          0.026771325159"
/>
<POINT_OBJECT
  FE_MODEL      = "/moving_sled/shoulder_FE"
  ID            = "303"
  NAME          = "PointObj_303"
  NODE          = "40"
/>
<BELT
  ID        = "1"
  NAME      = "floor_rrwc"
>
  <BELT_SEGMENT
    CHAR                = "/tiedown_char"
    ID                  = "1"
    NAME                = "seg1"
    POINT_REF_1         = "/an_rrfl"
    POINT_REF_2         = "/an_rrwc"
  />
</BELT>
<BELT
  ID        = "2"
  NAME      = "floor_rlwc"
>
  <BELT_SEGMENT
    CHAR                = "/tiedown_char"
    ID                  = "1"
    NAME                = "seg1"
    POINT_REF_1         = "/an_rlfl"
    POINT_REF_2         = "/an_rlwc"
  />
</BELT>
<BELT
  ID        = "3"
  NAME      = "floor_frwc"
>
  <BELT_SEGMENT
```

```
   CHAR                = "/tiedown_char"
   ID                  = "1"
   NAME                = "seg1"
   POINT_REF_1         = "/an_frfl"
   POINT_REF_2         = "/an_frwc"
  />
</BELT>
<BELT
  ID       = "4"
  NAME     = "floor_flwc"
>
  <BELT_SEGMENT
   CHAR                = "/tiedown_char"
   ID                  = "1"
   NAME                = "seg1"
   POINT_REF_1         = "/an_flfl"
   POINT_REF_2         = "/an_flwc"
  />
</BELT>
<BELT
  ID       = "6"
  NAME     = "lapbeltsys"
>
  <BELT_SEGMENT
   CHAR                = "/belt_char"
   ID                  = "1"
   NAME                = "SeatBelt6_Seg1"
   POINT_REF_1         = "/tiepoint1"
   POINT_REF_2         = "/Lfloor"
  />
  <BELT_SEGMENT
   CHAR                = "/belt_char"
   ID                  = "2"
   NAME                = "SeatBelt6_Seg2"
   POINT_REF_1         = "/Lfloor"
   POINT_REF_2         = "/tiepoint2"
  />
  <BELT_TYING
   FRIC_COEF       = "0.5"
   ID              = "1"
   NAME            = "Belt_tying_1"
   POINT_REF_1     = "/Lfloor"
   POINT_REF_2     = "/Lfloor"
  />
</BELT>
<BELT
```

```
  ID       = "7"
  NAME     = "end"
 >
  <BELT_SEGMENT
   CHAR               = "/belt_char"
   ID                 = "1"
   NAME               = "SeatBelt7_Seg1"
   POINT_REF_1        = "/LlapFE_node"
   POINT_REF_2        = "/Rfloor"
  />
 </BELT>
 <BELT
  ID       = "8"
  NAME     = "shoulder_sys"
 >
  <BELT_SEGMENT
   CHAR               = "/belt_char1"
   ID                 = "1"
   INITIAL_STRAIN     = "-0.1"
   NAME               = "SeatBelt8_Seg1"
   POINT_REF_1        = "/pillar_point"
   POINT_REF_2        = "/UshdrFE"
  />
 </BELT>
 <CHARACTERISTIC.LOAD
  ELAS_LIMIT          = "0.0"
  HYS_MODEL           = "2"
  HYS_SLOPE           = "5.000000E+008"
  ID                  = "1"
  LOAD_FUNC           = "tiedown_load"
  NAME                = "tiedown_char"
  UNLOAD_FUNC         = "tiedown_unload"
 />
 <FUNCTION.XY
  ID       = "1"
  NAME     = "tiedown_load"
 >
  <TABLE
   TYPE = "XY_PAIR"
  >
<![CDATA[
  |      XI              YI      |
   0.00000000E+000     0.00000000E+000
   2.50000000E-002     2.00000000E+004
   5.00000000E-002     2.93000000E+004
   7.50000000E-002     3.83000000E+004
```

```
    1.00000000E-001      4.91000000E+004
    1.25000000E-001      6.44000000E+004
    1.50000000E-001      8.10000000E+004
    1.15000000E+000      7.45000000E+005
     ]]>
    </TABLE>
  </FUNCTION.XY>
  <FUNCTION.XY
    ID       = "2"
    NAME     = "tiedown_unload"
  >
    <TABLE
      TYPE = "XY_PAIR"
    >
<![CDATA[
    |      XI               YI      |
     0.00000000E+000      0.00000000E+000
     1.00000000E+000      1.00000000E+003
     ]]>
    </TABLE>
  </FUNCTION.XY>
  <CHARACTERISTIC.LOAD
    ELAS_LIMIT           = "0.0"
    HYS_MODEL             = "1"
    HYS_SLOPE            = "3.000000E+005"
    ID                 = "2"
    LOAD_FUNC            = "belt_load"
    NAME               = "belt_char"
    UNLOAD_FUNC          = "belt_unload"
  />
  <CHARACTERISTIC.CONTACT
    CONTACT_MODEL      = "FORCE"
    HYS_MODEL          = "2"
    HYS_SLOPE          = "5.000000E+008"
    ID               = "9990"
    LOAD_FUNC          = "wheel_contact_func1"
    NAME             = "wheel_contact"
  />
  <FUNCTION.XY
    ID       = "9990"
    NAME     = "wheel_contact_func1"
  >
    <TABLE
      TYPE = "XY_PAIR"
    >
<![CDATA[
```

```
   |      XI                YI       |
     0.00000000E+000      0.00000000E+000
     5.00000000E-002      5.00000000E+003
      ]]>
     </TABLE>
  </FUNCTION.XY>
  <CHARACTERISTIC.LOAD
   ELAS_LIMIT           = "0.0"
   HYS_MODEL             = "1"
   HYS_SLOPE            = "5.000000E+005"
   ID                 = "3"
   LOAD_FUNC            = "belt_load1"
   NAME               = "belt_char1"
  />
  <FUNCTION.XY
   ID       = "3"
   NAME     = "belt_load"
  >
   <TABLE
    TYPE = "XY_PAIR"
   >
<![CDATA[
   |      XI                YI       |
     0.00000000E+000      0.00000000E+000
     6.00000000E-002      4.00000000E+003
      ]]>
     </TABLE>
  </FUNCTION.XY>
  <FUNCTION.XY
   ID       = "5"
   NAME     = "belt_load1"
  >
   <TABLE
    TYPE = "XY_PAIR"
   >
<![CDATA[
   |      XI                YI       |
     0.00000000E+000      0.00000000E+000
     2.50000000E-002      5.00000000E+003
     5.00000000E-002      7.32500000E+003
     7.50000000E-002      9.57500000E+003
     1.00000000E-001      1.22750000E+004
     1.25000000E-001      1.61000000E+004
     1.50000000E-001      2.02500000E+004
     1.15000000E+000      1.86250000E+005
      ]]>
```

```
    </TABLE>
  </FUNCTION.XY>
  <FUNCTION.XY
   ID       = "4"
   NAME     = "belt_unload"
  >
   <TABLE
    TYPE = "XY_PAIR"
   >
<![CDATA[
   |      XI               YI       |
     0.00000000E+000      0.00000000E+000
     1.00000000E-001      1.00000000E+003
      ]]>
     </TABLE>
  </FUNCTION.XY>
  <CHARACTERISTIC.CONTACT
   CONTACT_MODEL     = "FORCE"
   HYS_MODEL         = "2"
   HYS_SLOPE         = "1.000000E+010"
   ID                = "9999"
   LOAD_FUNC         = "dummy_contact_func"
   NAME              = "dummy_contact"
  />
  <FUNCTION.XY
   ID       = "9999"
   NAME     = "dummy_contact_func"
  >
   <TABLE
    TYPE = "XY_PAIR"
   >
<![CDATA[
   |      XI               YI       |
     0.00000000E+000      0.00000000E+000
     3.00000000E-001      5.00000000E+004
      ]]>
     </TABLE>
  </FUNCTION.XY>
  <CONTACT.MB_MB
   DAMP_COEF          = "800.0"
   FRIC_COEF          = "0.8"
   ID                 = "1"
   INITIAL_TYPE       = "CORRECT"
   MASTER_SURFACE     = "/moving_sled/sled_group"
   NAME               = "rrwh_floor"
   SLAVE_SURFACE      = "/wheelchair/rrwh_surface"
```

```
>
 <CONTACT_FORCE.CHAR
  CONTACT_TYPE      = "USER_MASTER"
  MAX_FORCE_PAR     = "0.01"
  USER_CHAR         = "/wheel_contact"
 />
</CONTACT.MB_MB>
<CONTACT.MB_MB
 DAMP_COEF          = "800.0"
 FRIC_COEF          = "0.8"
 ID                 = "11"
 INITIAL_TYPE       = "CORRECT"
 MASTER_SURFACE     = "/moving_sled/sled_group"
 NAME               = "rlwh_floor"
 SLAVE_SURFACE      = "/wheelchair/rlwh_surface"
>
 <CONTACT_FORCE.CHAR
  CONTACT_TYPE      = "USER_MASTER"
  MAX_FORCE_PAR     = "0.01"
  USER_CHAR         = "/wheel_contact"
 />
</CONTACT.MB_MB>
<CONTACT.MB_MB
 DAMP_COEF          = "800.0"
 FRIC_COEF          = "0.8"
 ID                 = "2"
 INITIAL_TYPE       = "CORRECT"
 MASTER_SURFACE     = "/moving_sled/sled_group"
 NAME               = "frwh_floor"
 SLAVE_SURFACE      = "/wheelchair/frwh_surface"
>
 <CONTACT_FORCE.CHAR
  CONTACT_TYPE      = "USER_MASTER"
  MAX_FORCE_PAR     = "0.01"
  USER_CHAR         = "/wheel_contact"
 />
</CONTACT.MB_MB>
<CONTACT.MB_MB
 DAMP_COEF          = "800.0"
 FRIC_COEF          = "0.8"
 ID                 = "22"
 INITIAL_TYPE       = "CORRECT"
 MASTER_SURFACE     = "/moving_sled/sled_group"
 NAME               = "flwh_floor"
 SLAVE_SURFACE      = "/wheelchair/flwh_surface"
>
```

```
 <CONTACT_FORCE.CHAR
  CONTACT_TYPE      = "USER_MASTER"
  MAX_FORCE_PAR     = "0.01"
  USER_CHAR         = "/wheel_contact"
 />
</CONTACT.MB_MB>
<CONTACT.MB_MB
 DAMP_COEF          = "800.0"
 FRIC_COEF          = "0.2"
 ID                 = "3"
 INITIAL_TYPE       = "CORRECT"
 MASTER_SURFACE     = "/wheelchair/wcseat_contact_surface"
 NAME               = "pelvis_wcseat"
 SLAVE_SURFACE      = "/Hybrid_III_6_year_old/Pelvis_gmb"
>
 <CONTACT_FORCE.CHAR
  CONTACT_TYPE      = "USER_MASTER"
  MAX_FORCE_PAR     = "0.01"
  USER_CHAR         = "/dummy_contact"
 />
</CONTACT.MB_MB>
<CONTACT.MB_MB
 DAMP_COEF          = "800.0"
 FRIC_COEF          = "0.2"
 ID                 = "4"
 INITIAL_TYPE       = "CORRECT"
 MASTER_SURFACE     = "/wheelchair/wcseat_contact_surface"
 NAME               = "UlegR_wcseat"
 SLAVE_SURFACE      = "/Hybrid_III_6_year_old/FemurKneeR_gmb"
>
 <CONTACT_FORCE.CHAR
  CONTACT_TYPE      = "USER_MASTER"
  MAX_FORCE_PAR     = "0.01"
  USER_CHAR         = "/dummy_contact"
 />
</CONTACT.MB_MB>
<CONTACT.MB_MB
 DAMP_COEF          = "800.0"
 FRIC_COEF          = "0.2"
 ID                 = "5"
 INITIAL_TYPE       = "CORRECT"
 MASTER_SURFACE     = "/wheelchair/wcseat_contact_surface"
 NAME               = "UlegL_wcseat"
 SLAVE_SURFACE      = "/Hybrid_III_6_year_old/FemurKneeL_gmb"
>
 <CONTACT_FORCE.CHAR
```

```
   CONTACT_TYPE      = "USER_MASTER"
   MAX_FORCE_PAR     = "0.01"
   USER_CHAR         = "/dummy_contact"
  />
</CONTACT.MB_MB>
<CONTACT.MB_MB
  DAMP_COEF          = "800.0"
  FRIC_COEF          = "0.3"
  ID                 = "6"
  INITIAL_TYPE       = "CORRECT"
  MASTER_SURFACE     = "/wheelchair/wcback_contact_surface"
  NAME               = "pelvis_wcback"
  SLAVE_SURFACE      = "/Hybrid_III_6_year_old/Pelvis_gmb"
>
  <CONTACT_FORCE.CHAR
   CONTACT_TYPE      = "USER_MASTER"
   MAX_FORCE_PAR     = "0.01"
   USER_CHAR         = "/dummy_contact"
  />
</CONTACT.MB_MB>
<CONTACT.MB_MB
  DAMP_COEF          = "800.0"
  FRIC_COEF          = "0.3"
  ID                 = "7"
  INITIAL_TYPE       = "CORRECT"
  MASTER_SURFACE     = "/wheelchair/wcback_contact_surface"
  NAME               = "dummyback1_wcback"
  SLAVE_SURFACE      = "/Hybrid_III_6_year_old/dummy_back_surface1"
>
  <CONTACT_FORCE.CHAR
   CONTACT_TYPE      = "USER_MASTER"
   MAX_FORCE_PAR     = "0.01"
   USER_CHAR         = "/dummy_contact"
  />
</CONTACT.MB_MB>
<CONTACT.MB_MB
  DAMP_COEF          = "800.0"
  FRIC_COEF          = "0.3"
  ID                 = "71"
  INITIAL_TYPE       = "CORRECT"
  MASTER_SURFACE     = "/wheelchair/wcback_contact_surface"
  NAME               = "dummyback2_wcback"
  SLAVE_SURFACE      = "/Hybrid_III_6_year_old/dummy_back_surface2"
>
  <CONTACT_FORCE.CHAR
   CONTACT_TYPE      = "USER_MASTER"
```

```
   MAX_FORCE_PAR      = "0.01"
   USER_CHAR          = "/dummy_contact"
  />
</CONTACT.MB_MB>
<CONTACT.MB_MB
  DAMP_COEF          = "800.0"
  FRIC_COEF          = "0.3"
  ID                 = "72"
  INITIAL_TYPE       = "CORRECT"
  MASTER_SURFACE     = "/wheelchair/wcback_contact_surface"
  NAME               = "dummyback3_wcback"
  SLAVE_SURFACE      = "/Hybrid_III_6_year_old/dummy_back_surface3"
>
  <CONTACT_FORCE.CHAR
   CONTACT_TYPE      = "USER_MASTER"
   MAX_FORCE_PAR     = "0.01"
   USER_CHAR         = "/dummy_contact"
  />
</CONTACT.MB_MB>
<CONTACT.MB_MB
  DAMP_COEF          = "800.0"
  FRIC_COEF          = "0.3"
  ID                 = "8"
  INITIAL_TYPE       = "CORRECT"
  MASTER_SURFACE     = "/wheelchair/footrest_contact_surface"
  NAME               = "shoeR_footrest"
  SLAVE_SURFACE      = "/Hybrid_III_6_year_old/ShoeR_gmb"
>
  <CONTACT_FORCE.CHAR
   CONTACT_TYPE      = "USER_MASTER"
   MAX_FORCE_PAR     = "1.0"
   USER_CHAR         = "/dummy_contact"
  />
</CONTACT.MB_MB>
<CONTACT.MB_MB
  DAMP_COEF          = "800.0"
  FRIC_COEF          = "0.3"
  ID                 = "9"
  INITIAL_TYPE       = "CORRECT"
  MASTER_SURFACE     = "/wheelchair/footrest_contact_surface"
  NAME               = "shoeL_footrest"
  SLAVE_SURFACE      = "/Hybrid_III_6_year_old/ShoeL_gmb"
>
  <CONTACT_FORCE.CHAR
   CONTACT_TYPE      = "USER_MASTER"
   MAX_FORCE_PAR     = "1.0"
```

```
    USER_CHAR         = "/dummy_contact"
   />
  </CONTACT.MB_MB>
  <CONTACT.MB_MB
   DAMP_COEF          = "800.0"
   FRIC_COEF          = "0.3"
   ID                 = "10"
   INITIAL_TYPE       = "CORRECT"
   MASTER_SURFACE     = "/wheelchair/tiepoint_contact_surface"
   NAME               = "tiepoint_dummy"
   SLAVE_SURFACE      = "dummy_body"
  >
   <CONTACT_FORCE.CHAR
    CONTACT_TYPE      = "MASTER"
   />
  </CONTACT.MB_MB>
  <CONTACT.MB_FE
   ID                 = "12"
   MASTER_SURFACE     = "GroupMB_103     /Hybrid_III_6_year_old/Abdomen_gmb"
   NAME               = "dummytolapfe"
   SLAVE_SURFACE      = "GroupFE_2"
  >
   <CONTACT_FORCE.KINEMATIC
    FRIC_COEF         = "0.5"
   />
  </CONTACT.MB_FE>
  <CONTACT.MB_FE
   ID                 = "13"
   MASTER_SURFACE          =  "GroupMB_102          /Hybrid_III_6_year_old/ArmUpR_gmb
/Hybrid_III_6_year_old/ArmLowL_gmb     /Hybrid_III_6_year_old/Thorax_gmb"
   NAME               = "dummytoshldrfe"
   SLAVE_SURFACE      = "GroupFE_3"
  >
   <CONTACT_FORCE.KINEMATIC
    FRIC_COEF         = "0.3"
   />
  </CONTACT.MB_FE>
  <GROUP_MB
   ID                 = "101"
   NAME               = "dummy_body"
   SURFACE_LIST       = "ALL"
   SYSTEM             = "Hybrid_III_6_year_old"
  />
  <GROUP_MB
   ID                 = "102"
   NAME               = "GroupMB_102"
```

```
  SURFACE_LIST          = "ClavicleL_bod_Ellip_52       ArmUpL_ell       AbdomenUp_ell
AbdomenMid_ell    Pelvis_ell    NeckLow_ell    HipR_ell    HipL_ell"
  SYSTEM            = "Hybrid_III_6_year_old"
 />
 <GROUP_MB
  ID              = "103"
  NAME            = "GroupMB_103"
  SURFACE_LIST          = "Pelvis_ell       HipL_ell       HipR_ell       AbdomenMid_ell
LumbarSpineLow_ell    FemurL_ell    FemurR_ell"
  SYSTEM            = "Hybrid_III_6_year_old"
 />
 <LOAD.SYSTEM_ACC
  AZ_FUNC     = "gravity"
  SYSTEM      = "Hybrid_III_6_year_old"
 />
 <LOAD.SYSTEM_ACC
  AZ_FUNC     = "gravity"
  SYSTEM      = "wheelchair"
 />
 <FUNCTION.XY
  ID       = "10"
  NAME     = "gravity"
 >
  <TABLE
   TYPE = "XY_PAIR"
  >
<![CDATA[
  |      XI              YI      |
    -1.00000000E+000     -9.81000000E+000
    2.00000000E+000      -9.81000000E+000
     ]]>
    </TABLE>
 </FUNCTION.XY>
 <FUNCTION.XY
  ID       = "11"
  NAME     = "sled_pulse"
 >
  <TABLE
   TYPE = "XY_PAIR"
  >
<![CDATA[
  |      XI              YI      |
    0.00000000E+000     -1.67346700E-002
    1.00000000E-004     -5.08848600E-002
    2.00000000E-004     -8.45877700E-002
    3.00000000E-004     -1.24289300E-001
```

4.00000000E-004 -1.63611500E-001
5.00000000E-004 -2.09132800E-001
6.00000000E-004 -2.54542100E-001
7.00000000E-004 -3.06435900E-001
8.00000000E-004 -3.58452100E-001
9.00000000E-004 -4.17099700E-001
1.00000000E-003 -4.75934800E-001

.
.
.

2.40000000E-002 -2.17388400E+001
2.41000000E-002 -2.16755600E+001
2.42000000E-002 -2.15962600E+001
2.43000000E-002 -2.15090600E+001
2.44000000E-002 -2.14091600E+001
2.45000000E-002 -2.13049400E+001
2.46000000E-002 -2.11917600E+001
2.47000000E-002 -2.10781700E+001
2.48000000E-002 -2.09595800E+001
2.49000000E-002 -2.08444900E+001
2.50000000E-002 -2.07281800E+001
2.51000000E-002 -2.06190100E+001
2.52000000E-002 -2.05121300E+001
2.53000000E-002 -2.04158400E+001
2.54000000E-002 -2.03251800E+001
2.55000000E-002 -2.02482000E+001
2.56000000E-002 -2.01796200E+001
2.57000000E-002 -2.01271100E+001
2.58000000E-002 -2.00849600E+001
2.59000000E-002 -2.00603600E+001
2.60000000E-002 -2.00470800E+001

.
.
.

1.98000000E-001 -1.73947100E-002
1.98100000E-001 -2.38375200E-002
1.98200000E-001 -3.32351200E-002
1.98300000E-001 -3.91539200E-002
1.98400000E-001 -4.79813500E-002
1.98500000E-001 -5.32860600E-002
1.98600000E-001 -6.14696000E-002
1.98700000E-001 -6.61103700E-002
1.98800000E-001 -7.36003700E-002
1.98900000E-001 -7.75071100E-002

```
   1.99000000E-001      -8.42365800E-002
   1.99100000E-001      -8.73630400E-002
   1.99200000E-001      -9.32840700E-002
   1.99300000E-001      -9.55818100E-002
   1.99400000E-001      -1.00668700E-001
   1.99500000E-001      -1.02131900E-001
   1.99600000E-001      -1.06375500E-001
   1.99700000E-001      -1.06965900E-001
   1.99800000E-001      -1.10301500E-001
   1.99900000E-001      -1.09969200E-001
   2.00000000E-001      -1.12405300E-001
    ]]>
    </TABLE>
</FUNCTION.XY>
<OUTPUT_BODY
 CORRECT_AX    = "ON"
 CORRECT_AY    = "ON"
 CORRECT_AZ    = "ON"
 CRDSYS        = "OBJECT"
 FILTER        = "CFC60"
 ID            = "1"
 NAME          = "WCcg_acc"
 SIGNAL_TYPE   = "LIN_ACC"
>
 <POINT_OBJECT_1
  BODY      = "/wheelchair/accelerometer"
  POS       = "0.0          0.0          0.0"
 />
</OUTPUT_BODY>
<OUTPUT_BODY
 CORRECT_AX    = "ON"
 CORRECT_AY    = "ON"
 CORRECT_AZ    = "ON"
 CRDSYS        = "OBJECT"
 FILTER        = "CFC60"
 ID            = "2"
 NAME          = "sled_acc"
 SIGNAL_TYPE   = "LIN_ACC"
>
 <POINT_OBJECT_1
  BODY      = "/moving_sled/sled_body"
  POS       = "0.0          0.0          0.0"
 />
</OUTPUT_BODY>
<OUTPUT_BODY_REL
 ID          = "6"
```

```
 NAME        = "Fhead_position"
 SIGNAL_TYPE = "REL_POS"
>
 <POINT_OBJECT_1
  BODY     = "/Hybrid_III_6_year_old/Head_bod"
  POS      = "0.0908      0.0         0.0"
 />
 <POINT_OBJECT_2
  BODY     = "/moving_sled/sled_body"
  POS      = "0.0         0.0         0.0"
 />
</OUTPUT_BODY_REL>
<OUTPUT_BODY_REL
 ID          = "7"
 NAME        = "knee_position"
 SIGNAL_TYPE = "REL_POS"
>
 <POINT_OBJECT_1
  BODY     = "/Hybrid_III_6_year_old/KneeR_bod"
  POS      = "0.0         0.0         0.0"
 />
 <POINT_OBJECT_2
  BODY     = "/moving_sled/sled_body"
  POS      = "0.0         0.0         0.0"
 >
</OUTPUT_BODY_REL>
<OUTPUT_BODY_REL
 ID          = "8"
 NAME        = "pointP_position"
 SIGNAL_TYPE = "REL_POS"
>
 <POINT_OBJECT_1
  BODY     = "/wheelchair/p_point"
  POS      = "0.0         0.0         0.0"
 />
 <POINT_OBJECT_2
  BODY     = "/moving_sled/sled_body"
  POS      = "0.0         0.0         0.0"
 />
</OUTPUT_BODY_REL>
<OUTPUT_BODY_REL
 ID          = "9"
 NAME        = "Hpt_position"
 SIGNAL_TYPE = "REL_POS"
>
 <POINT_OBJECT_1
```

```
   BODY      = "/Hybrid_III_6_year_old/Pelvis_bod"
   POS       = "-0.02         -0.12         0.015"
  />
  <POINT_OBJECT_2
   BODY      = "/moving_sled/sled_body"
   POS       = "0.0          0.0          0.0"
  />
</OUTPUT_BODY_REL>
<OUTPUT_BODY_REL
  ID         = "16"
  NAME       = "Rhead_position"
  SIGNAL_TYPE = "REL_POS"
>
  <POINT_OBJECT_1
   BODY      = "/Hybrid_III_6_year_old/Head_bod"
   POS       = "-0.0908       0.0          0.0"
  />
  <POINT_OBJECT_2
   BODY      = "/moving_sled/sled_body"
   POS       = "0.0          0.0          0.0"
  />
</OUTPUT_BODY_REL>
<OUTPUT_BELT
  EXTENDED      = "ON"
  ID            = "4"
  INPUT_REF     = "/floor_rrwc/seg1"
  INPUT_TYPE    = "BELT_SEGMENT"
/>
<OUTPUT_BELT
  EXTENDED      = "ON"
  ID            = "5"
  INPUT_REF     = "/floor_rlwc/seg1"
  INPUT_TYPE    = "BELT_SEGMENT"
/>
<OUTPUT_BELT
  EXTENDED      = "ON"
  ID            = "7"
  INPUT_REF     = "/end/SeatBelt7_Seg1"
  INPUT_TYPE    = "BELT_SEGMENT"
/>
<OUTPUT_BELT
  EXTENDED      = "ON"
  ID            = "8"
  INPUT_REF     = "/shoulder_sys/SeatBelt8_Seg1"
  INPUT_TYPE    = "BELT_SEGMENT"
/>
```

```
 <OUTPUT_CONTACT
  CONTACT_LIST        = "rrwh_floor rlwh_floor frwh_floor flwh_floor pelvis_wcseat
UlegR_wcseat UlegL_wcseat pelvis_wcback dummyback1_wcback dummyback2_wcback
dummyback3_wcback"
  EXTENDED        = "ON"
  ID              = "10"
 />
 <OUTPUT_JOINT_DOF
  ID        = "101"
  JOINT     = "/moving_sled/sled_joint"
  SIGNAL_TYPE = "ACC"
 />
 <GROUP_FE
  ELEMENT_LIST      = "3:24 26       29:51      1820:1821"
  FE_MODEL          = "/moving_sled/lap_FE"
  ID              = "2"
  NAME              = "GroupFE_2"
 />
 <GROUP_FE
  ELEMENT_LIST      = "3:36 38       41:75 301748 301751"
  FE_MODEL          = "/moving_sled/shoulder_FE"
  ID              = "3"
  NAME              = "GroupFE_3"
 />
 <GROUP_FE
  FE_MODEL          = "/moving_sled/shoulder_FE"
  ID              = "4"
  NAME              = "shoulderbelt_support"
  NODE_LIST         = "15:20       48:50"
 />
 <SUPPORT
  BODY          = "/Hybrid_III_6_year_old/Sternum_bod"
  DOF_ALL       = "ON"
  FE_MODEL      = "/moving_sled/shoulder_FE"
  NODE_LIST     = "15:20       48:50"
 />
</MADYMO>
```